Vol. 98 No. 2 June 1, 1978
Completing Vol. 98

ISSN 0003-2670

ANALYTICA CHIMICA ACTA

International journal devoted to all branches of analytical chemistry

ELSEVIER SCIENTIFIC PUBLISHING COMPANY

ANALYTICA CHIMICA ACTA

International journal devoted to all branches of analytical chemistry
Revue internationale consacrée à tous les domaines de la chimie analytique
Internationale Zeitschrift für alle Gebiete der analytischen Chemie

PUBLICATION SCHEDULE FOR 1978 (incorporating the section on Computer Techniques and Optimization).

	J	F	M	A	M	J	J	A	S	O	N	D
Analytica Chimica Acta	96/1	96/2	97/1	97/2	98/1	98/2	99/1	99/2	100	101/1	101/2	102
Section on Computer Techniques and Optimization			103/1			103/2			103/3			103/4

Scope. *Analytica Chimica Acta* publishes original papers, short communications, and reviews dealing with every aspect of modern chemical analysis, both fundamental and applied. The section on *Computer Techniques and Optimization* is devoted to new developments in chemical analysis by the application of computer techniques and by interdisciplinary approaches, including statistics, systems theory and operation research.

Submission of Papers. Manuscripts (three copies) should be submitted to:
for *Analytica Chimica Acta:* Dr. A. M. G. Macdonald, Department of Chemistry, The University, P.O. Box 363; Birmingham B15 2TT, England;
for the section on *Computer Techniques and Optimization:* Dr. J. T. Clerc, Laboratorium für Organische Chemie, Swiss Federal Institute of Technology, Universitätstrasse 16, CH-8092 Zürich, Switzerland.

Information for Authors. Papers in English, French and German are published. There are no page charges. Manuscripts should conform in layout and style to the papers published in this Volume. Authors should consult Vol. 93, p. 379 for detailed information. Reprints of this information are available from the Editors or from: Elsevier Editorial Services Ltd., Mayfield House, 256 Banbury Road, Oxford OX2 7DE (Great Britain).

Reprints. Fifty reprints will be supplied free of charge. Additional reprints (minimum 100) can be ordered. An order form containing price quotations will be sent to the authors together with the proofs of their article.

Advertisements. Advertisement rates are available from the publisher.

Subscriptions. Subscriptions should be sent to : Elsevier Scientific Publishing Company, P.O. Box 211, 1000 AE, Amsterdam, The Netherlands. The section on *Computer Techniques and Optimization* can be subscribed to separately.

Publication. *Analytica Chimica Acta* (including the section on *Computer Techniques and Optimization*) appears in 8 volumes in 1978. The subscription for 1978 (Vols. 96–103) is Dfl. 1000.00 plus Dfl. 120.00 (postage) (Total approx. US $486.96). The subscription for the *Computer Techniques and Optimization* sections only (Vol. 103) is Dfl. 125 plus Dfl. 15.00 (postage) (Total approx. US $60.87). Journals are sent automatically by air mail to the U.S.A. and Canada at no extra cost and to Japan, Australia and New Zealand for a small additional postal charge. All earlier volumes (Vols. 1–87) are available at Dfl. 115.00 (plus postage).

Claims for issues not received should be made within three months of publication of the issue, otherwise they cannot be honoured free of charge.

Customers in the U.S.A. and Canada who wish to obtain additional bibliographic information on this and other Elsevier journals should contact our Journal Information Center, 52, Vanderbilt Avenue, New York, NY 10017. Tel: (212) 867-9040.

Analytica Chimica Acta, 98 (1978) 193—203

A DETAILED STUDY OF SAMPLE INJECTION INTO FLOWING STREAMS WITH POTENTIOMETRIC DETECTION

Zs. FEHÉR and G. NAGY

EGYT Pharmacochemical Works, Budapest (Hungary)

K. TÓTH and E. PUNGOR*

Institute for General and Analytical Chemistry, Technical University of Budapest, 1502-Budapest (Hungary)

(Received 4th October 1977)

SUMMARY

A new method developed by combining manual or coulometric injection into flowing streams and potentiometric detection is described. The potential—time curves obtained in a flow-through detector as a result of single injections are handled theoretically and examined practically. The effects of experimental parameters, concentrations and flow rates on the signal are discussed. A systematic survey of the potential use of the technique in analysis is given. Species can be determined easily either in the flowing stream or in the injected sample. Some applications in pharmaceutical and other types of analysis are listed, and the main advantages of the technique are summarized.

In 1969, a new injection or spike technique for the analysis of flowing streams was developed in combination with a voltammetric flow-through detector cell. The principle of the method, the basic relationships between the signal obtained and the experimental parameters, and the application of the technique for serial analysis of samples in small volumes have been reported [1]. In solving different analytical problems the technique proved to be excellent, and it was further developed to broaden its applicability [2]. Long-term experience suggests that this technique is suitable for the determination of any component which can be detected by direct voltammetry or determined by classical amperometric titration.

Parallel to this work, other detector systems, e.g. potentiometric and spectrophotometric systems, have also been employed in solving analytical problems by means of the injection technique [3—5]. A survey of all the work done in this area — including the rather different systems proposed by Růžička et al. [6—10] — indicate that injection into flowing streams provides not only a very fast way of analysing individual samples, but one which can be easily automated. A well-designed apparatus operating on this principle can handle many more samples within a certain period of time than any other commercially available type, even considering the

Technicon AutoAnalyzers. This is so, because the methods do not generally require a long time to achieve steady-state signals.

The present paper reports some recent research concerning the injection technique. Further theoretical considerations, developments in the apparatus and in the technique of reagent addition, important improvements in the detection system, and new applications are discussed.

EXPERIMENTAL

Apparatus

Two different flowing systems were constructed and supplied with appropriate measuring instruments depending on the mode of injection.

Manual injection system

Figure 1 shows the experimental set-up constructed for volumetric injection. The flowing solution, of appropriate ionic strength and pH, is pumped from a reservoir (1) at a constant flow rate with a LKB Varioperpex 12000 peristaltic pump (2). The sample or the reagent solution to be injected is forced into the stream with a precision syringe (Hamilton 700) or with the help of a specially designed injector [11] at point (3). A flow-through mixing chamber (4) with a magnetic stirrer is placed between the point of injection and the detector cell (5). The flow-through detector cell is supplied with an ion-selective (Pungor-type) indicating electrode and a reference electrode.

The indicating electrodes were prepared in this laboratory in a form with a smaller active area (2—5 mm diameter) than the commercially available electrodes. For different problems, Ag^+, I^-, Cl^-, Br^-, CN^- and NH_4^+-sensitive electrodes were used. For the urea measurements, an ammonium-selective electrode based on a neutral carrier in a silicone-rubber matrix was converted to a urea enzyme electrode by placing a thin polyacrylamide gel layer containing urease [12] on the measuring surface. The glucose enzyme electrode was prepared from an iodide-selective electrode with a liquid reaction layer containing glucose oxidase and peroxidase enzymes (for more details see [13]

The flow-through arrangement shown in Fig. 1 can be used more advantageously than flow-through caps [14, 15] for the analysis of streaming

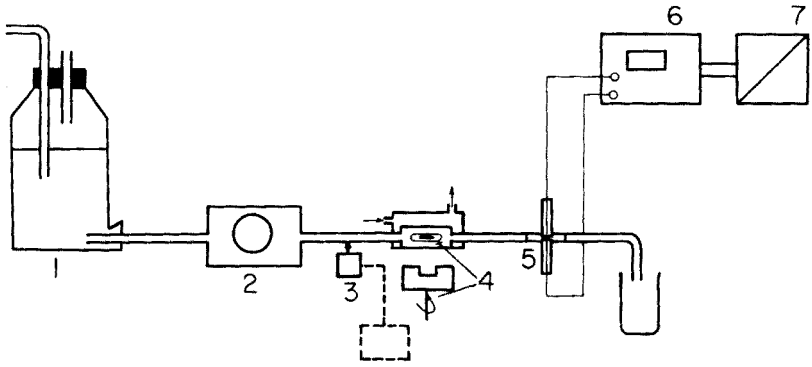

Fig. 1. Experimental set-up for measurements with volumetric injection. (Symbols are given in the text.)

solutions. With the flow-through cap — especially in the low concentration ranges — the electrode potential is affected greatly by oscillations in the flow rate, because the streaming potential contributes significantly to the total voltage measured.

The e.m.f. was measured with a differential electrometer (6; Keithley type 604) and recorded with an X-Y recorder (7; Bryans 201/A).

Coulometric injection system

Figure 2 shows the apparatus with which the injection was accomplished by coulometric generation in situ. The solution from the reservoir (1) is pumped (2) to the generating cell (3) which consists of two compartments separated with a dialysis membrane (4). The flow-through compartment of the generating cell contains the solid-state injector electrode (5) while the other compartment contains the counter electrode (6). The arrangement of the generating cell avoids mixing of the products of the electrode reactions because the flowing stream carries the products away from the electrodes.

The flow-through compartment also serves as a mixing chamber. The drip vessel (7) separates electrically the generating and the indicating units. For the coulometric generation, a potentiostat (8); Tacussel ASA 100-1) operating as a current generator is programmed externally with a function generator (9; Philips, type PM 5168). From the drip vessel, the solution flows through the detector cell which incorporates the appropriate sensors and measuring apparatus discussed above, i.e. a microcapillary-type ion-selective electrode (10), reference electrode (11), millivolt meter (12) and recorder (13).

Chemicals

All chemicals used were of analytical grade. The injector silver electrode was 99.999% pure silver (diameter, 4 mm).

Urease (E.C. 3.5.1.5.; Merck) was obtained as a lyophilized preparation

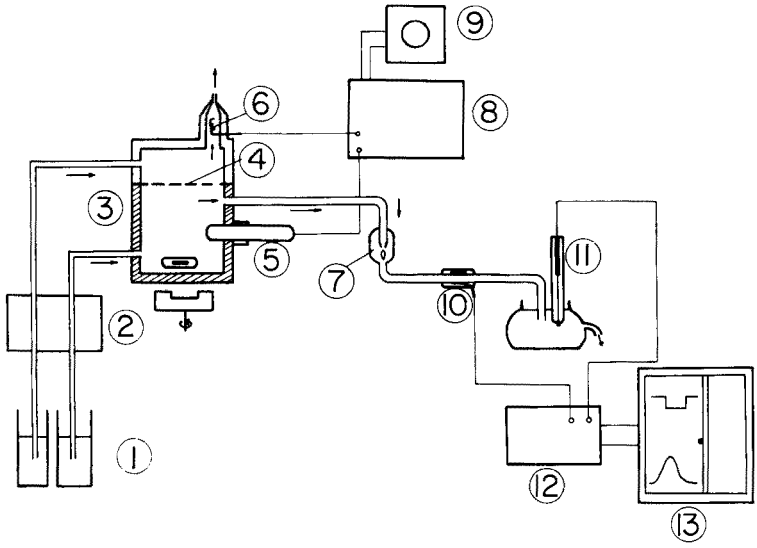

Fig. 2. Experimental set-up for measurements with coulometric injection. (Symbols are given in the text.)

with a declared activity of 5 U mg^{-1}. The glucose oxidase (E.C. 1.1.3.4) and horseradish peroxidase (E.C. 1.11.1.7.) used were obtained (Sigma Chemicals) with declared activities of 15 EU mg^{-1} and 100 purpurogallin units mg^{-1}, respectively.

Procedures

Measurements are carried out as follows. The solution from the reservoir or from the sample holder flows at a defined constant rate through the system while the base line is recorded. The volumetric or coulometric injection is started only after a stable base line has been achieved. Obviously, when potentiometric detection is used, stable base lines are obtained only if an appropriate species is present at a constant concentration which gives a steady electrode response. The potential changes arising from injections are recorded as peak signals.

To provide trouble-free detection, the flowing solution must contain a component to adjust the ionic strength (e.g. KNO_3) and the electroactive species at constant ionic activity to give a steady electrode potential. Moreover, if any reagent injection is to be done coulometrically, then the conditions suitable for coulometric generation must be provided, i.e. low resistance, appropriate pH, etc.

The values obtained experimentally for peak potential changes (ΔE_τ) were compared to those expected theoretically. For calculation of the theoretical data, several experimental parameters had to be measured. The actual measurements were carried out as follows.

The time duration of the coulometric injection was easily controlled by an electric switch in the coulometric generating circuit and by an appropriate timer. The flow rate of the streaming solution was periodically checked and measured volumetrically. The volume of the mixing chamber was established by filling it with distilled water from a precision syringe. The slope of the calibration graph of the ion-selective electrode used was determined by calibrating the electrode in flow-through conditions with standard solutions flowing through the detector cell. The slopes are the same under flowing conditions or static conditions. In the calculations the Faraday number was taken as 96 500.

THEORETICAL CONSIDERATIONS

The model introduced earlier was based on equations which described the concentration–time profile in the system after an injection [1]. To obtain these equations, it was assumed that: (a) the rate of injection is constant, i.e. a concentration gradient is not formed in the direction of flow inside a plug of the solution containing the material injected; and (b) the mixing of the solution in the stirrer is instantaneous and complete.

Accordingly, if $0 \leqslant t < \tau$, the concentration distribution is given by

$$\Delta c_t = (M/V\tau)\,(1 - e^{-\frac{V}{W}t}) \qquad (1)$$

whereas if $t \geqslant \tau$, the concentration distribution is given by

$$\Delta c_t = (M/V\tau)\,(1 - e^{-\frac{V}{W}\tau})\, e^{-\frac{V}{W}(t-\tau)} \qquad (2)$$

where V is the flow rate, W is the volume of the mixing chamber, and τ is the time required by the solution "plug" (containing the injected material) to pass the entrance section of the mixing chamber. If tailing is ignored, then τ is equal to the time of injection.

The validity of the model was readily confirmed for voltammetric detection.

If another assumption is introduced — namely, that no differentiation is made between differences in concentration and activity ($\Delta a = \Delta c$) — then eqns. (1) and (2) can be converted to "theoretical" potential—time equations by means of the signal transformation equation valid for potentiometric sensors

$$\Delta E_t = S \ln \left[1 + \Delta c_t / (c_0 + \sum_{i=0}^{n} K_i c_i)\right] \qquad (3)$$

where S is the slope of the electrode calibration graph; c_i is the concentration of the interfering ion; c_0 is the concentration of the flowing solution; and K_i is the selectivity coefficient.

Figure 3 shows a comparison between the theoretical and experimental electrode potential—time curves. The theoretical curves (thick lines) were calculated from eqn. (3) for the experimental parameters valid for the set-up used and for the conditions used in obtaining the experimental curves (thin lines). The agreement between the theoretical and experimental results provides excellent confirmation of the validity of the model used. However, in extreme conditions, e.g. with very long injection times or with long distances between the point of injection and detection — distortions are observed.

From the analytical point of view, it must be noted that the electrode potential difference is a signal basically dependent on two concentrations, i.e. the concentrations of the flowing and injected solutions. Accordingly, either of these concentrations can be determined. If the peak height is the signal utilized, then it can easily be given in an explicit form:

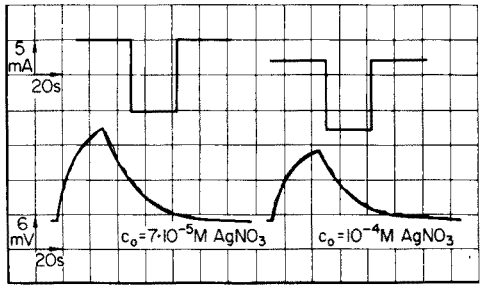

Fig. 3. Comparison of theoretical (——) and experimental (——) $\Delta E_t - t$ curves obtained after injection. Flowing solution, 10^{-4} M $AgNO_3$—10^{-1} M KNO_3. Silver-selective indicator electrode with saturated calomel reference electrode.

$$\Delta E_\tau = S\left[1 + \frac{(M/V\tau)\,(1 - e^{-\frac{V}{W}\tau})}{c_0 + \sum_{i=0}^{n} K_i\, c_i}\right] \qquad (4)$$

The time integral of eqn. (3), which would correspond to the area under the peak, has not yet been successfully solved and therefore cannot be expressed exactly.

RESULTS AND DISCUSSION

Before the injection technique was used with potentiometric detection for analytical purposes, the effect of different parameters on the peak height and peak area had to be studied. The most important relationships are those existing between the concentration of the flowing solution and the signal, and between the amount injected and the signal.

Figure 4 shows the relationships between the peak height or peak area and the amount of silver ion injected coulometrically. The dependence of the peak height on the amount of silver ion (Fig. 4A) injected corresponds very closely to the theoretically expected relation (eqn. 4). The dependence of peak area on the amount of silver ion injected (Fig. 4B) is also well defined and readily applicable in practice. Accordingly, the injection technique

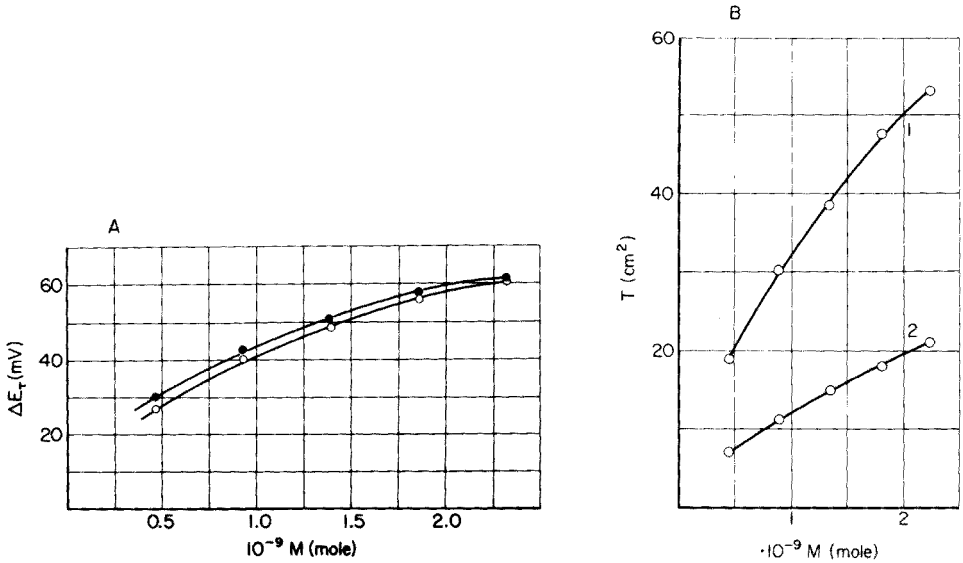

Fig. 4. The relationship between peak height or peak area and the amount coulometrically injected. (Flowing solution (c_0) 10^{-4} M $AgNO_3$—10^{-1} M KNO_3. Time of coulometric generation, 5, 10, 15, 20 and 25 s. Silver-selective indicator electrode. $W = 1.6 \times 10^3$ l). (A) Peak height dependence for $V = 2.5 \times 10^{-5}$ l s^{-1} and $i = 9.6 \times 10^{-3}$ A; (○) calculated; (●) measured. (B) Peak area dependence for $i = 9 \times 10^{-3}$ A; curve (1) for $V = 4 \times 10^{-5}$ l s^{-1}; curve (2) for $V = 6 \times 10^{-5}$ l s^{-1}.

with potentiometric detection is appropriate for the analysis of individual samples of small volume in the same way as has been reported for voltammetric detection. The average standard deviation of the measurements is about 1.5% whether the injection is done volumetrically with a syringe, or coulometrically.

As expected from eqns. (3) and (4), and in contrast to the situation with voltammetric detectors, the peak height and peak area are dependent not only on the amount of analyte injected but also on the concentration of the appropriate ion which is originally present in the flowing solution. It is therefore possible to determine the concentration of an appropriate ion in the flowing stream. Figure 5 shows a calibration curve of this type obtained by injecting the same species (cyanide) in the same amount into flowing solutions with different cyanide concentrations. Qualitatively, the effect can easily be understood by considering the nature of the potentiometric detection. Since the real relationship between the electrode potential and concentration is exponential, the same change in concentration will result in different changes in potential depending on the initial concentration level of the analyte concerned.

It is clear that the combination of the injection technique with potentiometric detection offers new and very interesting possibilities for the analysis of flowing solutions. In addition to the simple means of analysing discrete samples of small volume without chemical reactions, the general technique makes it easy to achieve a periodically operating automatic method for the analysis of flowing streams by injection of standards of the same nature.

When this method is applied, there are two ways of determining the concentration of streaming solutions.

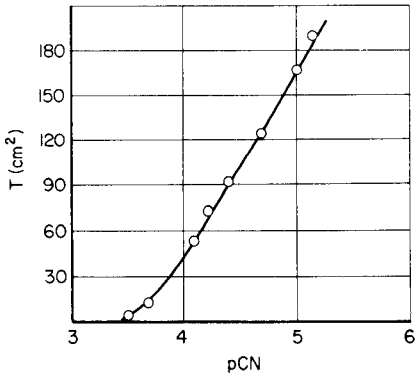

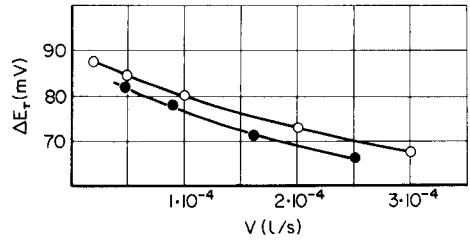

Fig. 5. The dependence of the area under the peak on the concentration of cyanide in the flowing stream when the same amount of cyanide (5×10^{-7} mol) is injected. A cyanide-selective indicator electrode is used.

Fig. 6. The dependence of the peak height on flow rate (V) of the solution. Flowing solution, 10^{-4} M $AgNO_3$—10^{-1} M KNO_3. Amount injected, 6.75×10^{-8} mol Ag^+. $W = 2.1 \times 10^{-3}$ l. Silver-selective indicator electrode. (○) Calculated; (●) measured.

One method depends on a calibration curve (e.g., Fig. 5), and the other is a matter of direct calculation. The concentration of the flowing solution can be calculated from eqn. (4), if the concentration profile is known. Probably the best accuracy is obtained if the peak height is used for the calculations. The calculation of the appropriate value of the slope, S, should also be made from the peak height values of the recording; for this purpose at least two different standard injections are necessary.

The flow rate (V) of the flowing solution might be expected to affect not only the shape of the peak obtained after an injection, but also the speed of analysis. To study this effect, a wide range of flow rates was applied, and the same amounts of material were injected into the flowing solution of constant concentration. As expected from eqn. (4), the peak heights showed only slight changes despite considerable changes in flow rate (Fig. 6). Figure 6 also shows a comparison of the experimental and calculated values of ΔE_τ; the latter were obtained by applying eqn. (4) with the actual experimental parameters.

Figure 7 shows the linear dependence of the area under the peak on the $1/V$ values. Since the peak height is only slightly influenced by the flow rate in the ranges studied, all the increase in peak area is due to peak broadening. Thus, the faster the flow, the shorter the time of an analysis.

Since it is quite difficult to keep the flow rate of a solution constant with very high precision, it must be concluded that the curves should be evaluated on a peak-height basis rather than on a peak-area basis. There is, therefore, no need to employ an integrator which would make the instrumentation more sophisticated and costly.

Figure 8 illustrates the relationship between the potentiometric signal and the duration of injection. The peak height as well as the peak area seem to be independent of the time duration of injection over the period 3—20 s if the amount injected is kept constant. The experimental values of ΔE_τ show an acceptable agreement with the calculated values.

The relationship between the peak heights recorded and the volume of the mixing chamber was also investigated. Figure 9 shows that the calculated peak heights are in good agreement with the experimental values.

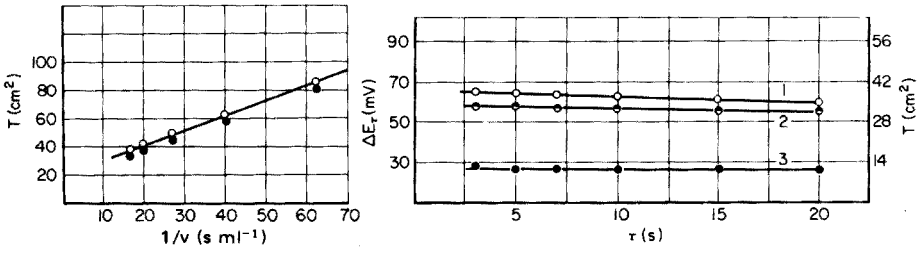

Fig. 7. The relationship between the peak area and the reciprocal value of the flow rate. Conditions as for Fig. 6. (○) Experiment 1; (●) experiment 2.

Fig. 8. The dependence of the peak area and peak height on the time of injection when the same amounts are injected into the flow streams. $i\tau$ = constant. V = 0.06 ml s^{-1}. (1) Calculated ΔE_τ; (2) measured ΔE_τ; (3) measured T.

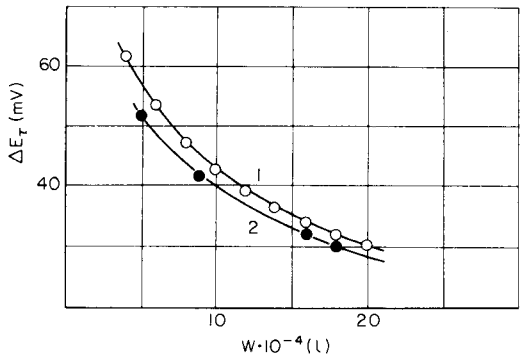

Fig. 9. Comparison of the calculated and measured peak heights obtained with mixing chambers of different volumes. $i = 9 \times 10^{-3}$ A. $\tau = 5$ s. $V = 2 \times 10^{-5}$ l s^{-1}. (1) Calculated; (2) measured.

The agreement between these calculated and measured values shows that the equation derived on the assumptions mentioned above is appropriate for describing the experimentally obtained data. The measured ΔE_τ values are always smaller than the calculated values, but the difference of a few millivolts can easily be explained. During the time of the relatively sharp transient concentration change, there must be differences between the ion activity in the bulk solution streaming through a certain cross-section and the activity of the solution which is actually in contact with the surface of an electrode placed in the same position.

There is no doubt that species other than the species originally present in the flowing stream can be injected, in carrying out determinations by this technique. If a chemical reaction is employed between the flowing and injected solutions, a great variety of possibilities is opened. For example, during the course of a reaction, the species giving the electrode response can be consumed, so that after an injection a "negative" peak appears. Both peak area and peak height can be utilized to determine either the amount injected or the concentration of the flowing solution. If the peaks recorded are negative, evaluation can be done in exactly the same manner as described earlier for positive peaks, i.e. either calibration or direct calculation is possible. Essentially, the latter can be considered as a standard-subtraction method.

Analyses can also be based on the formation of an electroactive component in the chemical reaction between the sample solution and a reagent. An illustration of methods based on this principle is provided by the determination of urease enzyme activity worked out in this laboratory. Here, the urea substrate solution is the flowing solution and urease samples of unknown activity are injected; an ammonium-sensitive, neutral-carrier electrode [16] is incorporated in the system as the detector, and the activity of ammonium ions produced in the enzyme reaction is followed.

Similarly, the concentration in a flow stream of a species which does not give an electrode response can be determined by injecting an appropriate

TABLE 1

A survey of applications of the injection technique with potentiometric detection

Flowing solution	Solution injected	Application	Detector
Components determined in the injected solution			
KI + KNO_3	I^-	I^- in pharmaceuticals	I^-
KI + KNO_3	I^- + Cl^-	I^- in Cl^-	I^-
KI + KNO_3	CN^-	CN^- samples	CN^-
KCl + KNO_3	Chlorpromazine HCl Diethazine HCl Melipramine HCl	Cl^- in pharmaceuticals	Cl^-
KBr + KNO_3	Gastrixone Methylhomatropinium bromide	Br^- in pharmaceuticals	Br^-
Tris (pH 7.0)	Urea	Urea samples	Urea electrode
Tris + urea	Urease	Urease activity	NH_4^+
Thiocholine ester	Cholinesterase	Cholinesterase activity	S^{2-}
I^- + buffer	Glucose	Glucose samples	Glucose enzyme electrode [13]
Cl^- + KNO_3	Cl^-	Cl^- content of drinking water	Cl^-
Components determined in the flowing stream			
CN^- + KNO_3	CN^-	CN^- content of sewages	CN^-
CN^- + KNO_3	Ag^+	CN^- content of sewages	CN^-, Ag^+
S^{2-} + NaOH	Ag^+	S^{2-} content in samples	S^{2-}
S^{2-} + NaOH	Hg^{2+}	S^{2-} content in samples	S^{2-}
Aqueous solutions	Acid or base	Buffer capacity	pH (glass)

reagent. In this case, the flowing solution must contain some component to ensure a stable base-line. After reagent injection, a positive peak then appears. If the reagent itself gives the electrode response, then the determination must be based on a reaction which consumes reagent; as the concentration of the flowing sample increases, the signals (peaks) will decrease. If a product of the chemical reaction is the electroactive species — and neither the sample nor the reagent gives an electrode response — then the higher the sample concentration, the greater the signal recorded.

This injection technique with potentiometric detection has now been applied in solving quite a number of different current analytical problems. An overview of the applications is given in Table 1. The principles of the individual methods listed should be clear from the above discussion. It must be emphasized that these examples cover only some of the possibilities. The examples presented prove the wide range of applicability of the injection technique. The range covers important fields such as environmental analysis [17], pharmaceutical product control, clinical analysis, etc.

Conclusions

In conclusion, the main advantages of the injection technique are that it is easily automated, and that it is suitable not only for the analysis of small volumes of relatively concentrated samples, but also for the analysis of streaming solutions by the standard addition technique; the high precision of coulometric reagent generation ensures the reliability of the standard or reagent addition. The technique is suitable for the analysis of samples which can cause electrode poisoning, e.g. cyanide. If a chemical reaction is employed, samples of low concentrations can be analysed. Finally, the technique is very useful for calibration in flowing streams, and simplifies checking the slope of the electrode response. This feature may be of the greatest analytical value when enzyme electrodes are used as detectors.

REFERENCES

1 G. Nagy, Zs. Fehér and E. Pungor, Anal. Chim. Acta, 52 (1970) 47.
2 Zs. Fehér and E. Pungor, Anal. Chim. Acta, 71 (1974) 425.
3 E. Pungor and K. Tóth, Vom Wasser, 42 (1974) 43.
4 E. Pungor, K. Tóth and G. Nagy, in M. Kessler (Ed.), Ion and Enzyme Electrodes in Biology and Medicine, Urban und Schwarzenberg, München, 1976.
5 E. Pungor, K. Tóth and G. Nagy, Hung. Sci. Instrum., 35 (1975) 1.
6 J. Růžička and E. H. Hansen, Anal. Chim. Acta, 78 (1975) 45; 87 (1976) 353.
7 J. Růžička and J. W. B. Stewart, Anal. Chim. Acta, 79 (1975) 79; 82 (1976) 137.
8 J. W. B. Stewart, J. Růžička, H. Bergamin-Filho and E. A. Zagatto, Anal. Chim. Acta, 81 (1976) 371.
9 J. Růžička, J. W. B. Stewart and E. A. Zagatto, Anal. Chim. Acta, 81 (1976) 387.
10 J. Růžička, E. H. Hansen and E. A. Zagatto, Anal. Chim. Acta, 88 (1977) 1.
11 Zs. Fehér, G. Nagy, E. Lindner, K. Tóth and E. Pungor, in preparation.
12 G. G. Guilbault, G. Nagy and S. S. Kuan, Anal. Chim. Acta, 67 (1973) 195.
13 G. Nagy, L. W. von Storp and G. G. Guilbault, Anal. Chim. Acta, 6 (1973) 443.
14 R. A. Llenado and G. A. Rechnitz, Anal. Chem., 45 (1973) 2165.
15 J. Mertens, P. Van der Winkel and D. L. Massart, Anal. Chem., 48 (1976) 272.
16 G. G. Guilbault and G. Nagy, Anal. Chem., 45 (1973) 417.
17 K. Tóth, G. Nagy, Zs. Fehér and E. Pungor, Z. Anal. Chem., 282 (1976) 379.

Analytica Chimica Acta, 98 (1978) 205—214

POLAROGRAPHIC DETERMINATION OF HYDROXYLAMINES: APPLICATION TO ANALYSIS OF PHOTOGRAPHIC PROCESSING SOLUTIONS

D. R. CANTERFORD

Research Laboratories, Kodak (Australasia) Pty. Ltd., P.O. Box 90, Coburg, 3058, Victoria (Australia)

(Received 23rd January 1978)

SUMMARY

Procedures for the determination of hydroxylamine and *N,N*-diethylhydroxylamine (DEHA), based on anodic polarographic waves, are described. The importance of using a strongly alkaline supporting electrolyte and of complete removal of dissolved oxygen is illustrated. With rapid alternating current (a.c.) polarography, 3×10^{-6} M hydroxylamine and 4×10^{-5} M DEHA can be detected. Detection limits with the differential pulse technique are approximately tenfold lower. In a practical application, rapid a.c. polarography is shown to be suitable for the direct determination of hydroxylamine and DEHA in photographic processing solutions. The only pretreatment of samples is dilution with a strongly alkaline supporting electrolyte. Possible interferences from other constituents of the processing solutions are avoided by using the standard addition method.

In a recent review [1] of the determination of hydroxylamine, the importance of quantitative methods in studies of biological processes and for industrial purposes was emphasized. Hydroxylamine and some of its derivatives are weak developing agents in alkaline solution [2] and are often constituents of photographic processing solutions. Published procedures for the determination of hydroxylamine in such solutions include spectrophotometric [3] and titrimetric [4] methods.

Hydroxylamine can be determined by a variety of electrochemical methods which utilize its oxidizing and reducing properties [1]; these include coulometry, polarography, potentiometry and chronopotentiometry. Iversen and Lund [5, 6] have shown that hydroxylamine and a number of *N*-substituted derivatives give anodic direct current (d.c.) polarographic waves in alkaline solution. These authors restricted their investigation to the rather narrow concentration range of 10^{-4}—10^{-2} M. In a recent article on the application of alternating current (a.c.) polarography to analysis of photographic processing solutions [7], the anodic wave of *N,N*-diethylhydroxylamine (DEHA) was used to illustrate the advantage of the a.c. technique, with its peak form of readout, for a wave occurring close to the anodic limit of the mercury electrode. Procedures for the determination of hydroxylamine and DEHA by rapid a.c.

and differential pulse polarography are now described in detail. This work was carried out in order to establish methods for the direct determination of these species in photographic processing solutions. The principal reason for using the rapid (short controlled drop-time) method was to enable fast scan rates of potential to be used.

EXPERIMENTAL

Apparatus

A.c. and d.c. polarograms were obtained with a Metrohm Polarecord E 261 used in conjunction with a Metrohm AC Modulator E 393. An applied alternating voltage of 10 mV (rms) at 50 Hz was used for a.c. polarography. Short controlled drop times were obtained with a Metrohm Drop Controller E 354S (0.16 s) and a Princeton Applied Research (PAR) Model 174/70 Drop Timer (0.25 s). Differential pulse polarograms were obtained with a PAR Model 174A Polarographic Analyzer and recorded with a Hewlett-Packard Model 7040A-383 X-Y Recorder. Currents have been corrected for the tenfold gain in output which is present when the PAR 174A is operated in the differential pulse mode.

All potentials reported are relative to a silver—silver chloride (sat. KCl) reference electrode. A tungsten wire auxiliary electrode was used. The reference electrode was separated from the test solution by a salt bridge containing 1 M KNO_3. This solution was replaced daily. A water-jacketed cell was used, with all results being obtained at 25.0°C.

Chemicals

Stock solutions of hydroxylamine were prepared from hydroxylammonium chloride (Baker Analyzed Reagent) or hydroxylammonium sulfate (Eastman). Eastman *N,N*-diethylhydroxylamine was used. Supporting electrolyte solutions were prepared from reagent-grade chemicals. Chemicals used for preparing photographic processing solutions were of normal photographic quality.

Procedures

To construct calibration curves, and when analyzing samples by the addition method, small aliquots of a concentrated stock solution were added by microsyringe to a known volume of sample in the polarographic cell. Oxygen-free nitrogen, obtained by scrubbing with vanadium(II) chloride solution, was passed over the surface of the test solution while polarographic measurements were being made.

RESULTS AND DISCUSSION

Before the optimum conditions for the determination of hydroxylamines are described, the necessity for complete removal of dissolved oxygen will be

illustrated. Iversen and Lund [5] reported that in the presence of oxygen, hydroxylamines gave irreproducible anodic double-waves which could not be removed by flushing with nitrogen. They offered no explanation as to the origin of the double-wave.

Figure 1 shows d.c. and corresponding a.c. polarograms for (a) reduction of oxygen in air-saturated 0.1 M NaOH and (b) oxidation of 4×10^{-4} M hydroxylamine in oxygen-free 0.1 M NaOH (oxygen was removed with nitrogen before hydroxylamine was added from a microsyringe). In the latter case, a single well-defined wave was observed. However, when 4×10^{-4} M hydroxylamine was added to air-saturated 0.1 M NaOH, two anodic waves similar to those reported by Iversen and Lund [5] were recorded (Fig 1c). Flushing with nitrogen did not remove the second wave at −0.14 V. This wave, which occurs at the same potential as the oxygen reduction wave (Fig. 1a), is undoubtedly due to hydrogen peroxide, which is one of the products of aerial oxidation of hydroxylamine [8, 9]. The first wave at −0.26 V is due to residual hydroxylamine. Similar observations were recorded with DEHA. (From Fig. 1c it appears that polarography, particularly the a.c. technique, may provide a simple method of monitoring aerial oxidation of hydroxylamines and the consequent build-up of hydrogen peroxide.)

Incorporation of sulfite in the supporting electrolyte, as suggested by Iversen and Lund [5], is probably the most convenient and rapid method of removing dissolved oxygen.

Rapid a.c. polarography

Hydroxylamine and DEHA both gave well-defined rapid a.c. polarograms in strongly alkaline supporting electrolytes. The peak potential for both species shifted to more negative potentials with increasing NaOH concentration. Rao and Meites [10] reported a similar shift for the d.c. half-wave potential of hydroxylamine.

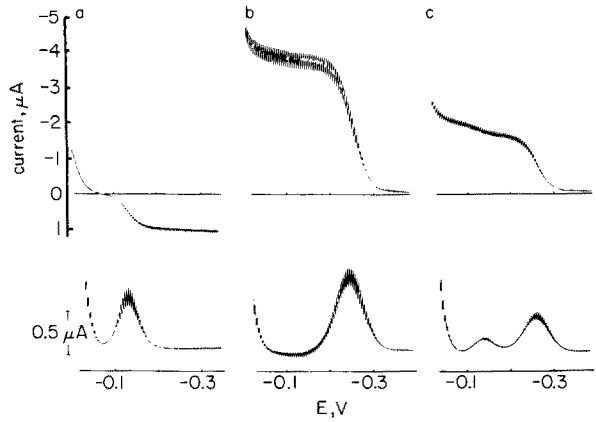

Fig. 1. Rapid d.c. and a.c. polarograms of (a) air-saturated 0.1 M NaOH, (b) 4×10^{-4} M hydroxylamine in oxygen-free 0.1 M NaOH, and (c) 4×10^{-4} M hydroxylamine in air-saturated 0.1 M NaOH. Drop time = 0.25 s.

For a given supporting electrolyte, the DEHA peak occurred at a more positive potential than the hydroxylamine peak. This is in contrast to a number of *N*-monoalkylhydroxylamines and *N,N*-dibenzylhydroxylamine studied by Iversen and Lund [5, 6], all of which had d.c. half-wave potentials more negative than that of hydroxylamine. Thus the choice of supporting electrolyte is more critical for DEHA than for the other hydroxylamines since it occurs closer to the anodic limit of the mercury electrode.

Iversen and Lund [5, 6] used a supporting electrolyte consisting of 0.16 M KOH—0.16 M Na_2SO_3. It is clear from Fig. 2 that this is not the optimum supporting electrolyte for determination of low DEHA concentrations. In 1.5 M NaOH—0.1 M Na_2SO_3 (Fig. 2b) not only is the DEHA peak at a more negative potential but the anodic limit is shifted to a more positive potential because of the lower sulfite concentration. Thus the DEHA peak is much better resolved from the background in the latter supporting electrolyte.

Figure 2 also illustrates clearly why the a.c. technique is preferred. Even in 1.5 M NaOH—0.1 M Na_2SO_3 it would be difficult to measure the d.c. limiting current accurately for 2×10^{-4} M DEHA.

The detection limit of a technique can be defined as the smallest quantity or concentration of a substance that can be detected at a chosen probability level [11]. As previously illustrated [12], it is difficult to apply this definition to the rapid polarographic method where the background is smooth and thus the limiting factor is the double-layer charging current rather than instrumental "noise". In such cases, the detection limit can be qualitatively estimated by gradually increasing the concentration of the electroactive species until a definite wave is observed by comparison with the background polarogram. When this procedure was used, 3×10^{-6} M hydroxylamine and 4×10^{-5} M DEHA could be detected with the rapid a.c. technique. (Calibration curves and reproducibility data are discussed in a later section illustrating practical

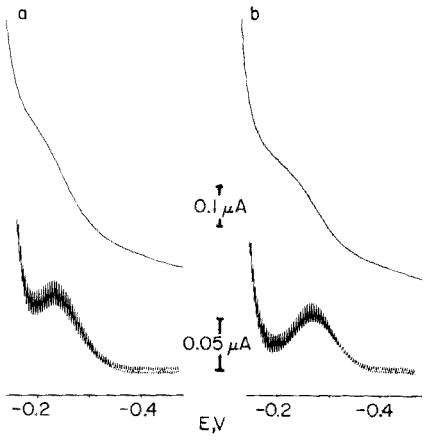

Fig. 2. Rapid d.c. and a.c. polarograms of 2×10^{-4} M DEHA in (a) 0.16 M KOH—0.16 M Na_2SO_3 and (b) 1.5 M NaOH—0.1 M Na_2SO_3. Drop time = 0.25 s.

applications of the method.) Because of the fast scan rate of potential with the rapid method a complete polarogram can be recorded in less than 30 s.

Differential pulse polarography

The feasibility of using the differential pulse technique for the determination of lower hydroxylamine and DEHA concentrations was investigated. Both compounds gave well-defined differential pulse peaks in 1.5 M NaOH—0.1 M Na_2SO_3. The effect of pulse amplitude was examined in order to establish the optimum conditions for determination of low concentrations. Figure 3 shows the dependence of peak current on pulse amplitude. The plot for hydroxylamine shows the expected behavior [13] of linearity at low pulse amplitudes with some departure from linearity at high amplitudes. For DEHA the plot was also linear at low amplitudes. However, increasing the amplitude from 50 to 100 mV did not result in a further increase in peak current. This was due to the closeness of the DEHA peak to the anodic limit and the fact that differential pulse peaks usually become broader with increasing amplitude. Indeed, as illustrated in Fig. 4, a distinct peak was not observed for 1×10^{-5} M DEHA when the pulse amplitude was 100 mV. Figure 4 also illustrates the empirical method used to measure peak current (i_p).

Table 1 gives the dependence of peak potential and peak half-width on pulse amplitude. As expected for an anodic process [14], both peaks shifted

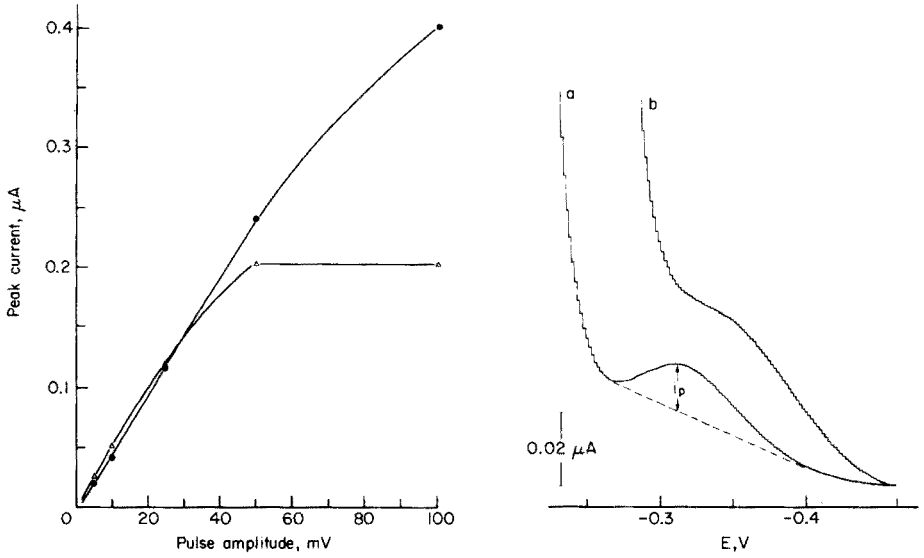

Fig. 3. Dependence of differential pulse peak current on pulse amplitude for (•) 1.2×10^{-5} M hydroxylamine and (△) 1×10^{-4} M DEHA in 1.5 M NaOH—0.1 M Na_2SO_3. Drop time = 2 s.

Fig. 4. Effect of pulse amplitude on differential pulse polarogram of 1×10^{-5} M DEHA in 1.5 M NaOH—0.1 M Na_2SO_3. Pulse amplitude: (a) 50; (b) 100 mV. Drop time = 2 s.

TABLE 1

Dependence of peak potential (E_p) and peak half-width ($W_{1/2}$) on pulse amplitude (ΔE) for 1×10^{-4} M hydroxylamine (HA) or DEHA in 1.5 M NaOH—0.1 M Na_2SO_3

ΔE (mV)	E_p (HA) (V)	$W_{1/2}$ (HA) (mV)	E_p (DEHA) (V)
5	−0.320	70	−0.265
10	−0.325	71	−0.269
25	−0.332	71	−0.275
50	−0.345	75	−0.290
100	−0.365	100	−0.310

to more negative potentials with increasing pulse amplitude. Although the hydroxylamine peak became broader with increasing pulse amplitude, the broadening was only slight for amplitudes up to 50 mV. Because of the highly asymmetrical shape of the DEHA peak a meaningful half-width could not be measured for this species. These results indicate that 50 mV is probably the optimum pulse amplitude for determination of hydroxylamines.

With a pulse amplitude of 50 mV and a drop time of 2 s, 2×10^{-7} M hydroxylamine and 5×10^{-6} M DEHA could be detected. Calibration curves, although linear, did not pass through the origin (Fig. 5).

Loss of hydroxylamine either by oxidation or some other process such as adsorption on the walls of the cell, was a problem at very low hydroxylamine concentrations. For example, the peak current for 8×10^{-7} M hydroxylamine decreased by 50% in 4.5 min. It was thus essential to record the differential pulse polarogram as soon as possible after introducing the hydroxylamine

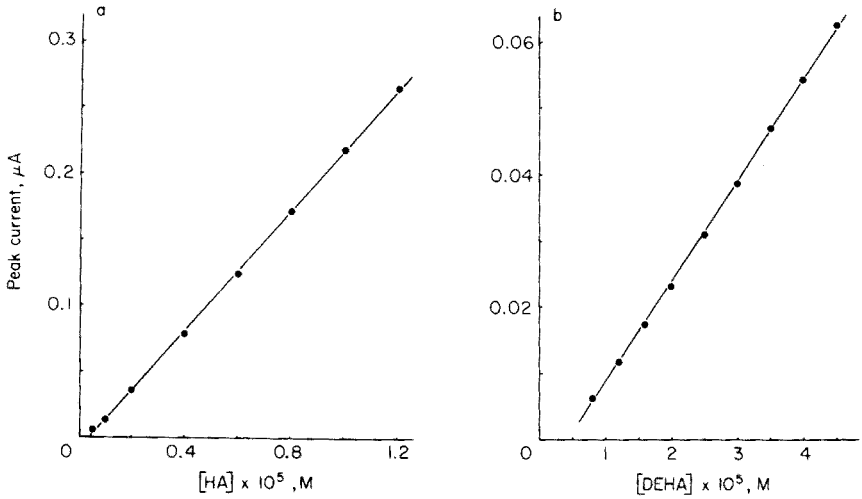

Fig. 5. Differential pulse calibration curves for (a) hydroxylamine and (b) DEHA in 1.5 M NaOH—0.1 M Na_2SO_3. Pulse amplitude = 50 mV. Drop time = 2 s.

stock solution by microsyringe. Because of the slow response of the PAR 174A when used in the differential pulse mode (this is due to the long time constant of the memory circuit), there was inevitably a significant delay between introducing the sample and beginning the polarographic scan. This time could be reduced by using a shorter drop time, although this would also decrease the sensitivity of the method.

Application to analysis of photographic processing solutions

Photographic processing solutions, because of their complex chemical composition, often present difficult analytical problems. Many existing methods require complicated separation procedures before a constituent can be determined [15]. Apart from being time-consuming, these separation steps may create health hazards and waste disposal problems because of the organic solvents used. Thus there is considerable incentive to develop more rapid and direct methods which avoid extraction procedures.

It has been established that rapid a.c. polarography can be used for the direct determination of hydroxylamine and DEHA in a variety of photographic processing solutions. Because these constituents occur at high concentrations, it was unnecessary to utilize the higher sensitivity of the differential pulse method.

Well defined rapid a.c. peaks corresponding to hydroxylamine oxidation have been observed for a number of processing solutions. For example, Fig. 6 shows the peaks obtained for Kodacolor II (C-41) and Ektaprint-3 (EP-3) developers diluted 100-fold with 1 M NaOH—0.1 M Na_2SO_3. For the processing solutions of interest, considerable dilution was necessary before analysis could be attempted. With little or no dilution the hydroxylamine peak was so broad, because of *iR* drop distortion, as to be useless for analytical purposes. Furthermore, at high hydroxylamine concentrations the large *iR* drop resulted in non-linearity of calibration curves. Dilution with a strongly alkaline supporting electrolyte also enabled the pH to be adjusted upwards from its normal value of about 9—10.

Calibration curves for hydroxylamine in 1 M NaOH—0.1 M Na_2SO_3 and in various processing solutions diluted with this supporting electrolyte are show in Fig. 7. In these solutions the concentration of hydroxylamine is expressed in terms of g l^{-1} of the sulfate salt (abbreviated as HAS). Although all the curves pass through the origin, the curves for processing solutions diluted with 1 M NaOH—0.1 M Na_2SO_3 do not coincide with the curve for 1 M NaOH—0.1 M Na_2SO_3 only. One reason for this can be seen by examining background polarograms recorded in the absence of hydroxylamine. For example, as shown in Fig. 8, a constituent of the Ektaprint-R (EPR) developer shifts the anodic limit to more negative potentials. Because of the empirical method by which hydroxylamine peak current is measured, this results in an apparent decrease in peak current. Similar results were obtained for the other processing solutions investigated. It is also possible that other constituents of the solutions such as *p*-phenylenediamine color developing

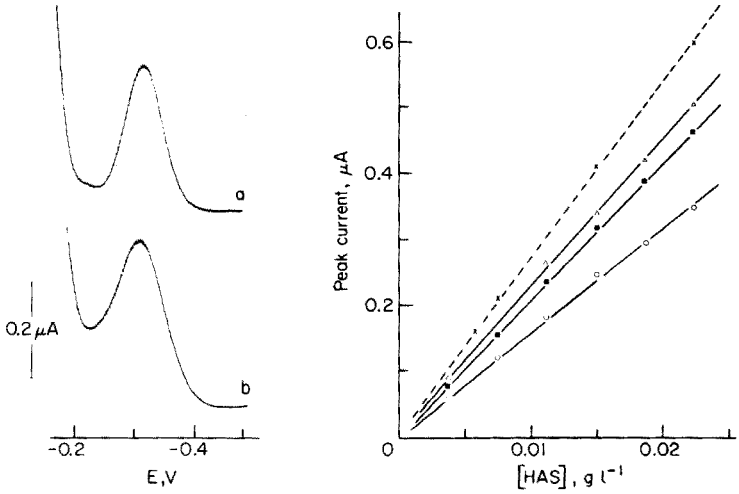

Fig. 6. Rapid a.c. polarograms of hydroxylamine in (a) C-41 and (b) EP-3 developers diluted 100-fold with 1 M NaOH—0.1 M Na_2SO_3. Drop time = 0.16 s.

Fig. 7. Rapid a.c. calibration curves for hydroxylamine in 1 M NaOH—0.1 M Na_2SO_3 (×) and in processing solutions diluted with 1 M NaOH—0.1 M Na_2SO_3. Processing solution: (▪) C-41 developer (× 100 dilution); (○) EP-3 developer (× 100 dilution); (△) EPR developer (× 500 dilution). Drop time = 0.16 s.

agents, which are known to be surface-active [16, 17], may suppress the hydroxylamine peak and thus interfere indirectly.

DEHA occurs in the cyan and yellow developers used for processing Kodachrome transparencies (K-14 Process). As for hydroxylamine, well-defined rapid a.c. peaks were obtained when these solutions were diluted with a strongly alkaline supporting electrolyte. Although other constituents of these developers did not interfere directly with the DEHA peak, there was evidence of indirect interference. For example, Fig. 9 shows calibration curves for DEHA in 1.5 M NaOH—0.1 M Na_2SO_3 and in cyan developer at various dilutions. With increasing dilution, the curves for the cyan developer approach the curve for 1.5 M NaOH—0.1 M Na_2SO_3 only. It was established that lowering of the peak current in the presence of the processing solution was not due to differences in the background (i.e., not due to direct interference). However, as previously shown [7], one of the other constituents of cyan developer, Kodak Coupling Agent C-16 (*N*-[*o*-acetamidophenethyl]-1-hydroxy-2-naphthamide), suppresses the DEHA peak. Of course, it is possible that other surface-active constituents of the solution, such as the color developing agent and polyethylene glycol [16—18], also suppress the DEHA peak. For the yellow developer, suppression of the DEHA peak was less severe. With 11-fold dilution or greater, calibration curves in the presence and absence of the processing solution coincided.

If all other constituents of a particular processing solution are at their specified concentrations, the hydroxylamine or DEHA concentration can

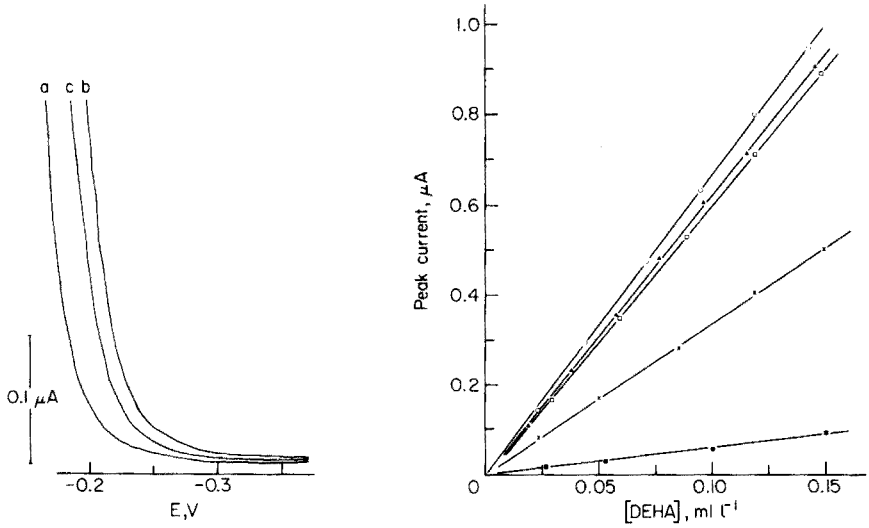

Fig. 8. Rapid a.c. background polarograms for (a) 1 M NaOH—0.1 M Na_2SO_3, (b) EPR developer (× 100 dilution), and (c) EPR developer (× 500 dilution). Drop time = 0.16 s.

Fig. 9. Rapid a.c. calibration curves for DEHA in 1.5 M NaOH—0.1 M Na_2SO_3 (○) and in K-14 cyan developer diluted with 1.5 M NaOH—0.1 M Na_2SO_3. Dilution factor: (▪) 5; (×) 12.5; (□) 21; (▲) 26. Drop time = 0.16 s.

be taken directly from the appropriate calibration curve (e.g., Figs. 7 and 9). However, in practice, the analyst will usually not be in a position to know if the above condition is met. Thus the addition method should be used to avoid errors caused by the direct and indirect interferences noted above which change the slopes of the calibration curves. Since the calibration curves pass through the origin (confirmed by least-squares regression analysis) no "blank" correction is necessary when the addition method is used.

The rapid a.c. technique has proved a very simple and rapid method of determining hydroxylamine and DEHA in photographic processing solutions. It has now been used in our laboratories for several years for routine process control (particularly in the case of DEHA). Because the only sample pretreatment required is dilution with an alkaline supporting electrolyte, the time-consuming separation steps of most other methods are avoided. Reproducibility of the method is excellent. For example, ten replicate scans on a sample of K-14 yellow developer (diluted 13.5-fold with 1.5 M NaOH—0.1 M Na_2SO_3) had a relative standard deviation of 0.38%. When the addition method is used, it is necessary to make only one addition of standard solution, with the original concentration being calculated from the appropriate equation. With this procedure, which adds little time to each analysis, seven replicate analyses of the above developer for DEHA had a relative standard deviation of 1.4%.

The differential pulse behavior of hydroxylamine and DEHA in processing

solutions was similar to the a.c. behavior. From preliminary experiments, it is apparent that the differential pulse method could be used for the present application if a.c. polarography is not available (as with the basic PAR 174A instrument).

The author is grateful to Thelma Lobb for technical assistance, R. J. Taylor for helpful discussion, and J. T. van Gemert for encouragement and helpful criticism of the manuscript.

REFERENCES

1 T. Kolasa and W. Wardencki, Talanta, 21 (1974) 845.
2 W. E. Lee in C. E. K. Mees and T. H. James (Eds.), The Theory of the Photographic Process, Macmillan, New York, 3rd edn., 1966.
3 W. Brune and E. Rieger, Zeit. Wiss. Photogr. Photophys. Photochem., 46 (1951) 179.
4 E. J. Birr, Zeit Wiss. Photogr. Photophys. Photochem., 47 (1952) 122.
5 P. E. Iversen and H. Lund, Acta Chem. Scand., 19 (1965) 2303.
6 P. E. Iversen and H. Lund, Anal. Chem., 41 (1969) 1322.
7 D. R. Canterford, Photogr. Sci. Eng., 20 (1976) 230.
8 M. N. Hughes and H. G. Nicklin, J. Chem. Soc. A, (1971) 164.
9 R. Tomat, A. Rigo, and R. Salmaso, J. Electroanal. Chem., 59 (1975) 255.
10 G. R. Rao and L. Meites, J. Phys. Chem., 70 (1966) 3620.
11 R. Gabriels, Anal. Chem., 42 (1970) 1439.
12 D. R. Canterford, Anal. Chem., 47 (1975) 88.
13 E. P. Parry and R. A. Osteryoung, Anal. Chem., 37 (1965) 1634.
14 D. R. Canterford and A. S. Buchanan, J. Electroanal. Chem., 44 (1973) 291.
15 G. Russell, Chemical Analysis in Photography, Focal Press, London, 1965.
16 D. R. Canterford, J. Electroanal. Chem., 73 (1976) 247.
17 D. R. Canterford, Photogr. Sci. Eng., 21 (1977) 215.
18 D. R. Canterford, Anal. Chim. Acta, 94 (1977) 377.

Analytica Chimica Acta, 98 (1978) 215—220

THE POLAROGRAPHIC BEHAVIOUR OF COPPER COMPLEXES OF PILOCARPINE AND SOME RELATED IMIDAZOLES

G. C. F. CLARK, G. J. MOODY and J. D. R. THOMAS*
Chemistry Department, UWIST, Cardiff CF1 3NU (Gt. Britain)
(Received 3rd January 1978)

SUMMARY

The polarographic behaviour of copper in the presence of citrate and pilocarpine and other imidazoles has been studied. The half-wave potentials of the copper(II)—copper(I) citrate system are controlled by the concentration of the second ligand when this is an imidazole nucleus. The effect can be used as the basis of an analytical procedure for these ligands.

Imidazole compounds are of considerable biomedical importance; for example, pilocarpine is used to induce localized sweating in the pilocarpine iontophoresis stage of testing sweat for chloride and sodium when diagnosing or screening for cystic fibrosis [1]. The present investigation was undertaken to evaluate the polarographic behaviour of pilocarpine when complexed with copper, as a possible means of determining pilocarpine at low concentrations or in very small samples.

The imidazole nucleus is polarographically inert and the lactone ring of pilocarpine is not reducible at a mercury electrode down to —2.5 V. Although Kirkpatrick [2] reported a catalytic wave for pilocarpine at —1.95 V, it was found to be of little value. In this paper, it is shown that by using the polarographic waves or peaks of copper complexes, it is possible to achieve adequate sensitivity for analytical purposes.

As shown by Meites [3], the behaviour of copper in citrate media is complex, and ammonia at high concentrations splits the single copper(II) polarographic wave into two waves of equal height corresponding to copper(II) and copper(I). With low concentrations of copper, a similar behaviour has been observed in the present study with imidazole derivatives.

Imidazoles (Im) form strong copper(I) complexes [4, 5] so that the following overall reaction can occur:

$$Cu^{II}(citrate)_2 + 2Im + e \rightarrow Cu^{I}(Im)_2 + 2\ citrate \qquad (1)$$

If the copper concentration is maintained below that of the imidazole derivative, the half-wave potentials of the reduction waves are a function of the imidazole concentration.

The general equation for the half-wave potential, $E_{\frac{1}{2}}$, for the reduction of a complexed metal ion to a lower valence state in the presence of an excess of ligand at 25°C [6] is:

$$E_{\frac{1}{2}} \approx E_0 + (0.0591/n) \log (K_o/K_r - (p/n)\ 0.0591 \log C_x \quad (2)$$

where E_0 is the standard potential of the reaction, K_o and K_r are the stability constants of the oxidized and reduced complexes, n is the number of electrons transferred, p is the change in the number of ligands, and C_x is the ligand concentration. For the reduction to the metal, the corresponding equation is:

$$E_{\frac{1}{2}} \approx E_0 + (0.0591/n) \log K_r - (p/n)\ 0.0591 \log C_x \quad (3)$$

Thus, depending on the value of p, the half-wave potential is a function of log [ligand].

For copper in a citrate medium, the addition of a second ligand will cause the appearance of two reduction waves obeying the above equations if the stability constant of the copper(II) citrate complex exceeds that of the copper(II)X complex, and the stability constant of the copper(I)X complex is large enough to stabilize the copper(I) state. Hence,

$$Cu^{II}\ (citrate)_2 + pX + e = Cu^{I}X_p + citrate \quad (4)$$

and

$$Cu^{I}X_p + e + Hg = Cu^{O}\ (Hg) + pX \quad (5)$$

It also requires that the concentration of X exceed that of copper.

EXPERIMENTAL

Apparatus and materials

A three-electrode cell with either a dropping mercury (DME) or a hanging mercury drop electrode (HMDE) versus a saturated calomel electrode, was used in a PAR 174A polarographic analyzer coupled to a Gould HR 2000 X-Y recorder.

All chemicals were reagent grade, except for *N*-methylimidazole which was prepared by treating imidazole with dimethyl sulphate followed by distillation (90—98°C at 15 mm Hg). Identity was confirmed by n.m.r. spectroscopy.

The copper—citrate medium contained 1 M citric acid (4.4 cm^3), 1 M trisodium citrate (95.6 cm^3), 1 M copper sulphate (0.1 cm^3) and 0.2% Antarox CO-880 suppressor (10 cm^3) made up to 1 dm^3 with water.

Procedures

The polarographic measurements were made at 25°C on 2.5 cm^3 of the copper—citrate medium after deaeration for 5 min with oxygen-free nitrogen. Test samples were added to the copper—citrate medium with a Hamilton syringe.

Polarographic curves were recorded for the DME by the sampled d.c. mode with a 0.5-s drop time and a scan speed of 2 mV s^{-1}. Differential pulse polarograms were obtained with a 0.5-s drop time, a scan speed of 0.2 mV s^{-1} and modulation amplitude of 5 mV.

With the HMDE the sample volume was 5 cm^3. For pulse voltammetry in this mode the pulse time was 0.5 s, modulation amplitude 50 mV, and scan speed 5 mV s^{-1}. For differential pulse anodic stripping voltammetry, the plating potential was −500 mV, plating time 20 s, pulse time 0.5 s, pulse amplitude 50 mV and the scan speed 5 mV s^{-1}.

RESULTS

Polarography

Pilocarpine. The polarographic waves obtained for the copper-citrate medium in the presence of pilocarpine are shown in Fig. 1. The half-wave potentials (Table 1) were measured by differential pulse polarography, corrected for pulse amplitude by the relation $E_{\frac{1}{2}} = E_{peak}$ − (pulse amplitude)/2 [7].

The copper(II) wave is split into two waves in the presence of pilocarpine, each corresponding to 1 e reductions. The wave heights are effectively independent of the pilocarpine concentration, while the half-wave potential relation of the first wave, $E_{\frac{1}{2}}^{I} = 0.195 + 0.069$ log [pilocarpine], holds over the 0.04 − 6 mM pilocarpine range. The relation for the half-wave potential of the second wave is $E_{\frac{1}{2}}^{II} = -0.78 - 0.075$ log [pilocarpine].

The first wave may be adopted as the basis of an analytical method for

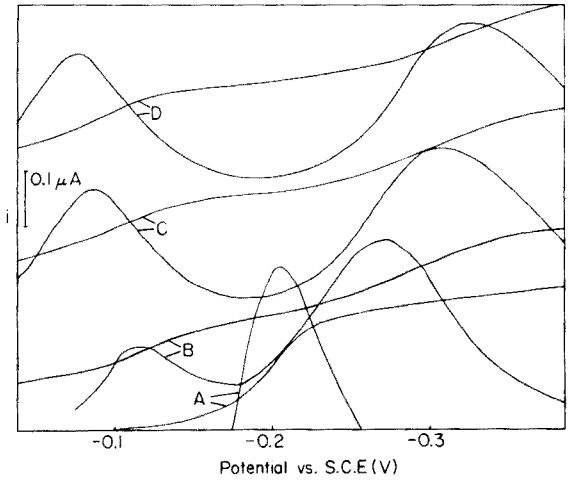

Fig. 1. Polarographic and differential pulse polarographic waves for pilocarpine in copper—citrate medium. 2.5 cm^3 of copper—citrate medium plus pilocarpine nitrate. Curve A is for copper—citrate only. Curves B, C and D correspond to additions of 0.04, 0.12 and 0.20 mM pilocarpine nitrate, respectively.

TABLE 1

Half-wave potentials of reduction waves of pilocarpine in a copper—citrate medium

First wave			Second wave		
Concentration of pilocarpine nitrate in copper citrate medium (mM[a])		$E'_{\frac{1}{2}}$ (mV)	Concentration of pilocarpine nitrate in copper citrate medium (mM[a])		$E''_{\frac{1}{2}}$ (mV)
0.04	(5)	−106.0	0.04	(5)	−497.4
0.06	(7.5)	−91.8	0.06	(7.5)	−519.0
0.079	(10)	−86.3	0.08	(10)	−527.0
0.158	(20)	−68.9	0.10	(12.5)	−532.6
0.234	(29.5)	−56.7	0.12	(15)	−536.7
0.310	(39)	−45.6	0.14	(17.5)[b]	−539.7
0.385	(48)	−38.5			
0.741	(92.5)	−19.6			
1.470	(184)	+1.3			
2.900	(362)	+20.65			
5.63	(704)[b]	+43.9			

[a]Parenthesized numbers are corresponding concentrations (mM) of the standard pilocarpine nitrate solutions of which 20 mm^3 was taken with 2.5 cm^3 of copper—citrate medium for each measurement of $E_{\frac{1}{2}}$. [b]$E_{\frac{1}{2}}$ values were not measurable at higher concentrations.

pilocarpine by adding 20 mm^3 samples to 2.5 cm^3 of the copper citrate medium. The half-wave potential may be measured by differential pulse polarography, and measurements with solutions of known pilocarpine concentrations can be used for calibration purposes (see Table 1). Results of measuring concentrations of replicate samples are shown in Table 2.

Imidazole. Imidazole behaves similarly to pilocarpine, the equations for the two waves being $E'_{\frac{1}{2}} = 0.091 + 0.061 \log [\text{imidazole}]$, and $E''_{\frac{1}{2}} = -0.570 - 0.088 \log [\text{imidazole}]$. For the first wave, the upper limit was fixed by an impurity in the imidazole producing a wave at 0.0 V but despite this, the relation held over the 0.04—10 mM range.

TABLE 2

Pilocarpine concentrations obtained from calibrated shifts of $E'_{\frac{1}{2}}$ resulting from addition of 20 mm^3 of pilocarpine nitrate solutions to 2.5 cm^3 of copper—citrate medium

Pilocarpine taken (mM)	Pilocarpine found (mM)	Error (%)	Pilocarpine taken (mM)	Pilocarpine found (mM)	Error (%)
10	9.5	−5	70	71.0	+1.4
	10.8	8		69.5	−0.7
	8.9	−11		70.2	+0.28
30	31.5	5	100	98.0	−2.0
	29.5	−1.7		101.4	+1.4
	30.5	+1.7		100.4	+0.4

Brucine. Since a great many alkaloids are polarographically inert, it was interesting that brucine in this procedure gave a splitting into two waves for the 1—10 mM range. However, only the first wave was sufficiently well-defined to measure accurately $E'_{\frac{1}{2}}$ according to the relation $E'_{\frac{1}{2}} = 0.210 + 0.050$ log [brucine].

N-*Methylimidazole.* This showed the same behaviour as imidazole over the range 10—700 mM, but the first wave was less clearly defined than the second. The linear relation between $E_{\frac{1}{2}}$ and log [concentration] did not hold for the first wave above 80 mM, possibly because of the formation of copper(II)—imidazole complexes of the same stoichiometry as those of copper(I). The respective wave equations are: $E'_{\frac{1}{2}} = 0.296 + 0.079$ log [*N*-methylimidazole] and $E''_{\frac{1}{2}} = -0.386 - 0.087$ log [*N*-methylimidazole].

Amines. Ammonia, dimethylaniline and trimethylamine were tested for the 0.04—1.2 mM range and no effect was observed on the reduction wave of the copper in the copper—citrate medium. Although this is apparently in conflict with the results of Meites [3] in ammonium citrate, it must be realised that in the present study the level of amine was only of the order of 1% or less than that of the ammonium ion used by Meites.

Hanging mercury drop electrode experiments

Only pilocarpine was investigated with the HMDE. It showed similar behaviour to that at the DME, except that noise was less troublesome. The lower limit of the linear relationship for the first wave, $E'_{\frac{1}{2}} = 0.013 + 0.065$ log [pilocarpine], is 1.6 mM. The change in the constant term from that observed for the DME is present for the copper—citrate system in the absence of nitrogen ligands. With the DME the peak height in differential pulse polarography is not proportional to ligand concentration. However, for the HMDE with differential pulse polarography the peak height is proportional to pilocarpine concentration over the 0.4—1.6 mM concentration range. The peaks corresponding to the reduction of copper(I) were not well defined and were not investigated.

When differential pulse anodic stripping voltammetry was used, the behaviour was quite different (Fig. 2). Splitting of the copper wave was observed only for pilocarpine concentrations above about 0.2 mM. Below this level a single peak was observed, at about −170 mV, and the peak height ranged from 1 to 10 μA. Above 0.8 mM, two resolved peaks were observed, with approximately constant heights. The more positive peak, corresponding to the oxidation to copper(II), had a potential of about − 120 mV (Fig. 2) and could not be related to pilocarpine concentration. The other peak, corresponding to oxidation to copper(I), gave a peak potential proportional to log [pilocarpine] according to $E_{peak} = -0.239 + 0.102$ log [pilocarpine].

DISCUSSION

There have been relatively few reports of analytical methods for determining polarographically inert substances by complexing them to metal ions.

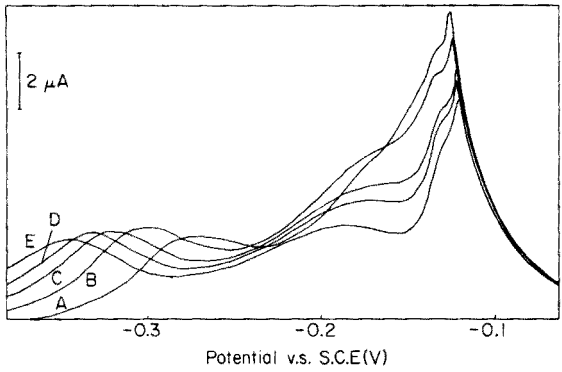

Fig. 2. Differential pulse anodic stripping voltammetry of copper in the presence of pilocarpine. Curves A—E correspond to 120, 200, 300, 400 and 600 mm^3, respectively, of 0.1 M pilocarpine nitrate solution added to 5 cm^3 of copper—citrate medium.

The method most usually employed has been the measurement of current as a function of ligand concentration [8].

On the splitting of copper differential peaks, Smyth et al. [9] have observed that in the anodic stripping voltammetry of copper the single peak was split into two by the presence of bromazepam. However, they did not report on variations of peak potential as the bromazepam concentration was varied.

Behaviour of the type observed here will occur only if the metal ion can exist in two soluble oxidation states, and if in changing from one to the other the number of ligands complexed changes. Thus, in the present case, in the absence of citrate there would be no change in complexation or reduction from copper(II) to copper(I) so that the half-wave potential would remain constant. The effect depends on the copper(II) ions being complexed by citrate, and the copper(I) ions by the ligand of interest. This means that the technique may be applicable to all ligands capable of forming stable copper(I) complexes in solution.

The authors thank the Medical Research Council for financial support.

REFERENCES

1 See, e.g., P. T. Bray, G. C. F. Clark, G. J. Moody and J. D. R. Thomas, A Perspective of Sodium and Chloride Ion-Sensitive Electrode Sweat Tests for Screening in Cystic Fibrosis, UWIST, Cardiff, 1975, p. 13.
2 H. F. W. Kirkpatrick, Q. J. Pharm. Pharmacol., 19 (1946) 526.
3 L. Meites, J. Am. Chem. Soc., 72 (1950) 180.
4 B. R. James and R. J. P. Williams, J. Chem. Soc., (1961) 2007.
5 C. J. Hawkins and D. D. Perrin, J. Chem. Soc. (1962) 1351.
6 I. M. Kolthoff and J. J. Lingane, Polarography, Interscience, New York, 2nd edn., 1952, p. 211.
7 G. J. M. Heijne, and W. E. Van der Linden, Anal. Chim. Acta, 82 (1976) 231.
8 R. Prasad, Analyst, 102 (1977) 601.
9 M. R. Smyth, T. S. Berg and W. F. Smyth, Anal. Chim. Acta, 92 (1977) 129.

Analytica Chimica Acta, 98 (1978) 221—226

THE FORMATION OF MIXED COPPER SULFIDE–SILVER SULFIDE MEMBRANES FOR COPPER(II)-SELECTIVE ELECTRODES
Part IV. Selectivity Coefficients and Complexometric Titrations

G. J. M. HEIJNE, W. E. van der LINDEN* and G. den BOEF

Laboratory for Analytical Chemistry, University of Amsterdam, Nieuwe Achtergracht 166, Amsterdam (The Netherlands)

(Received 28th November 1977)

SUMMARY

The analytical applicability of a mixed sulfide copper-selective electrode has been evaluated, with special attention given to end-point indication in complexometric titrations. In acidic medium, several metals can be titrated satisfactorily. The determination of calcium and magnesium in alkaline medium is discussed briefly. Selectivity coefficients are presented for several metal ions in acidic medium.

The preparation, composition and behaviour of a copper(II)-selective electrode based on a mixed copper—silver sulfide has already been described in detail [1—3]. The application of copper(II)-selective electrodes in analysis has been dealt with in several papers; yet it seems desirable to report the results obtained with this new electrode to indicate its possibilities, especially in complexometric titrations (cf. [4]). Since few reports are available which present selectivity coefficients (see e.g. [4, 5]), values of these coefficients have been determined for a number of metal ions. In general, the values found were low ($< 10^{-3}$). For silver(I) and mercury(II), the performance of the electrode deteriorated completely; iron(III) caused some other anomalies.

EXPERIMENTAL

The preparation of the electrodes and the equipment used for the measurements were the same as before [1—3]. The selectivity coefficients were determined in acetate buffer (0.05 M, pH 4.7), adjusted with potassium nitrate to ionic strength 0.1. Titrations were carried out in this medium, and also in 0.25 M ammonia—ammonium nitrate buffer (pH 9.9) and in 0.25 M cyclohexylamine—cyclohexylamine nitrate buffer (pH 11.0). All chemicals used were of analytical-reagent grade. Metal ions were added as nitrates, except for iron(II) which was added as sulfate.

RESULTS AND DISCUSSION

Selectivity coefficients and limit of detection

Recently, recommendations have been published by the IUPAC [6] with respect to the definition of the practical limit of detection, D_M, and the potentiometric selectivity coefficient, $k^{pot}_{M,N}$, of ion-selective electrodes, as well as methods for the determination of these values. According to these recommendations, which give preference to the so-called fixed interference method, selectivity coefficients were determined in acidic medium for several metal ions at 10^{-3} M. Free ion activities were calculated by using activity coefficients as discussed by Kielland [7], and side-reaction coefficients of the metal ions with acetate according to the equations and the stability constants presented by Ringbom [8]. The values of $k^{pot}_{M,N}$ obtained in this way, as well as those of D_{Cu} appeared to depend strongly on the pretreatment of the electrode, which was to be expected from previous results [1]. The results are presented in Tables 1 and 2, together with logarithmic values of the activity coefficient, f_i, and the side-reaction coefficient, $\alpha_{M(Ac)}$. The results given in Table 1 represent the practical limit of detection of the electrode in copper(II)-solutions, while those in Table 2 give values of $k^{pot}_{M,N}$. If the determination was carried out with electrodes which had been kept for some time in 10^{-3} M free EDTA, for instance after the performance of a titration, in nearly all cases the logarithmic values were about 0.3—0.6 lower. This might be due to exhaustion of the membrane surface with respect to copper, because of the enhanced dissolution process discussed earlier [3]. This seems more likely than adsorption of the ligand, since relatively low potential values occurred also in the presence of 10^{-3} M cadmium and zinc, which form complexes with EDTA easily, and therefore should have caused restoration of the original values because of desorption of the ligand.

Values of $k^{pot}_{M,N}$ and D_M can be obtained also by calculation from the relation [4]:

$$E = E' + S \log (a_{M^{2+}} + k^{pot}_{M,N} \cdot a_{N^{2+}} + D_M) \quad (1)$$

or from the linearized form:

$$a_{M^{2+}} + k^{pot}_{M,N} \cdot a_{N^{2+}} + D_M = 10^{(E - E')/S} \quad (2)$$

TABLE 1

Limit of detection of two copper-i.s.e.'s in acidic medium

Electrode	$-\log f_i$	$\log \alpha_{Cu(Ac)}$	Limit of detection, $\log D_{Cu}$	
			After contact with free Cu(II)	After contact with EDTA
1	0.39	0.41	−7.14, −7.21, −7.20, −7.22	−7.54, −7.82
2	0.39	0.41	−7.13, −7.35	−7.53

TABLE 2

Selectivity coefficients $k^{pot}_{Cu,N}$ and $k'^{pot}_{Cu,N}$ of the copper-i.s.e. in acidic medium for $c_N = 10^{-3}$ M

metal N	$-\log f_i$	$\log \alpha_{N(Ac)}$	$\log k^{pot}_{Cu,N}$ after contact with:		$\log k'^{pot}_{Cu,N}$ after contact with:		Lit. data [reference]
			Free Cu(II)	Free EDTA	Free Cu(II)	Free EDTA	
Zn	0.39	0.20	−3.6	−4.1	−3.4	−3.9	−3.0 [4]
Cd	0.42	0.11	−3.5	−4.0	−3.2	−3.7	−3.0 [4]
Ni	0.39	0.06	−3.7	−4.0	−3.3	−3.6	−3.3 [4]
Mn	0.39	0.04	−3.8	−4.2	−3.4	−3.8	
Pb	0.44	0.63	−2.7	−2.9	−3.0	−3.2	
Fe(II)	0.39	0.21	−3.3	−3.4	−3.1	−3.2	

E' and S can be found from measurements at such high concentrations of the primary ion that $a_{M^{2+}} \gg k^{pot}_{M,N} \cdot a_{N^{2+}}$. The logarithmic values of $k^{pot}_{M,N}$ obtained in this way are slightly higher than those given in Table 2, both when the electrode has been in contact with free copper ions (+0.01 to 0.05) and in contact with free EDTA (+0.07 to 0.2).

The application of the more elaborate method of Srinavasan and Rechnitz [9] for the evaluation of small selectivity coefficients in mixed solutions gave about the same results at the lowest copper concentrations, although the relation found was not linear for the entire concentration range. Possibly the values of the selectivity coefficients are too low in this case.

Because the values tabulated in Table 3 include corrections for activity and side-reaction coefficients, it might be useful to define a conditional selectivity coefficient $k'^{pot}_{M,N} = (f_N \cdot \alpha_M / f_M \cdot \alpha_N) \cdot k^{pot}_{M,N}$. Introduction of this coefficient in eqn. (1) leads to:

$$E = E' + S \log (f_M/\alpha_M) + S \log (c_{M^{2+}} + k'^{pot}_{M,N} \cdot c_{N^{2+}} + D'_M) \qquad (3)$$

where $c_{M^{2+}}$ and $c_{N^{2+}}$ denote analytical concentrations. $E' + S \log (f_M/\alpha_M)$ can be replaced by a new constant, E''. This conditional coefficient gives a direct indication of the interference to be expected, because concentration levels are involved instead of activities. Values of $k'^{pot}_{M,N}$ are also presented in Table 2.

The interference of iron(II) needs some comment. As far as could be observed, iron(II) itself showed little interference, as long as oxygen was excluded by working in a nitrogen atmosphere. The fact that measurements in solutions containing iron(II) without being deoxygenated showed positively drifting potentials is probably due to the oxidation of iron(II) to iron(III).

Iron(III) showed some anomalies. It can be calculated that in the acetate buffer used, nearly all iron(III) is complexed by acetate ($\alpha_{Fe(III)(Ac)} = 10^{3.82}$) or precipitated as hydroxide ($\alpha_{Fe(III)(OH)} = 10^{3.1}$). Nevertheless, a large potential jump corresponding to a jump caused by the addition of 10^{-5} M copper(II) was observed on the addition of 10^{-3} M iron(III), followed by a

negative drift until a stable potential was reached, corresponding to 10^{-6} M copper(II). This relatively high value might be due to a reaction of iron(III) with copper(I) in the membrane material, which has been shown [2] to consist mainly of jalpaite ($\sim Ag_{1.5}Cu_{0.5}S$), leading to the formation of free copper(II). The influence of iron(III) on the potential of a copper-i.s.e. has recently been used to develop an analytical procedure for the determination of iron(III) [10].

It was found that after measurements in the presence of iron(III), the interference of other ions increased: $\log k^{pot}_{Cu,Cd} = -3.1$ and $\log k^{pot}_{Cu,Pb} = -2.5$, whereas the limit of detection of the electrode still had the same value in calibrations as well as titrations. Extensive polishing of the electrode by hand with Perspex A2 polishing fluid (ICI) gave no improvement of the selectivity. Apparently, the limit of detection of the electrode and its selectivity do not depend on the same properties of the membrane material.

Complexiметric titrations

The results of titrations in acidic media are summarized in Table 3. End-points were determined from logarithmic curves as well as from curves linearized by means of eqn. (2). Since complexiметric titrations with ion-selective electrodes have been treated in detail by van der Meer et al. [4, 11, 12] there is no need to go into all details of the tabulated results. These comprise titrations of copper(II) alone, mixtures of copper(II) and several other metal ions at the 10^{-3} M level, and — as an example — mixtures of zinc and copper at lower concentrations, and a range of zinc concentrations with copper—EDTA as indicator. In the latter case, good results were obtained from logarithmic curves for concentrations of zinc down to 5×10^{-6} M. At low concentrations it is important that the waiting time after additions is long enough to make sure that equilibrium has been established; otherwise positive deviations up to 30% at the 10^{-6} M level can be expected in direct titrations of copper as well as in indicator-ion titrations. The results obtained in the presence of iron need some comment. According to the stability constants, it would be expected that copper(II) could be determined separately in the presence of iron(II), but not in the presence of iron(III). In practice, the opposite was found. In the case of iron(III), this is probably due to the slow formation of the iron(III)—EDTA complex, while iron(II) is readily oxidized to iron(III)—EDTA (see e.g. [13]). In the former case, copper can be determined with acceptable accuracy provided that the titration is carried out quickly. Linearization is a prerequisite in that case.

In alkaline medium the electrode showed drifting potentials, especially in ammoniacal solution, and became insensitive after a few days. In cyclohexylamine this deterioration was slower, and correct end-points were observed for the titration of 10^{-3} M EDTA with copper. The direct titration of 4×10^{-4} M calcium with EDTA gave small but sharp potential breaks. In back-titrations, it was found that both 4×10^{-4} M magnesium alone and the sum of 4×10^{-4} M calcium + 4.10^{-4} M magnesium could be determined reasonably well, when

TABLE 3

Determination of metals by titration with EDTA in acidic medium (pH 4.7)[a]

Composition of the solution (mol l^{-1})	Equiv. point considered	Logarithmic curve			Linearized curve		
		R.e. (%)	s_r (%)	n	R.e. (%)	s_r (%)	n
10^{-3} Cu	Cu	−0.7	0.5	6	−0.0	0.3	6
10^{-4} Cu	Cu	+0.2			+0.3		
10^{-5} Cu	Cu	0.0			+0.3		
10^{-6} Cu	Cu	0.0			−1.8		
10^{-3} Cu + 10^{-3} Mn	Cu	−1.9	0.2	2	−1.7	0.5	2
	Cu + Mn	−2.5	0.4	2	+0.7	0.3	2
10^{-3} Cu + 10^{-3} Cd	Cu	unreliable			+2.9	0.5	2
	Cu + Cd	−1.0	0.2	2	+1.1	0.3	2
10^{-3} Cu + 10^{-3} Pb	Cu	unreliable			+16	10[b]	
	Cu + Pb	−1.4	0.0	2	−1.4	0.3	2
10^{-3} Cu + 10^{-3} Ni	Cu	impossible			impossible		
	Cu + Ni	−0.2					
10^{-3} Cu + 10^{-3} Fe(II)	Cu	impossible			impossible		
	Cu + Fe	−1.4			−4.1		
10^{-3} Cu + 10^{-3} Fe(III)	Cu	unreliable			+6.0		
	Cu + Fe	−8.6			−5.3		
10^{-3} Cu + 10^{-3} Zn	Cu	unreliable			+2.1	0.5	2
	Cu + Zn	−0.8	0.4	2	−1.0	0.3	2
5.10^{-4} Cu + 5.10^{-4} Zn	Cu	+10	9	3			
	Cu + Zn	−0.8	0.3	3			
10^{-4} Cu + 10^{-4} Zn	Cu + Zn	−1.0					
5.10^{-5} Cu + 5.10^{-5} Zn	Cu + Zn	−0.5	1.0	3			
10^{-5} Cu + 10^{-5} Zn	Cu + Zn	+1.0					
5.10^{-6} Cu + 5.10^{-6} Zn	Cu + Zn	+5.3	2.3	3			
5.10^{-7} Cu + 5.10^{-7} Zn	Cu + Zn	+8.8	7.7	3			
10^{-4} Cu + 10^{-3} Zn	Cu + Zn	−0.5	0.2	3			
10^{-5} Cu + 10^{-3} Zn	Cu + Zn	0.0	0.3	3			
10^{-6} Cu + 10^{-3} Zn	Cu + Zn	+0.6	1.2	3			
10^{-3} Zn + 10^{-6} Cu—EDTA		−0.1	0.6	4	+19		
10^{-4} Zn + 10^{-6} Cu—EDTA		+3.0	0.8	4	+4.5		
10^{-5} Zn + 10^{-6} Cu—EDTA		+2.2	1.0	4	+10		
5.10^{-6} Zn + 10^{-6} Cu—EDTA		+3.3	1.5	3	+10		
2.10^{-6} Zn + 10^{-6} Cu—EDTA		+12.3	1.5	4	+20		
1.10^{-6} Zn + 10^{-6} Cu—EDTA		+27	0.8	5	+36		

[a]R.e. = relative error, s_r = relative standard deviation, n = number of determinations.
[b]When corrected for the amount of Pb—EDTA formed, r.e. = +1.0%, s_r = 0.5% (n = 2).

the excess of EDTA (10^{-3} M was added) was titrated quickly with copper(II). An electrode with a quick response is needed in this case; probably that is the reason why van der Meer et al. [12] could not titrate magnesium in their experiments. Although titrations in alkaline medium are possible in some cases, they are less attractive, especially in ammoniacal solution, because of the deterioration of the electrode.

REFERENCES

1 G. J. M. Heijne, W. E. van der Linden and G. den Boef, Anal. Chim. Acta, 89 (1977) 287.
2 G. J. M. Heijne and W. E. van der Linden, Anal. Chim. Acta, 93 (1977) 99.
3 G. J. M. Heijne and W. E. van der Linden, Anal. Chim. Acta, 96 (1978) 13.
4 J. M. van der Meer, G. den Boef and W. E. van der Linden, Anal. Chim Acta, 76 (1975) 261.
5 G. J. Moody and J. D. R. Thomas, Selective Ion-Sensitive Electrodes, Merrow Publishing Co., 1971, p. 23.
6 Commission on Analytical Nomenclature, Pure Appl. Chem., 48 (1976) 129.
7 J. Kielland, J. Am. Chem. Soc., 59 (1937) 1675.
8 A. Ringbom, Complexation in Analytical Chemistry, Interscience, New York, 1963.
9 K. Srinavasan and G. A. Rechnitz, Anal. Chem., 41 (1969) 1203.
10 Y. S. Fung and K. W. Fung, Anal. Chem., 49 (1977) 497.
11 J. M. van der Meer, G. den Boef and W. E. van der Linden, Anal. Chim. Acta, 79 (1975) 27.
12 J. M. van der Meer, G. den Boef and W. E. van der Linden, Anal. Chim. Acta, 85 (1976) 309.
13 A. Hulanicki and R. Karkowska, Talanta, 18 (1971) 239.

Analytica Chimica Acta, 98 (1978) 227—232

A SIMPLE POTENTIOMETRIC METHOD FOR THE DETERMINATION OF REDUCING SUBSTANCES IN URINE WITH A COPPER-SELECTIVE ELECTRODE

D. P. NIKOLELIS, D. S. PAPASTATHOPOULOS and T. P. HADJIIOANNOU*

Laboratory of Analytical Chemistry, University of Athens, Athens (Greece)

(Received 12th October 1977)

SUMMARY

A potentiometric method for the determination of reducing substances in urine is described. Samples are treated with Stanley—Benedict reagent and the unused copper(II) is determined with a copper(II)-selective electrode by the standard addition technique. Glucose in the range 25—200 μg in 0.1-ml samples can be determined with an average error of about 2%. The recovery of added glucose for six samples was 96—107% (average 100.5%). Comparison with the conventional titrimetric method shows good agreement. The effect of other non-glucose reducing substances present in urine is reported.

Benedict's method for the determination of reducing substances in urine is still widely used, in various modifications, for the diagnosis of several diseases. Qualitative tests based on the same principle are also employed but lack sensitivity [1—4]. Although glucose is the commonest urinary reducing constituent present in conditions such as diabetes mellitus or renal glucosuria, and its presence or absence can be confirmed by specific enzymatic methods, Benedict's method remains useful, because of the diagnostic importance of other non-glucose reducing substances, such as galactose, fructose, lactose, homogentisic acid, etc., which may be present in urine in other clinical conditions [1, 2].

Ion-selective electrodes have been successfully adapted as sensors for use in various clinical analyses because of their low cost, high selectivity and indifference to optical interferences [5—9]. It was recently shown that reducing sugars in natural products can be determined rapidly by a new potentiometric method with a copper ion-selective electrode [10]. The simplicity, sensitivity and speed obtained suggested that the method could be applied to the determination of urinary reducing substances. Results are now presented which show that a similar procedure is suitable for the determination of reducing substances in urine. The urine samples are treated with a standard amount of Stanley—Benedict reagent, and the unreduced copper(II) is determined with a copper ion-selective electrode by a standard addition technique.

EXPERIMENTAL

Apparatus

A solid-state copper(II)-selective electrode (Orion model 94-29A) and a single-junction reference electrode (Orion model 90-01) were used with a digital pH/mV meter (Orion model 801). All measurements were carried out in a thermostatically controlled 10-ml cell at 25 ± 0.2°C.

The glucose standards and the urine samples were treated with the Stanley—Benedict reagent in 30-ml Kjeldahl flasks on an electrically heated micro-Kjeldahl digestion stand.

The surface of the copper(II)-selective electrode was polished with diamond paste and treated with silicone oil daily, in order to achieve the best electrode performance [10, 11]. To eliminate any effects of ambient light fluctuations, the electrodes and the cell were placed in a black-painted wooden box [10, 12].

Reagents

Solutions of 0.1000 M copper(II) nitrate (stock solution), 0.2 M acetate buffer (pH 4.1) containing fluoride, glucose standards and Stanley—Benedict reagent were prepared with deionized-distilled water from reagent-grade materials, as previously described [10, 13]. A solution of 0.0100 M copper(II). nitrate prepared from the stock solution was used for determination of the calibration slope and for the standard addition technique.

Fresh urine samples were collected daily from healthy personnel in this laboratory and from members of their families, 3—70 years old. The samples were stored under refrigeration and used without pre-treatment.

Procedures

Determination of the calibration slope. Calculate the slope S graphically from a conventional calibration plot in the range 10^{-3}—10^{-5} M copper(II). Construct this plot from the results obtained by adding 0.0100 M copper(II) nitrate solution (5 μl to 0.5 ml) to the thermostated cell containing a solution of 2.50 ml of the acetate buffer and 2.50 ml of water. The calibration slope must be checked daily.

Sample treatment with Stanley—Benedict reagent. Transfer 0.100-ml aliquot of glucose standard solution or unknown urine sample to a 30-ml Kjeldahl flask containing 5.0 ml of water and 0.050 ml of Stanley—Benedict reagent. Add a few anti-bumping granules to avoid excessive foaming, and boil on an electric heater for 10 min. Allow to cool to room temperature, and filter through a Whatman No. 42 filter paper into a 10-ml volumetric flask. Wash the flask and the precipitate of copper(I) oxide on the filter twice with 1.0 ml of water into the volumetric flask. Add 5.0 ml of the acetate buffer by pipette, and dilute to the mark with water (solution A).

Standard addition procedure. Pipette a 5.0-ml portion of solution A into the thermostated cell and immerse the electrode pair. Measure the potential

while stirring, after a steady-state reading is established (1—3 min). Then, add 0.100 ml of 0.0100 M copper(II) nitrate solution to the cell and measure the new steady-state potential.

Preparation of the working curve. Calculate the unknown concentration C_0 of the unreduced copper(II) for each glucose standard solution from the standard addition equation [14]: $C_0 = C_\Delta/[\text{antilog}\ (\Delta E/S)-1]$, where C_Δ is the change in copper(II) concentration, ΔE is the observed potential change, and S is the calibration slope. Plot the working curve of C_0 vs. μg of glucose/0.1 ml, using three glucose standard solutions of 25.0, 100 and 200 μg/0.1 ml.

Determination of reducing substances. For the determination of reducing substances in urine samples, use the same standard addition procedure as for glucose standards. Calculate the concentration C_0 of the unreduced copper(II) as above, and establish the amount of the reducing substances from the working curve.

RESULTS AND DISCUSSION

Procedures for eliminating the effect of the electrode surface condition on the performance of the copper electrode, and reasons for the choice of experimental conditions, have been reported [10, 11].

The proportionality between the unreduced copper(II) concentration and glucose is linear in the range of 25—200 μg glucose/0.1 ml of sample, which is equivalent to 25—200 mg/100 ml. This range covers the normal range for total reducing substances in urine, which is 50—150 mg/100 ml expressed as glucose [2, 4]. The correlation coefficient for a working curve in this range was —0.9994.

Results obtained for aqueous glucose solutions are shown in Table 1. The error was 1—2% and the relative standard deviation for six replicate complete analyses of 50.0 and 100 μg of glucose in 0.1 ml of sample was less than 2%.

TABLE 1

Results for aqueous glucose solutions

Glucose (mg/100 ml)		Relative error (%)	s_r (%)
Taken	Found[a]		
25.0	25.5	+2.0	—
50.0	49.5	—1.0	1.82 (n = 6)
100	97.4	—2.6	1.63 (n = 6)
150	151	+0.7	—
200	203	+1.5	—
		Av. 1.56	

[a]From calibration curve, average of two values.

The results obtained for reducing substances in 12 urine samples by the proposed method and by Benedict's titrimetric method [15] are compared in Table 2; the mean deviation between the potentiometric and titrimetric results is +0.2% (+4.1% to −3.8%). The results from another set of 50 urine samples analyzed by both methods are shown in a correlation plot (Fig. 1); clearly, there is satisfactory agreement between the two methods. The accuracy of the method was further checked by recovery experiments carried out on six representative urine samples (Table 3); the recoveries ranged from 95.6% to 107% (average 100.5%). To check the reproducibility, twenty complete determinations were made on three different urine samples. The

TABLE 2

Comparison of the titrimetric and potentiometric methods for determination of reducing substances in urine

Sample no.	Reducing substances (mg/100 ml)[a]		Difference (%)
	Titrimetric method	Potentiometric method	
1	28.3	29.1	+2.8
2	53.3	51.3	−3.8
3	42.1	43.2	+2.6
4	75.5	74.7	−1.1
5	32.0	33.3	+4.1
6	61.5	60.3	−2.0
7	25.8	25.2	−2.3
8	98.4	98.7	+0.3
9	88.9	87.4	−1.7
10	65.6	66.5	+1.4
11	58.8	58.4	−0.7
12	38.0	39.3	+3.4

[a]Average of two determinations for each sample and method.

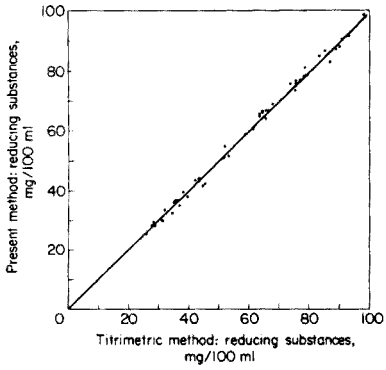

Fig. 1. Comparison of the potentiometric and the Benedict titrimetric methods for the determination of reducing substances in 50 samples of urine (correl. coef. 0.997, slope 0.998, intercept −0.062 mg/100 ml).

TABLE 3

Recovery of glucose added to six urine samples

Reducing substances (mg/100 ml)	Glucose added (mg/100 ml)	Glucose recovery (%)	Reducing substances (mg/100 ml)	Glucose added (mg/100 ml)	Glucose recovery (%)
25.1	50.0	106.2	60.2	50.0	95.6
	100	97.9		100	102.0
33.3	50.0	103.8	72.3	25.0	100.8
	100	98.7		50.0	99.4
40.6	25.0	99.6	93.1	25.0	95.6
	50.0	107.0		50.0	105.8
	100	97.4		100	96.9

TABLE 4

Effect of various reducing substances added to urine

Reducing substance added	Initial reducing substances present (mg/100 ml)	Amount of substance added (mg/100 ml)	Total reducing substances found (mg/100 ml)	Amount of substance found (mg/100 ml)	Recovery (%)
Lactose[b]	67.2	25.0	87.8	20.6	82.4
		50.0	107	39.8	79.6
		100	148	80.8	80.8
Galactose[c]	67.2	25.0	92.2	25.0	100.0
		50.0	116	48.8	97.6
		100	171	104	104.0
Arabinose[c]	67.2	25.0	92.1	24.9	99.6
		50.0	118	50.8	101.6
		100	161	93.8	93.8
Xylose[c]	67.2	25.0	90.5	23.3	93.2
		50.0	114	46.8	93.6
		100	148	80.8	80.8
Glucuronic acid[d]	39.5	25.0	64.3	24.8	99.2
		50.0	91.4	51.9	103.8
		100	114	74.5	74.5
Ascorbic acid[d]	39.5	50.0	103	63.5	127.0
		100	146	106.0	106.0
Creatinine[a]	39.5	50.0	68.5	29.0	58.0
		100.0	99.7	60.2	60.2
Uric acid[a]	39.5	50.0	84.6	45.1	90.2
		100	96.8	57.3	57.3
Salicylates[d]	36.1	50.0	76.3	40.2	80.4
		100	118	81.9	81.9
p-Aminosalicylic acid	36.1	50.0	75.9	39.8	79.6
		100	66.7	30.6	30.6
Isoniazid[d]	36.1	50.0	54.5	18.4	36.8
		100	54.4	18.3	18.3
Oxalic acid[c]	36.1	25.0	62.3	26.2	104.8
		50.0	91.2	55.1	110.2

[a]Common substance in urine. [b]Common substance in urine during pregnancy and lactation. [c]Rare substance in urine. [d]Substance present in urine under drug therapy.

mean values found for reducing substances expressed as glucose, were 37.1, 76.8 and 97.9 mg/100 ml, with relative standard deviations of 1.51, 2.43 and 1.81%, respectively.

The Stanley—Benedict reagent is not specific for glucose, but also reacts with other reducing substances which may be present in human urine [1, 2, 4]. The effect of such substances was examined by recovery experiments on various urine samples. The results obtained, summarized in Table 4, are in good agreement with results reported by others [2, 16—19].

The proposed potentiometric method for the determination of reducing substances in urine offers several advantages over the conventional procedures based on the Benedict method, in terms of simplicity, reliability high analysis rate and very small sample requirements. Because of these advantages, the method can be useful for routine screening tests on samples from newborns and infants.

This research was supported in part by a research grant from the National Institute of Research.

REFERENCES

1 J. F. Zilva and P. R. Pannall, Clinical Chemistry in Diagnosis and Treatment, Lloyd-Luke, London, 2nd edn., 1975, pp. 210, 371.
2 I. Davidsohn and J. B. Henry (Eds.), Todd-Sanford Clinical Diagnosis by Laboratory Methods, W. B. Saunders, Philadelphia, 15th edn., 1974, pp. 19, 55.
3 R. J. Henry, D. C. Cannon and J. W. Winkelman (Eds.), Clinical Chemistry, Principles, and Technics, Harper & Row, New York, 2nd edn., 1974, p. 1297.
4 N. W. Tietz (Ed.), Fundamentals of Clinical Chemistry, W. B. Saunders, Philadelphia, 1976, p. 258.
5 G. J. Moody and J. D. R. Thomas, Analyst, 100 (1975) 609.
6 P. J. Elving, Bioelectrochem. Bioenerg., 2 (1975) 251.
7 D. S. Papastathopoulos and G. A. Rechnitz, Anal. Chem., 47 (1975) 1792.
8 D. S. Papastathopoulos and G. A. Rechnitz, Anal. Chim. Acta, 79 (1975) 17.
9 C. E. Hjemdahl-Monsen, D. S. Papastathopoulos and G. A. Rechnitz, Anal. Chim. Acta, 88 (1977) 253.
10 D. S. Papastathopoulos, D. P. Nikolelis and T. P. Hadjiioannou, Analyst, 102 (1977) 852.
11 G. Johansson and K. Edström, Talanta, 19 (1972) 1623.
12 Cupric Ion Electrode Instruction Manual, Form IM 94-29/1721, Orion Research Inc., 1971.
13 I. M. Kolthoff and R. Belcher, Volumetric Analysis, Vol. III, Interscience, New York, 1957, pp. 357 and 361.
14 P. L. Bailey, Analysis with Ion-Selective Electrodes, Heyden, London, 1976, p. 187.
15 CRC, Manual of Clinical Laboratory Procedures, The Chemical Rubber Co., Cleveland, Ohio, 2nd edn., 1970, p. 51.
16 W. W. Wells, T. Chin and B. Weber, Clin. Chim. Acta, 10 (1964) 352.
17 V. J. Harding and C. E. Downs, J. Biol. Chem., 101 (1933) 487.
18 J. P. Comer, Anal. Chem., 28 (1956) 1748.
19 M. Samson, J. Am. Chem. Soc., 61 (1939) 2389.

Analytica Chimica Acta, 98 (1978) 233—241

BEHAVIOUR OF MEMBRANE GRAPHITE ELECTRODES IN POTENTIOMETRIC TITRATION OF BASES AND REDUCING SUBSTANCES IN ACETIC ACID MEDIA

T. J. PASTOR*, V. J. VAJGAND and Ž. SIMONOVIĆ
Department of Chemistry, Faculty of Sciences, University of Belgrade (Yugoslavia)
É. SZEPESVÁRY
Institute for General and Analytical Chemistry, Technical University, Budapest (Hungary)
(Received 10th December 1977)

SUMMARY

Potentiometric titrations of bases with perchloric acid, and of reducing substances with lead(IV) acetate, in acetic acid medium and in a mixture of acetic acid and acetic anhydride are discussed. The indicator electrodes used were: a Radelkis membrane graphite electrode (OP-C-7112 C), laboratory-prepared silicone rubber-based graphite electrodes, an Elektrokarbon graphite electrode (SU 106), a Radiometer glass electrode (G 200 B), and a platinum electrode. In addition, new types of silicone rubber-based electrodes were prepared by incorporating mixtures of graphite and manganese dioxide, graphite and quinhydrone, and manganese dioxide in their membranes. A manganese dioxide electrode was also prepared by electrolytic precipitation of manganese on a platinum anode. The properties of all the cited electrodes are compared. The influence of oxidants, especially potassium permanganate, on the behaviour and sensitivity of graphite membrane electrodes in the potentiometric acid—base and redox titrations is described.

The behaviour of graphite electrodes in potentiometric acid—base titrations has been studied intensively only since the discovery of the possibility of decreasing their surface porosity by impregnation and the development of procedures for obtaining special types of compact graphite. Pioneers in this field, Berčik et al. [1—9] investigated titrations in aqueous [1] and non-aqueous [2—9] media, using impregnated graphite indicator electrodes [1—9] as well as electrodes prepared from natural graphite from Sri Lanka [2, 7] and glassy carbon electrodes [6, 7, 9]. In his first study [1], Berčik observed that the potential of wax-impregnated graphite electrodes changes linearly with pH in aqueous solutions and that their sensitivity can be increased by brief immersion in an acidified aqueous solution of a suitable oxidant, such as potassium bromate, dichromate or permanganate. In almost all the solvents used, the most sensitive electrodes were those which had been kept in potassium permanganate solution. This was explained as resulting from the formation of a quinone—hydroquinone redox system on the electrode surface during the activation process [1—6] or from the establishment

of a mixed potential between separated manganese dioxide on the electrode surface and the solution [7—9].

Pyrolytic graphite indicator electrodes were used by Miller [10] and Thomason [11] in the potentiometric titration of acids and bases in aqueous and non-aqueous media. On the basis of their properties, Miller [10] assumed that these electrodes function like an oxygen electrode.

Glassy carbon indicator electrodes were studied in detail in potentiometric, bipotentiometric and biamperometric titrations of acid—base systems in aqueous media [12—14]. The *i—E* curves of electrodes recorded in titrated systems show that the potential of polarized electrodes is determined by the reduction of dissolved oxygen at the cathode and by the oxidation of water at the anode [12, 13]. A couple comprising a glassy carbon electrode and a glassy carbon graphitic oxide electrode gives titration curves with a definite maximum at the titration end-point, when either strong or weak acids are determined [14].

The potential of carbon-fibre pH-sensitive electrodes does not depend on the presence of oxygen in the test solution [15], but is thought to be due to the ionization of carboxylic acid groups formed on the electrode surface by reactions with atmospheric oxygen [16].

Pungor and Szepesváry [17] described the preparation of silicone rubber-based graphite electrodes of low porosity. These electrodes were used as indicator electrodes for potentiometric acid—base titrations in water and acetone [18, 19]; again, electrodes activated by an acidic solution of potassium permanganate showed the greatest potential jumps at the titration end-point.

Non-activated graphite electrodes made of pyrolytic graphite [10] and glassy carbon [14] are also suitable for redox titration in aqueous media. Preliminary investigations have shown that carbon fibre electrodes [16] and graphite-activated Selectrodes [20] can also be used for end-point detection in potentiometric redox titrations.

Because of the low porosity of silicone rubber-based graphite electrodes, and because their preparation allows other components to be incorporated easily in the membrane so that the electrodes of different compositions and properties can be obtained, it was considered worthwhile to investigate their behaviour further. Accordingly, new types of electrodes were prepared by incorporating manganese dioxide, and mixtures of graphite and manganese dioxide or graphite and quinhydrone in the membranes. The properties of electrodes obtained in this manner were compared with the features of other indicator electrodes used in potentiometric acid—base and redox titrations in highly-corrosive solvents such as acetic acid and acetic anhydride.

EXPERIMENTAL

Electrodes

The following electrodes were used:

(1) glass electrode (Radiometer type G 200 B);

(2) membrane graphite electrode (Radelkis type OP-C-7112C);

(3) silicone rubber-based membrane electrodes prepared by the method of Pungor and Szepesváry [17], with membranes (active surface area, 2 mm or 5 mm in diameter) containing (a) finely powdered spectrographically-pure graphite, (b) mixture of graphite and manganese dioxide in 3:1, 1:1 and 1:3 ratios, (c) mixture of graphite and quinhydrone in 1:1 ratio, and (d) manganese dioxide;

(4) manganese dioxide electrode obtained by electrolytic precipitation of manganese on a platinum anode of 0.5-cm^2 area from a solution containing manganese(II) sulfate, sodium formate and formic acid [21];

(5) graphite electrode (Elektrokarbon SU 106, Topolčany) of 2-cm^2 surface area;

(6) platinum electrode, of 6-cm^2 area;

(7) mercury—mercury(I) acetate reference electrode [22].

Chemicals and solutions

The solvents, reagents and titrated substances used were either of analytical grade or high-quality pharmaceutical industry products and were not further purified.

Lead(IV) acetate was prepared by dissolving minium (Pb_3O_4) in acetic acid by heating [23]. A 5×10^{-2} M lead(IV) acetate solution was prepared by dissolving the appropriate amount of this salt in acetic acid; it was standardized by the method of Berka et al. [24]. A 5×10^{-3} M lead(IV) acetate solution was prepared by exact dilution.

Solutions of perchloric acid in acetic acid were prepared as described previously [25].

Apparatus and procedure

Changes in solution acidity, i.e. in the e.m.f. cells during titration, were measured with a tube voltmeter (Radiometer pH meter type 22p and PHM 26). The volumes of the solutions to be titrated were 18—25 ml in a 50-ml beaker and the solutions contained 5×10^{-5}—5×10^{-4} mol of the substance determined.

The membrane electrodes were kept in distilled water for 16—24 h prior to use. Immediately before measurement, the graphite electrodes were treated by brief immersion (3—5 min) in one of the following solutions: acidified aqueous 2×10^{-3} M, 2×10^{-2} or 2×10^{-1} M potassium permanganate solution, 2×10^{-1} M potassium dichromate solution, 5×10^{-1} M cerium(IV) sulfate solution, or a saturated solution of lead(IV) acetate in acetic acid. After activation, the electrodes were washed with water, and dried with filter paper and a cold air stream. When necessary, the activated electrodes were reduced at the end of titration by immersion in a 5×10^{-2} M solution of tin(II) chloride in 1 M hydrochloric acid or in dilute solutions of other suitable reductants.

RESULTS

Titrations of bases

Initially, the behaviour of Radelkis membrane graphite electrodes was examined in detail for the potentiometric titration of sodium acetate with 0.1 M perchloric acid in acetic acid. The non-activated electrode showed exceedingly small potential changes during titration, and it was impossible to determine the titration end-point exactly (Fig. 1). Its characteristics and properties changed very little even after immersion in an acidified aqueous solution of cerium(IV) sulfate or in a saturated solution of lead(IV) acetate in acetic acid. Somewhat greater potential changes at the titration end-point, 30—40 mV, were exhibited after activation in a potassium dichromate solution. The greatest effect on the sensitivity of this electrode, similarly to other types of graphite electrodes [1—9, 18, 19], was exercised by the higher concentrations of potassium permanganate solution. For this reason, in the later phases of the work, the graphite electrodes were activated only with the 2×10^{-1} M solution of potassium permanganate.

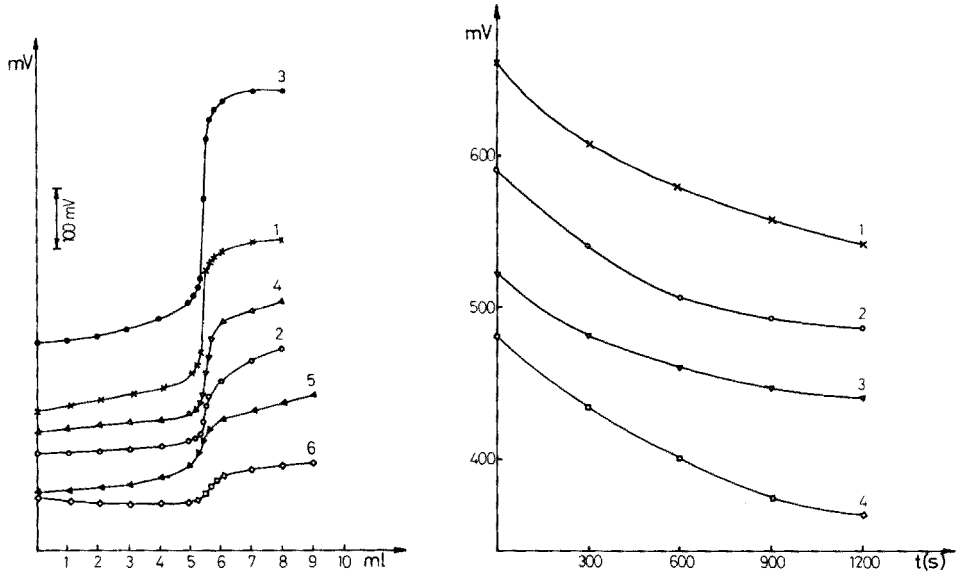

Fig. 1. Potentiometric titration curves of sodium acetate with perchloric acid obtained with a glass electrode (1); a non-activated Radelkis membrane graphite electrode (2); and this electrode activated by immersion in an acidified aqueous solution of potassium permanganate (3), potassium dichromate (4) and cerium(IV) sulfate (5), and a saturated solution of lead(IV) acetate in acetic acid (6).

Fig. 2. Variation with time of the Radelkis membrane graphite electrode potential in a solution of sodium acetate in acetic acid after electrode pre-treatment with an acidified aqueous solution of 5×10^{-1} M cerium(IV) sulfate (1), 2×10^{-1} M potassium permanganate (2), 2×10^{-1} M potassium dichromate (3), and a saturated solution of lead(IV) acetate in acetic acid (4).

Several successive determinations can be made with an activated electrode but the sensitivity decreases; it is approximately halved even in the second titration. Therefore, it is necessary to activate the electrode prior to each determination in order to conduct the titration successfully. This causes a constant increase in the initial value of the electrode potential but does not affect its sensitivity or the accuracy of determination. In order to obtain fair reproducibility of the potential values of successive titrations, the membrane graphite electrode should be reduced after every determination and activated immediately before a new titration.

It is characteristic that regardless of the oxidant used, the potential of a freshly-activated electrode changes significantly on immersion in a test solution, usually by 100—150 mV in 20 min (Fig. 2). The electrode potential then becomes almost steady and titration can be carried out. Under these working conditions, a steady potential is achieved quickly after each addition of titrant; only in the vicinity of the end-point, 2—3 min must be allowed before further addition of the titrant.

The nature and composition of the solvent used does not greatly affect the behaviour of the non-activated electrode. However, they do affect the behaviour of activated electrodes. When antipyrine is titrated in pure acetic acid or in a 1:1 mixture of acetic acid and acetic anhydride, not even the use of electrodes activated with a potassium permanganate solution gives greater changes of potential at the end-point; in pure acetic anhydride, the potential jumps are enhanced considerably (40—50 mV/0.1 ml $HClO_4$).

The results obtained with a Radelkis membrane graphite electrode activated with a potassium permanganate solution are shown in Table 1. It can be seen that this electrode can be used successfully for the determination of base hydrochlorides in the presence of mercury(II) acetate. Small amounts of bases can also be successfully titrated with a 10^{-2} M solution of perchloric acid, because the decrease in the potential jump at the equivalence point is smaller when this electrode is used than is the case with glass electrodes.

Silicone rubber-based graphite electrodes, prepared by the method of Pungor and Szepesváry [17], behave similarly to the electrode described above but are somewhat more sensitive. These electrodes, after activation with a 2×10^{-1} M potassium permanganate solution, give a potential jump of 160—170 mV at the end-point in titrations of bases with a 0.1 M solution of perchloric acid in acetic acid.

In order to interpret correctly the functioning of these electrodes, it was considered relevant to study the properties and behaviour of electrodes with membranes containing both manganese dioxide and graphite. Such electrodes showed some differences as well as a number of common properties with the permanganate-activated membrane graphite electrodes. For example, their potential on first immersion in a solution of a base in acetic acid increased slowly (30—40 mV during the first 20 min), whereas in later determinations the potential decreased if the electrode was kept in distilled water between two titrations. The establishment of potential was rapid

TABLE 1

Potentiometric titrations of bases with a 0.1 M solution of perchloric acid in acetic acid with a Radelkis membrane graphite electrode activated by permanganate

Substance titrated	Taken (mg)	Electrodes used[a]	
		MA—G found[b] (%)	MA—C found[c] (%)
Sodium acetate	41.0	99.98	100.10 ± 0.09
Nicotinamide	61.1	100.03	100.23 ± 0.07
Isoniazid	68.6	99.92	99.93 ± 0.29
Sodium *p*-aminosalicylate	105.6	99.94	100.13 ± 0.07
Aminopyrine	115.7	99.95	99.99 ± 0.16
Promethazine—HCl	160.4	100.04	100.22 ± 0.25
Pyridoxine—HCl	102.8	99.98	99.83 ± 0.19

[a]MA — Mercury—mercury(I) acetate electrode. G — Glass electrode. C — Graphite electrode (Radelkis). [b]Mean result of 4 titrations. [c]Mean result of 8 titrations with average deviation.

except at the equivalence point, as for the graphite membrane electrodes. However, when the electrodes were kept in acetic acid between titrations, they showed a stable potential as soon as they were immersed in the sample solution. The sensitivity of the electrodes based on graphite and manganese dioxide increased after storage for 60 h in acetic anhydride or for 20 h in a dilute solution of perchloric acid in acetic acid; longer treatment with the latter solution led to a decrease in electrode sensitivity, probably because of dissolution of manganese dioxide from the surface layer of the membrane. However, the establishment of potential on electrodes treated in this manner was slow, so that the potentials near the end-point had to be read 10 min after each addition of titrant. It should be emphasized that the nature of the solvent used again affected the behaviour of these electrodes. Thus, in three consecutive titrations of sodium acetate with 0.1 M perchloric acid in acetic acid, the potential jumps at the end-point were 160, 90 and 50 mV, whereas the jumps obtained in similar titrations in acetic anhydride were 180, 130 and 100 mV.

The membrane electrodes which incorporated only manganese dioxide were not suitable for measuring solution acidity because of their high resistance.

Electrodes prepared by electrolytic precipitation of manganese dioxide on a platinum anode showed stable potential values during titration and larger potential jumps at the end-point (about 300 mV/0.1 ml $HClO_4$) than any of the above electrodes (Fig. 3).

Membrane graphite electrodes with quinhydrone incorporated showed a somewhat higher sensitivity than the non-activated graphite electrodes only in the first titration. This can be explained by the dissolution of quinhydrone

from the electrode surface and by the insufficient quantity of an active component in the solution for the formation of a redox couple with a potential dependent upon the concentration of hydrogen ions. The correctness of this interpretation is supported by the fact that when silicone rubber-based graphite electrodes were used in titrations of quinhydrone-saturated solutions of a base, sharp potential jumps were obtained at the end-point (up to 300 mV), as in the case of a platinum electrode (Fig. 3).

Titration of reducing substances

On the basis of the above results, it could be considered that silicone rubber-based graphite indicator electrodes should also give good results in potentiometric redox titrations in non-aqueous solutions. In order to prove this, hydroquinone in acetic acid was titrated with a 0.05 M lead(IV) acetate solution. Figure 4 shows that the platinum electrode and the freshly-prepared silicone rubber-based graphite electrode gave regularly-shaped titration curves

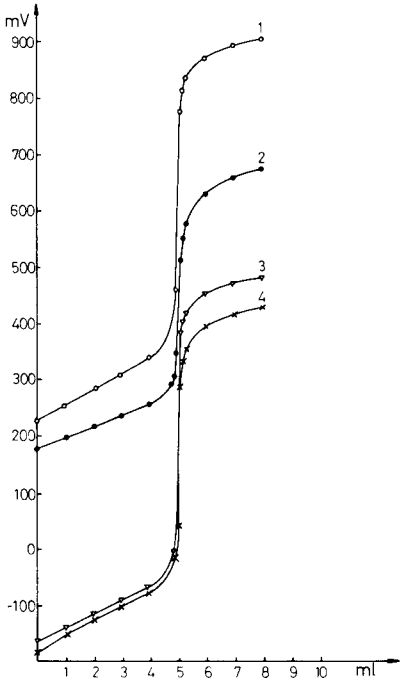

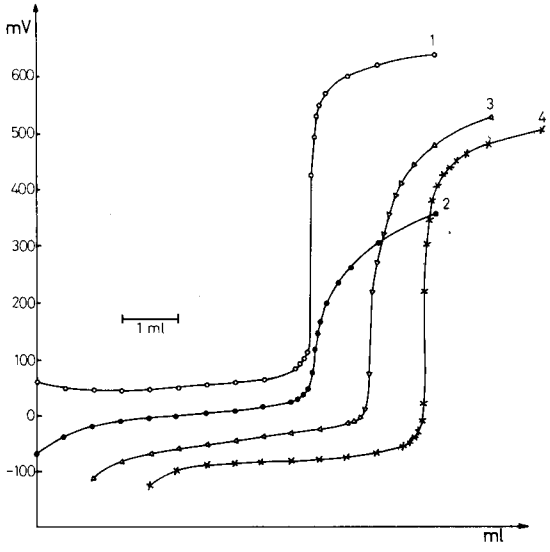

Fig. 3. Potentiometric titration curves of sodium acetate with 0.1 M perchloric acid obtained with a manganese dioxide electrode prepared electrolytically (1), a silicone rubber-based graphite electrode with incorporated manganese dioxide (2), a platinum electrode in the presence of quinhydrone (3) and a silicone rubber-based graphite electrode in the presence of quinhydrone (4).

Fig. 4. Potentiometric titration curves of hydroquinone with a 0.05 M solution of lead(IV) acetate in acetic acid obtained with a platinum electrode (1), a Radelkis membrane graphite electrode (2), an Elektrokarbon graphite elektrode (3), and a laboratory-prepared silicone rubber-based graphite electrode with a fresh surface (4).

with a sharp potential jump at the end-point. The establishment of potential at these electrodes was rapid except at the equivalence point. However, in the determination of very dilute solutions of hydroquinone with a 5×10^{-3} M solution of lead(IV) acetate, only the platinum indicator electrode gave acceptable results (Table 2). The silicone rubber-based graphite electrodes also behaved similarly in direct titrations of 2-mercaptoethanol (Table 2). The presence of acetic anhydride in the test solution did not improve the results, but caused a shift in the potential value, i.e. in the position of the titration curves.

The Radelkis membrane graphite electrode pre-treated with oxidants and the Elektrokarbon graphite electrode cannot be used for end-point detection in titrations with lead(IV) acetate solutions in acetic acid, because the potential jumps are not well defined (Fig. 4). This is probably due to contamination of the surface of the former electrode and to the porosity of the surface of the latter electrode.

DISCUSSION

The results show that the sensitivity of membrane graphite electrodes towards changes in the hydrogen ion concentration in acetic acid solutions is low. Pre-treatment of these electrodes with a saturated solution of lead(IV) acetate in acetic acid or with an acidified aqueous solution of cerium(IV) sulfate does not significantly improve their properties, whereas somewhat larger changes of potential are obtained after treatment with a solution of potassium dichromate. However, the greatest improvement in the sensitivity of these electrodes was achieved by pre-treatment with solutions of potassium permanganate. The positive influence of this oxidant can, on the basis of literature data and on the present observations, be explained both by oxidation of the surface layer of graphite [1—6, 16, 26, 27] and by the separation of manganese compounds of higher oxidation state on their surface [7—9, 28, 29] during activation. In this study, electrodes were made

TABLE 2

Potentiometric titrations of reducing substances with lead(IV) acetate solution in acetic acid with a silicone rubber-based graphite electrode

Substance titrated	Taken (mg)	Electrodes used[a]			
		MA—Pt		MA—C	
		No. of titns.	Found (%)	No. of titns.	Found (%)
Hydroquinone	27.6	12	100.07 ± 0.52	12	100.57 ± 0.37
	2.75	7	100.60 ± 0.22	20	101.79 ± 0.69
2-Mercaptoethanol	9.82	5	100.23 ± 0.04	6	100.24 ± 0.16

[a]MA — Mercury—mercury(I) acetate electrode. C — Silicone rubber-based graphite electrode (freshly-prepared).

from membranes containing manganese dioxide or quinhydrone in addition to graphite. There is a similarity in behaviour between the electrodes with incorporated manganese dioxide and membrane graphite electrodes activated by potassium permanganate solution. Their properties are akin to those of the manganese dioxide electrodes described in the literature [28, 29]. Quinhydrone incorporated in the membrane of graphite electrodes has a small influence on the form of the curves obtained in titrations of bases with perchloric acid, but only in the first titration.

Unused silicone rubber-based graphite electrodes, i.e. with fresh surfaces, behave as almost ideal indifferent electrodes and can be used successfully as indicating electrodes for potentiometric redox titrations in acetic acid.

The authors are grateful to the Serbian Research Fund for financial support. We are indebted to Professor E. Pungor for helpful discussions and suggestions.

REFERENCES

1 J. Berčik, Chem. Zvesti, 14 (1960) 372.
2 J. Berčik and Z. Hladký, Proc. Conf. Appl. Phys.-Chem. Methods Chem. Anal., Budapest, 1 (1966) 99; Chem. Abstr., 69 (1968) 23959h.
3 J. Berčik and Z. Hladký, Chem. Zvesti, 17 (1963) 95.
4 J. Berčik and M. Čakrt, Chem. Zvesti, 22 (1968) 755.
5 J. Berčik, M. Čakrt and K. Derzsiová, Chem. Zvesti, 22 (1968) 761.
6 J. Berčik and Z. Hladký, Chem. Zvesti, 22 (1968) 768.
7 J. Berčik, M. Čakrt and Z. Hladký, Chem. Zvesti, 24 (1970) 290.
8 J. Berčik, Z. Hladký and M. Čakrt, Chem. Zvesti, 24 (1970) 298.
9 J. Berčik, Z. Hladký and M. Čakrt, Z. Anal. Chem., 261 (1972) 113.
10 F. J. Miller, Anal. Chem., 35 (1963) 929.
11 P. F. Thomason, Microchem. J., 8 (1964) 234.
12 J. Doležal and K. Štulik, J. Electroanal. Chem., 17 (1968) 87.
13 E. Samcová, K. Štulik and J. Doležal, Collect. Czech. Chem. Commun., 37 (1972) 60.
14 A. Dodson and V. J. Jennings, Anal. Chim. Acta, 72 (1974) 205.
15 V. J. Jennings and P. Pearson, Nature (London), 256 (1975) 31.
16 V. J. Jennings and P. Pearson, Anal. Chim. Acta, 82 (1976) 223.
17 E. Pungor and É. Szepesváry, Anal. Chim. Acta, 43 (1968) 289.
18 É. Szepesváry and E. Pungor, Anal. Chim. Acta, 54 (1971) 199.
19 É. Ráth Szepesváryné and E. Pungor, Magy. Kém. Folyoirat, 77 (1971) 502.
20 J. Ružička, C. G. Lamm and J. Chr. Tjell, Anal. Chim. Acta, 62 (1972) 15.
21 A. Schleicher, Elektroanalytische Schnellmethoden, Ferdinand Enke, Stuttgart, 1947, p. 124
22 W. B. Mather, Jr. and F. C. Anson, Anal. Chim. Acta, 21 (1959) 468.
23 A. I. Vogel, A Text-Book of Practical Organic Chemistry, Including Qualitative Organi Analysis, 3rd edn., Longman, London, 1970, p. 199.
24 A. Berka, J. Janata and J. Zýka, Collect. Czech. Chem. Commun., 29 (1964) 2242.
25 V. Vajgand and T. Pastor, Bull. Soc. Chim. Beograd, 34 (1969) 267.
26 A. Clauss, R. Plass, H. P. Boehm and U. Hofmann, Z. Anorg. Allg. Chem., 291 (1957) 205.
27 V. Majer and J. Veselý, J. Electroanal. Chem., 45 (1973) 113.
28 I. I. Zhukov and Yu. A. Boltunov, Zh. Obshch. Khim., 2 (1932) 407.
29 R. S. Johnson and W. C. Vosburgh, J. Electrochem. Soc., 99 (1952) 317.

Analytica Chimica Acta, 98 (1978) 243—250

DETERMINATION OF CHROMIUM(III) AND CHROMIUM(VI) IN SEA WATER BY ATOMIC ABSORPTION SPECTROMETRY

G. J. de JONG and U. A. Th. BRINKMAN*

Department of Analytical Chemistry, Free Reformed University, Amsterdam (The Netherlands)

(Received 24th October 1977)

SUMMARY

A method is described for the selective determination of chromium(VI) and chromium(III) in sea water. Chromium(VI) is quantitatively extracted with Aliquat-336 from weakly acidic (pH 2) sample solutions. Successful extraction of chromium(III) is achieved from neutral (pH 6—8) solutions containing at least 1 M thiocyanate. The chromium content of the organic extracts is measured by flameless atomic absorption spectrometry at 357.9 nm. The detection limits are 0.01 and 0.03 $\mu g\ l^{-1}$ of chromium(VI) and chromium(III), respectively. Alternatively, chromium(III) can be extracted, as chromium(VI), after oxidation by ammonium persulphate.

An understanding of the chemical speciation and oxidation state of trace elements in sea water is important from both environmental and geochemical view-points. Chromium is one of the elements that is present in sea water in two valency states. The mechanism of the toxicity of chromium(VI) is not yet well understood, but it seems to interfere with the enzymatic sulphur uptake of the cell [1] and it can affect the lungs, liver and kidneys [2, 3]. There have been no reports of oral toxicity of chromium(III); indeed, it is necessary for the maintenance of a normal glucose tolerance factor [2, 4, 5].

According to Elderfield [6], thermodynamic considerations suggest the predominance of chromium(VI) in sea water but the analytical data contradict this conclusion. Elderfield points out several reasons for the discrepancy between calculation and analysis: (1) it is likely that the kinetics of the chromium(III)—chromium(VI) oxidation are such that equilibrium, i.e., the formation of chromium(VI) as a major species, is only slowly attained; (2) because of lack of pertinent data, several relevant equilibrium species, such as organic complexes of chromium(III), and reactions such as reduction of chromium(VI) by organic substances, were not considered in the model; (3) prior to analysis, sea-water samples are often filtered through 0.45-μm membrane filters; the presence of any sub-0.45-μm particulates may bias the chromium oxidation ratio towards the trivalent ion.

In the analysis, many sampling techniques and separation and/or preconcentration procedures may disturb, to some extent, the equilibria between

TABLE 1

Literature data on the chromium(III) and (VI) contents of sea water

Sampling locality	Method of concentration	Method of determination	Chromium content ($\mu g\ l^{-1}$)			Ref
			Cr(III)	Cr(VI)	Total Cr	
Boston Harbour	Extraction with APDC—MIBK after oxidation	Flame a.a.s.			0.27—3.69	7
Japanese coastal water	Extraction with DDTC—MIBK	Flame (less) a.a.s.		0.35—1.3		8
North Sea	Coprecipitation with iron(III) hydroxide	Flame a.a.s.			0.38—1.41	10
Irish Sea	Coprecipitation with iron(III) hydroxide	Spectrometry with diphenylcarbazide			0.46	11
Ligurian Sea	Coprecipitation with iron(III) hydroxide (with and without sulphite treatment)		<0.02—0.23	0.05—0.36		12
North Sea	Adsorption on activated carbon	Neutron activation analysis			0.6—3.3	13

the various species in solution. For example, adsorption losses and contamination occur easily during filtration and centrifugation. A normal preservation method, such as acidification, can affect the speciation; yet, if no such method is used, significant changes in the water composition are known to occur quite rapidly. Some typical literature data on the analysis of sea water are recorded in Table 1. As for the results obtained by means of extraction with ammonium pyrrolidine dithiocarbamate (APDC)—methyl isobutyl ketone or diethyl dithiocarbamate (DDTC)—methyl isobutyl ketone, one should realize that the extractability of chromium(VI) has been shown to vary from 50—100% [7—10]. In such cases, the extraction efficiency is strongly dependent on the composition of the sea-water sample and a yield determination is always necessary. Coprecipitation of chromium(III) with iron(III) hydroxide suffers from the disadvantage that chromium(VI) also appears to be, partly, adsorbed on the precipitate [10—12]. The separate determination of chromium(III) and chromium(VI) by neutron activation analysis after preconcentration on activated carbon is hampered by the high chromium blank of the carbon and by the necessity of measuring the adsorption percentage of chromium(VI) on carbon [13].

In this paper, a method is presented for the quantitative separation and preconcentration of chromium(III) and chromium(VI) in sea water, with a high-molecular-weight ammonium salt as extractant. In this way, the application of an inaccurate difference determination is circumvented.

EXPERIMENTAL

Materials

Standard solutions were prepared from analytical-grade chromium(III) nitrate and potassium chromate; the chromium(III) solutions were acidified to 0.01 M with hydrochloric acid. Aliquat-336 (General Mills, Kankakee, Illinois), a yellow viscous liquid, is a mixture of methyltri-n-alkylammonium chlorides with alkyl groups that consist mainly of C_8—C_{10} chains; its mean molecular weight is 475. All other chemicals were of analytical-grade quality and were tested for low chromium blanks.

Samples

Sea-water samples (2—25 l) were collected in polyethylene bottles, which were conditioned by shaking with ca. 1 M nitric acid and deionized water. In order to prevent the adsorption of chromium(III) on the wall of the bottles [7, 14, 15], an amount of hydrochloric acid sufficient to acidify the samples to pH 2 was put into the containers prior to sampling for the chromium(III) analyses. With chromium(VI), losses were shown to be negligible from neutral solutions (also see ref. 15). However, at pH 2, the hexavalent ion is slowly reduced to chromium(III), the rate of reduction being dependent on the composition of the sea-water sample. In the present investigation, chromium(VI) was found to be absent from all samples acidified immediately after the sampling, and analyzed after a period of time of 24 (or more) h.

For the preliminary investigations, solutions of chromium(III) and (VI) in deionized-distilled water were used. To 500 ml of these solutions 14 g of sodium chloride were added to equal the concentration in sea water.

Extraction

Glass separatory funnels (1 l) were carefully cleaned with a (1 + 1) mixture of 4 M nitric acid and 4 M hydrochloric acid and subsequently with deionized water. For the extraction of chromium(VI), the sea water was acidified to pH 2 with hydrochloric acid. For the extraction of chromium(III), enough potassium thiocyanate was added to obtain a concentration of 1 M; the solution was then neutralized with sodium hydroxide to pH 6—8. For the oxidation of chromium(III), 1 ml of a 0.1 M ammonium persulphate solution and 500 ml of sea water were boiled for 15 min.

After these additions of the appropriate reagents, 500 ml of sea water were equilibrated with 5 (chromium(VI)) + 15 (chromium(III)) ml of a 0.1 M solution of Aliquat-336 in toluene. After shaking for ca. 3 min, the phases were allowed to separate for 15—30 min. The chromium content of the organic phase was then measured by flameless atomic absorption spectrometry at 357.9 nm. Aliquots (50-μl) were injected for the following heating program: drying at 130°C for 1 min, ashing at 1350°C for 1.5 min and atomization at 2650°C for 15 s.

Apparatus

A Perkin-Elmer Model 403 atomic absorption spectrophotometer equipped with an HGA 72 graphite cell with no. 71868 carbon tubes was used.

RESULTS AND DISCUSSION

Extraction of chromium(VI)

The extraction of chromium(VI) from various acidic solutions with tertiary amines, substituted quaternary ammonium salts and other similar extractants has often been studied [16—20]. The nature of the species extracted into the organic phase appears to depend on the experimental conditions: $HCrO_4^-$, $Cr_2O_7^{2-}$, $HCr_2O_7^-$ and CrO_3Cl^- are the species reported in the literature. The influence of the hydrochloric acid concentration on the extractability of chromium(VI) was investigated for the extraction of 0.2 $\mu g\ l^{-1}$ of chromium(VI) with a 0.1 M solution of Aliquat-336 in toluene. The data in Table 2 demonstrate that the optimum acid concentration is not very critical: extraction is quantitative between about 0.005 and 0.02 M.

When sea-water samples spiked with up to 0.8 $\mu g\ l^{-1}$ of chromium(VI) were used, recovery of the hexavalent ion was quantitative after a single extraction: the relative signal of the second extract was invariably negligible (<1%), provided that a suitable correction was applied for the amount of organic phase dissolved in the sea-water sample during the first extraction.

TABLE 2

Dependence of the relative absorbance (Abs.) of the organic phase on the HCl molarity for organic extracts obtained after extraction of chromium(VI) (0.2 $\mu g\ l^{-1}$) (Organic phase, 0.1 M Aliquat-336 in toluene. Aqueous phase, 0.2 μg Cr(VI) l^{-1} in 0—0.5 M HCl + 2.8% NaCl. V_{aq} = 500 ml; V_{org} = 5 ml.)

HCl (M)	0	0.001	0.005	0.01	0.02	0.05	0.10	0.20	0.5
Abs.	3	18	22.5	22	21	16	15.5	15	11

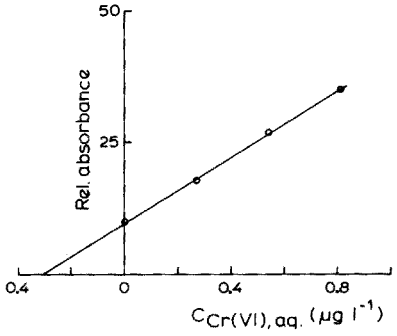

Fig. 1. Determination of the chromium(VI) content of a sea-water sample from the North Sea (53°45′ N, 5°20′ E; 16th February 1977) by standard addition. For experimental details, see text.

The result of the analysis of a sea-water sample by means of standard addition is shown in Fig. 1; a chromium(VI) content of 0.31 ± 0.02 $\mu g\ l^{-1}$ was found. For the selected phase ratio $V_{aq.}/V_{org.}$ = 500:5, the detection limit — defined as twice the standard deviation of the blank signal — for chromium(VI) is ca. 0.01 $\mu g\ l^{-1}$.

Extraction of chromium(III)

It has been shown [21] that about 10^{-4} M chromium(III) is extracted quantitatively from concentrated (>1 M) thiocyanate solutions with a solution of 0.1 M Aliquat-336 in, for example, tetrachloromethane, provided that the acidity of the aqueous phase is closely controlled. At such low concentrations, $Cr(SCN)_4(H_2O)_2^-$ is the predominant species in the organic extracts, but some $Cr(SCN)_6^{3-}$ may also be present. In this investigation, preliminary experiments showed that in the concentration range of chromium(III) encountered in sea water, the dependence of the percentage extraction on the acidity of the aqueous phase is again very critical. With about 4 M potassium thiocyanate, quantitative extraction of chromium(III) (0.2 $\mu g\ l^{-1}$) can be achieved from solutions acidified to pH 2. However, under these conditions, the chromium blanks are high and rather irreproducible. Besides, such a high thiocyanate concentration is not attractive for a routine method of analysis for large numbers of samples. When the thiocyanate concentration is lowered to 1 M, extraction of 0.2 $\mu g\ l^{-1}$ of chromium(III) is incomplete at $V_{aq.}/V_{org.}$ = 500:5, even if the solution is neutral. Therefore, to improve the percentage extraction, the amount of extractant solution was increased from 5 to 15 ml. Quantitative extraction is then possible and the blank signal has a low and constant value or is even negligible. Data on the dependence of the extraction efficiency of chromium(III) on the thiocyanate concentration and acidity of the aqueous phase are given in Table 3. It can be concluded that a thiocyanate concentration equal to or higher than ca. 1 M is required and that the extraction is complete only in the pH range 6—8. With the samples used here, addition of a buffer solution to maintain pH 6—8 was found to be superfluous. If, with other types of samples, pH control is necessary, care should be taken to limit the amount of buffer. For example, the addition of a relatively high amount of a phosphate buffer decreases the chromium(III) signal because of complexation, whereas the chromium blank increases.

As with chromium(VI), sea-water samples containing added chromium(III) were used to demonstrate the quantitative recovery after a single extraction. Analysis of a sea-water sample (Fig. 2A) showed a chromium(III) content of 0.09 ± 0.03 $\mu g\ l^{-1}$. The detection limit for this method (at $V_{aq.}/V_{org.}$ = 500:15) is ca. 0.03 $\mu g\ l^{-1}$.

Lastly, it can be concluded from Tables 2 and 3 that chromium(VI) is not extracted in the pH range required for the extraction of chromium(III). Conversely, chromium(III) does not interfere in the determination of the hexavalent ion. Both conclusions were confirmed by the successive extraction of the ions from appropriate aqueous solutions.

TABLE 3

Dependence of the relative absorbance of the organic phase on the thiocyanate concentration and pH value for organic extracts obtained after extraction of chromium(III) (0.7 $\mu g\ l^{-1}$)
(Organic phase, 0.1 M Aliquat-336 in toluene. Aqueous phase, 0.7 μg Cr(III) l^{-1} in 2.8% NaCl. $V_{aq.}$ = 500 ml. $V_{org.}$ = 15 ml.)

At pH 7		At 1 M KSCN	
KSCN (M)	Relative absorbance	pH	Relative absorbance
0	3	4.0	17
0.25	5	5.0	18.5
0.50	11	6.0	31
1.0	24	7.0	31
1.5	24.5	8.0	28
		9.0	23

[a]The pH was adjusted with HCl and/or NaOH solution.

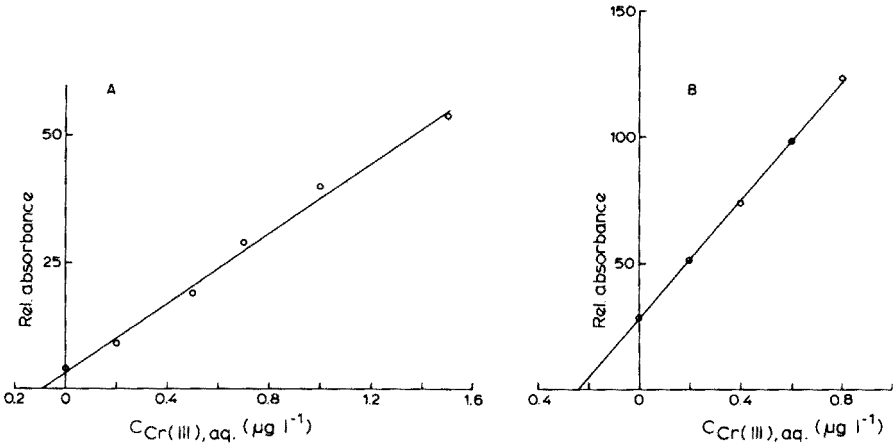

Fig. 2. Determination of the chromium(III) content of a sea-water sample from the North Sea (55°23′ N, 6°56′E; 22nd April 1977) by standard addition. For experimental details, see text. A, Thiocyanate method. B, Oxidation method.

Oxidation of chromium(III)

Determination of chromium(III) in sea water can also be carried out by its oxidation to chromium(VI), and subsequent extraction of the latter ion as described above. Gilbert and Clay [7] reported the complete oxidation of chromium(III) in sea-water samples (pH 8) heated to 50°C in less than 30 min, using a few drops of permanganate. In the present study, permanganate was added to heated chromium(III) solutions, as needed to maintain a pink colour. However, even after boiling solutions at either pH 8 or lower pH values, quantitative oxidation did not occur. The amount of

permanganate had to be limited, because this ion is also effectively extracted by Aliquat-336 and attacks the carbon tube during the subsequent analysis; also, when a relatively high permanganate concentration is used, the blank signal is significant. Incomplete oxidation of nanogram amounts of chromium(III) by permanganate has also been observed by Beyermann [22], who recommended ammonium persulphate. This reagent was applied successfully for the oxidation of chromium(III) in sea water. When an acidified sample was boiled for 15 min with 1 ml of a 0.1 M ammonium persulphate solution, quantitative recovery was observed, while the blank signal was negligible. The dependence of the percentage oxidation on the amount of ammonium persulphate and on the boiling time is shown in Table 4. Analysis of a sea-water sample (Fig. 2B) gave a chromium(III) content of 0.24 ± 0.02 $\mu g\ l^{-1}$.

DISCUSSION

The results of the above analyses are in the range of chromium concentrations reported in the literature (cf. Table 1). They demonstrate the applicability of all three procedures to the analysis of sea-water samples. However, the thiocyanate method gave a distinctly lower chromium(III) result than did the oxidation method (Fig. 2). Probably, the powerful oxidation carried out under acidic conditions releases (part of) the chromium(III) from such forms as colloids and highly stable complexes of chromium(III) with organic ligands, while these chromium(III)-containing species are unaffected by the treatment with thiocyanate. The presence of major amounts of chromium as particulate or non-dialyzable chromium has been reported for both sea [23] and river [24] water.

The hypothesis was confirmed by analyses of some samples of coastal water on the beach of Zandvoort (North Holland). These showed the

TABLE 4

Dependence of the percentage oxidation of chromium(III) on the ammonium persulphate concentration and on the boiling time
(Organic phase, 0.1 M Aliquat-336 in toluene. Aqueous phase, 0.8 μg Cr(III) l^{-1} in 0.01 M HCl + 2.8% NaCl. $V_{aq.}$ = 500 ml; $V_{org.}$ = 5 ml.)

At constant boiling time (15 min)		At constant 2×10^{-4} M $(NH_4)_2S_2O_8$	
$(NH_4)_2S_2O_8$ (M)	Relative absorbance	Boiling time (min)	Relative absorbance
5×10^{-5}	60	0	3
1×10^{-4}	105	1	31
2×10^{-4}	115[a]	2	46
1×10^{-3}	120	10	83
2×10^{-3}	115	15	110[a]
		30	110

[a]Relative absorbance after repeated treatment with ammonium persulphate, 0—5.

presence of 0.5—1.0 $\mu g\ l^{-1}$ for chromium(VI) and 1.0—1.5 $\mu g\ l^{-1}$ for chromium(III), as determined by the thiocyanate method. However, when the chromium(III) content of the unfiltered samples was determined by the oxidation method, the values obtained were higher by about one order of magnitude. In good agreement with this result, a total chromium concentration of ca. 10 $\mu g\ l^{-1}$ was found by direct analysis of the coastal sea water, i.e., without prior extraction. Consequently, it can be concluded that the combined use of the thiocyanate and oxidation methods should be of value in differentiating between the several forms of chromium present in natural waters.

The authors thank Mr. H. Bruins for skilful assistance in carrying out part of the experimental work, and Dr. P. Hagel of the Netherlands Institute for Fishery Investigation at IJmuiden for supplying sea-water samples.

REFERENCES

1 J. F. Pankow and G. E. Janauer, Anal. Chim. Acta, 69 (1974) 97.
2 V. Valković, Trace Element Analysis, Taylor and Francis Ltd., London, 1975, p. 107.
3 U. Förstner and G. Müller, Schwermetalle in Flüssen und Seen, Springer-Verlag, Berlin, 1974, p. 24.
4 K. Schwarz and W. Mertz, Arch. Biochem. Biophys., 72 (1957) 515.
5 K. Schwarz and W. Mertz, Arch. Biochem. Biophys., 85 (1959) 292.
6 H. Elderfield, Earth Planet. Sci. Lett., 9 (1970) 10.
7 T. R. Gilbert and A. M. Clay, Anal. Chim. Acta, 67 (1973) 289.
8 K. Hiiro, T. Owa, M. Takaoka, T. Tanaka and A. Kawahara, Bunseki Kagaku, 25 (1976) 122.
9 T. Matsuo, J. Shida, M. Abiko and K. Konno, Bunseki Kagaku, 24 (1975) 723.
10 C. H. v. d. Weijden, L. Vasak, P. Seeverens, L. Belle, M. Reith and H. A. van der Sloot, Chem. Weekbl., 71(13) (1975) 10.
11 L. Chuecas and J. P. Riley, Anal. Chim. Acta, 35 (1966) 240.
12 R. Fukai, Nature, 213 (1967) 901.
13 H. A. van der Sloot, J. Radioanal. Chem., 37 (1977) 727.
14 D. E. Robertson, Anal. Chim. Acta, 42 (1968) 533.
15 A. D. Shendrikar and P. W. West, Anal. Chim. Acta, 72 (1974) 91.
16 C. J. Deptula, J. Inorg. Nucl. Chem., 30 (1968) 1309.
17 W. Zmijewska, J. Radioanal. Chem., 10 (1972) 187.
18 V. M. Rao and M. N. Sastri, J. Indian Chem. Soc., 53 (1976) 1006.
19 J. Adam and R. Přibil, Talanta, 18 (1971) 91.
20 J. Hála, O. Navrátil and V. Nechuta, J. Inorg. Nucl. Chem., 28 (1966) 553.
21 G. J. de Jong and U. A. Th. Brinkman, J. Radioanal. Chem., 35 (1977) 223.
22 K. Beyermann, Fresenius Z. Anal. Chem., 190 (1962) 4.
23 B. A. Loveridge, G. W. C. Milner, G. A. Barnett, A. M. Thomas and W. M. Henry, AERE Rep. R-3323, 1960.
24 P. Benes and E. Steinnes, Water Res., 8 (1974) 947.

Analytica Chimica Acta, 98 (1978) 251—259

SPECIES-SPECIFIC ANALYSIS FOR NANOGRAM QUANTITIES OF ARSENIC IN NATURAL WATERS BY ARSINE GENERATION FOLLOWED BY GRAPHITE FURNACE ATOMIC ABSORPTION SPECTROMETRY

ALI U. SHAIKH and DENNIS E. TALLMAN*

Department of Chemistry, North Dakota State University, Fargo, North Dakota 58102 (U.S.A.)

(Received 25th October 1977)

SUMMARY

The determination of total arsenic as well as its speciation in natural waters has been carried out with excellent precision and accuracy and with nanogram sensitivity by flameless atomic absorption spectrometry. The various arsenic species in a water sample are reduced to the corresponding hydrides, collected in a liquid nitrogen cold trap from which they are selectively vaporized and then swept directly through the sample port into a graphite furnace for detection. The relative accuracy of the method is better than ±5% as determined by EPA reference samples. In order to test further the reliability of the method, total arsenic calculated from speciation analysis is compared to total arsenic determined by a procedure involving sample digestion.

Much attention has been focused on the determination of arsenic in the environment, largely because of the high toxicity of certain of its compounds. Moreover, the substantial differences in the toxicities of the various forms of arsenic [1] justify the continued development of improved techniques for the speciation analysis of environmental samples. The various arsenic forms may be separated by reduction of the arsenic compounds to the corresponding arsines followed by separation of the arsines either by gas chromatography [2, 3] or by sequential volatilization [4]. Detection schemes have consisted of microwave emission spectrometry [2], electron capture and flame ionization detection [3], d.c.-discharge emission [4] and hydrogen—air flame atomic absorption [3].

A procedure by which inorganic arsenic can be determined at the nanogram level by graphite-furnace atomic absorption spectrometry has already been reported [5]. A method by which the determination of total arsenic as well as its speciation can be achieved at the nanogram level by using a commercially available graphite-furnace a.a.s. detection system is described here. Arsines are generated and collected in a cold trap and are then selectively vaporized by a method similar to that of Braman et al. [4]. The vaporized arsines are then sequentially swept directly through the sample

port into the graphite tube furnace. Results are reported for the analysis of EPA reference samples and for the analysis of several urine and natural water samples, with comparative data.

The principal advantages of this approach are [1] simplicity of experimental requirements, [2] excellent precision and accuracy, and [3] linearity of the working curves over more than two orders of magnitude. It should be noted that a method similar to the one described here was employed by McDaniel et al. [6] for the determination of selenium, though speciation of selenium was not attempted.

EXPERIMENTAL

Apparatus

A Perkin-Elmer Model 603 AA spectrometer equipped with a deuterium background corrector and a Perkin-Elmer Model HGA-2100 graphite tube furnace were used; the absorbances were recorded on either the digital display of the spectrometer or a Perkin-Elmer Model 165 recorder. The peak height mode of absorbance measurement gave excellent precision and linearity and was used throughout this study. Background correction, though not essential, was used to alleviate possible interference from atmospheric moisture which, on humid days, tended to condense on the furnace windows. A Perkin-Elmer arsenic electrodeless discharge lamp was used, and all measurements were made at the most sensitive As resonance line (193.7 nm). A PDP-11/40 computer with a CRT graphics terminal was used to compute the best-fit least-squares curves for the standard addition experiments.

The arsine generator and its connection to the graphite furnace are depicted in Fig. 1. Arsines were generated in a 250-ml round-bottom flask fitted with a capped side tube. The ground-glass stopper was fitted with a purge gas system, as shown, with two three-way stopcocks which enabled the

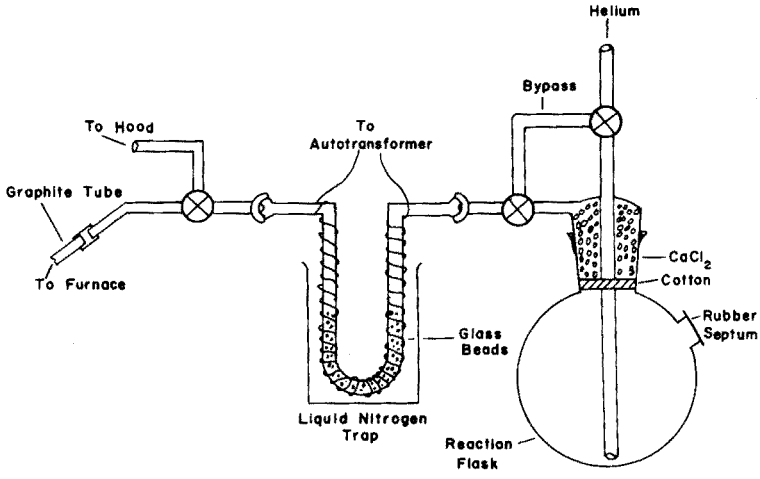

Fig. 1. Arsine generation, trapping and volatilization apparatus.

purge gas stream to be directed through the generator flask during arsine generation and trapping and through the bypass during volatilization and detection.

The pyrex U-tube, about 40 cm long and 1.2 cm in diameter, was half-filled with 60-80 mesh glass beads, and was connected by ball and socket joints. A heating coil (22-gauge bare chromium wire; Consolidated, Chicago, Illinois) about 2 m long, was wound around the U-tube. The three-way stopcock attached to the U-tube permitted the gas stream to be directed either to a hood for venting hydrogen produced during arsine generation or to the graphite furnace for atomization and detection of the arsines. The end of the tube extending from the trap to the furnace was joined to a graphite tube about 4 cm long (0.30-cm i.d., 0.45-cm o.d.). This tube was fabricated by drilling a hole coaxially through a solid emission spectrographic electrode (Union Carbide, New York), and was joined to the glass tubing by heat shrinking the glass tube around one end. This graphite gas injection tube is capable of withstanding the high atomization temperatures of the furnace. The sample inlet hole of the furnace tube was enlarged to 0.45-cm diameter, so that the tip of the graphite gas injection tube fitted snugly, ensuring complete passage of the arsines into the furnace.

Reagents

Distilled deionized water (Millipore Inc.) was used to prepare all solutions. As reported previously [4, 7], considerable loss of arsenic was observed when polystyrene or polypropylene bottles were used for storage of arsenic standards. Therefore, all arsenic solutions were prepared and stored in glass containers. Standard solutions of As(III) and As(V) were prepared in 0.1 M NaOH from Baker Analyzed As_2O_3 and As_2O_5, respectively. Methylarsonic acid (MAA; >95% purity, Alfa Chemicals) was used without further purification. Dimethylarsinic acid (DMAA; "purified" grade, Fisher Scientific) was purified further by the method of Kilpatrick [8]. Stock solutions of As(III) and As(V) were found to be quite stable up to two weeks, but MAA and DMAA solutions lost arsenic on standing and were discarded after 3—4 days. Solutions containing less than 1 ppm As were prepared on the day of the experiment.

Sodium borohydride (Alfa Chemicals) was used as a 5% solution in 0.1 M NaOH. Analytical-grade HCl (Dupont) was used for acidifying solutions. Acetate and citrate buffers were prepared from reagent-grade chemicals. Very small amounts of arsenic were present in the sodium borohydride and in the citrate buffers, hence all absorbance values were corrected for blanks.

EPA reference samples (Cincinnati, Ohio) were diluted according to the instructions and were stored in glass containers.

Procedures

Sample digestion. Portions of selected samples were digested prior to analysis for total arsenic. Three standard digestion procedures were attempted

[9]. Appreciable losses of arsenic from natural water samples were observed when the more vigorous $HClO_4/HNO_3$ and H_2SO_4/HNO_3 digestion methods were used. Therefore, the less vigorous $H_2SO_4/K_2S_2O_8$ method was employed as follows: to 100 ml of sample were added 1 ml of concentrated H_2SO_4 and 1 ml of 5% $K_2S_2O_8$. The solution was boiled strongly for 10 min, and cooled. An additional 10—15 ml of water was added, and the solution was boiled gently for another 10 min and made up to volume. Complete conversion of organic arsenicals to inorganic arsenic can be achieved in this way without apparent loss of arsenic. Urine samples were digested for a longer period (~1 h) to ensure complete conversion of organic arsenic to inorganic forms.

Analytical procedure. Arsenic was determined by placing a 1—90-ml aliquot of sample, depending on the As level, in the arsine generation flask and adding the appropriate amount of buffer or HCl to establish the desired pH (see below). The final volume was brought to 100 ml and the apparatus was then assembled as illustrated in Fig. 1. The stopcocks were set so that a helium flow of 400 cm^3 min^{-1} was directed through the flask and U-tube and then vented to the hood. The U-tube was immersed in liquid nitrogen, and after a 2-min cooling period, 2 ml of 5% $NaBH_4$ solution was injected through the rubber septum into the sample solution. After 30 s, a second 2-ml injection of $NaBH_4$ was made. This amount of $NaBH_4$ was usually sufficient for complete reduction of the arsenic species. The helium flow was continued for 5—6 min to ensure complete generation and trapping of the arsines and to vent completely the hydrogen formed during the reduction reaction. The helium flow was then stopped, and the liquid nitrogen was removed from around the U-tube which was allowed to warm at room temperature for 30 s. Next, the stopcocks were adjusted so that the helium would bypass the generator and flow from the U-tube to the graphite furnace. The U-tube heating coil, recorder, graphite furnace controller and gas flow were simultaneously activated, and absorbance was recorded for the requisite length of time (typically 30—50 s). A flow rate of 350 cm^3 min^{-1} yielded optimum resolution of the arsenic peaks. An atomization temperature of 2600°C was selected (see below). A convenient U-tube temperature ramp was obtained with an autotransformer setting of 35 V.

Total inorganic arsenic (inorganic As(III) plus As(V)), MAA and DMAA were determined at pH 0. No significant decomposition of the organoarsines was observed under these conditions. Inorganic As(III) alone was determined at pH 5 in acetate buffer by employing a second aliquot of sample. Inorganic As(V) was obtained by difference. Total arsenic in digested samples was determined at pH 0.

For standard addition analyses, one or more of three standards (As(III), MAA and DMAA) were added to the samples prior to hydride generation. Four such additions of the appropriate standards were used for each standard addition analysis.

RESULTS AND DISCUSSION

The absorbance resulting from analysis of a sample for inorganic arsenic was determined as a function of the atomization temperature; the results are summarized in Fig. 2. The sensitivity of detection increases with increasing atomization temperature and appears to reach a maximum at a temperature somewhat greater than 2800°C. Since arsine decomposes at temperatures considerably lower than 2800°C [10, 11], this observed atomization behavior may be due to deposition of elemental arsenic on the furnace tube from which it is slow to volatilize [10, 11]. A somewhat similar atomization behavior is observed when the silver diethyldithiocarbamate complex of arsine is injected into the graphite furnace [5], although the maximum in the atomization curve appears to occur at a somewhat lower temperature [2300—2400°C]. In this latter case, the silver diethyldithiocarbamate may provide a more efficient pathway for arsenic atomization. In any event, the furnace tube deteriorated very rapidly at the 2800°C atomization temperature, lasting for only 15—20 determinations, whereas at 2600°C, a tube could be used for 150 determinations. For this reason, an atomization temperature of 2600°C was selected, approximately 14% in sensitivity being sacrificed in exchange for prolonged tube life. Very little difference in sensitivity was noted when pyrolytically coated graphite tubes were used in place of uncoated tubes [12]. Mixing a small amount of hydrogen with the helium purge gas as suggested by Parris et al. [11] had no significant effect on the measured absorbances, but rather led to very rapid furnace tube deterioration.

Total inorganic arsenic was determined in samples acidified either with HCl to pH 0 or pH 1 or with oxalic acid to pH 1. Determinations in HCl at pH 0 yielded slightly larger absorbance signals than the other determinations,

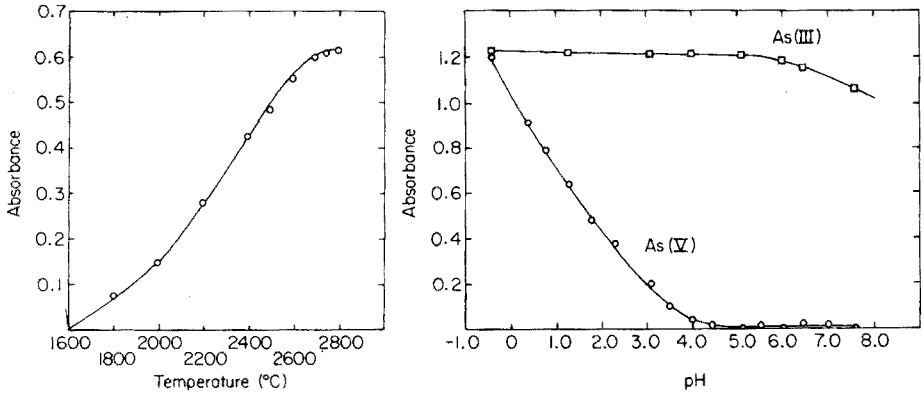

Fig. 2. Optimization of the atomization temperature for inorganic arsenic; 100 ng As(III) was used.

Fig. 3. A.a.s. response for As(III) and As(V) reduction at various pH values; 250 ng As as either As(III) or As(V) was used.

suggesting more complete generation of arsine from this medium. The variation in absorbance resulting from analyses for As(III) and As(V) as a function of pH is shown in Fig. 3. Although it has been reported [4] that As(III) can be determined selectively in the presence of As(V) at pH 3.5—4, Fig. 3 shows that a higher pH is required to alleviate interference by As(V). At pH 5, As(III) could be reduced selectively and determined without interference from up to a 100-fold amount of As(V). Similar behavior was observed in citrate buffer although this buffer system exhibited a small but constant background absorbance. Moreover, interference by As(V) in the determination of As(III) at pH 5 was less in acetate buffer than in citrate buffer. For these reasons, acetate buffer was preferred in determining inorganic As(III). A pH of 5 was chosen for the selective determination of As(III) since lower pH values gave rise to interference from As(V) (Fig. 3) whereas higher pH values led to lower rates of arsine generation.

Figure 4 displays typical absorbance signals for arsine, methylarsine and dimethylarsine. Phenylarsine and possibly other higher-molecular-weight organo-arsines, though most likely formed during the reduction step of the analysis, are not carried over to the cold trap because of their relatively low vapor pressures. However, their levels in natural waters are generally very low and, thus, they were of less interest to the present study. Trimethylarsine oxide, which can be detected by the proposed method at levels above 10 ng, was not detected in any of the natural water samples analyzed and, therefore, is not considered further here.

The reproducibility of the method is quite good. At the 100-ng level, corresponding to arsine generation from 50 ml of a 2-ppb water sample, ten replicate determinations of inorganic arsenic in reference samples yielded a r.s.d. of 2%. Somewhat poorer precision was obtained for MAA (r.s.d. 5%) and DMAA (r.s.d. 4%). Figure 5 illustrates the linearity and sensitivity of the method for the various forms of arsenic. For inorganic arsenic, linearity up to approximately 400 ng is observed with a sensitivity (corresponding to 1% absorption) of 0.7 ng. For MAA and DMAA, linearity to 600 ng is obtained, with a sensitivity of 10 ng As for MAA and 7 ng As for DMAA. Detection limits, in terms of ng As, are 1, 15 and 10 ng for inorganic arsenic, MAA and DMAA, respectively. The detection limits were determined from the amount of arsenic compound required to produce an increase in absorbance which was twice as large as the uncertainty associated with a blank analyzed in identical fashion.

Analysis of reference and other samples

To test the accuracy of the method, EPA reference samples were analyzed for inorganic arsenic by the method of standard additions. The reference samples were diluted so as to bring their arsenic concentration into the range commonly found in natural waters. The results of these analyses (Table 1) indicate a relative error of less than ±5%. Percentage recoveries were computed from the standard addition data for the EPA reference

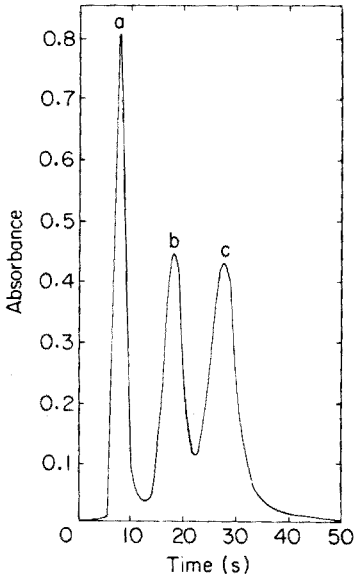

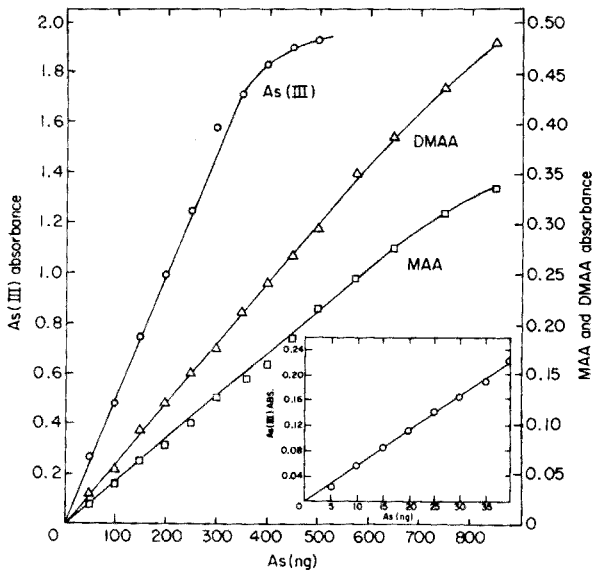

Fig. 4. A.a.s. response for sequential volatilization of arsine, methylarsine and dimethylarsine; (a) 150 ng As as As(III). (b) 500 ng As as MAA. (c) 325 ng As as DMAA.

Fig. 5. Standard calibration curves for inorganic arsenic, MAA and DMAA. Inset: As(III) in the range 0—35 ng.

TABLE 1

Analysis of EPA reference samples and river water for inorganic arsenic by standard additions[a]

Sample	Dilution factor[b]	As concentration (ppb)		Relative error (%)	Av. recovery of added As (%)
		Observed	Accepted		
EPA 1	3:50	1.63	1.56	+4.5	94.1 ± 2.5
EPA 2	1:50	2.09	2.18	—4.2	96.3 ± 4.0
River water 1	—	1.20	—	—	97.6 ± 2.0
River water 2	—	12.8	—	—	93.5 ± 1.6

[a]Four standard additions were performed.
[b]The EPA samples were diluted to bring their concentrations into the range commonly encountered with natural water samples. The results reported are for the diluted samples.

samples and for two river water samples (Table 1). Recoveries of inorganic arsenic from all samples averaged approximately 95 ± 3%. Similar recoveries were obtained from natural water samples for MAA and DMAA, averaging 94 ± 5%.

A variety of natural water samples from rivers, lakes and groundwaters in addition to a few urine samples were analyzed by this technique. These

TABLE 2

Analysis of natural water samples for various arsenic species
(All concentrations are given in ppb.)

Sample	As(III)	As(V)	As as MAA	As as DMAA	Total As (by summation)	Total As (by digestio
Red River (N.D.)	1.15	2.10	(0.2)[a]	1.75	5.2	5.50
Cedar Creek (N.D.)	6.10	6.70	(0.2)	3.0	16.0	17.80
Battle Lake (MN)	0.80	1.45	(0.2)	3.5	5.9	5.80
Silver Lake (MN)	1.27	1.47	(0.2)	2.0	4.9	5.00
Ground water 1	12.50	7.75	ND[b]	ND	20.2	19.20
Ground water 2	0.62	0.44	ND	ND	1.1	1.06
Urine 1	0.51	1.00	3.7	9.5	14.7	18.15
Urine 2	2.10	2.90	8.1	11.0	24.1	28.20

[a]Numbers in parentheses are at the detection limit (15 ng); 75-ml samples were used.
[b]Not detectable.

samples were analyzed for inorganic As(III) and As(V), MAA and DMAA and also for total arsenic after digestion. A few typical results are summarized in Table 2. For the natural water samples, agreement within 10% is observed in most cases between the total As computed from the speciation analysis and total As obtained by analysis of digested samples. The agreement is not quite as good for the urine samples for which total arsenic by digestion is consistently higher than that obtained by speciation. The method of standard additions, employed throughout this study, should minimize the effects of those inorganic ions known to interfere with arsine generation [7]. Therefore, this difference observed with urine samples probably results from the presence of higher-molecular-weight organic arsenicals in urine which are not separated and detected by the present technique. Trimethylarsine oxide was barely detectable in the urine samples and its concentration is estimated to be no larger than 0.4 ppb.

Most of the surface water samples analyzed from North Dakota and neighboring Minnesota exhibit a total arsenic concentration of less than 10 ppb. Arsenic concentrations in ground-water samples from western North Dakota varied widely, although generally below 5 ppb and almost exclusively inorganic in form. The ratio of As(III) to As(V) also varied widely in these ground-waters, perhaps reflecting the oxidation—reduction potential of the particular system from which the sample was obtained. This latter concept is being explored more fully and will be reported later.

Financial support from the U.S. Department of the Interior, Office of Water Resources Research (C-6307) and from the Environmental Protection Agency (R803727-01-1) is gratefully acknowledged.

REFERENCES

1 A Toxic Substance List, 1972, U.S. Department of Health, Education and Welfare, Rockville, Md.
2 Y. Talmi and D. T. Bostick, Anal. Chem., 47 (1975) 2145.
3 M. O. Andreae, Anal. Chem., 49 (1977) 820.
4 R. S. Braman, D. L. Johnson, C. C. Foreback, J. M. Ammons and J. L. Bricker, Anal. Chem., 49 (1977) 621.
5 A. U. Shaikh and D. E. Tallman, Anal. Chem., 49 (1977) 1093.
6 M. McDaniel, A. D. Shrendikar, K. D. Reiszner and P. W. West, Anal. Chem., 48 (1976) 2240.
7 F. D. Pierce and H. R. Brown, Anal. Chem., 48 (1976) 693.
8 M. L. Kilpatrick, J. Am. Chem. Soc., 71 (1949) 2607.
9 M. J. Taras (Ed.), Standard Methods for the Examination of Water and Wastewater, American Public Health Association, Washington, D.C., 1971, p. 524.
10 J. W. Robinson, R. Garcia, G. Hindman and P. Slevin, Anal. Chim. Acta, 69 (1974) 203.
11 G. E. Parris, W. R. Blair and F. E. Brinkman, Anal. Chem., 49 (1977) 378.
12 R. E. Sturgeon and C. L. Chakrabarti, Anal. Chem., 49 (1977) 378.

Analytica Chimica Acta, 98 (1978) 261—267

DETERMINATION OF BERYLLIUM, BARIUM, VANADIUM AND SOME OTHER ELEMENTS IN WATER BY ATOMIC ABSORPTION SPECTROMETRY WITH ELECTROTHERMAL ATOMIZATION

P. LAGAS

National Institute for Water Supply, P.O. Box 150, Leidschendam (The Netherlands)

(Received 4th November 1977)

SUMMARY

The determination of beryllium, barium and vanadium by atomic absorption spectrometry in an uncoated graphite furnace poses several problems, e.g. bad reproducibility, memory effects, etc. These difficulties can be avoided by using tubes coated with pyrolytic graphite and carbide. The optimal temperature for the pyrolytic graphite coating and the quantity of lanthanum that should be introduced for the carbide coating are discussed. Beryllium, barium and vanadium in surface water and tap water can be determined without memory effects and with detection limits of 0.01, 1 and 1 $\mu g\ l^{-1}$, respectively. Good agreement was found with the results obtained by activation analysis and flame or flameless (with uncoated tubes) atomic absorption spectrometry after preconcentration. The lifetime of the coated tubes was increased, and improved results were also found for the determination of other carbide-forming and/or high-melting elements such as molybdenum, cobalt, nickel, copper and chromium.

Little work has been done on the determination of beryllium, barium and vanadium in tap and surface waters by conventional flameless atomic absorption spectrometry because the detection limits available are relatively high compared with the usual concentrations of these elements in waters. Moreover, the reproducibility is poor, which may be caused by formation of barium carbide (m.p. 3000°C) or vanadium carbide (m.p. 2810°C) residues in the furnace. If the furnace is provided with a pyrolytic graphite coating and a carbide coating, the sensitivity and the detection limits are greatly improved and memory effects can be avoided.

Pyrolytic graphite coating of the graphite furnace was first advocated in 1968 by L'vov [1] and was later applied by many other workers [2—7]. Sturgeon and Chakrabarty [7] have summarized the advantages of pyrolytic graphite-coated tubes compared to normal graphite tubes, as lower permeability to gases, lower porosity, higher purity, higher sublimation point (3970 K), higher resistance to oxidation and higher thermal conductivity. As a result of these properties, improvements in sensitivity, detection limit and precision, and longer lifetimes of the tubes can be expected.

To supply the graphite furnace with a carbide coating, the inner surface of the tube can be treated with a suitable carbide-forming element such as lanthanum or zirconium [8]. The coating prevents physical contact between

the carbon of the furnace and the sample constituents and thus inhibits carbide formation by elements in the sample.

EXPERIMENTAL

Instrumentation

The Perkin-Elmer model 603 atomic absorption spectrophotometer used was equipped with an HGA model 74 graphite furnace atomizer, a sampler type AS 1, a model 56 recorder and suitable hollow-cathode lamps. Table 1 shows the operating conditions.

The temperatures mentioned in this paper are the temperatures that should be reached with uncoated tubes as reported in the HGA 74 manual. Because of the higher conductivity of pyrolytic graphite and the increased weight of the tube, the resistance of the coated furnace will be lower. According to the equations $Q = I^2R$ and $V = IR$, and because the HGA 74 is voltage-stabilized, the heat released and the real temperature of the graphite tube will therefore be higher (probably 50—75°C at maximum temperature) than mentioned.

Reagents

Diluted stock solutions containing Be, V and Ba in the ratio 1:100:1000 were prepared with ultrapure water from stock solutions of the metal ions (1.000 g l^{-1}; Merck Titrisols).

Procedures

Pyrolytic coating. A mixture of 10% methane—90% argon at a flow rate of 300 ml min^{-1} was added to the normal internal argon flow of 300 ml min^{-1} while the furnace was heated at 2400°C for 8 min. Treatment under these conditions gave a deposit of about 70 mg of pyrolytic graphite.

Carbide coating. An aliquot (100 μl) of a solution containing 1 mg La ml^{-1} (from $LaCl_3$) was injected into the graphite furnace and the program was run under the following conditions: drying at 100°C for 100 s, charring at

TABLE 1

Operating conditions for the determination of Be, Ba and V
(Argon was used as purge gas, and during the first 8 s of the atomization stage the flow was 50 ml min^{-1} (miniflow). Deuterium background correction was applied for Be and V.)

		Be	Ba	V
Wavelength	(nm)	234.9	553.6	318.3
Slit width	(nm)	0.7	0.2	0.7
Char temperature[a]	(°C)	1000	1500	1500
Atomization time[b]	(s)	10	15	15
Injection volume	(μl)	50	10	50

[a]Charring time, 30 s. [b]Maximum atomization temperature.

1000°C for 30 s, and atomization at the maximum temperature for 10 s. This procedure was repeated three times to obtain a deposit of 400 μg of lanthanum in the furnace tube.

Sample preparation. All samples and standard solutions were acidified with nitric acid to pH 2 before injection.

RESULTS AND DISCUSSION

The optimum temperature for pyrolytic coating and the optimum amount of lanthanum

Four graphite furnaces were treated with the argon—methane mixture at different temperatures. The time required to obtain a deposit of 70 mg of pyrolytic graphite was measured, and the absorbances of Be, Ba and V were determined for each tube before and after the lanthanum carbide coating (Table 2). At 2200°C and 2400°C the pyrolytic coating is formed very quickly with an efficiency for methane of about 50%; the absorbance values for the standard solution containing Be, Ba and V are then at a maximum, and there are no memory effects.

The optimum quantity of lanthanum seems to be about 400 μg. For a solution containing 0.2 μg Be ml^{-1}, the absorbance increased from 0.015 with a coating of 40 μg La to about 0.030 with a coating of 400 μg La. More lanthanum resulted in slightly higher absorbance values for beryllium, but the reproducibility was reduced when the amount of lanthanum was 500—1000 μg. The lanthanum solution should be introduced into the furnace with the maximum injection quantity (100 μl) to obtain a large coated area inside the tube; the solution should not contain more than 1.0 g La l^{-1} to prevent smoke development.

Under the recommended conditions, the detection limits (signal:noise = 2:1) for beryllium, barium and vanadium were 0.01, 1.0 and 1.0 μl l^{-1}, respectively.

TABLE 2

Time of pyrolytic coating and absorbance of Be, Ba and V before carbide coating (—c.c.) and after carbide coating (+c.c.) as a function of the temperature of pyrolytic coating

Temp. of coating (°C)	Required time (min)	Absorbance for 0.2 μg Be l^{-1} (50 μl)		Absorbance for 200 μg Ba l^{-1} (10 μl)		Absorbance for 20 μg V l^{-1} (50 μl)	
		—c.c.	+c.c.	—c.c.	+c.c.	—c.c.	+c.c.
Uncoated	—	0.014	0.028	0.02+[a]	0.02+	0.008+	0.007+
1800	30	0.007	0.030	0.04+	0.04±	0.012+	0.014±
2000	15	0.009	0.042	0.07+	0.09±	0.014+	0.020±
2200	10	0.009	0.050	0.16+	0.30—	0.015±	0.036—
2400	8	0.009	0.050	0.16+	0.34—	0.015—	0.033—

[a] + = much memory; ± = little memory; — = no memory.

Choice of purge gas

The results were improved with argon rather than nitrogen as purge gas. The determination of barium with coated tubes and argon as purge gas was about 15 times more sensitive than with nitrogen as purge gas. For Be and V, the sensitivities were improved by factors of 1.8 and 1.2, respectively, when argon was used as purge gas. The reason is presumably that nitrogen is not inert and forms nitrogen compounds in the graphite furnace which prevent atomization of Be, V and particularly Ba.

Charring and atomization temperatures

The maximum charring temperature where no loss of analyte occurs is 1500°C for V and Ba (Fig. 1A). At the highest atomization temperature that can be reached (2650°C), the absorbances of the vanadium and barium standard solution are still not constant, so that the real optimum temperature will be higher than 2650°C (Fig. 1B). However, an atomization temperature of 2650°C is satisfactory in practice for the determination of V and Ba in tap and surface waters.

For vanadium and barium, in contrast to beryllium, there was no difference in response between standard solutions and samples of tap and surface waters (Fig. 2). The optimum charring and atomization temperatures for beryllium are, respectively, 1000°C and 2650°C.

The lifetime of the coated tubes is sufficient for about 200—400 analyses, which is about twice the number possible with uncoated tubes. Visual inspection showed that the insides of the coated tubes were still in good condition after about 200 barium determinations.

Method of standard additions

The results obtained by the method of standard additions and from a calibration curve were compared. For tap and surface water, there was good agreement in the results for barium and vanadium. However, the concentrations of beryllium found in tap and surface waters by the method of

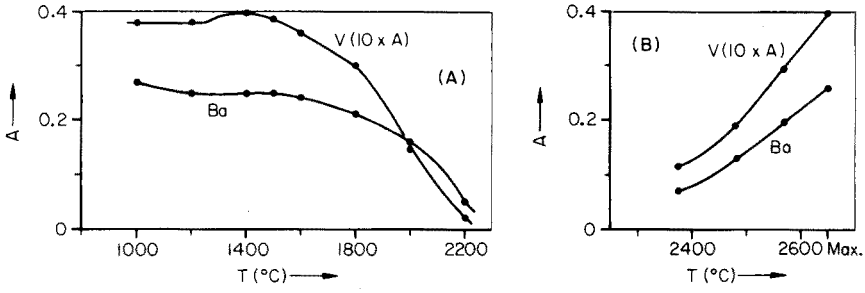

Fig. 1. Charring and atomization temperatures vs. the absorbance of a barium standard solution (200 μg Ba l^{-1}, 10 μl) and a vanadium standard solution (20 μg V l^{-1}, 50 μl). (A) Variable charring temperature with constant maximum atomization temperature. (B) Variable atomization temperature with a charring temperature of 1500°C.

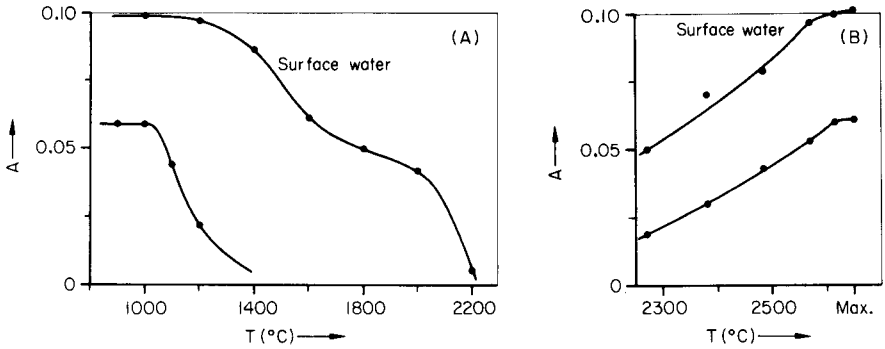

Fig. 2. Charring temperature (A) and atomization temperature (B) vs. the absorbance of a beryllium standard solution (0.2 μg Be l^{-1}, 50 μl) and of a sample of surface water with the addition of 0.2 μg Be l^{-1}. For (A) constant (maximum) atomization temperature was used. For (B) the charring temperature was 1000° C.

standard additions were 1.5—2 times lower than the concentrations determined from a calibration curve; this is probably caused by matrix effects (see also Fig. 2). Obviously the standard additions method is essential in the case of beryllium.

Comparison of different analytical methods

A sample of surface water (river Meuse) and a sample of tap water were analyzed by the proposed method with pyrolytic graphite- and carbide-coated tubes; both calibration curves and the method of standard additions were used.

The samples were also analyzed by other laboratories which applied different analytical methods:

(1) Atomic absorption spectrometry for beryllium and vanadium with a graphite furnace (uncoated tubes) after preconcentration with hydrated iron oxide (J. van Haren, Municipal Waterworks, Rotterdam Berenplaat).

(2) Activation analysis for vanadium [9] (H. A. van der Sloot, Netherlands Energy Research Foundation).

(3) Atomic absorption spectrometry for barium in a C_2H_2/N_2O flame after preconcentration with thenoyl trifluoroacetone in methyl isobutyl ketone [10, 11] (C. Dullaart, Municipal Waterworks, Rotterdam Berenplaat).

The results obtained are shown in Table 3.

The use of coated tubes for the determination of other elements

Table 4 shows the absorbance values of standard solutions obtained with uncoated tubes (U), carbide-coated tubes (C), pyrolytic graphite-coated tubes (P) and pyrolytic graphite-coated and carbide-coated tubes (PC).

Although the carbide-coated tubes enhance the response of some elements, e.g. molybdenum, and the pyrolytic graphite-coated tubes greatly improve the absorbance signals for cobalt, copper and nickel, in the same way as for barium and vanadium, the most remarkable improvements of absorbance

TABLE 3

Results obtained by different methods for the determination of Be, Ba, and V in tap and surface water (All concentrations in $\mu g\ l^{-1}$)

		Proposed method		
		Calibration curve	Standard addition	Alternative method
Ba	Surface water	102	100	103[a]
	Tap water	35	35	47[a]
V	Surface water	5.0	5.2	4.5[b]
				6.0[c]
	Tap water	<1	—	0.07[b]
				0.1[c]
Be	Surface water	<0.01	—	0.008[c]
	+0.17 μg Be l^{-1}	0.31	0.20	0.17[c]
	Tap water	<0.01	—	0.002[c]
	+0.10 μg Be l^{-1}	0.17	0.11	0.11[c]

[a]A.a.s. with TTA—MIBK extraction. [b]Activation analysis. [c]A.a.s. with preconcentration on hydrated iron oxide.

TABLE 4

Absorbance values of standard solutions obtained with U, P, C and PC tubes. Deuterium background correction was applied for all determinations, except Cu, Cr, and Ni

Element	Concn. ($\mu g\ l^{-1}$)[a]	Absorbance				
		U-tube	C-tube	P-tube	PC-tube	A(PC)/A(U)
Al	10	0.024	0.045	0.006	0.050	2.1
As[b]	10	0.040	0.040	0.032	0.052[c]	1.3
Cd	1	0.125	0.135	0.125	0.130	1.0
Co	5	0.009	0.009	0.030	0.040	4.5
Cr	10	0.080	0.095	0.200	0.240	3.0
Cu	10	0.040	0.040	0.100	0.125	3.1
Mn	10	0.110	0.120	0.200	0.200	1.8
Mo	20	0.011	0.016	0.013	0.055	5.0
Ni[d]	10	0.008	0.006	0.026	0.032	4.0
Pb	10	0.038	0.036	0.036	0.038	1.0
Sb	10	0.017	0.022	0.022	0.030	1.7
Se[b]	10	0.019	0.020	0.020	0.020[c]	1.1

[a]50 μl injection; [b]In 0.02% Ni solution; [c]Reduced reproducibility; [d]Measurement at 352.5 nm.

values were obtained with the combination of pyrolytic graphite coating and carbide coating. It seems that such tubes can be applied for all the elements investigated except arsenic and selenium which showed reduced

reproducibility, although for some elements (lead and cadmium) there was no enhancement of absorbance.

The coated tubes seem to be particularly suitable for the determination of carbide-forming and/or high-melting elements like molybdenum, cobalt, nickel, copper, and chromium. The sensitivities and consequently the detection limits were improved by factors of 3—5.

REFERENCES

1 B. V. L'vov, Spectrochim. Acta, 24 (1969) 53.
2 D. C. Manning and R. D. Ediger, At. Absorpt. Newsl., 15 (1976) 42.
3 S. A. Clyburn, T. Kantor and C. Veillon, Anal. Chem., 46 (1974) 2213.
4 A. C. Thompson, R. G. Godden and D. R. Thompson, Anal. Chim. Acta, 74 (1975) 289.
5 K. I. Aspila, C. L. Chakrabarti and M. P. Bratzel, Anal. Chem., 44 (1972) 1718.
6 D. D. Siemer, R. Woodriff and B. Watne, Appl. Spectrosc., 28 (1974) 582.
7 R. E. Sturgeon and C. L. Chakrabarti, Anal. Chem., 49 (1977) 90.
8 J. H. Runnels, R. Merryfield and H. B. Fisher, Anal. Chem., 47 (1975) 1258.
9 H. A. van der Sloot and H. A. Das, J. Radioanal. Chem., 35 (1977) 139.
10 G. D. Renshaw, At. Absorpt. Newsl., 12 (1973) 158.
11 W. M. Jackson, G. T. Gleason and P. J. Hammonds, Jr., Anal. Chem., 42 (1970) 1242.

Analytica Chimica Acta, 98 (1978) 269—277

FILTER PAPER STANDARDS FOR TRACE ELEMENTS

D. E. RYAN* and J. HOLZBECHER

Trace Analysis Research Centre, Chemistry Department, Dalhousie University, Halifax, Nova Scotia B3H 4J1 (Canada)

(Received 7th November 1977)

SUMMARY

Filter papers spotted with microliter amounts of relatively concentrated (1000 $\mu g\ ml^{-1}$) solutions of metal ions can serve as excellent sources for the preparation of solution standards at trace concentration levels. The metal ions are eluted from the filter paper matrix by acidic or saline solutions. The reproducibility of preparation, elution efficiency, and stability with time were studied for manganese, copper, and zinc standards. The presence of these elements in the eluates was confirmed for small volumes by direct neutron activation analysis (n.a.a.) of the liquids; large volumes were analyzed directly by Zeeman-modulated atomic absorption (Zn) or by n.a.a. after preconcentration by co-precipitation (Mn). Multielement standards are readily prepared.

There is an increasing need for trace element standards at the microgram level. Many approaches have been used (NBS type standards, secondary standards, or commercially available standard solutions). The use of natural systems (e.g., Orchard Leaves) requires a guarantee of adequate mixing since distribution in the matrix may be heterogeneous; prepared solutions require careful stabilization, and powdered mixtures depend on particle size and type of mixing, and are generally of poor precision.

Most laboratories require high-quality secondary standards suitable for daily checking of techniques, which can be prepared or purchased at minimal cost; multielement analysis, for which multielement standards are required, is becoming increasingly necessary. Laboratory-generated standard solutions are usually bulk solutions (of strength *thought* to be stable) prepared by weighing and dissolution in a known volume of solvent; solutions of appropriate final concentration (e.g., 0.01—1 $\mu g\ ml^{-1}$) are prepared by successive dilutions as required and it is assumed that there is no loss of element to vessel walls as solutions are diluted.

Established procedures rely on (a) confidence in the results obtained in replicate determinations, preferably involving several techniques, (b) confidence that weighing and dilution errors are minimal and that stability persists on dilution. Weighing and dilution errors, with today's apparatus, are insignificant. Of major concern, however, are both the rapid loss of species of interest to vessel walls and the interactions that take place in

multielement solutions. Although stabilizers are of value in preventing loss by adsorption, they may add to the interactions in multielement solutions. Reversible fixation of the species of interest on a sorbent, from which the "standard" can be released just prior to use, seems to be a possible solution to the problem. If trace amounts of the element of interest are fixed reversibly on a carrier with a low ion-exchange capacity (e.g., cellulose), trace element standards that are stable with time, are easy to handle and store, and are not subject to the losses (through adsorption) or change of species (through interaction) that occur in solution standards, should be obtained. The trace metals could then be eluted immediately before use to give solutions containing known trace metal concentrations.

Trace element standards prepared by fixation on filter papers are the subject of this study. N.a.a. was chosen as the method for determination of the trace metals as it enables direct measurement in either solids or liquids to be made without introducing any reagents and is thus especially suitable for monitoring the efficiency of elution processes. Manganese, copper, and zinc were used as they are common trace metals that are easily determined by n.a.a.

EXPERIMENTAL

Stock solutions (1000 μg ml^{-1}) of manganese, copper, and zinc were prepared by dissolution of $Mn(C_2H_3O_2)_2 \cdot 4H_2O$ (Fisher), $Cu(NO_3)_2 \cdot 3H_2O$ (Fisher) and $Zn(NO_3)_2 \cdot 6H_2O$ (Baker), respectively. Their concentrations were checked against Fisher Certified AA Standards (1000 μg ml^{-1} in HNO_3 with Mn, CuO and ZnO as solute, respectively).

Whatman No. 1 filter papers, 4.25 cm in diameter, were divided in quarters. For manganese they were used as such; for copper and zinc, however, acid-washed filter papers were necessary to decrease the background in the γ-ray spectrum. The papers were immersed in 100 ml of 0.1 M HNO_3 for 1 h and then air-dried; the acid was prepared by fresh dilution of 12 M nitric acid, previously purified by distillation. To prevent brittleness of older batches caused by some acid retained after the nitric acid washing, the papers were washed with distilled water and soaked in an additional 100 ml of distilled water for 1 h. The dried filter papers were spotted with the stock solutions; 1 μl (Hamilton syringe) was used for manganese and copper to give spots containing 1 μg of metal; for zinc, 10 μl of solution was used to give spots containing 10 μg because of the lower sensitivity of n.a.a. for zinc. The standards were air-dried for 2 min.

The elements of interest were determined by n.a.a. in a small swimming-pool-type research reactor (SLOWPOKE) developed by Atomic Energy of Canada Limited. It uses enriched ^{235}U fuel with a light water moderator and beryllium reflector. The γ-ray spectra were taken by a TN-11 pulse-height analyzer (Tracor Northern) with a Ge(Li) detector (Canberra Industries).

Zinc in sea-water eluates was determined by a.a.s. with Zeeman background correction. The principles of the method and instrumentation are described elsewhere [1—4].

Table 1 shows the short-lived isotopes, produced by (n,γ) reactions with thermal neutrons in the reactor, that were measured. Another isotope of copper, ^{66}Cu (1039.6 keV, $T_{½}$ = 5.10 min) was also tried, but its very short half-life made its measurement difficult, especially when low concentrations were investigated after elution.

The irradiation and measurement conditions were as follows. A large (outer) site in the reactor was used; a series of six samples encapsulated in small containers could be irradiated at the same time under the same conditions. The neutron flux was 10^{12} n cm^{-2} s^{-1} with irradiation times of 15 min for manganese, and 3 h for copper and zinc; the decay period before measurement was ca. 30 min for manganese, and ca. 1 h for copper and zinc, and the count time was 300 s. The regions integrated (keV) are shown in Table 2. For counting, the filter papers were removed from their polyethylene containers, centered on an aluminium plate at a fixed distance from the detector, and flattened with a metal weight. Liquid or powder samples were measured directly in their small polyethylene containers.

RESULTS AND DISCUSSION

Comparison and treatment of filter papers

Regular filter papers can be used for manganese as washing by acid results in a decrease from 0.01 μg to 0.005 μg Mn only, although the overall background is substantially decreased. As the signal-to-background ratio for 1 μg Mn is very high (ca. 46:1) the acid treatment is unnecessary.

TABLE 1

Short-lived isotopes produced in the reactor

Isotope	Target abundance (%)	Peak measured (keV)	Half-life (h)
^{56}Mn	100	846.9	2.582
^{64}Cu	69.17	511.0 (β^+)	12.75
^{69m}Zn	18.57	438.7	13.7

TABLE 2

Regions integrated (keV)

Isotope	Low energy background	Peak	High energy background
^{56}Mn	827—833	844—850	861—867
^{64}Cu	493—500	507—514	521—528
^{69m}Zn	426—430	436—440	446—450

The determination of copper and zinc is, however, much less sensitive, so that background and blank values become important. For example, the blank is about 20% of the signal for 1 μg Cu with filter papers. This does not mean, necessarily, that a substantial amount of copper is present, since other elements (e.g., sodium and chlorine) also contribute to the 511-keV peak and no significant blank was found with the short-lived ^{66}Cu isotope. The blank value is decreased to about 6% of the signal for 1 μg Cu on treatment with acid; the signal-to-background ratio is then ca. 16:1.

Although there is virtually no blank reading for zinc (with either regular or acid-treated filter papers), acid-washing results in enhancement of the signal-to-background ratio from ca. 1.6:1 to 4.3:1.

Table 3 shows results obtained for the copper, manganese and sodium contents of various filter papers; zinc was not determined because of its relatively low sensitivity (ca. 1 μg under the analytical conditions) by n.a.a. Acid- and water-washed Whatman No. 1 filter papers are comparable to ashless analytical filter papers. Since preconditioning of cation-exchange matrices, through acid washing, is desirable for increased rate of exchange, acid- and distilled water-washed Whatman No. 1 filter papers are recommended. Extensive comparisons of the suitability of various filter papers for spot test [5] and ring oven techniques [6] in terms of trace metal impurities are available.

Reproducibility

The reproducibility of preparation of standards was investigated for a series of 5 standards of each respective metal, together with one blank for each series. The relative standard deviations found were: 5.0% for Mn (regular filter papers), 3.6% for Cu (acid-washed filter papers), and 5.6% for Zn (acid-washed filter papers). These compare with r.s.d. values of ca. 10% for zinc spotted on regular filter papers and ca. 7% for short-lived ^{66}Cu. The overall reproducibility of the preparation and measurement of standards is thus ca. 5% relative.

TABLE 3

Comparison of the trace metal contents (in $\mu g\ g^{-1}$) of different filter papers

Paper[a]	Cu	Mn	Na
SS 589 black ribbon	1.2	0.01	13
SS 589 white ribbon	1.3	0.10	19
SS 589 blue ribbon	1.0	0.14	14
W1 untreated	4.6	0.12	153
W1 acid washed	1.0	0.05	30
W1 acid and H_2O washed	0.8	0.04	15
W30	6.0	0.31	63
W41	1.5	0.03	42
W54	1.1	0.04	32

[a]SS, Schleicher & Schüll. W, Whatman.

Elution with dilute acid

The preliminary manganese elution studies showed that ca. 30% of the manganese remained on the filter paper even after elution for 5.5 h with distilled water; an exchange medium is necessary to achieve effective elution. On elution with 100 ml of 0.1 M HNO_3 for 30 min, ca. 0.5%, 6%, and 0% of the original amounts remain on the filter paper for Mn, Cu, and Zn, respectively, and there is essentially no further change with time (see Fig. 1). Thus for other experiments (e.g. aging, etc.) 30 min was chosen as the standard elution time for copper and zinc and 60 min was used for manganese (some difficulties were expected with manganese because of a possible change of the species with time). The elution results are virtually the same as the blank values, so that complete elution was achieved. Standard trace solutions are thus easily obtained by the elution process.

Elution with 1 ml of 0.1 M HNO_3 was also investigated. The elution efficiency is time-dependent (see Fig. 1); 8% Mn is left after 30 min, 6% Cu after 60 min, and 11% Zn after 5 min; there is no further change with time. The experimental results do not imply that elution is poorer with small volumes; they arise from the retention of the relatively concentrated eluate (1 $\mu g\ ml^{-1}$ for Mn and Cu, 10 $\mu g\ ml^{-1}$ for Zn for complete elution) on the filter papers. This can be removed by washing the filter papers with 2 ml of distilled water after elution. There is no time-dependence (from 5 to 60 min studied) and the amounts of metals remaining on the filter papers are about 2.5%, 5%, and 0.5% for Mn, Cu, and Zn, respectively. Except for the manganese result (which is slightly higher) these results compare well with the respective blanks.

Aging

Aging can result in a change of species on the filter paper with time (e.g., oxidation of Mn(II) to Mn(IV)) and, consequently, in a different elution efficiency of older standards compared with those freshly spotted. It is also necessary to confirm that the metals of interest remain on the

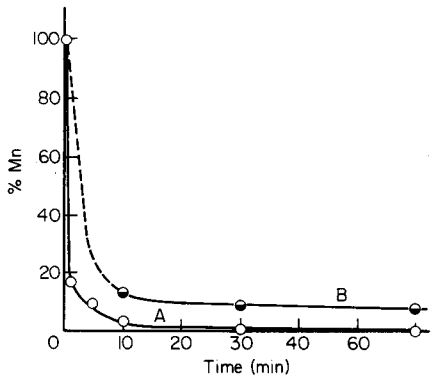

Fig. 1. Manganese elution; (A) 100 ml of 0.1 M HNO_3, (B) 1 ml of 0.1 M HNO_3.

papers for prolonged periods of time, although their "loss" seems to be very unlikely. A series of standards was spotted and investigated after various periods of time.

Copper, zinc, and manganese standards did not show any appreciable change in the their elution ability up to 21, 20 and 6 d, respectively; after 20 d, the manganese standard had about 0.9% of the original amount of Mn left instead of the usual 0.5%. After 63 d, the copper and zinc standards showed unchanged elution capability, while after 69 d, the manganese standard showed about 1.5% Mn left on the paper after elution. A yellow-brown spot (MnO_2 ?) was visible on the old standard; it disappeared, however, during elution (no visible changes were observed for old copper and zinc standards). Although there was a slight decrease of elution efficiency for manganese with time, it was negligible within the time period investigated. All the above elutions were done in 100 ml of 0.1 M HNO_3 for 30 min (Cu and Zn) and 60 min (Mn).

The following results were obtained by comparison of the metal content of the freshly spotted and aged filter paper standards: the manganese standard, 13 d old, gave readings ca. 2.5% higher than the freshly spotted one, while 9-d copper and zinc standards were 15% higher and 1.4% lower, respectively. Still older standards (Mn — 69 d, Cu and Zn — 63 d) were 15%, 10%, and 9% higher, respectively, than the freshly spotted ones. Although there seems to be a trend for older standards to give higher readings than the freshly spotted ones, this difference is not significant considering the amounts of the trace metals involved, the standard deviation of their determination, and the limited number of results. The metals of interest remain on the filter papers and spotted filter paper standards can be used up to two months at least.

Measurement of 1-ml eluates

To confirm that the metals of interest eluted from the filter paper standards were indeed present in the eluates, elutions with 1 ml of 0.1 M HNO_3 were performed (60 min for Mn, 30 min for Cu and Zn). The eluates were irradiated in small plastic containers and counted directly in them (to avoid losses in transfer); respective blanks were also run. Volumes of 1 ml were selected as the metal concentrations obtained by elution permitted ready determination.

Manganese, copper, and zinc were eluted with 90%, 96%, and 90% efficiency, respectively; this is in excellent agreement with the results from previous experiments which showed that, because of the small volume of eluate, typically 8%, 6% and 11% of Mn, Cu and Zn, respectively, were retained on the filter papers (removed by washing with water as outlined in the "elution with dilute acid" section).

Elution with 3% sodium chloride

To approximate the conditions existing in sea water, elution with 3% sodium chloride solution was studied. There was a high background in the

spectrum from the sodium chloride retained on the papers in the course of elution. Measurement was still possible but, to lower the background, the filter papers were washed after the sodium chloride elution with two 100-ml portions of distilled water for 30 min each. All three metals were effectively eluted with 3% NaCl solution (the amounts left on the filter papers, i.e., 0.34%, 3.6%, and 0% for Mn, Cu, and Zn, respectively, compare well with the normal blanks). The elution times were 60 min for manganese, and 30 min for copper and zinc.

Elution with sea water

The sea water used was from the Northwest Arm, Halifax, Nova Scotia, taken from a tap in the Oceanography Laboratories of the University; the water, filtered through sand before entering the building, was not treated further before use.

Elutions (60 min for Mn, 30 min for Cu and Zn) were made with 100 ml of regular and acidified (to become 0.1 M in HNO_3) sea water. If, after sea-water elution, the filter papers were washed with a squeeze bottle only, there was a relatively high background in the spectrum which was due mainly to sodium chloride retained on the papers; although measurement was still possible, some papers were (after elution) washed twice in 100 ml of distilled water, 30 min each time. This gave a substantial decrease in background. With the exception of copper there was virtually no difference in elution efficiency between regular and acidified sea water, and manganese and zinc were effectively eluted. Typical amounts remaining on filter papers after elution with acidified sea water and subsequent washing with distilled water were 0.16% Mn, 5.4% Cu, and 0% Zn. These values compare well with the usual blanks. About 14% of copper remain, however, on the paper after elution with regular sea water; acidified sea water is necessary to remove copper effectively.

The sea-water eluates were also checked for the trace elements by neutron activation (after preconcentration from the 100-ml volume by co-precipitation) and measured directly by Zeeman-modulated a.a.s. (essential for reliable background correction).

Co-precipitation

Manganese was studied first as its determination by n.a.a. is the most sensitive. Calcium oxalate co-precipitation was used [7—9]; with this collector, ca. 50% of manganese (1 μg present originally) was co-precipitated from 100 ml of distilled water; for the same volume of sea water the collection efficiency was only ca. 15%. In the complex sea water matrix, competing equilibria decrease the amount of "free", collectable manganese. Even though the co-precipitation is far from complete, excellent results are obtained for standard addition of manganese to sea water; a plot of signal versus manganese concentration gave a straight line through the origin. The amount of manganese present in sea water is less than 2.5 ng ml^{-1} since the

reagent blank signal (about the same for distilled water and sea water) is ca. 25% of the signal for 1 μg Mn. The reproducibility of co-precipitation of manganese from sea water is very good, with a relative standard deviation of about 7% (five results). To confirm that manganese released from filter paper standards on elution is indeed in the acidified sea-water eluates, it was co-precipitated from these eluates and also from sea-water standards prepared by injecting 1 μg of Mn into acidified sea water from a syringe; respective blanks were also run. Good agreement between these two sets of standards was found with differences of about 10% relative. It was proved that, after elution from the paper standards, manganese is indeed present and sea-water standards containing known amounts of added manganese are obtained.

Manganese was also collected after complexation with oxine and subsequent adsorption on activated carbon [10]. The collection efficiency for 1 μg Mn in 100-ml volumes was excellent; 97% and 91% were recovered from distilled water and sea water, respectively.

Zeeman-modulated atomic absorption

Zinc (10 μg) released from filter paper standards on elution with 100 ml of acidified sea water was determined in these eluates (and also in sea-water standards prepared by injecting 10 μg Zn into 100 ml of acidified sea water from a syringe); respective blanks were also analyzed. The method used was a.a.s. with Zeeman background correction. Excellent agreement was obtained between the sea-water eluates and sea-water standards (the mean reading was the same for both sets); 10 μg of Zn was eluted from the spotted paper standards into acidified sea water in 30 min.

Multielement paper standards

Multielement paper standards containing 1 μg of manganese, 1 μg of copper and 10 μg of zinc were prepared by spotting the acid- and distilled water-washed filter papers successively with the respective metal solutions and allowing them to air-dry.

The overall relative standard deviation for the preparation and measurement of five multielement standards was 4.2%, 7.3%, and 10.8% for Mn, Cu, and Zn, respectively (the corresponding results for single-element standards were 5.0%, 3.6%, and 5.6%). In the previous studies, manganese standards were irradiated for much shorter periods (15 min) than copper and zinc standards (3 h); ^{56}Mn has a shorter half-life than ^{64}Cu and ^{69m}Zn and its determination is much more sensitive. The multielement standards were irradiated for 3h (necessary to activate copper and zinc sufficiently) and, as a result, ^{56}Mn became activated to such a degree that samples had to be placed farther from the detector for counting. The reproducibility of copper and zinc determination was, therefore, poorer than in single-element standards. The results do not imply, however, that the preparation of single-element standards is more reliable than that of multielement standards.

The multielement standards were eluted with 100 ml of 0.1 M HNO_3 for various periods of time. There is virtually no difference in the elution of copper and zinc from multielement or single-element standards. Manganese, however, was eluted faster from the multielement standard (about 5 min) while it took ca. 20—30 min from a single element standard. For multi-element standards, acid- and distilled water-washed filter papers were used; for manganese alone, untreated filter papers were employed. The acid treatment apparently improved the ion-exchange properties of the filter papers.

After 21 days multielement standards were compared with freshly spotted ones; their elution capability remained unchanged and their metal content differed insignificantly. Similar results were obtained for multielement standards after 51 days.

Conclusions

Filter papers can be used as matrices in the preparation of standards for trace elements. They can be spotted with metal solutions reproducibly, the spotted standards are stable with time, and the metal ions are readily eluted to give standard solutions containing known trace concentrations of the elements of interest. It is also possible to spot the filter papers with microliter volumes of many metal solutions in such a manner that the spots are separate and any possible interactions among the species present are, therefore, avoided. This is a major advantage over multielement solutions. Multielement standards for manganese, copper and zinc show generally the same properties as single-element standards in terms of elution capability and stability with time; no appreciable interaction of these spotted elements was noted, even when the spots were not separate. Another attractive feature of filter paper standards is the possibility of their certification by non-destructive neutron activation analysis.

This work was supported under a contract (Marine Analytical Standards Program) from the National Research Council of Canada.

REFERENCES

1 R. Stephens and D. E. Ryan, Talanta, 22 (1975) 655.
2 R. Stephens and D. E. Ryan, Talanta, 22 (1975) 659.
3 D. E. Veinot and R. Stephens, Talanta, 23 (1976) 849.
4 R. Stephens, Talanta, 24 (1977) 233.
5 P. W. West and W. C. Hamilton, Mikrochem. Ver. Mikrochim. Acta, 38 (1951) 100.
6 H. Weisz, Microanalysis by the Ring Oven Technique, Pergamon Press, Oxford, 1961.
7 D. E. Ryan, R. J. Prime, J. Holzbecher and R. E. Young, Anal. Lett., 6 (1973) 721.
8 D. E. Ryan, H. Rollier and J. Holzbecher, Can. J. Chem., 52 (1974) 1942.
9 D. E. Ryan, J. Holzbecher and H. Rollier, Anal. Chim. Acta, 73 (1974) 49.
10 B. M. Vanderborght and R. E. Van Grieken, Anal. Chem., 49 (1977) 311.

Analytica Chimica Acta, 98 (1978) 279—290

APPLICATION OF RAPID FURNACE HEATING TO THE CARBON-FURNACE ATOMIC EMISSION DETERMINATION OF INVOLATILE ELEMENTS

D. LITTLEJOHN and J. M. OTTAWAY*

Department of Pure and Applied Chemistry, University of Strathclyde, Cathedral Street, Glasgow G1 1XL (Gt. Britain)

(Received 25th January 1978)

SUMMARY

Improved or new detection limits are reported for the measurement of the atomic emission of involatile elements with a HGA 2200 carbon-furnace atomizer incorporating maximum power heating and temperature control. The optimization of the instrument and the preset temperature for each element are described. Measurements of the temperatures of the tube wall and the vapour phase inside the furnace during atomization are compared for both conventional and maximum power heating.

A useful feature of electrothermal atomizers in atomic absorption or atomic emission spectrometry is the facility to control, over a wide range, the temperature of the atomization surface. Any preselected temperature may be chosen and within limits, caused by long-term changes in the nature of the surface and/or volatilization losses of carbon, the temperature achieved is highly reproducible. Accurate calibration is, however, necessary if a knowledge of the precise temperature under any given set of conditions is required. In contrast, although flames can give constant and reproducible temperatures in all reaction zones, major changes of the temperatures reached in any zone are not possible without introducing gross variations in the chemistry or structure of the flame. Besides control of the final temperature, many commercial carbon-furnace atomizers also permit control of the rate at which a preselected temperature is reached. A slow rate of heating is generally found useful for the drying and thermal pre-treatment of liquid samples, as this prevents spluttering and random distribution of the sample in the tube and often improves both the reproducibility and sensitivity of the atomization signals. During atomization, a fast rate of heating generally improves peak-height sensitivity particularly for the more involatile elements. When the temperature of the carbon tube is increased rapidly to temperatures above the minimum needed for appearance of the atomic species of interest, atomization is rapid and the atomic population reaches a maximum value determined by the rate of atomization in competition with losses by convection, diffusion etc. Fast heating rates therefore

lead to an improvement in peak-height sensitivity in atomic absorption and should lead to a similar improvement in atomic emission measurements. In this case, however, any lag of the temperature of the vapour phase behind that of the carbon tube [1, 2], which might be increased at faster tube heating rates, could be an additional important factor.

In most of the early designs of electrothermal atomizers, the furnace is heated by applying a constant voltage across the carbon tube. The temperature increases until the heat losses are balanced by the power supplied. By voltage selection, both the heating rate and final temperature are changed. The heating rate also varies during the atomization cycle and is fast at the beginning but much slower as the maximum temperature at any particular voltage is reached. This has two distinct disadvantages. For the atomic absorption determination of elements such as cadmium, which are volatilized below 1000°C, it is still necessary to use an atomization temperature of 1800—2000°C to achieve maximum sensitivity, as this final temperature must be set in order to achieve a fast heating rate below 1000°C. For involatile elements that are volatilized at temperatures near the maximum achieved by the atomizer, it is impossible to carry out atomization at fast heating rates. In 1974, Lundgren et al. [3] demonstrated the advantages of temperature-controlled heating in which the heating rate and final temperature could be set independently by use of a triac that regulated power and an infrared sensor that measured and was used to control the temperature. The rate of atomization can then be increased by an increase in heating rate rather than by an increase in the final temperature of the tube. Maximum sensitivity for cadmium was achieved at final temperatures below 1000°C, and at 820°C the signal for cadmium could be measured in the presence of 2% sodium chloride without significant volatilization of the matrix [3]. With faster heating rates, maximum atomic absorption sensitivity for most elements can be obtained at much lower temperatures than those adopted previously on instruments with slower heating rates.

The possibility of achieving fast heating rates at and near the maximum tube temperatures would be a considerable advantage for the analysis of refractory and carbide-forming elements. Although pyrolytic graphite tubes or coatings [4—6] have been reported to give increases in sensitivity for a number of elements, the slow heating rate, at the high temperatures required for atomization of involatile elements, impairs the sensitivity for these elements in most instruments currently available.

In carbon-furnace atomic emission spectrometry, modifications to an HGA 72 furnace atomizer by reducing the carbon wall thickness at the centre [1] or ends [7] of the tube have yielded improved detection limits for involatile and volatile elements, respectively, and detection of a wide range of elements in the sub-ppm region has been reported [1, 7]. Although reduction of the tube wall thickness at the centre [1] increased both the final atomization temperature and the heating rate, the heating rates achieved did not compare with those reported by Lundgren et al. [3] and analytically

useful detection limits have yet to be reported for many of the more involatile elements.

Perkin-Elmer have recently introduced a new electrothermal atomizer (HGA 2200) in which a temperature-feedback system, similar in principle to that proposed by Lundgren et al. [3], is used to achieve maximum power heating and hence maximum heating rates to any preset atomization temperature. The application of this instrument to the determination of involatile elements by carbon-furnace atomic emission spectrometry is reported here. Temperature-controlled heating is shown to be advantageous in this application, and new or improved detection limits have been achieved for many involatile elements. The optimization of the furnace and spectrometer for atomic emission measurements is described, and a simple modification which can also be applied to other similar atomizer units is reported.

EXPERIMENTAL

Instrumentation

A Perkin-Elmer HGA 2200 carbon tube atomizer was mounted in a PE 272 atomic absorption/emission spectrometer coupled to a Hitachi 056 strip-chart recorder. The PE 272 was optimized for measurements of atomic emission as reported previously [1, 8]. Where available, hollow-cathode lamps were used to adjust the monochromator to the required wavelength. In other cases, the monochromator was adjusted by means of the atomic emission signal obtained during atomization of a 20-μl aliquot of a standard solution of the element of interest, at a concentration 10—50 times the detection limit. The monochromator slit was set to give a bandpass of 0.2 nm by using the alternative slits of reduced height provided with the instrument. These prevent the ring of continuum from the tube wall, which is focused on the entrance slits, from directly entering the monochromator with the analyte emission. Because of reflection of the wall radiation by the windows of the HGA 2200, it was necessary to replace the right-hand quartz window (i.e., furthest from the entrance slit) with a black non-reflecting material to reduce the background signal to a minimum (see below).

The HGA 2200 atomizer incorporates maximum power heating with temperature control that allows the graphite tube to be heated with maximum power and speed to any preset atomization temperature. The temperature is monitored optically by a silicon photodiode which measures the intensity of the black-body radiation emitted by the graphite tube during atomization and activates the electronics to switch over to voltage control as soon as the preset temperature is reached. The photodiode is calibrated at the required temperature when the temperature/time parameters are set at the start of each analytical procedure. With maximum power heating, the background signal reaches a maximum at the same time as the combined background and analyte atomic emission signal. Both signals were measured

separately by using either the chart recorder (chart speed, 160 mm min^{-1}) or the spectrometer peak-height facility and microprocessor digital readout. The net analyte atomic emission signal was obtained by subtraction of the appropriate background signal from the peak height of the combined signal.

Pyrolytically coated graphite tubes were used, unless otherwise indicated. Samples were transferred to the centre of the graphite tube with a 20-μl Oxford micropipette and were dried for 45 s at 100°C and atomized with maximum power heating and temperature control, under gas-stop conditions, for 5—7 s at selected atomization temperatures as indicated in the text. To remove any analyte remaining at the completion of the atomization stage, a burn-off period of 5—10 s at 2700°C was incorporated. During the drying of samples, research-grade argon (99.996%) or nitrogen (99.9%) was employed as the purge gas at a flow rate of 0.04 l min^{-1}.

The temperatures of the tube wall were measured with an IRCON optical pyrometer as described previously [2]. The vapour-phase temperatures during atomization under conventional and maximum power heating were measured and compared with the corresponding wall temperatures. Temperatures were obtained from comparisons of the atomic emission measurements of four iron lines by a procedure described previously [2].

Chemicals

Stock solutions were prepared from reagents of the highest available purity by dissolving the appropriate amount of a suitable salt in distilled water and adding nitric or sulphuric acid to give a final acid concentration of 10^{-2} M (unless otherwise indicated). Stock solutions were diluted with distilled water as required. Detection limits were calculated from 5—8 injections of a low standard aqueous solution, and are defined as that concentration which gives a signal equal to the background signal plus two standard deviations of the peak height from the sample injections.

RESULTS AND DISCUSSION

Optimization of the HGA 2200 for atomic emission measurements

Detection limits for graphite-furnace atomic emission for systems without wavelength-modulation background correction [9], depend on the ratio of atomic emission to tube-background emission as well as on the statistical reproducibility of the signals. Generally, experimental conditions giving the lowest background emission are preferred. The nature and magnitude of tube background and its influence on atomic emission sensitivity has been discussed previously for several instrumental systems [10]. With open-ended furnaces such as the Perkin-Elmer HGA 70 and 72, the magnitude of the background signal is controlled by the ability of the spectrometer to form a sharp and clearly defined image of the tube radiation on the entrance slits of the monochromator. Optical baffling can then be used to prevent the continuum radiation from the walls of the tube from reaching the detector

directly, and the small residual background signal is caused by Rayleigh scattering of tube wall radiation by the atoms and/or molecules in the vapour phase of the furnace [10].

Although most atomic absorption/emission spectrometers fail to reach this degree of optical purity, instruments such as the PE 272, designed for operation with electrothermal atomizers, have monochromator slits of reduced height that reduce to a low level the amount of tube wall radiation reaching the detector. However, when such a spectrometer is used in conjunction with a graphite furnace that is sealed at both ends with quartz windows, such as the HGA 2200, an additional contribution to the background is obtained from reflection of black-body radiation, from the tube into the monochromator, by the furnace window furthest (on the optical path) from the monochromator. For atomizers such as the Perkin-Elmer HGA 2200, 2100, 74, 76 and 76B mounted in spectrometers such as the Perkin-Elmer 272, 360, 370 and 460, this window is on the right-hand side of the furnace head. The effect was first noted on an IL 151 spectrometer operated with an IL 455 furnace, where the window is on the left-hand side [11].

When the alternative slits provided with the PE 272 spectrometer were used, additional baffling offered no advantage. The influence of reflection of light from the right-hand furnace window of the HGA 2200 and from the window of the hollow-cathode lamp compartment to the right-hand side of the atomizer is illustrated by the relative tube background signals shown in Fig. 1. With the monochromator set at the manganese wavelength of 403.08 nm, the tube background signal was measured under conditions of maximum power heating to 2100°C with different modifications for reducir reflection. With the unmodified furnace and spectrometer, a relatively large background signal was obtained, mostly from reflection of tube radiation at the furnace window but with a small contribution from reflection at the window of the lamp compartment. Replacing the furnace window with an opaque non-reflecting material (condition d) reduced the background to a level comparable to that when there was no reflection (condition e, Fig. 1 The removal of the furnace window during atomization did not impair the sensitivity of either atomic absorption or atomic emission measurements, and for some elements, such as Mn and Cr, peak-height signals were improved when the window was completely removed after the drying stage. However, for consistency, the results reported here were obtained under condition (d), i.e., when a black, non-reflecting material was used in place of the right-hand furnace quartz window. This modification is recommended for all the furnaces mentioned above.

This is the only modification necessary with the PE 272—HGA 2200 system. With PE 360 and PE 370 spectrometers, further improvements in signal-to-background ratio were achieved with HGA 74 and 76 atomizers when the dimensions of the aperture stop located before the monochromato of these spectrometers were reduced.

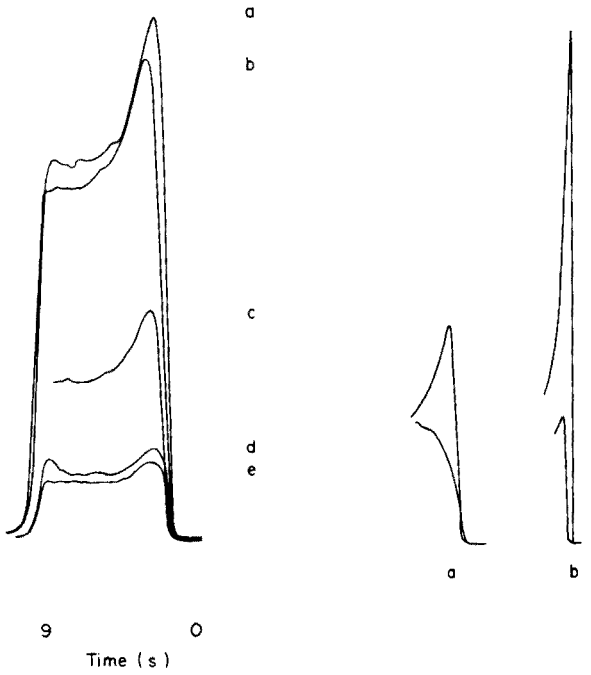

Fig. 1. HGA 2200 tube background signals measured at 403.08 nm for maximum power heating to 2100°C for (a) the unmodified HGA 2200—PE 272 system; (b) the unmodified furnace unit, but with a black card over the window of the hollow-cathode lamp compartment; (c) the right furnace quartz window blackened with a marker pen; (d) the right furnace quartz window removed and replaced with a piece of black non-reflecting sandpaper; (e) the right furnace quartz window completely removed and black card placed over the window of the hollow-cathode lamp compartment. Chart recorder speed, 160 mm min^{-1}.

Fig. 2. Carbon-furnace atomic emission and tube background signals for molybdenum. 20 μl of 0.1 μg ml^{-1} solution, wavelength 379.83 nm, PE 272 bandpass 0.2 nm, and chart recorder speed 160 mm min^{-1}. Atomization under argon gas-stop conditions with pyrolytically coated tubes at (a) normal heating rate, (b) maximum power heating with temperature control, to a top preset temperature of 2500°C.

Maximum power heating with control of final temperature

With the background signal reduced to a minimum as described above, the sensitivity of the HGA 2200—PE 272 system for atomic emission can be further optimized by maximizing the concentration of atoms in the furnace at the time of measurement. Under maximum power heating, the tube temperature is increased rapidly, and atoms are released from the carbon surface more quickly and form a more concentrated atomic vapour than under slower heating rates. However, the concentration of atoms at any time during atomization will depend on a balance between the rate of production and the rate of dissipation of atoms. Under gas-stop conditions, it is likely that the rate of diffusional loss will increase at higher temperatures

[12], and this must also be considered when the optimum heating rate and final temperature for the measurement of atomic emission are chosen for each element. For atomic emission, the Boltzmann equation predicts an exponential rise in emission intensity as the temperature is increased, and it is therefore likely than an improvement in sensitivity for most elements will be achieved under conditions of increased heating rate. Both diffusional and Boltzmann effects will depend on the vapour phase rather than the tube wall temperature, and the degree to which the former lags behind the latter will also be important.

The practical effect of the combination of these factors is illustrated for molybdenum in Fig. 2. At a final temperature of 2500°C, maximum power heating gave a × 3 enhancement of peak emission intensity and a × 2 increase in the ratio of atomic emission to background emission, compared to conventional heating to the same final temperature. The rapid increase in temperature on applying maximum power is reflected in the more rapid rise in tube background in Fig. 2b compared to 2a.

Comparison of the effect of heating rate on the tube wall temperature as measured by the optical pyrometer is shown in Fig. 3. As the constant voltage applied for conventional heating (Fig. 3A) is increased, both the final temperature and the rate of increase in temperature are increased. With maximum power heating, however, the same rapid increase in temperature is achieved at all temperature settings (Fig. 3B), and the instrument switches over to voltage control when the silicon photodiode indicates that the preset final temperature has been reached. In general, temperatures slightly lower than the preset value (as indicated) were obtained but deviations were always within ±50°. Although no substantial temperature overshoot was observed on maximum power heating, background signals invariably gave peaks on the rise curve at applied temperatures below 2600°C, as shown in Figs. 1 and 2.

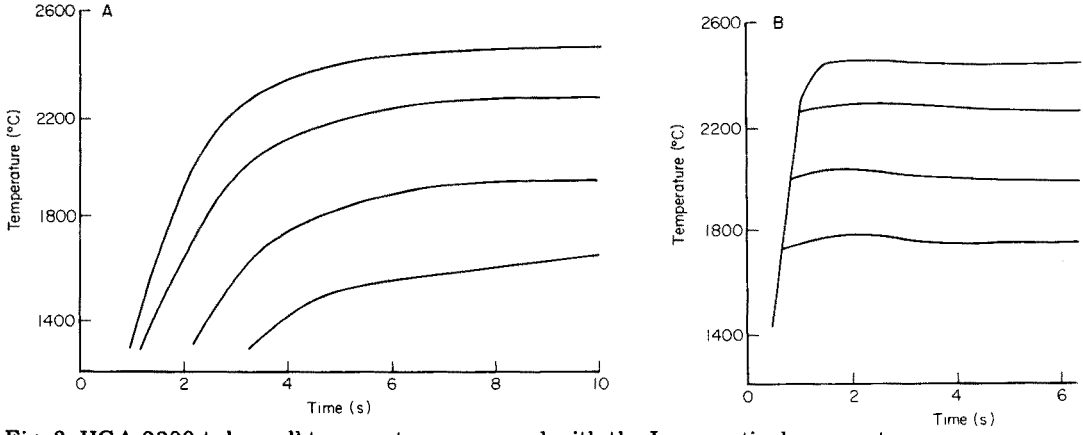

Fig. 3. HGA 2200 tube wall temperature measured with the Ircon optical pyrometer, under gas-stop conditions in an argon atmosphere. (A) Conventional heating to preset temperatures of 1750, 2000, 2300 and 2500°C. (B) Maximum power heating with temperature control to preset temperatures of 1750, 2000, 2300 and 2500°C.

The reason for this is unknown, but the effect was not observed at preset temperatures above 2600°C, where no similar drop in background intensity was observed.

A comparison of the temperatures of the tube wall and vapour phase under maximum power heating showed an apparent lag of about 0.5 s of the vapour phase temperature behind the tube wall temperature during the rapid rise in temperature, but that both temperatures were similar soon after the maximum had been reached (Fig. 4). The lag is 100 times greater than the time lag predicted from heat transfer coefficients for a furnace employing conventional heating rates and gas stop [13]. Although maximum power heating may account for this, it is likely that the response time of the recorder used in the present work was a significant contributing factor. The method used to measure the vapour phase temperature was that applied recently [2] to measurements with an HGA 72 carbon furnace. When the four iron lines at 370.56, 373.49, 373.71 and 392.29 nm were used, and corrections were applied for the variations in the spectral response of the spectrometer, a plot of $\ln([I\lambda_{ij}]/[g_i A_{ij}])$ against E_i was linear with a slope equal to $-1/kT$ from which the absolute temperature T can be obtained. In this expression, I is the corrected emission intensity measured under conditions of negligible self absorption at wavelength λ_{ij}; g_i is the statistical weight of the upper energy level i of energy E_i; A_{ij} is the transition probability; and k is Boltzmann's constant.

This 'slope' procedure was used to measure vapour phase temperatures at many points during the atomization step at a preset temperature of 2500°C under both conventional and maximum power heating. The results are compared with the corresponding tube wall temperatures obtained from the optical pyrometer in Fig. 4. The agreement between tube wall and vapour phase temperatures is within the experimental error of 80—120°C. When maximum power heating is used and constant temperature is reached, the vapour phase rapidly approaches the same temperature as the tube wall,

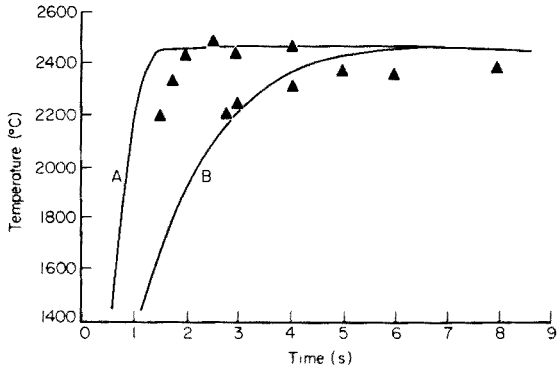

Fig. 4. Variation with time of the tube wall temperature (——) and vapour temperature (▲) for the HGA 2200 atomizer with maximum power heating (A) and conventional heating (B).

but under conventional heating the vapour phase appears to deviate from the tube wall temperature at the later stages of the atomization cycle.

Carbon-furnace atomic emission measurements of involatile elements

It was expected that maximum power heating would be advantageous for the measurement of atomic emission from involatile elements, both on the grounds of an increase in the maximum transient atom concentration and an increase in the vapour phase temperature during the lifetime of that atom population. Optimized detection limits for eleven such elements are given in Table 1 and compared with detection limits reported for flame emission [14, 15] and carbon-furnace atomic absorption [16]. Although the latter were not defined or measured under the same conditions, they allow a general comparison. The modified HGA 2200—PE 272 system was used, and for each element the detection limit was measured at the optimum preset temperature at which the signal-to-background ratio is maximized. Temperature optimization is a function of atom appearance temperatures and other factors, and was found to be significant on the HGA 2200 with maximum power heating but not under conventional heating with voltage control.

Detection limits under maximum power heating were significantly improved compared to conventional heating; except for beryllium, they compare favourably with those reported for flame emission and carbon-furnace atomic absorption. The detection limit for titanium compares reasonably with a value of 0.010 $\mu g\ ml^{-1}$ reported previously for c.f.a.e.s. with simultaneous background correction [9, 17]. Values for molybdenum [18] and beryllium [1] are almost identical to values reported previously for similar instruments without background correction, but are inferior to the most recent work incorporating the use of background correction [17] in which limits of 0.001 and 0.002 $\mu g\ ml^{-1}$ were achieved for molybdenum and beryllium, respectively. C.f.a.e.s. detection limits for the other eight elements have not been reported previously.

With maximum power heating, optimum conditions of signal-to-background ratio and reproducibility were achieved at temperatures below 2700°C for most of the elements considered; even for boron, iridium and uranium, where higher temperatures were used, the maximum temperature was still not required. In addition, atomic emission signals generally peaked within 3—4 s after the start of atomization. The combination of reduced temperatures and shorter atomization periods should extend tube lifetime under maximum power heating compared to conventional heating, particularly for the pyrolytically coated tubes used here.

In general, the analytical reproducibility obtained for electrothermal devices employing manual injection of microsamples is poorer than for continuous nebulization of solutions into flames. A recent study [17] has suggested that variations in heating rate and tube temperature would make carbon-furnace atomic emission less reproducible than carbon-furnace atomic absorption. For the more involatile elements, the possibilities of carbide formation and between-run memory effects and the requirement

TABLE 1

Detection limits for involatile elements by carbon-furnace atomic emission spectrometry, compared to flame emission and carbon-furnace atomic absorption spectrometry

Element	Wavelength (nm)	Optimum c.f.a.e.s. temperature (°C)	Detection limits (μg ml^{-1})		
			C.f.a.e.s.[a]	F.e.	C.f.a.a.s.[b]
Vanadium	318.40				0.019
	437.92	2500	0.0088	0.01[h]	
Molybdenum	313.26				0.005
	379.83	2600	0.016	0.03[i]	
	390.30			0.10[h]	
Ruthenium	349.89				0.02
	372.80	2600	0.023[c]	0.02	
Rhodium	343.49				0.008
	369.24	2400	0.031[d]	0.02	
Titanium	365.35				0.05
	399.86	2500	0.037	0.20	
Palladium	247.64				0.006
	363.47	2300	0.062	0.05	
Silicon	251.61	2500	0.088	10.0	0.01
Boron	249.68	2850	0.20[e]	30.0	0.75
Beryllium	234.86	2550	0.46[f]	10.0	0.0002
Iridium	263.97				0.075
	380.01	2700	0.86	30.0	
Uranium	591.54	2800	2.5[g]	10.0	—

[a] 20-μl aliquot of solutions. [b] Sensitivity in μg ml^{-1}/0.0044 A; based on 20-μl aliquots of solution (see ref. 16). [c] PE 306 spectrometer. [d] Nitrogen atmosphere; other elements measured in argon. [e] 100 μg ml^{-1} calcium added to boron standard solution. [f] 1% hydrochloric acid solution. [g] 0.01 M hydrochloric acid solution. [h] Nitrous oxide/acetylene flame for V, Mo, Ru, Rh, Ti, Pd [14]. [i] Premixed oxyacetylene flame for Mo, Si, B, Be, Ir, U [15].

for high atomization temperatures, might suggest that reproducibilities would be poorer than for more volatile elements. The HGA 2200 was therefore used with maximum power heating to compare the reproducibility of a number of elements classified for convenience as medium volatile (optimu temperatures of 2100—2300°C) and involatile (optimum temperatures 2500—2800°C), the results are given in Table 2. The background signal was subtracted in each case prior to calculation of the relative standard deviation The deviations vary between 1.0 and 7.0%, and no significant variation is apparent between the two sets of elements or as a function of the optimum atomization temperature. At the concentrations used, the values would appear acceptable for analytical purposes. They are similar to values reporte for a furnace operated under conventional heating but with automatic sample injection [17] and some improvement may result from the combination of the temperature control of the HGA 2200 and automatic sampl injection.

TABLE 2

C.f.a.e.s. reproducibility for some medium volatile and involatile elements at concentrations giving comparable signal-to-background ratios

Element	Optimum temperature (°C)	Concentration (μg ml^{-1})	Signal-to-background ratio	RSD (%)
Iron	2100	0.2	2.0	4.3
Nickel	2300	0.2	1.3	3.8
Chromium	2300	0.05	1.2	5.3
Cobalt	2300	1.0	1.8	1.0
Titanium	2500	0.5	1.2	3.9
Silicon	2500	1.0	1.8	3.7
Beryllium	2550	5.0	3.4	7.0
Molybdenum	2600	0.5	3.6	1.6
Uranium	2800	50.0	1.0	2.5

TABLE 3

Carbon-furnace atomic emission detection limits for peak-height signals measured by chart recorder and digital readout

Element	Wavelength (nm)	Optimum atomization temperature (°C)	Detection limits[a] (μg ml^{-1})	
			Recorder chart	Digital readout
Chromium	425.43	2300	0.0055	0.0040
Cobalt	345.35	2300	0.038	0.032
Iron	371.99	2100	0.022	0.017
Manganese	403.08	2150	0.011	0.006

[a]For 20-μl aliquots of solutions with nitrogen as furnace gas and normal unpyrolysed tubes.

Because of the transient existence of the atomic vapour in the carbon tube, the signals recorded in c.f.a.a.s. and c.f.a.e.s. are dependent on the response time of the electronic measurement system, and usually the amplifier or recorder determines the overall speed of response [12]. With the PE 272, improved signal-to-background ratios were achieved with the peak-height digital readout facility compared to those obtained with the Hitachi recorder. The detection limits were improved by factors of 1.2—1.8; this is shown for four elements in Table 3. Background signals of the same magnitude were obtained on both recording systems but the microprocessor system, which processes the signal every 0.1 s, was preferable to the 0.5-s response time of the recorder for measurement of the sharp atomic emission peaks. The improvement of detection limit is small but the peak-height measurement facility of the PE 272 is always advantageous in allowing operation without a strip chart recorder. This is satisfactory for operation under maximum power heating but might be unsatisfactory in cases where the background is

not at its maximum at the same time as the atomic emission signal, which will usually happen under conventional heating.

The main advantages of the HGA 2200—PE 272 system for atomic emission measurements of involatile elements are the maximum power heating and control of temperature, the simplicity of instrumental optimization and the availability of pyrolytically coated tubes. The use of the HGA 72—PE 306 system discussed previously [1, 8, 10] requires that the tubes have reduced wall thickness at the centre [1] in order to achieve detection limits approaching those reported in this paper. This modification allowed higher temperatures and faster heating rates to be used; when it was combined with pyrolytically coated graphite tubes, detection limits of 0.016 and 0.089 $\mu g\ ml^{-1}$ were obtained for rhodium and palladium, respectively, at an optimized temperature of 2550°C. These results are comparable to those from the HGA 2200—PE 272 system but can be obtained only with a modified HGA 72 tube. The application of maximum power heating offered in the HGA 2200 has allowed an extension of the range of elements that can be determined at sub-$\mu g\ ml^{-1}$ levels by carbon-furnace atomic emission spectrometry. The combination of wavelength-modulation background correction with such a system should further improve the detection limits reported and should add further to the substantial range of elements that can now be determined at analytically useful levels by this technique.

The authors are indebted to the Perkin-Elmer Corp. for the short-term loan of the HGA 2200—PE 272 system, and to The Salters' Company for the award of a research scholarship to D. L.

REFERENCES

1 J. M. Ottaway and F. Shaw, Appl. Spectrosc., 31 (1977) 12.
2 D. Littlejohn and J. M. Ottaway, Analyst, 103 (1978) July issue.
3 G. Lundgren, L. Lundmark and G. Johansson, Anal. Chem., 46 (1974) 1028.
4 B. V. L'vov, Atomic Absorption Spectrochemical Analysis, translated by J. H. Dixon, Adam Hilger Ltd., London, 1970, p. 206.
5 D. C. Manning and R. D. Ediger, At. Absorpt. Newsl., 15 (1976) 42.
6 R. E. Sturgeon and C. L. Chakrabarti, Anal. Chem., 49 (1977) 90.
7 J. M. Ottaway and R. C. Hutton, Analyst, 101 (1976) 683.
8 J. M. Ottaway and F. Shaw, Analyst, 100 (1975) 438.
9 M. S. Epstein, T. C. Rains and T. C. O'Haver, Appl. Spectrosc., 30 (1976) 324.
10 D. Littlejohn and J. M. Ottaway, Analyst, 102 (1977) 553.
11 J. K. Hunter, unpublished results.
12 F. J. M. J. Maessen and F. D. Posma, Anal. Chem., 46 (1974) 1439.
13 W. M. G. T. Van den Broek and L. de Galan, Anal. Chem., 49 (1977) 2176.
14 E. E. Pickett and S. R. Koirtyohann, Anal. Chem., 41 (1969) 28A.
15 V. A. Fassel and D. W. Golightly, Anal. Chem., 39 (1967) 466.
16 Standard Conditions for the HGA, Perkin-Elmer Corp., Norwalk, Connecticut, U.S.A., March, 1977.
17 M. S. Epstein, J. R. Moody, T. J. Brady, T. C. Rains and I. L. Barnes, Anal. Chem., in press.
18 J. F. Alder, A. J. Samuel and R. D. Snook, Spectrochim. Acta, Part B, 31 (1976) 509.

Analytica Chimica Acta, 98 (1978) 291—298

THE DETECTION OF MERCURY VAPOUR BY MAGNETICALLY INDUCED OPTICAL ROTATION

R. STEPHENS*

Trace Analysis Research Centre, Department of Chemistry, Dalhousie University, Halifax, N.S. (Canada)

(Received 1st November 1977)

SUMMARY

Equations to describe magnetically-induced optical rotation signals obtained from mercury atoms in the vapour phase are described and tested. The method gives good analytical sensitivity and selectivity. Its advantages over the conventional techniques of analytical spectrometry include the automatic tolerance of continuum background absorption and of source drift.

Magnetically-induced optical rotation (m.i.o.r.) is a phenomenon which has not been utilized for analytical atomic spectrometry. Nevertheless, the sensitivity and selectivity of m.i.o.r. appear likely to be quite satisfactory for its analytical application. In addition, the noise levels and spectral interference effects encountered are influenced by parameters which are different from, and in some ways more favourable than, those affecting conventional spectroscopic techniques. For these reasons, the investigation of m.i.o.r. becomes a matter of potential interest. Such an investigation has been carried out here for the specific case of mercury, an element which is particularly suitable because of its significant vapour pressure at room temperature, as well as the availability of intense spectroscopic sources.

THEORY

The following equations are applicable to the instrumental arrangement described in the Experimental section. Radiation from a d.c. resonance line source is passed through an atom reservoir positioned between crossed polarizers within a longitudinal oscillating magnetic field. Only the a.c. components of the transmitted radiation are measured.

Let H = magnetic field strength; f = oscillation frequency of H; ϕ = angle of rotation of the plane of polarization as radiation passes through the atom reservoir; l = path length of atom reservoir; N = atom density in atom reservoir; I = incident intensity at the photomultiplier; I_0 = source intensity; and S = electrical signal corresponding to I.

Mitchell and Zemansky give a relationship of the form $\phi = KHNl$, where K is a constant [1]. Although the relation was derived for frequencies away from the centre of the absorption line, it was found to describe the experimental behaviour of the present system quite well when used in the following derivation. Thus in general

$$\phi = \phi_0 + KHNl \tag{1}$$

where $H = H_0 \sin 2\pi ft$, t being the time, H_0 the peak value of H, and ϕ_0 the value of ϕ for $H = 0$.

The law of Malus gives $I = \frac{1}{2}I_0 \sin^2 \phi \simeq \frac{1}{2}I_0 \phi^2$ for small ϕ

$$= \tfrac{1}{2}I_0(\phi_0 + KNlH_0 \sin 2\pi ft)^2 = \tfrac{1}{2}I_0(\phi_0^2 + \tfrac{1}{2}K^2N^2l^2H_0^2 + 2\phi_0 KNlH_0 \sin 2\pi ft - \tfrac{1}{2}K^2N^2l^2H_0^2 \cos 4\pi ft).$$

Thus two simultaneous a.c. signals will be generated, at frequencies f and $2f$, where

$$S_f = GI_0\phi_0 KNlH_0 \tag{2}$$

and

$$S_{2f} = \tfrac{1}{4}GI_0K^2N^2l^2H_0^2 \tag{3}$$

G being the electronic gain.

The above relations apply to low atom densities, where negligible attenuation is caused by absorption in the atom reservoir. If this condition is not satisfied, I_0 must be replaced by $I_0 e^{-kNl}$ where k is the Beer's Law absorptivity of the vapour.

EXPERIMENTAL

Figure 1 shows the optical arrangement used. A Hg electrodeless discharge source was used, radiation being observed from the centre of a capillary pinch (5 mm × 1 mm i.d.) drawn in the centre of the silica tube lamp envelope (8 cm × 8 mm diameter). The source was capacitively coupled to a 2 MHz r.f. supply as described elsewhere [2], and mounted at the focus of the lens L (5-cm focal length, f/2.5 aperture) to give an approximately collimated beam through the atom reservoir and polarizers. The polarizers were ultraviolet-transmitting calcite prisms (8-mm aperture; Oriel Corp.) with an extinction coefficient of less than 10^{-5}. The Hg 253.7-nm line was isolated by a Baird-Atomic Hg-line interference filter and was detected with an IP 28 photomultiplier. The filter was mounted directly against the window of the photomultiplier housing to permit the two to be moved as a single unit. The photomultiplier signal was fed to a PAR model 117 pre-amplifier and 124 lock-in. D.c. intensities were measured by switching the photomultiplier signal through a d.c. amplifier to a digital voltmeter.

Two atom reservoirs were used: these are shown in Fig. 1. The smaller unit (Fig. 1A) was used only to determine the magnitude of any fluorescence

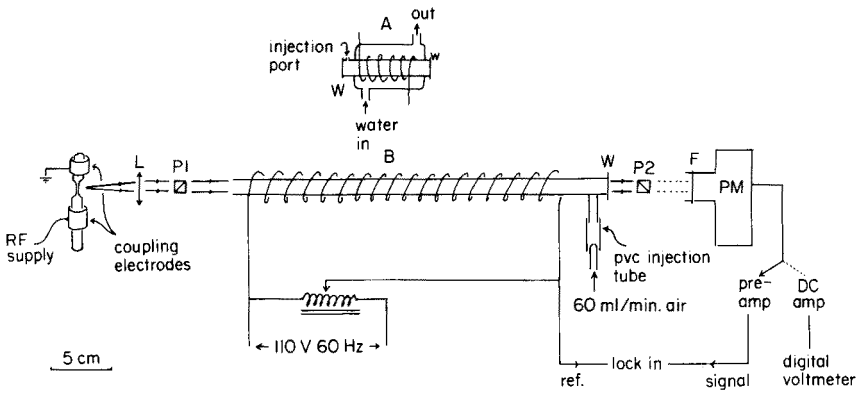

Fig. 1. Apparatus. P_1, P_2: polarizers. L: collimating lens. F: filter. PM: photomultiplier. W: silica windows.

contribution to the observed signals (see below). All other measurements were made with the larger unit (Fig. 1B), which consisted of a pyrex tube (30 cm × 1.3 cm i.d.), carrying 3000 turns of 22-gauge magnet wire. At the maximum r.m.s. current of 5 A used, this solenoid gave a peak field of 900 G at the centre of the coil. All magnetic field strengths were measured by insertion of a search coil at the centre of the solenoid. The solenoid was driven at the 60-Hz mains frequency through a variable auto-transformer. The transformer output also provided the reference voltage for the lock-in amplifier.

Mercury vapour was introduced by drawing up a measured volume of saturated vapour into a (calibrated) syringe, diluting with air to a constant volume of 2 ml, and injecting the vapour through the PVC connecting tube over a period of about 5 s. A constant air flow of about 60 ml min^{-1} carried the injected vapour through the atom reservoir. All quantitative measurements of the resulting signals were made with the lock-in amplifier in its integration mode, to minimize the effects of variable delivery time. The syringe was purged with clean air between readings to eliminate the slight memory effects otherwise apparent.

It was necessary to measure precisely the relative angle, Θ, between the polarizer axes. This was done by use of a He—Ne laser as a light pointer. The beam was reflected from a small mirror attached to the edge of one polarizer onto a fixed linear scale: the system was calibrated from the position of minimum optical transmission ($\Theta = 90°$).

RESULTS AND DISCUSSION

Effect of resonance fluorescence

Atomic fluorescence under the type of experimental conditions used here has been discussed in detail by Mitchell and Zemansky [1]. With the

particular optical alignment of the present apparatus, fluorescence is expected to show circular polarization in the presence of the magnetic field, and to be unpolarized in its absence. It is not apparent that such radiation will be amplitude-modulated by the magnetic field, in which case no fluorescent contribution to the observed signal would be expected.

Experimentally, the relative contributions of m.i.o.r. and fluorescence to the observed signals were evaluated as follows. For perfectly collimated source radiation, the m.i.o.r. signal is independent of the distance between the atom reservoir and the detector, whereas the fluorescence signal is approximately proportional to $L/R(R + L)$, where L is the length of the atom reservoir and R is the distance between the atom reservoir and the detector. Signal measurement over increasing values of R for $R > L$ should therefore indicate the relative contributions of m.i.o.r. and of fluorescence. In practice, the lack of collimation of the source radiation was apparent for the R values used (up to 60 cm). This was corrected by determining simultaneously the variations of transmitted intensity with R, by rotating one polarizer through 90° and multiplying all readings by the ratio of the intensity at R (minimum) to that at R. Rotations of + 90° and −90° were used with sequential consistency, because of a slight asymmetry in the polarizer transmission on rotation through 180°. The maximum correction introduced by this procedure was a factor of 2 at R = 60 cm.

The results thus obtained are shown in Fig. 2. It is apparent that neither

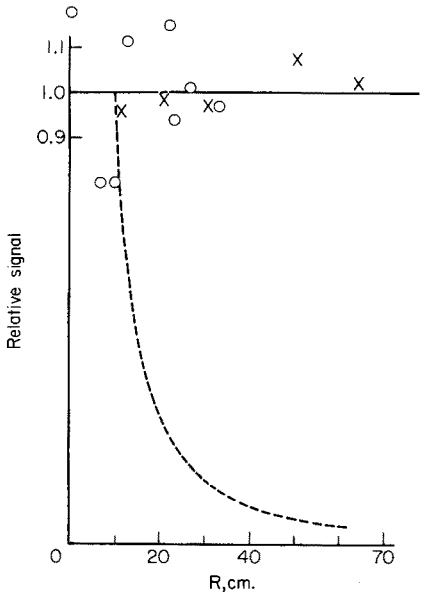

Fig. 2. Signal vs. the distance between photomultiplier and atom reservoir (R). All signals obtained by injecting 2 ml of Hg vapour at a field of 650 G. ○ = S_{2f}; × = S_f. The S_{2f} and S_f signals have been normalized with respect to their respective average values. The dotted curve is the relative fluorescence intensity given by the equation $L/R(R + L)$.

the f nor the $2f$ signals are markedly affected by fluorescence. Accordingly, any fluorescence contribution to the signals observed has been ignored in the data presented below.

Calibration curves

Figure 3 shows the f and $2f$ calibration curves measured at increasing field strength. The general form of the curves is qualitatively as expected from eqns. (2) and (3), i.e. linear and square-law dependence on concentration and field strength. The curves do not rise as sharply as would be expected; this behaviour is attributed to neglect of the e^{-kNl} term already mentioned. Quantitatively, the adherence of the f and $2f$ signals to eqns. (2) and (3) can be judged from Fig. 4, in which the function $S_{2f}/(H_0S_f)$ is plotted against N for all the data shown in Fig. 3. Equations (2) and (3) show that such a plot should be linear irrespective of attenuation caused by atomic absorption. It is apparent from Fig. 4 that, while relatively good linearity is in fact obtained from such a plot, the slope is not identical for each set of data points, i.e. the constant K in eqns. (2) and (3) is in fact influenced slightly by the magnitude of H_0.

Signal variations caused by variations in polarizer angle

Figure 5 shows the dependence of the f and $2f$ signals on the angle, Θ, between the polarizer axes. Again the curves can be interpreted from eqns. (2) and (3), which require the f and $2f$ signals respectively to be proportional

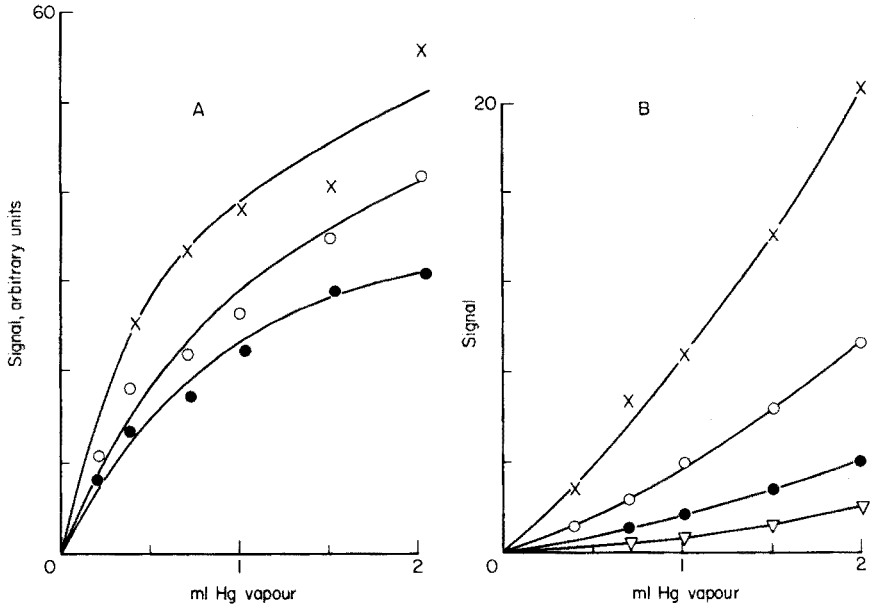

Fig. 3. Calibration curves for the S_f (A) and S_{2f} (B) signals. × = 900 G; ○ = 650 G; ● = 400 G; ▽ = 160 G.

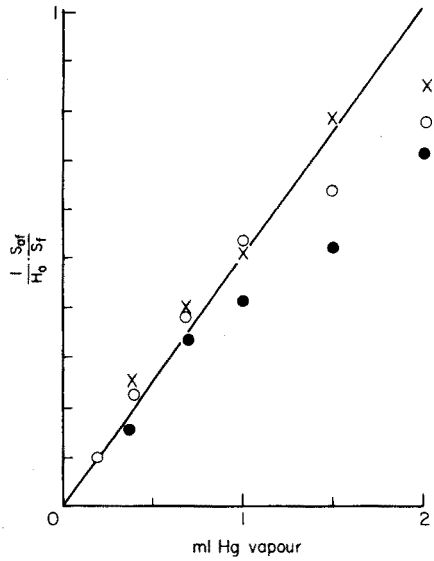

Fig. 4. S_{2f}/H_0S_f vs. volume of Hg vapour injected, based on the data given in Fig. 3. × = 900 G; ○ = 650 G; • = 400 G.

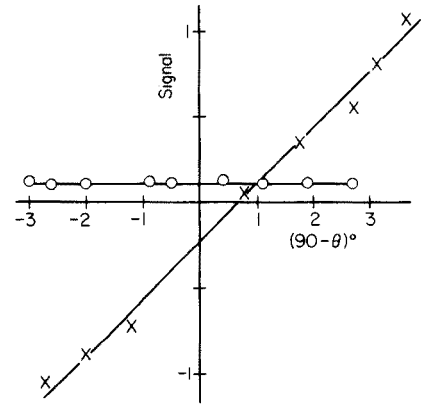

Fig. 5. S_f (×) and S_{2f} (○) vs. polarizer displacement, (90—Θ)°. 0.6 ml of Hg vapour injected; field strength 650 G.

to Θ and constant. From eqn. (2) the f curve should go through the origin: the failure to do this is attributed to a stray d.c. magnetic field around the apparatus, with a component along the axis of the atom reservoir. That such a field would give a displacement of the observed form can be seen by substitution of $H = H_{dc} + H_0 \sin 2\pi ft$ into eqn. (1).

Analytical parameters

Two variables of analytical interest associated with the present apparatus will be discussed in detail here. These are (a) spectroscopic selectivity, and (b) sensitivity.

Selectivity. When the formulae derived in Mitchell and Zemansky are applied (which is felt to be reasonable since they permit the experimental data obtained here to be described quite well), then optical rotation of an emission frequency ν by an absorption frequency ν_0 is proportional to $(\nu - \nu_0)^{-2}$. Because a resonance line source is used, the values of $(\nu - \nu_0)^{-2}$ over the whole emission line are large. This will not be the case for absorption lines which do not fall within the emission line profile. Thus spectroscopic selectivity is inherent to the m.i.o.r. technique, for reasons which are similar to those responsible for the selectivity of line-source a.a.s.

However, the selectivity of m.i.o.r. has certain features which suggest that it may offer an unusually powerful tool for analytical atomic spectrometry. The first of these features is the lack of sensitivity to a continuum absorption

caused by wide-band molecular absorption or particle scatter (since a small separation between emission or absorption line frequencies is required to give significant vapour-phase optical rotation). This behaviour is illustrated in Fig. 6, which shows responses obtained for mercury vapour and for saturated acetone and benzene vapours. Secondly, the system is insensitive to changes of source intensity, since the source is not viewed directly. Thirdly, large transient signals and associated noise, such as are encountered with dual-beam background-corrected atomic absorption measurements upon finite changes in optical transmission efficiency, do not occur with m.i.o.r. because its transmission efficiency is negligible in the first place.

Sensitivity. A full discussion of the sensitivity inherent to m.i.o.r. is not given here. However, in an optimized m.i.o.r. system, a consideration of photon noise levels shows that the source intensity transmitted through the crossed polarizers should be less than the background emission intensity from the atomizer over the optical bandwidth of the system. Moreover, the present apparatus is ideally suited to giving good sensitivity, because there is no noise from atomizer emission. The detection limit obtained (4×10^{-12} g) does not represent the limit of the system, but rather is a limit imposed by the finite extinction coefficient of the polarizers used.

S_f and S_{2f} detection limits of 4×10^{-12} and 1×10^{-11} g, respectively, with an integration time of 1 s were obtained with the present apparatus. These values are considered to be sufficiently good to support the comments made earlier concerning the potentially useful sensitivity of the technique. Greater sensitivity could be obtained by use of a more efficient polarizing system,

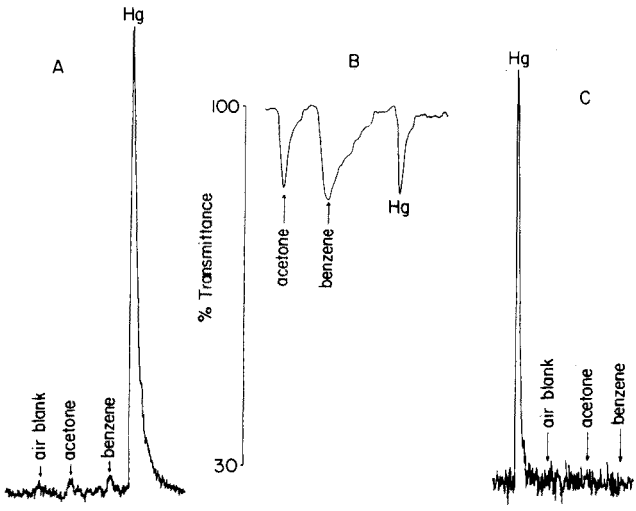

Fig. 6. Signals obtained by injection of 0.4 ml of mercury vapour and of 2 ml of saturated acetone and benzene vapour. (A) S_f m.i.o.r. signal. (B) Corresponding absorption signals obtained by measurement of the transmitted d.c. intensity with polarizer P2 removed. (C) S_{2f} m.i.o.r. signals.

greater magnetic field strength, longer integration time and/or higher source intensity.

Conclusions

This work has shown that m.i.o.r. represents a viable technique for the detection of mercury atoms. The automatic tolerance of continuum background absorption and source drift, etc., together with the ability to correct signal magnitudes for variable optical transmission efficiency (as shown in Fig. 5) give the method some advantages over conventional spectrometric techniques. The data obtained support the validity of the equations and associated assumptions used to describe the m.i.o.r. response for the specific case of mercury.

M.i.o.r. is instrumentally similar to atomizer-modulated, Zeeman background-corrected (ZBC) atomic absorption spectrometers which have been described recently [3, 4], although it avoids certain of their inherent noise sources (schlieren, photon). Indeed, ZBC spectrometers of this type could be readily modified for m.i.o.r. operation.

However, the spectroscopic requirements of m.i.o.r. (high intensity sources and a low emission background atomizer) are closer to those of atomic fluorescence instrumentation. Probably therefore, the natural development of the technique lies in the application of tunable lasers; these devices satisfy the intensity requirement of m.i.o.r. At the same time, m.i.o.r. is complementary to the laser source, because of its tolerance for absorption background, source drift, etc., combined with the fact that the detector is not directly exposed to source emission. Such a combination is felt to be of sufficient potential interest to warrant future investigation.

The author is indebted to the National Research Council of Canada for support of this work.

REFERENCES

1 A. C. G. Mitchell and M. W. Zemansky, Resonance Radiation and Excited Atoms, Cambridge University Press, 1934.
2 R. Stephens, Talanta, 24 (1977) 233.
3 J. B. Dawson, E. Grassan, D. J. Ellis and M. J. Keir, Analyst, 101 (1976) 315.
4 H. Koizumi and K. Yasuda, Spectrochim. Acta, Part B, 31 (1977) 523.

Analytica Chimica Acta, 98 (1978) 299—306

DOSAGE PAR FLUORESCENCE X DU CHLORE ET DU BROME DANS LES EAUX NATURELLES, LES SAUMURES ET LES EVAPORITES

MARIE-CLAUDE SICHÈRE* et FABIEN CESBRON

Laboratoire de Mineralogie-Cristallographie associé au C.N.R.S., Université P. et M. Curie, 75230 Paris Cedex 05 (France)

GIAN-MARIA ZUPPI

Laboratoire de Géologie Dynamique, Université P. et M. Curie, 4 place Jussieu, 75230 Paris Cedex 05 (France)

(Reçu le 21 Novembre 1977)

RÉSUMÉ

Des concentrations en brome de 0,6—120 mg l^{-1} peuvent être déterminées directement sur liquide par fluorescence x en utilisant le sélénium comme étalon interne pour éliminer les effets d'interférence; pour de plus faibles concentrations il faut avoir recours à la concentration du brome sur papier résine. Il est également possible de doser le chlore directement dans une gamme de 0,6—120 g l^{-1}, du baryum est ajouté pour réduire l'influence des carbonates et des sulfates. L'influence des ions SO_4^{2-}, CO_3^{2-}, Ca^{2+}, K^+, Mg^{2+}, Na^+, Sr^{2+}, Fe^{3+}, est examiné.

SUMMARY

X-ray fluorescence analysis for chlorine and bromine in natural waters and brines

Bromine concentrations of 0.6—120 mg l^{-1} may be determined directly in liquids by x-ray fluorescence with selenium as internal standard to eliminate interference effects; for lower concentrations, bromine is concentrated on a filter disk containing an exchange resin. It is possible to measure chlorine directly in the 0.6—120 g l^{-1} range; barium is added to reduce the influence of carbonates and sulfates. The influence of some ions e.g. SO_4^{2-}, CO_3^{2-}, Ca^{2+}, K^+, Mg^{2+}, Na^+, Sr^{2+}, Fe^{3+}, has been examined.

L'analyse par spectrométrie de fluorescence x a été choisie de préférence à toutes les autres méthodes car elle permet d'atteindre un très large éventail de concentration sans qu'il soit nécessaire de faire appel à des traitements préalables généralement fastidieux par voie humide; de plus c'est une méthode non destructive. Quelques méthodes de dosage ont déjà été décrites, en particulier par Dunton [1], Rose et Cuttita [2], Kokotailo et Damon [3], Wahlberg et Myers [4], Radcliffe [5] et enfin Erämetsa et Särkkä [6] mais elles ne s'appliquent qu'au brome. Le problème se posait de doser le chlore et le brome avec une précision suffisante tout en s'affranchissant des interférences dues à la présence d'autres éléments, interférences qui n'ont pas été étudiées jusqu'alors.

Des essais infructueux d'analyse sur les phases solides obtenues soit en précipitant le brome par le nitrate d'argent, soit en évaporant des solutions, ont conduit à abandonner cette technique; en effet dans le premier cas le métal lourd absorbe une partie du rayonnement tandis que dans le second le brome s'évapore dès que la température dépasse 50°C. C'est donc finalement en phase liquide que le chlore et le brome ont été dosés, les sels des évaporites étant alors dissous.

CONDITIONS EXPERIMENTALES

Le dosage en phase liquide s'effectue sous flux d'hélium (50 l h^{-1}) pour diminuer l'absorption par l'air du rayonnement de fluorescence émis puisqu'il n'est pas possible de travailler sous vide. Les conditions opératoires optimales sont résumées dans le Tableau 1.

L'épaisseur utile "d" qui doit être traversée par le faisceau de rayonnement x et qui contribue pour 99,9% au rayonnement de fluorescence est donnée par la formule

$$d_{cm} = 6{,}91 \left(\frac{\mu_1}{\sin\phi} + \frac{\mu_2}{\sin\psi}\right)$$

compte-tenu du fait que l'intensité due à la contribution des couches comprises entre 0 et d est

$$I_{2d} = \left(c\, k\, I_1 \Big/ \left[\frac{\mu_1}{\sin\phi} + \frac{\mu_2}{\sin\psi}\right]\right) \left(1 - \exp\, -\left(\frac{\mu_1}{\sin\phi} + \frac{\mu_2}{\sin\psi}\right) d\right)$$

où ϕ = angle d'incidence du faisceau de longueur d'onde λ_1; ψ = angle d'émergence du faisceau de longueur d'onde λ_2; μ_1 = coefficient d'absorption de la longueur d'onde λ_1; μ_2 = coefficient d'absorption de la longueur d'onde λ_2; On choisit de plus $I_{2d} = 0{,}999\, I_{2\infty}$.

TABLEAU 1

Conditions expérimentales

	Br	Cl	Se
Raie analysée	Br $K\alpha_1$ $n = 1$ $2\theta = 29{,}89°$	Cl $K\alpha_1$ $n = 1$ $2\theta = 65{,}35°$	Se $K\alpha_1$ $n = 1$ $2\theta = 31{,}82°$
Fond	$2\theta = 28{,}89°$	$2\theta = 66{,}35°$	$2\theta = 30{,}82°$
Tube	Mo, 45 kV, 22 mA	Cr, 20 kV, 36 mA	Mo, 45 kV, 22 mA
Cristal analyseur	LiF	P.E	LiF
Compteur	Flux gazeux 1520 V	Flux gazeux 1520 V	Flux gazeux 1520 V
Fente de Soller	0,15°	0,4°	0,15°
Discrimination:			
seuil	0,48 V	0,48 V	0,48 V
canal	0,78 V	0,90 V	0,78 V
Comptage	200 s	400 s	200 s

Dans le cas de l'appareillage SRS Siemens utilisé, $\phi = \psi = 45°$ ce qui permet de simplifier la formule: $d_{cm} = 6{,}91/(\mu_1 + \mu_2)$.

Dans le cas du dosage du brome dans l'eau de mer avec une anticathode de molybdène l'épaisseur optimale "*d*" est égale à 0,877 cm, dans le cas du chlore analysé avec une anticathode au chrome elle est de 0,015 cm. Le dosage du chlore et du brome en phase liquide a été effectuée en utilisant un volume égal à 10 ml ce qui représentait une hauteur de 1 cm dans la cuve utilisée; d'où une épaisseur plus que suffisante en particulier dans le cas du chlore.

INFLUENCE DES IONS ETRANGERS ET DISCUSSION DES RESULTATS

Dosage du brome

L'influence des anions et des cations lors du dosage du brome doit être envisagée avec soin car l'absorption de la raie d'émission du brome par d'autres éléments présents, dépend des teneurs en ces éléments susceptibles d'être gênants.

Si les anions SO_4^{2-} et CO_3^{2-} sont pratiquement sans effet sur le dosage du brome, il n'en est pas de même du chlore qui produit un affaiblissement du rayonnement de fluorescence du brome. La Fig. 1 montre la variation de pente des différentes courbes obtenues en faisant varier la teneur en NaCl (l'ion Na^+ a un effet négligeable) pour des concentrations en brome constante: on y voit nettement que plus la teneur en brome est élevée plus l'effet dépressif est important; pour des solutions contenant 5 mg l^{-1} Br^- il n'y a pratiquement

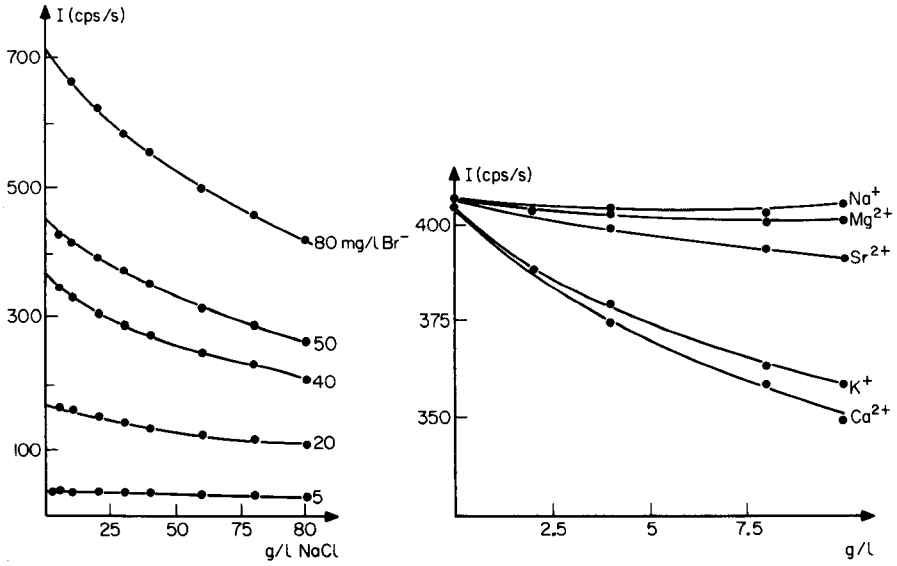

Fig. 1. Variation de l'intensité du rayonnement du brome en fonction de teneurs croissantes en NaCl.

Fig. 2. Influence des ions Na^+, K^+, Mg^{2+}, Sr^{2+}, Ca^{2+}, sur l'intensité émise par le brome.

pas de perturbation. Des teneurs en chlore ne dépassant pas 2,5 g l^{-1} ne gênent pas le dosage du brome jusqu'à des concentrations de 20 mg l^{-1} en Br^-, dans le cas de teneurs plus élevées il convient de diluer les solutions.

L'influence des ions Ca^{2+}, K^+, Mg^{2+}, Na^+, Sr^{2+} est traduite sur la Fig. 2: dans le cas de solutions contenant 50 mg l^{-1} de brome, pour des concentrations de 10 g l^{-1} en ion K^+ et Ca^{2+} (sous forme d'acétate), on note un affaiblissement de l'intensité respectivement de 11,2 et 14,9%. Par contre l'effet dépressif est moindre pour le strontium puisque l'intensité du rayonnement émis ne diminue que de 3,4% pour des teneurs en ion Sr^{2+} de 10 g l^{-1}; de plus cet élément est rarement présent en concentrations notables dans les eaux naturelles, les saumures et les évaporites. Pour Mg^{2+} et Na^+ l'effet dépressif est pratiquement négligeable.

Enfin, en ce qui concerne le fer, l'affaiblissement de l'intensité émise du brome n'est notable que lorsque la teneur dépasse 0,3 g l^{-1} Fe.

L'influence de la matrice peut donc être, dans certains cas, considérable, en particulier dans les évaporites: la Fig. 3 montre les variations de l'intensité du rayonnement de fluorescence du brome en fonction de la teneur (en g l^{-1}) de NaCl de la matrice; l'utilisation du sélénium préconisé par Kokotailo et Damon [3] et Erämetsa et Särkkä [6] semble alors s'imposer.

En effet le sélénium étant voisin du brome dans la classification périodique, il subit les mêmes effets, dépressifs ou exaltateurs, que lui; cet élément est introduit sous forme de sélénite d'ammonium avec une concentration constante de 100 mg Se l^{-1}.

Le dosage en phase liquide du brome avec étalon interne de sélénium a été réalisé facilement. Pour des concentrations de 0,6—100 mg l^{-1}, la courbe d'étalonnage obtenue en portant le rapport I_{Br}/I_{Se} (0—1.40) en ordonnée et la teneur en brome en abscisse, est très sensiblement une droite. Par exemple l'erreur relative pour l'analyse d'une solution contenant 50 mg l^{-1} de brome et 10 mg K l^{-1} peut atteindre 1,3% en présence de l'étalon de sélénium alors qu'elle serait de l'ordre de 11,2% en l'absence de cet étalon, l'effet

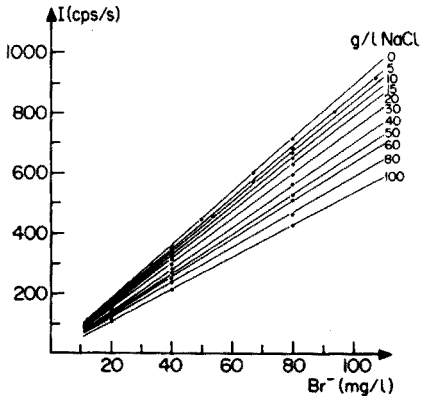

Fig. 3. Variation de l'intensité du rayonnement du brome en fonction de la teneur en NaCl de la matrice.

dépressif du potassium étant très notable. L'influence du chlore est encore plus spectaculaire; le dosage d'une solution contenant 50 g l^{-1} de chlore et 25 mg l^{-1} de brome est effectué avec une erreur relative de 2,6% avec étalon interne et de 36% sans étalon. L'intérêt de ce dernier est donc évident.

Pour des gammes de teneur en brome inférieures à 0,6 mg l^{-1} il faut envisager de concentrer la solution sur papier résine [5, 7]. Les papiers utilisés sont chargés de résine Amberlite à 50% en poids (papier Reeve, Angel Type SB_2) capable de fixer les anions en milieu fortement basique. Cette méthode de concentration du brome semble être d'un emploi plus aisé que celle que préconisent Wahlberg et Myers [4] qui concentrent sur des disques imprégnés d'acides gras.

Les disques de papier résine, coupés au diamètre de 30 mm, sont traités par une solution 0,5 M de $NaNO_3$ afin d'éliminer toute trace de chlorure éventuellement présente dans la résine [8], plusieurs passages sont effectués et après rinçage à l'eau distillée les disques sont mis à sécher; il suffit de les faire gonfler dans l'eau avant usage. Les disques sont alors placés dans une colonne de chromatographie Chromaflex; ils reposent sur une plaque en verre frittée (40—60 μm), les deux parties de la colonne sont réunies par une pince métallique pour rodage sphérique, un joint torique assurant l'étanchéité. Pour récupérer au moins 99% du brome présent sept passages s'avèrent nécessaires; il faut éviter de filtrer des volumes trop importants sinon la capacité d'échange de la résine risque d'être dépassée, en général un volume de 40 ml est convenable. Il s'avère aussi nécessaire d'employer successivement trois papiers (avec autant de passages pour chacun) pour être certain de fixer pratiquement tout le brome présent dans la solution. Les papiers rincés à l'eau distillée sont ensuite mis à sécher. Une courbe d'étalonnage établie pour une gamme de 0,06 à 1 mg l^{-1} de brome est linéaire; la valeur de l'intensité portée en ordonnée est la somme des valeurs des intensités des trois papiers moins celle obtenue pour un blanc: papier traité uniquement par $NaNO_3$.

Il est donc possible de doser le brome de 0,06—120 mg l^{-1} soit directement soit après concentration sur papier résine si la teneur est inférieure à 0,6 mg l^{-1}.

Dosage du chlore

Le dosage direct sur phase liquide peut également s'appliquer au chlore. De même que pour le brome nous avons examiné les différentes interférences possibles.

La Fig. 4 montre l'influence des ions SO_4^{2-}, CO_3H^- et CO_3^{2-} qui provoquent un affaiblissement non négligeable de l'intensité du rayonnement émis du chlore. Pour des teneurs en ions variant de 0 à 20 g l^{-1}, l'erreur relative est de 2,7% dans le cas des ions CO_3H^-, de 6,5% dans le cas des ions CO_3^{2-} et de 7,5% dans le cas des ions SO_4^{2-}. Sur la Fig. 5 des courbes établies en faisant varier la teneur en SO_4^{2-} pour différentes solutions de teneur en chlore constantes montrent que la pente moyenne augmente avec la teneur croissante en chlore, de 4 à 30 g l^{-1}.

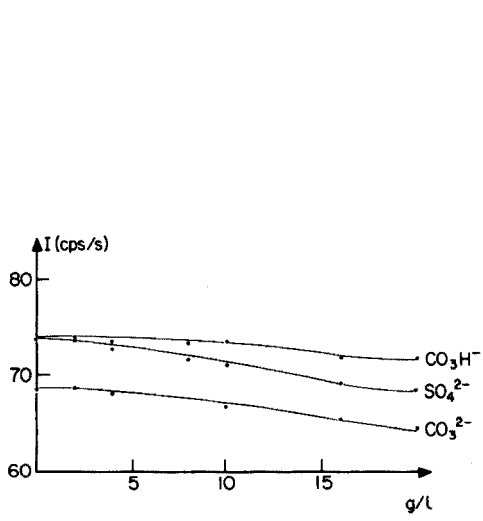

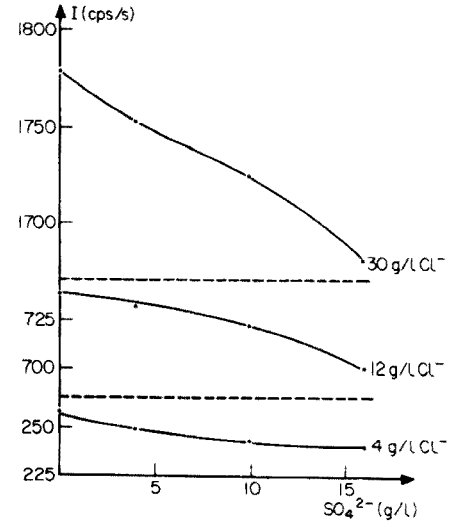

Fig. 4. Influence des ions CO_3^{2-}, CO_3H^-, SO_4^{2-}, sur le dosage du chlore.

Fig. 5. Influence des ions SO_4^{2-} sur l'intensité du rayonnement du chlore.

En ce qui concerne le brome aucun effet n'est notable pour des teneurs inférieures à 150 mg l^{-1}.

De plus des solutions de KCl, NaCl, $MgCl_2$, $SrCl_2$ ont été préparées pour examiner une éventuelle influence des ions K^+, Na^+, Mg^{2+}, Sr^{2+}. Seul Sr^{2+} a un effet dépressif: pour une solution de $SrCl_2$ contenant 10 g Cl_2 l^{-1}, on observe un affaiblissement de l'intensité émise de l'ordre de 7% par rapport à celle émise par une solution de NaCl contenant la même quantité de chlore.

Le choix d'un étalon interne s'est avéré impossible et, pour diminuer fortement les interférences, il faut avoir recours à l'adjonction d'un élément lourd, ici, le baryum. Les sulfates étant gênants il est aisé de les précipiter par addition d'acétate de baryum, il suffit de tenir compte du rapport SO_4/Ba = 0,7. Pour diminuer fortement l'influence des carbonates, il suffit d'ajouter de l'acétate de baryum en tenant compte du rapport CO_3/Ba = 0,436.

Par exemple si l'on a dans la solution à doser 2,5 g l^{-1} de CO_3 et 5 g l^{-1} de SO_4 il faut 5,7 g l^{-1} de Ba pour éliminer l'effet de CO_3^{2-} et 3,5 g l^{-1} de Ba pour éliminer l'effet de SO_4^{2-} ce qui se vérifie aisément dans le Tableau 2.

TABLEAU 2

Effet d'un élément lourd (baryum) pour corriger les effets dépresseurs de CO_3^{2-} et SO_4^{2-}

	Intensité
10 g l^{-1} Cl^-	124.437
10 g l^{-1} Cl^- + 2,5 g l^{-1} CO_3 + 5 g l^{-1} SO_4	121.914
10 g l^{-1} Cl^- + 2,5 g l^{-1} CO_3 + 5 g l^{-1} SO_4 + 3 g l^{-1} Ba	122.351
10 g l^{-1} Cl^- + 2,5 g l^{-1} CO_3 + 5 g l^{-1} SO_4 + 9,9 g l^{-1} Ba	124.473

Il est donc ainsi possible de doser le chlore pour des teneurs allant de 0,05 à 150 g l^{-1} sans avoir recours à une technique de concentration, on peut couvrir de la sorte la gamme des teneurs en chlore des eaux naturelles, des saumures et des évaporites et on atteint des concentrations telles que le brome associé n'est plus décelable.

La Fig. 6 est la courbe d'étalonnage du chlore de 0,05 à 150 g l^{-1}; une courbe d'étalonnage plus précise a également été établie pour les faibles teneurs allant jusqu'à 2 g l^{-1}. La courbe d'étalonnage du chlore a été traitée du point de vue paramétrique à l'aide d'une équation du troisième degré tandis que l'approximation du premier degré est suffisante pour la courbe d'étalonnage du brome. Les valeurs permettant d'établir les courbes d'étalonnage ont été traitées à l'ordinateur.

CONCLUSION

Ce mode de dosage par fluorescence x permet d'analyser le chlore et le brome pour des gammes de concentrations allant de la centaine de g l^{-1} à la fraction de mg l^{-1} avec une déviation standard meilleure que 1% relatif.

L'influence des anions et des cations présents en général dans les eaux et les saumures naturelles a été étudiée: c'est ainsi que l'effet dépressif important du chlore et du calcium, par exemple, sur l'intensité du rayonnement émis par le brome a été mis en évidence; il a été démontré également que les ions carbonates et les sulfates affaiblissent l'intensité émise par le chlore.

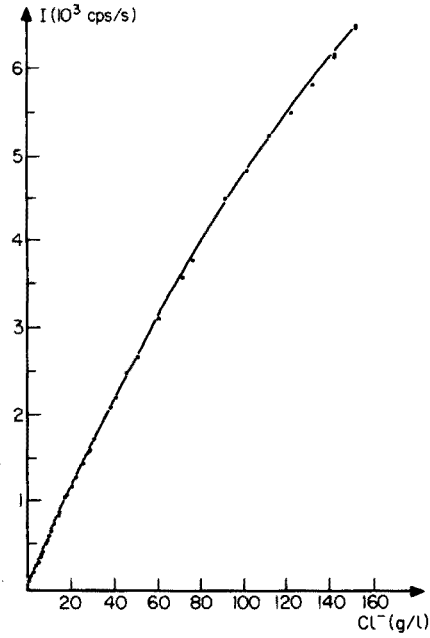

Fig. 6. Courbe d'étalonnage du chlore.

Cette étude de la détermination du chlore et du brome était principalement orientée vers la détermination du rapport $Br \times 10^3/Cl$ qui est un indicateur génétique des conditions de formation des horizons stratigraphiques des évaporites et de l'origine possible des eaux de sources thermales.

La méthode mise au point a d'ailleurs été appliquée à un certain nombre de problèmes géologiques et hydrogéologiques; les résultats devant faire l'objet d'une publication séparée.

BIBLIOGRAPHIE

1 P. J. Dunton, Appl. Spectrosc., 22 (1968) 99.
2 H. J. Rose Jr. et F. Cuttita, Advan. X-ray Anal., 11 (1968) 23.
3 G. T. Kokotailo et G. F. Damon, Anal. Chem., 25 (1953) 1185.
4 J. S. Wahlberg et A. T. Myers, U.S. Geol. Surv. Prof. paper n° 600 D, (1968) 214.
5 D. Radcliffe, Anal. Lett., 3 (1970) 573.
6 O. Erämetsa et M. Särkkä, Suom. Kemistil. B, 43 (1970) 4.
7 M.-C. Sichère et G. M. Zuppi, C.R. Acad. Sci. Paris, Sér. D., 276 (1973) 2935.
8 R. C. De Geiso, W. Rieman III et S. Lindenbaum, Anal. Chem., 26 (1954) 1840.

Analytica Chimica Acta, 98 (1978) 307—313

EFFECTS OF SEVERAL EXPERIMENTAL PARAMETERS ON THE RELATIVE SENSITIVITY FACTORS IN SPARK-SOURCE MASS SPECTROMETRIC ANALYSIS OF STEEL

KAZUO YANAGIHARA* and SHOKI SATO

Central Research Laboratory, Daido Steel Co., Ltd., Minami-ku, Nagoya City (Japan)

SHOHEI ODA and HITOSHI KAMADA

Department of Industrial Chemistry, Faculty of Engineering, University of Tokyo, Bunkyo-ku, Tokyo (Japan)

(Received 15th November 1977)

SUMMARY

The effects of spark gap, sample electrode size, spark technique, spark position, and energy-pass bandwidth of the ion beam, on the relative sensitivity factors in analysis for trace elements in steel by spark-source mass spectrometry have been investigated by means of electrical-detection, peak-switching techniques. The effects of spark gap and spark position are of the greatest importance. The energy distributions of both matrix and impurity ions were measured. For several elements, changes in spark position produced corresponding changes in the distribution of ion energies. These changes of energy distribution were partly responsible for variations in relative sensitivity factors with changing spark position.

It is well known that experimental parameters such as spark gap and spark position affect the accuracy and precision of trace elemental analysis by spark-source mass spectrometry (s.s.m.s.). Franzen and Hintenberger [1], Halliday et al. [2], and Yamaguchi et al. [3] have shown that variation of ion-accelerating voltage, spark voltage, pulse duration, and repetition rate can cause gross changes in elemental sensitivities. Magee and Harrison [4] investigated spark-gap effects in a number of different matrices with electrical-detection peak-switching techniques, and demonstrated that the sensitivities for most elements varied according to gap width. Wadlin and Harrison [5] reported that spark position affected resolution, line intensity, and relative sensitivity factor (RSF). Franzen and Schuy [6] discussed the effects of the sample electrode shape on analytical precision.

The precision (relative standard deviation) of repeat determinations in the analysis of steel by s.s.m.s. with electrical-detection peak-switching techniques is known to be within 5% for successive analyses [7]. However, the relative standard deviation may increase to as much as 15% when repeat analyses are done on different days. This is probably caused by variation of experimental parameters such as spark gap, spark position, sample electrode shape

etc., which affect the RSF. The purpose of this investigation was to determine the direction and extent of the effects of five experimental parameters, i.e. spark gap, sample electrode shape, spark technique, spark position, and energy-pass bandwidth of the ion beam, on the RSF for different elements.

EXPERIMENTAL

Apparatus

A JEOL JMS-01BM mass spectrometer with electrical detection equipment was used. The electrical-detection, peak-switching system of the apparatus was operated by the magnetic peak-switching method with a Hall probe magnetic-field monitor, thus allowing coverage of the entire mass range at a constant accelerating voltage [8]. The spark gap width was checked with an automatic spark gap controller [9]. The vacuum in the analyzer was maintained at about 4×10^{-8} torr, and the source pressure just before sparking was usually in 10^{-7} torr region.

Sample preparation

NBS low-alloy steel No. 462 and NBS stainless steel No. 443 were used as the standard steel samples. The compositions of these steels are (nominal weight %):

NBS 462: 0.40 C, 0.94 Mn, 0.045 P, (0.025 S), 0.28 Si, 0.20 Cu, 0.70 Ni, 0.74 Cr, 0.058 V, 0.08 Mo, 0.053 W, 0.11 Co, 0.037 Ti, 0.046 As, 0.066 Sn, 0.02 Al, 0.096 Nb, 0.036 Ta, 0.063 Zr, 0.006 Pb, (<0.0002 Ag), (0.003 Ge, 0.006 O, 0.008 N);

NBS 443: 3.38 Mn, (0.15 Si), 0.14 Cu, 9.4 Ni, 18.5 Cr, 0.064 V, 0.12 Mo, (0.09 W), 0.12 Co, 0.003 Ti, 0.006 Sn, 0.056 Nb, (0.0008 Ta), 0.0012 B, 0.0025 Pb, (0.005 Zn).

The samples were machined into two cylindrical electrodes, 15 mm long with diameters of 1 mm and 3 mm. These sample electrodes were etched with dilute hydrochloric acid, rinsed in distilled water, and then cleaned in high-purity ethanol with the aid of an ultrasonic cleaner. After drying, the electrodes were mounted on the electrode holders in the source chamber, and pre-sparked for an appropriate time.

Procedure

Electrical-detection, peak-switching techniques give more precise data than can be expected with photographic detection.

Spark-gap effects were determined with the use of the automatic spark gap controller, for gap widths of 15 μm, 25 μm, and 35 μm. The desired gap width was obtained by keeping the spark breakdown voltage, read on the gap monitor meter, at a given value. The correlation between the spark breakdown voltage and the gap width was calibrated previously for each sample

Two possible arrangements of the electrodes were considered, either head-to-head (point sparking) or side-by-side (line sparking). For point sparking, sample electrode heads were machined into hemispheres in order to minimize effects of inter-electrode self-shielding. For line sparking, sample electrodes were set parallel to the No. 1 slit vertically to make the sparking section coincide with the No. 1 slit of length 2 mm.

Effects of sample electrode size were studied for electrodes having diameters of 1 mm and 3 mm.

The energy-pass bandwidth of the ion beam was set at 200, 450, or 700 eV, by adjusting the energy-selective slit (α-slit) and the energy limiting slit (β-slit) width.

Spark position effects were determined by changing the distance between the electrodes and the No. 1 slit from 3 to 10 mm.

Eleven elements were determined: Fe (internal standard), Ti, V, Cr, Mn, Ni, Co, Cu, Mo, W and Pb. Spark conditions were 1000 pulses/s of 40 μs duration at about 80 kV; the ion-accelerating voltage was about 24 kV, and the total charge accumulations were 0.1 nC.

The procedure for measuring the energy distribution of ions has been reported [10].

RESULTS AND DISCUSSION

Effects of spark gap and spark technique

The effects of gap width variation on the RSF are shown in Fig. 1A. As the gap width increased, the RSF of Mn, Pb, Ni and Co increased, while

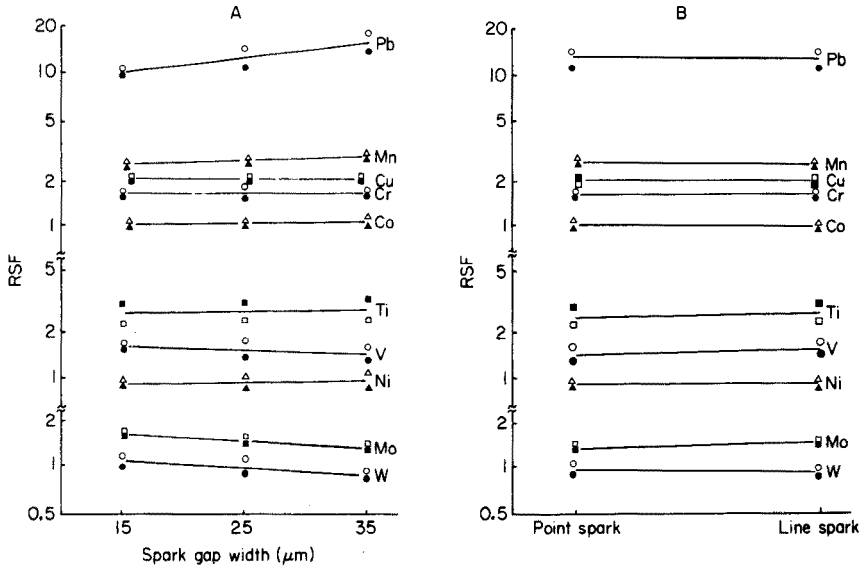

Fig. 1. Effects of spark gap width (A) and spark techniques (B) on relative sensitivity factors. Closed symbols indicate NBS 443; open symbols indicate NBS 462.

the RSF of Mo, W and V decreased; there was no significant effect for the other elements. This particular effect was common to the low-alloy steel sample and the stainless-steel sample, and was reproducible.

Franzen [11] and others [10, 12] have reported that the energy distribution of ions in the beam is affected by the gap width. According to Magee and Harrison [4], the changes in sensitivity with gap width are related to the ratio of the ionization potentials between the matrix and impurity elements. Although a definite correlation between gap width effects and ionization potentials was not observed in the present study, differences in gap width may produce changes in spark breakdown voltage and spark current. With these changes, parameters such as electron density and electron temperature vary in the spark plasma, and such changes affect sample vaporization processes and ion formation processes, leading to changes in the ion populations which are ultimately reflected in the RSF.

Figure 1B shows that there was no significant difference between the two spark techniques. However, line sparking gave less spark-ceasing and fewer inter-electrode self-shielding effects caused by erosion of the electrodes than point sparking. Therefore, when the automatic spark-gap controller is used, more precise data would be obtained by the line-spark technique.

Effect of sample electrode size, energy-pass bandwidth and spark position

The effects of sample electrode size on the RSF are shown in Fig. 2A. As the diameter of sample electrodes increased, the RSF of nearly all elements increased slightly. The reason is not clear, but parameters such as electrode temperature and ion extraction efficiency may vary with electrode size.

As shown in Fig. 2B, differences in the energy-pass bandwith of the ion beam did not affect the RSF very much. When the bandwidth of the ion beam was narrowed to 200 eV, the difference in RSF between low-alloy steel and stainless steel increased for lead and titanium, though the resolution improved. It appears that in steel analysis, it is not advisable to set the energy-pass bandwidth of the ion beam too narrow to achieve better resolution.

Changes in the RSF with variation of spark-to-slit distance are shown in Fig. 2C. In determinations made with a spark-to-slit distance of 10 mm, compared with that of 3 mm, the RSF for molybdenum and tungsten increased by about 25%, whereas the RSF for Mn, Ni and Cu decreased by a similar amount. Since all the experimental parameters except spark position were kept constant throughout these measurements, these significant changes in RSF are very unlikely to have been caused by variations in the sample vaporization processes or ion formation processes as in the case of gap effects. The energy components in the ion beam extracted by the accelerating field are known [10] to vary with spark positions, even though the energy distribution of ions produced in the spark discharge is presumably constant. Hence, the energy distribution of ions for several elements was measured under the same experimental condition as the RSF.

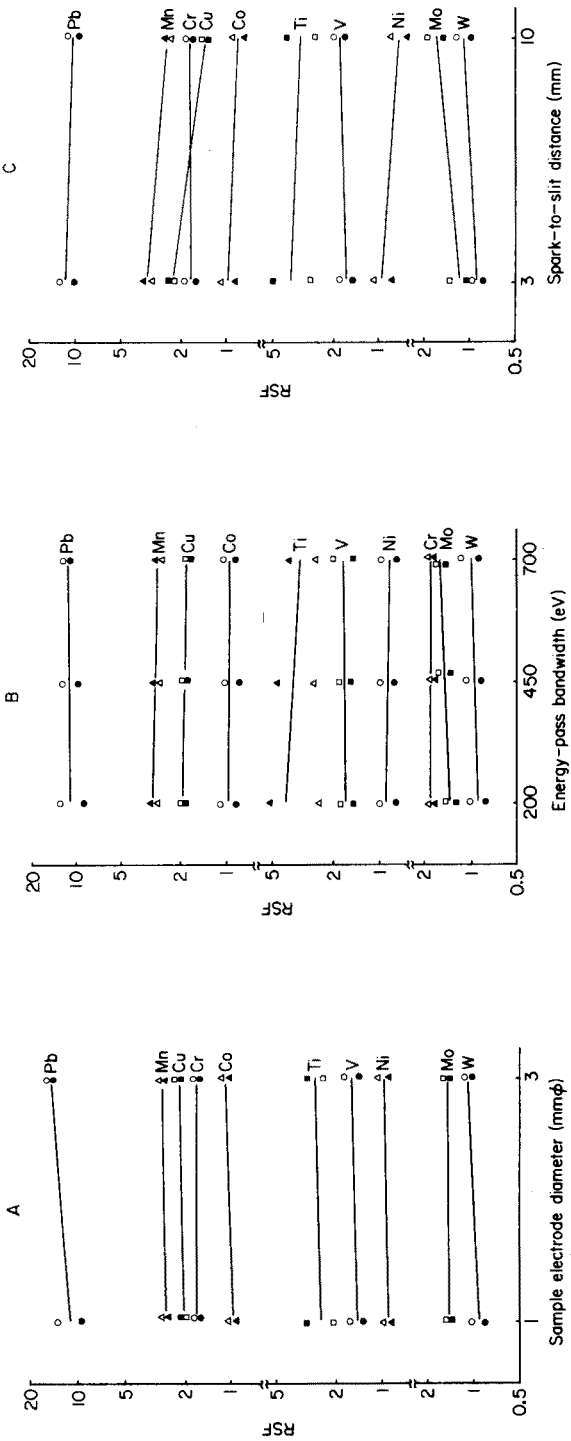

Fig. 2. Effects of sample electrode size (A), energy-pass bandwidth (B) and spark position (C) on relative sensitivity factors. Symbols as in Fig. 1.

Figure 3 shows the results of measurements of the energy distribution of ions. The spark-to-slit distance of 3 mm gives almost symmetrical curves whereas the distance of 10 mm gives asymmetrical curves. In addition, the energy distributions of Mn and Cu ions were found in higher energy regions than those of Fe, Cr and V ions, while that of Mo ion was found in a lower energy region.

In trace elemental analysis by s.s.m.s. the applied accelerating voltage was usually adjusted so as to maximize the total ion current which passed the β-slit. Presumably in this procedure the applied accelerating voltage would coincide approximately with the energy distribution peak of single charged ions of the matrix element. Therefore, with the energy-pass bandwidth of the ion beam set at 500 eV, only ions in the area represented by hatching in Fig. 3 could pass the β-slit and finally reach the ion detector. Consequently, the ratio of integrated intensities of the areas calculated from Fig. 3 for Fe ions and other ions should be closely related to the RSF of the elements.

Figure 4 shows the calculated values of the integrated intensity ratios of Fe ions and ions of other elements plotted against spark-to-slit distance. For every element, the changes in these values caused by the alteration in spark position was less than the change in the RSF. However, as the spark-to-slit distance increased, the value for molybdenum increased as is seen in the RSF variation, whereas the values for Mn and Cu decreased, as did their RSF variations. This variation of energy distribution in ion extraction processes appears to have a definite influence on RSF variation with spark positions. However, there are clearly other larger effects, as yet unidentified, also operating.

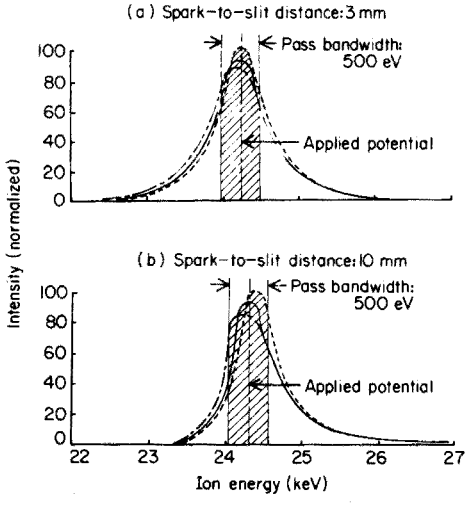

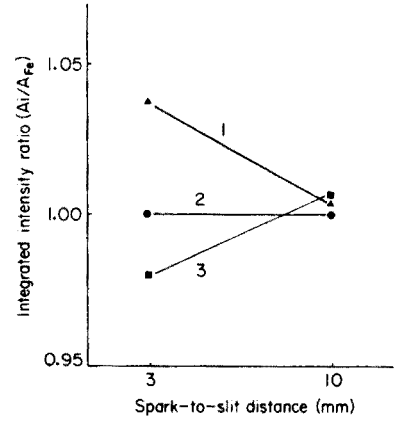

Fig. 3. Energy distribution for Fe ion and several impurity ions for NBS 462. —— Fe^+, Cr^+, V^+; -------- Mn^+, Cu^+; —·— Mo^+,

Fig. 4. Effects of spark-to-slit distance on integrated intensity ratios. (1) Mn, Cu; (2) Cr, V; (3) Mo.

Conclusion

Throughout this study it was observed that spark gap and spark position effects are particularly significant, and that sample electrode size effects are never negligible. These changes in RSF with variation of experimental parameters must be caused by complex interactions of many factors which had not been studied as yet. However, variation of energy distribution in ion extraction processes is undoubtedly one of the factors related to RSF variation with spark position. Although similar investigations on matrices other than iron are necessary in order to obtain a clearer understanding of the effects of experimental parameters on relative sensitivity factors, precise and reproducible control over spark gap, spark position, and sample electrode size are essential for precise and accurate analysis by s.s.m.s.

REFERENCES

1 J. Franzen and H. Hintenberger, Z. Naturforsch., Teil A, 18 (1963) 397.
2 J. S. Halliday, P. Swift and W. A. Wolstenholme, Advances in Mass Spectrometry, Vol. 3, Institute of Petroleum, London, 1964, p. 143.
3 N. Yamaguchi, R. Suzuki and O. Kammori, Bunseki Kagaku, 18 (1969) 3.
4 C. W. Magee and W. W. Harrison, Anal. Chem., 45 (1973) 852.
5 W. H. Wadlin and W. W. Harrison, Anal. Chem., 42 (1970) 1399.
6 J. Franzen and K. D. Schuy, Advances in Mass Spectrometry, Vol. 4, Institute of Petroleum, London, 1968, p. 449.
7 K. Yanagihara, S. Sato, M. Ito and T. Adachi, J. Iron Steel. Inst., 61 (1975) 347.
8 E. Watanabe, M. Naito and T. Ota, Proceedings of the International Conference on Mass Spectrometry, Kyoto, 1969, University of Tokyo Press.
9 M. Arai, M. Naito and T. Takagi, 21st Annual Conference on Mass Spectrometry and Allied Topics, San Francisco, 1973.
10 S. Oda, H. Aihara and H. Kamada, Bunseki Kagaku, 22 (1973) 757.
11 J. Franzen, Z. Anal. Chem., 91 (1963) 197.
12 J. R. Woolston and R. E. Honig, Rev. Sci. Instrum., 35 (1964) 69.

Analytica Chimica Acta, 98 (1978) 315—321

A NEW PROCEDURE FOR THE WET CHEMICAL ANALYSIS OF THE LEAD—NOBLE METALS BUTTON

A. DIAMANTATOS

J.C.I. Minerals Processing Research Laboratory, Knights (South Africa)

(Received 10th December 1977)

SUMMARY

Thiobarbituric acid can be used as a group precipitant for the recovery of Pt, Pd, Rh and Au from the lead perchlorate—perchloric acid solution obtained after the lead—noble metals button has been parted with perchloric acid. By integration of this procedure with the recovery of Ir, Ru and Os from the parting residue, a scheme is evolved which makes possible the determination of all the platinum metals and gold from a single button. The results of analyses of various platiniferous materials by the proposed lead—wet method and the classical lead-cupellation method are compared.

The procedural details for the recovery of the six platinum metals and gold after lead fusion and perchloric acid parting have been described in a series of recent papers [1—4]. The scheme developed was compared with the lead cupellation, the tin and the nickel sulphide collection schemes, and the data [4] demonstrated that the wet chemical analysis of the lead button yielded the highest recoveries. Beamish and van Loon [5, 6] after reviewing the various collection and fire-assay techniques, concluded that there is no recorded proof that the newer collectors, tin, iron-nickel-copper, copper, and nickel sulphide, provide better accuracy than the lead collector in the case of recovery of platinum, palladium, gold and perhaps rhodium. This statement refers, of course, to lead fusion followed by cupellation, and in full knowledge that some small losses of the above four metals occur during the cupellation. It is hardly necessary to refer to the advantages offered by avoidance of the cupellation step and its replacement by an entirely wet chemical treatment of the lead button. In view of this, efforts to develop new non-cupellation procedures seem fully justified.

Since the disintegration of the lead button by perchloric acid (160—180°C) is accomplished easily, and gives simultaneous removal of Ir, Ru, Os as metallic insolubles [1, 2], it can be understood that the crux of the problem for the wet analysis of the lead button is the recovery of Pt, Pd, Rh and Au from the perchloric acid filtrate.

Thiobarbituric acid has been found to be a suitable reagent for the gravimetric determination of palladium in hydrochloric acid solutions [7] and has also become established as one of the most frequently recommended

precipitants for the gravimetric standardization of hydrochloric acid solutions of rhodium [7]. It was therefore considered worthwhile to investigate the possible use of this reagent for the precipitation of the noble metals in perchloric acid medium, provided of course, that it does not, in the first place, precipitate lead.

This paper describes the successful use of thiobarbituric acid for the purpose outlined.

EXPERIMENTAL

Apparatus, solutions and reagents

A fire-assay electric furnace with a silicon carbide element was used for the lead fusion. A Techtron AA-5 atomic-absorption spectrometer, a Zeiss PMQII spectrophotometer and a Philips PW1220 x-ray fluorescence spectrometer were used for analytical measurements.

The lead fusion flux contained (parts by weight): litharge 50, borax 20, soda ash 60, silica 20, flour 5—6.

The standard copper—nickel matte contained: Pt 958 ppm, Pd 536 ppm, Rh 93 ppm, Ir 24.6 ppm, Ru 205 ppm, Os 19 ppm, Au 47.9 ppm, Ag 81 ppm, Cu 28.9%, Ni 48.2%, S 22.4%, Fe 1.4%, Co 0.45%, Te 0.02%, silica, etc.

Standard hydrochloric acid solutions of platinum, palladium, rhodium and gold were prepared and standardized as described previously [8]. The reagent solution was a 1% (w/v) thiobarbituric acid solution in glacial acetic acid.

Recommended procedure for Pt, Pd, Rh, Au, Ir

Mix 2—60 g of the sample as required (leach and/or roast, if necessary) with 150—180 g of lead flux and transfer to a suitable fireclay crucible. Fuse at 1200°C for 1 h and then pour the molten fluid into a conical iron mould. After cooling, detach the lead button from the slag by tapping. (Re-fuse the slag if high quantities of iridium are present in the sample.) Place the button in 100 ml of a 30% (w/v) sodium hydroxide solution and boil in order to remove completely any adhering slag. Compress the button to produce a disc of approximately 4 mm thickness. Place the lead disc in a 1-l squat beaker and add 300 ml of perchloric acid (70%) and 30 ml of acetic acid (glacial). Cover the beaker with a watchglass and introduce a thermometer. Heat to 180°C initially, remove the heat source for a while and then maintain the temperature between 160 and 180°C until complete dissolution of lead is achieved. Continue heating for another 20 min at ca. 150°C, to ensure complete dissolution of platinum, palladium, rhodium, and gold. Cool somewhat (70°C), and slowly dilute the perchlorate solution with 200 ml of water while stirring. Boil this solution gently for 5 min, and then cool. Filter the solution through a No. 540 filter paper into a 1-l beaker. Retain the black unattacked residue containing all the iridium and ruthenium and most of the osmium for later use.

Dilute the lead perchlorate—perchloric acid filtrate to ca. 600 ml with water, and bring to the boil gently, using a boiling rod. Remove the beaker from the hot plate, cool somewhat, and carefully add 20 ml of 1% thiobarbituric acid in glacial acetic acid while stirring. Bring to the boil again and continue boiling gently for 1 h. Cool the beaker and contents in cold water for at least 40 min, to ensure complete coagulation of the gold precipitate. Filter off the noble metals—thiobarbituric acid precipitate (containing all the Pt, Pd, Rh and Au) on a No. 540 filter paper and wash with hot water; it is not necessary to transfer the precipitate quantitatively to the filter. (The filtrate contains Pb, Ni, etc., and is rejected.)

Place the filter and precipitate in the original beaker, destroy the paper and organic matter by heating with 20 ml of a (2 + 1) mixture of nitric and perchloric acids, and then evaporate to dryness. Add 5 ml of concentrated sulphuric acid and a little sodium chloride and heat strongly for 20—30 min, before again fuming to dryness. Dissolve, and convert the residue to a hydrochloric acid solution, by boiling with 20 ml of 11 M hydrochloric acid for 15 min, and evaporating to incipient dryness. Repeat the hydrochloric acid treatment once more. Finally add 20 ml of 11 M hydrochloric acid and 3—5 drops of 100-vol. hydrogen peroxide, boil for 5—6 min and then cool. Determine the platinum, palladium, rhodium and gold directly in this hydrochloric acid solution by atomic absorption spectrometry [9].

To determine the iridium in the unattacked residue, transfer the filter paper to a zirconium crucible, char, ignite, and then fuse the residue with 2—3 g of sodium peroxide. Cool, leach the melt with water, acidify with hydrochloric acid and evaporate to dryness. Add 10 ml of perchloric acid (70%), boil for 10 min, and fume to complete dryness to volatilize all ruthenium and osmium. Proceed with the extraction and determination of iridium as detailed previously [10].

RESULTS AND DISCUSSION

The precipitation of Pt, Pd, Rh and Au

A sample (25 g) of the standard matte was leached with 300 ml of 11 M hydrochloric acid in presence of 100 g of ammonium chloride by boiling for 2 h, to dissolve the nickel, copper and iron. After dilution with 300 ml of hot water, the solution was filtered through a No. 40 filter paper. The filter with the residue containing the noble metals was placed on a bed of silica in a porcelain crucible and roasted at 850°C for 30 min to remove the last traces of sulphur. The residue was then mixed with the lead flux and fused as usual. The lead button was cleaned, compressed to a disc and parted as described in the recommended procedure. The resulting perchlorate solution, after dilution to 600 ml with water, was filtered to remove the metallic iridium, ruthenium and osmium and finally the filtrate was made up to 1 l in a volumetric flask.

A 100-ml aliquot of this filtrate solution (containing 2.39 mg Pt, 1.34 mg Pd, 0.232 mg Rh, 0.12 mg Au) was pipetted into a 400-ml beaker and 80 ml of perchloric acid (70%) was added before dilution to 250 ml with water. The solution was brought to the boil and 20 ml of 1% thiobarbituric acid in acetic acid was added while stirring. This addition resulted in the immediate appearance of a brownish coloration which after boiling for 5 min turned to a dark brown precipitate. After boiling for 1 h and cooling, the precipitate was filtered off and examined by x-ray fluorescence spectrometry. The x-ray scan indicated an abundance of Pt, Pd, Rh and Au, thus suggesting that thiobarbituric acid, could, under optimal conditions, precipitate quantitatively the above four metals in the lead perchlorate solution.

Effect of perchloric acid concentration on the precipitation

Six 100-ml aliquots of the above working solution were transferred to 400-ml beakers and different amounts (10—100 ml) of perchloric acid (70%) were added to each aliquot before dilution to ca. 250 ml with water. The precipitation of the noble metals with thiobarbituric acid and the filtration were done as in the previous test. The efficiency of the precipitation at the various perchloric acid concentrations was checked by examining the filtrates for platinum, palladium, rhodium and gold. The filtrates were evaporated and fumed to dryness. The organic matter was destroyed by taking the residues to fumes with sulphuric acid, as usual, and then evaporated to complete dryness.

Each dry residue was boiled with 25 ml of 11 M hydrochloric acid, the solution being evaporated to a small volume; then, after addition of 10 ml of 11 M hydrochloric acid, the mixtures were boiled again for a few minutes. The cooled solutions were filtered to remove the precipitated lead, and the filtrates were diluted to 10 ml in 5—6 M hydrochloric acid and tested by a.a.s. Platinum and palladium were not detected in the filtrates when more than 20 ml of extra perchloric acid was added. Rhodium was not detected when 60 ml or more of perchloric acid was added. However, 4.1—9.1% of the original gold was detected in all the filtrates, probably because of incomplete coagulation of the gold precipitate. Indeed, when two 100-ml aliquots were treated as above, but the noble metal—thiobarbituric acid precipitate was filtered after the solutions had been cooled in cold water for 30 and 45 min, respectively, complete retention of gold on the filter was achieved in both solutions.

Effect of boiling time and reagent concentration on precipitation

Another 1-l of lead perchlorate solution was prepared exactly as described above. Five 100-ml aliquots were pipetted into 400-ml beakers and 100 ml of perchloric acid (70%) was added to each before dilution to 250 ml with water. The solutions were brought to the boil, 20 ml of the thiobarbituric acid solution were added, and the solutions were kept boiling for times of 10—60 min. After the solutions had cooled in cold water for 30 min, the

precipitates were filtered off and the filtrates were analysed by a.a.s. as above. Platinum, palladium and gold were not detected in any of these filtrates. Rhodium, however, required boiling for at least 30 min for complete precipitation. The amounts of rhodium detected in the filtrates of the samples boiled for 10 and 25 min were 5.6% and 0.42%, respectively, of the original content. A boiling time of 60 min was therefore chosen.

Precipitations were carried out as described for the boiling time test, with different amounts of thiobarbituric acid (25—200 mg), each dissolved in 20 ml of glacial acetic acid. The precipitation of all the four metals was complete in all cases. This indicates that 25 mg of thiobarbituric acid is sufficient to precipitate 4.1 mg of total precious metals. However, the addition of a large excess of reagent is considered safer. The use of 20 ml of 1% (w/v) reagent solution is therefore, in general, recommended.

Co-precipitation of base metals

The fate of the base metals which are likely to be present in the most noble metal-bearing samples, was also investigated. A flotation concentrate (10 g) containing Ni, Cu, Fe, Al, Ca, Mg, Te, Se etc., was fused with 180 g of lead flux. The parting of the lead button and the subsequent steps were done exactly as in the recommended procedure. The (Pt + Pd + Rh + Au)—thiobarbituric acid precipitate was dried and examined by the x-ray fluorescence technique. The full scan revealed that only the copper and tellurium which were retained in the button, were co-precipitated with the noble metals. However, these two contaminants are in such small quantities that they have no effect on the final determinations of the precious metals either by atomic absorption spectrometry [9, 11] or by extraction-colorimetry [12, 13].

The integrated scheme (inclusion of Os and Ru)

The two volatile noble metals, osmium and ruthenium, can be conveniently determined in a separate button as described in a recent paper [2] or as recommended by Thiers et al. [14]. However, when necessary, e.g. if sufficient sample is not available, these two metals can be easily determined on the same lead button as the non-volatile noble metals. In such cases, the button must be dissolved in a distillation flask connected to a receiver trap containing sodium hydroxide solution, to absorb the small amount of osmium tetroxide developed during the parting treatment. This operation and the treatment of the parting residue to recover ruthenium, osmium, and iridium, have been described [2, 4].

Application of the proposed method to various samples and a comparison with the classical lead-cupellation

As a test of the accuracy of the proposed method, three 5-g portions of the standard matte and three lead fluxes spiked with standard hydrochloric acid solutions of platinum, palladium, rhodium and gold, were taken through

TABLE 1

Recovery of Pt, Pd, Rh, Au from Cu—Ni matte and from spiked lead fluxes

Element	Cu—Ni matte			Spiked lead fluxes		
	Present (mg)	Found (av., mg)	Recovery (%)	Added (mg)	Found (av., mg)	Recovery (%)
Pt	4.790	4.772	99.6	1.008	1.005	99.7
Pd	2.680	2.672	99.7	0.502	0.501	99.8
Rh	0.465	0.462	99.3	0.205	0.204	99.5
Au	0.239	0.233	97.5	0.103	0.101	98.1

TABLE 2

Comparison of lead—wet chemical and lead—cupellation procedures (All measurements were done by a.a.s.)

Sample	Method	Results in ppm[a]			
		Pt	Pd	Rh	Au
Ore (Merensky Reef)	Pb—wet analysis	3.98	1.62	0.31	0.29
(50 g)	Pb-cupellation	3.65	1.59	0.31	0.30
Ore (Canada)	Pb—wet analysis	2.79	15.65		0.58
(50 g)	Pb-cupellation	2.57	15.1		0.58
Matte	Pb—wet analysis	954	528	92.7	46.3
(5 g)	Pb-cupellation	942	519	92.5	46.0
Pt—Rh silicate	Pb—wet analysis	1618		368	
(5 g)	Pb-cupellation	1570		359	
Pt—catalyst	Pb—wet analysis	8775			
(2 g)	Pb-cupellation	8708			

[a]Average of 3 determinations.

the recommended procedure. The results of these tests are given in Table 1. These satisfactory recoveries confirm the high efficiency of thiobarbituric acid for the precipitation of these noble metals from perchloric acid solutions.

Different types of platiniferous materials were analysed, in triplicate, for Pt, Pd, Rh and Au by the proposed lead button—wet chemical method and by the classical lead-cupellation method. Comparative results for the two procedures (Table 2) confirm the higher efficiency of the non-cupellation scheme, and provide a general indication of the extent of the cupellation losses.

REFERENCES

1 A. Diamantatos, Anal. Chim. Acta, 90 (1977) 179.
2 A. Diamantatos, Anal. Chim. Acta, 91 (1977) 281.
3 A. Diamantatos, Anal. Chim. Acta, 92 (1977) 171.
4 A. Diamantatos, Anal. Chim. Acta, 94 (1977) 49.

5 F. E. Beamish and J. C. van Loon, Min. Sci. Eng., 4 (1972) 3.
6 F. E. Beamish and J. C. van Loon, Recent Advances in the Analytical Chemistry of the Noble Metals, Pergamon Press, Oxford, 1972.
7 J. E. Currah, W. A. E. McBryde, A. J. Cruikshank and F. E. Beamish, Ind. Eng. Chem. Anal. Ed., 18 (1946) 120.
8 A. Diamantatos, Anal. Chim. Acta, 66 (1973) 147.
9 R. C. Mallett, D. C. G. Pearton, E. J. Ring and T. W. Steele, Talanta, 19 (1972) 181.
10 A. Diamantatos and A. A. Verbeek, Anal. Chim. Acta, 86 (1976) 169.
11 M. M. Schnepfe and F. S. Grimaldi, Talanta, 16 (1969) 591.
12 A. Diamantatos, Anal. Chim. Acta, 67 (1973) 317.
13 A. Diamantatos and A. A. Verbeek, Anal. Chim. Acta, 91 (1977) 287.
14 R. Thiers, W. Graydon and F. E. Beamish, Anal. Chem., 20 (1948) 831.

Analytica Chimica Acta, 98 (1978) 323—333

INORGANIC INTERFERENCES IN THE 2,4-XYLENOL SPECTROPHOTOMETRIC METHOD FOR NITRATE AND THEIR ELIMINATION

GEORGE NORWITZ and PETER N. KELIHER*

Chemistry Department, Villanova University, Villanova, PA 19085 (U.S.A.)

(Received 23rd January 1978)

SUMMARY

A study of inorganic interferences with the 2,4-xylenol spectrophotometric method for nitrate and their elimination is reported. Fifty-three substances do not interfere with the original method. Nitrite interferes somewhat by producing a faint yellow color. Certain reducing agents (Fe^{2+}, S^{2-}, $S_2O_3^{2-}$, and SCN^-) cause low results by reducing the nitrate in the strong sulfuric acid solution, while some oxidizing agents (Mn^{7+}, Cr^{6+}, V^{5+}, and ClO_3^-) cause low results by inactivating or destroying the 2,4-xylenol. Persulfate and small amounts of H_2O_2 produce a slight deepening of the color; larger amounts of H_2O_2 cause low results, as do Cl^-, Br^-, I^-, and metals. The recommended maximum permissible limits (mg per 10-ml aliquot) for the original method are NO_2^--N, Fe^{2+}, S^{2-}, SCN^-, V^{5+}, ClO_3^-, Cl^-, I^-, 0.2; Mn^{7+}, Cr^{6+}, $S_2O_8^{2-}$, 5; H_2O_2, 0.02; $S_2O_3^{2-}$, Br^-, 0.1; metals, none. Procedures for the elimination of most of the interferences are described. Nitrite is destroyed with sulfamic acid. The interferences of reductants (Fe^{2+}, S^{2-}, $S_2O_3^{2-}$, and SCN^-) and oxidants (Mn^{7+} and Cr^{6+}) are eliminated with hydrogen peroxide, the excess of which (and $S_2O_8^{2-}$) is destroyed by boiling in the presence of Fe^{3+}. The interference of Cl^-, Br^-, and I^- is eliminated by precipitation with silver sulfate. An alternative to the sulfamic acid procedure is to oxidize nitrite to nitrate with peroxide and deduct NO_2^--N from the total NO_3^--N. After elimination of interferences, a 10-ml aliquot of sample solution is treated with 17.0 ml of sulfuric acid and 2,4-xylenol, the 6-nitro-2,4-xylenol is steam-distilled into an ammonia—water—isopropanol mixture, and the yellow color is measured.

Recently, an improved technique was proposed for the spectrophotometric determination of nitrate by use of 2,4-xylenol [1]. In order to apply this method to the determination of nitrate in a variety of materials, it was decided to undertake a comprehensive study of interferences and to investigate ways of eliminating them; in this regard, it should be pointed out that known spectrophotometric methods for nitrate are not entirely satisfactory in the presence of strong interferences [2]. Previously, a study was made of the interferences of chloride and nitrite with the 2,4-xylenol method, and a means was proposed for eliminating chloride interference [1]. Earlier investigators of the 2,4-xylenol method [3—7] mention other interferences besides chloride and nitrite, but their data are sketchy and contradictory; significantly different techniques were used for developing the color, so that conclusions about interferences would not be universally applicable in any case. In the present paper, methods of eliminating most of the interferences

are suggested. Nitrite is destroyed with sulfamic acid [8]. The interferences of certain reductants and oxidants are eliminated by use of hydrogen peroxide, excess of which is then destroyed. Chloride, bromide, and iodide are eliminated by precipitation with silver sulfate.

EXPERIMENTAL

Apparatus and reagents

A Bausch and Lomb Spectronic 20 colorimeter and a Parnas-Wagner Kjeldahl distillation apparatus (Arthur H. Thomas Co., Philadelphia; Cat. No. 7051-G10) were used [1].

Potassium nitrate (dried at 150°C for 1 h) and the other chemicals used were of reagent grade.

Standard nitrate solution (1 ml = 0.50 mg NO_3^--N). Dissolve 3.6100 g of KNO_3 in water and dilute to 1 l in a volumetric flask.

Silver sulfate solution (0.44%). Dissolve 4.40 g of Ag_2SO_4 in boiling water, cool, and dilute to 1 l.

Iron(III) solution (4.4%). Dissolve 22 g of $FeNH_4(SO_4)_2 \cdot 12H_2O$ in water containing a few drops of sulfuric acid and dilute to 500 ml with water.

2,4-Xylenol solution (2.5%). Dilute 5 ml of 2,4-xylenol (Eastman-Kodak) to 200 ml with acetone.

Preparation of calibration curve

Transfer 1.00, 2.00, 3.00, and 4.00 ml of standard nitrate solution to 100-ml volumetric flasks and dilute to the mark. Pipet 10-ml aliquots into 100-ml beakers, cover with watch glasses, and cool in cracked ice for 10 min or more. While keeping the beakers in cracked ice, add 17.0 ml of sulfuric acid very slowly dropwise from a buret while swirling. Carry along a reagent blank. Adjust the solutions to room temperature. Add 1.0 ml of 2,4-xylenol solution (2.5%), swirl to mix thoroughly, and allow to stand for 10—60 min.

Add 20 ml of water, 35 ml of isopropanol, and 5 ml of (0.88) ammonia liquor to five 100-ml volumetric flasks. Place one of the flasks under the condenser extension tube of the distillation apparatus so that the tube reaches to the bottom of the flask. Place an asbestos board between the burner and the flask. Introduce the sample through the entry funnel and wash in with 5—10 ml of water. Steam-distil in the usual manner [1] until the volume of liquid in the volumetric flask is about 95 ml. Remove the volumetric flask.

Dilute the solutions in the volumetric flasks to the mark and mix. Measure the absorbance at 455 nm against the reagent blank and plot absorbance against mg of NO_3^--N (per 10-ml aliquot).

Procedures

In all the following modifications, unless specified otherwise, an accurately measured portion (up to 75 ml) of the solution or dissolved sample containing up to 2.0 mg of NO_3^--N is used.

A. In the absence of interferences. Transfer the sample solution to a 100-ml volumetric flask and dilute to the mark. Pipet a 10-ml aliquot into a 100-ml beaker, cool in ice, and proceed as described for the calibration curve.

B. In the presence of metals as the elements. Transfer the sample solution to a 250-ml beaker. Filter as soon as possible through a No. 40 Whatman filter paper into a 100-ml volumetric flask, wash with water, and dilute to the mark. Pipet a 10-ml aliquot into a 100-ml beaker and proceed as described in procedure A.

C. In the presence of nitrite. Transfer the sample solution containing up to 50 mg of NO_2^--N to a 250-ml beaker. Dilute to about 75 ml (if necessary) and add 10 ml of sulfamic acid solution (10%). Cover with a watch glass, and boil for 1—2 min. Cool to room temperature and dilute to 100 ml in a volumetric flask. Pipet a 10-ml aliquot into a 100-ml beaker, and proceed as described in procedure A.

An alternative technique for handling NO_2^--N interference is to oxidize the NO_2^--N to NO_3^--N, determine the total NO_3^--N, and then deduct the NO_2^--N from the total NO_3^--N. For this method, transfer a portion of the sample with a total NO_3^--N + NO_2^--N content up to 2.0 mg to a 250-ml beaker, dilute to about 75 ml, add dilute sulfuric acid, iron(III) reagent, and hydrogen peroxide, and proceed as described in procedure D. Deduct the NO_2^--N (which should be determined at about the same time as the NO_3^--N) from the total NO_3^--N.

D. In the presence of Fe^{2+}, S^{2-}, $S_2O_3^{2-}$, SCN^-, *other interfering reductants,* $S_2O_8^{2-}$, H_2O_2, Mn^{7+}, *and* Cr^{6+}. Transfer the sample solution containing up to 250 mg of Fe^{2+}, S^{2-}, $S_2O_3^{2-}$, $S_2O_8^{2-}$, Mn^{7+}, and Cr^{6+}, up to 50 mg of SCN^-, and up to 1000 mg of H_2O_2 to a 250-ml beaker, and dilute to about 75 ml (if necessary). Add 5 ml of dilute sulfuric acid (10%), 5 ml of the iron(III) solution (4.4%), and 10 ml of hydrogen peroxide (30%); a smaller quantity of hydrogen peroxide can be used if the amount of reductants or oxidants is small. Dilute to about 125 ml with water, cover with a watch glass, and boil vigorously for 15 min (do not confuse effervescence with boiling). While the beaker is on the hot plate, wash down the watch glass and sides of the beaker, replace the watch glass, and boil vigorously for another 15 min. Cool to room temperature and dilute to 100 ml in a volumetric flask. Pipet a 10-ml aliquot into a 100-ml beaker and proceed as described in procedure A.

This procedure cannot be used in the presence of more than 15 mg of Cl^- or Br^- or 10 mg of I^- in the original portion.

E. In the presence of Cl^-, Br^-, *and* I^-. Transfer the sample solution (which may contain up to 4.0 mg of NO_3^--N if the solution after filtration is diluted to 200 ml), containing up to 100 mg of Cl^-, up to 200 mg of Br^-, and up to 250 mg of I^- to a 250-ml beaker. Dilute to about 75 ml (if necessary) and add 5 ml of dilute sulfuric acid (10%). Insert a stirring rod and heat almost to boiling. Remove from the hot plate and add sufficient silver sulfate solution (0.44%) from a graduated cylinder, while stirring, to precipitate the halide and provide a moderate excess of silver(I); 1 mg of Cl^-, Br^- or I^- is equivalent to 1.0, 0.44

or 0.28 ml of the silver sulfate solution (0.44%), respectively. Heat to boiling and boil for 1—2 min. Remove the beaker from the hot plate and test for complete precipitation by adding 1—2 drops of silver sulfate solution. If necessary, add more silver sulfate solution and reboil. Allow to stand for 15 min or more, filter through a Whatman No. 42 filter paper into a 100- or 200-ml volumetric flask (depending on the size of the original aliquot and the amount of silver sulfate solution used), and wash with water. Cool to room temperature and dilute to the mark. Pipet a 10-ml aliquot into a 100-ml beaker and proceed as described in procedure A.

DISCUSSION AND RESULTS

Study of interferences with the unmodified method

The study of interferences with the original unmodified method required the use of several techniques. When soluble salts were used, standard solutions of the interferences were prepared (chloride salts were avoided) and aliquots were transferred to 100-ml volumetric flasks, to which 2.0 ml of the standard nitrate solution were added before dilution to the mark. Aliquots (10 ml) were then treated with the 17.0 ml of sulfuric acid and the nitrate was determined as in the method. In dealing with interferences from those metals for which only the acid-insoluble oxides (SnO_2, ThO_2, TiO_2, Nb_2O_5, Ta_2O_5, UO_2, and ZrO_2) could be used, the oxides were weighed into a platinum crucible and fused with potassium hydrogensulfate. The melts were dissolved by heating with about 50 ml of water and 10 ml of sulfuric acid (Nb_2O_5 and Ta_2O_5 did not completely dissolve). The solutions were cooled, 2.0 ml of the standard nitrate solution were added, the solutions were diluted to 100 ml in volumetric flasks, and 10-ml aliquots were treated with 1.0 ml of water and 16.0 ml of sulfuric acid. In dealing with BaO, Bi_2O_3, SrO, S (elemental), and Se (elemental), the materials were weighed directly into 100-ml beakers and 8.0 ml of water and 2 ml of diluted standard nitrate solution (1 ml = 0.05 mg NO_3^--N) were added, followed by the 17.0 ml of sulfuric acid.

The substances (of which there were 53) that did not interfere with the original method are listed in Table 1. The substances that interfered and the recoveries in the presence of varying amounts of interferences are shown in Table 2, which provides a useful indication of what to expect in borderline cases of interference.

The manner of interference is complex. Nitrite interferes somewhat by producing a yellow color. The interference is inclined to be greater when no nitrate is present [1]; this follows because the NO_2^--N competes with the NO_3^--N by forming a nitroso compound with 2,4-xylenol, which is only slightly volatile with steam. The reducing agents Fe^{2+}, S^{2-}, $S_2O_3^{2-}$, and SCN^- cause low results by reducing the nitrate or the 6-nitro-2,4-xylenol in the strong sulfuric acid solution. It would be expected that Sn^{2+}, Cr^{2+}, Ti^{3+}, Cu^+, and Hg^+ would also cause low results; however, this could not be tested because only the chloride salts of these cations were available. In any case,

TABLE 1

Substances that did not interfere with the unmodified 2,4-xylenol method for nitrate when present in amounts up to 25 mg (0.10 mg of NO_3^--N present)

Substance	Added as	Substance	Added as	Substance	Added as
Al^{3+}	$AlK(SO_4)_2 \cdot 12H_2O$	Mn^{2+}	$MnSO_4 \cdot H_2O$	NH_4^+	$(NH_4)_2SO_4$
Sb^{3+}	$KSbOC_4O_6 \cdot \frac{1}{2}H_2O$	Hg^{2+}	$HgSO_4$	SO_4^{2-}	Na_2SO_4
As^{3+}	$NaAsO_2$	Mo^{6+}	$(NH_4)_6Mo_7O_{24} \cdot 4H_2O$	F^-	KF
As^{5+}	As_2O_5	Ni^{2+}	$NiSO_4 \cdot 7H_2O$	CO_3^{2-}	Na_2CO_3
Ba^{2+}	BaO	Nb^{5+}	Nb_2O_5[a]	PO_4^{3-}	K_2HPO_4
Be^{2+}	$BeSO_4 \cdot 4H_2O$	K^+	K_2SO_4	PO_2^{3-}	KH_2PO_2
Bi^{3+}	Bi_2O_3	Ag^+	Ag_2SO_4	ClO_4^-	NH_4ClO_4
B^{3+}	H_3BO_3	Na^+	Na_2SO_4	SO_3^{2-}	Na_2SO_3
Cd^{2+}	$CdSO_4$	Sr^{2+}	SrO	CN^-	KCN (hood)
Ca^{2+}	$CaSO_4$	Ta^{5+}	Ta_2O_5[a]	$Fe(CN)_6^{3-}$	$K_3Fe(CN)_6$
Ce^{4+}	$(NH_4)_4CeSO_4$	Tl^+	Tl_2SO_4	$Fe(CN)_6^{4-}$	$K_4Fe(CN)_6 \cdot 3H_2O$
Cr^{3+}	$CrK(SO_4)_2 \cdot 12H_2O$	Th^{4+}	ThO_2[a]	$C_2O_4^{2-}$	$(NH_4)_2C_2O_4 \cdot H_2O$
Co^{2+}	$CoSO_4 \cdot 7H_2O$	Sn^{4+}	SnO_2	$C_2H_2O^-$	$NaC_2H_3O_2$
Cu^{2+}	$CuSO_4 \cdot 5H_2O$	Ti^{4+}	TiO_2[a]	$C_6H_5O_7^{3-}$	$Na_3C_6H_5O_7 \cdot 2H_2O$
Fe^{3+}	$Fe(NH_4)(SO_4)_2 \cdot 12H_2O$	W^{6+}	$Na_2WO_4 \cdot 2H_2O$	$C_4H_4O_6^{2-}$	$Na_2C_4H_4O_6 \cdot 2H_2O$
Pb^{2+}	$Pb(C_2H_3O_2)_2 \cdot 3H_2O$	U^{4+}	UO_2[a]	S	S powder
Li^+	Li_2SO_4	Zn^{2+}	$ZnSO_4$	Se	Se powder
Mg^{2+}	$MgSO_4 \cdot 7H_2O$	Zr^{4+}	ZrO_2[a]		

[a]See text.

the interference of these reducing agents would be readily eliminated by the hydrogen peroxide treatment to be discussed below. As can be seen from Table 1, not all reducing agents interfere with the unmodified method (SO_3^{2-}, PO_2^{3-} and As^{3+} are in this category). The oxidizing agents Mn^{7+}, Cr^{5+}, V^{5+}, and ClO_3^- interfere by deactivating the 2,4-xylenol or destroying it. The oxidant $S_2O_8^{2-}$ produces a slight deepening of the color. Hydrogen peroxide in small amounts likewise produces a slight deepening of the color; larger amounts cause low results by hindering the color development and producing effervescence (and loss of solution) by catalytic decomposition of the hydrogen peroxide when the 2,4-xylenol solution is added. As can be seen from Table 1, not all oxidizing agents interfere; Fe^{3+} and Ce^{4+} are in this category. The anions Cl^-, Br^-, and I^- cause low results, apparently because of volatilization of nitrogen—halogen compounds, e.g. nitrosyl chloride, from the hot sulfuric acid solution (especially during the initial stages of the distillation) or by their reducing action. Aluminum and magnesium and other metals that react with sulfuric acid to produce hydrogen cause low results by reducing the nitrate. Aluminum dissolves rather slowly in sulfuric acid, and hence interferes more than magnesium which dissolves almost instantaneously. Silicon (as silicate) does not affect the color; however, if a large amount is present (25 mg or more), the flocculent precipitate of silicic acid produced on the addition of the sulfuric acid is partially driven over in the distillation. This unusual interference is readily eliminated by filtering a portion of the solution after the distillation.

The recommended maximum limits (mg per 10-ml aliquot) for the original

TABLE 2

Interferences with the unmodified 2,4-xylenol method for nitrate (0.10 mg of NO_3^--N present)

Interference	Added as	NO_3^--N (mg) recovered in presence of varying amounts of interference					
		0.1 mg	0.2 mg	0.5 mg	5 mg	10 mg	25 mg
NO_2^--N[a]	KNO_2	0.104	0.098	0.114			
Fe^{2+}	$FeSO_4 \cdot 7H_2O$		0.102	0.092	0.020	0.028	0.040
S^{2-}	$Na_2S \cdot 9H_2O$	0.103	0.104	0.074	0.010	0.006	
$S_2O_3^{2-}$	$Na_2S_2O_3 \cdot 5H_2O$	0.097	0.074	0.008			
Mn^{7+}	$KMnO_4$			0.100	0.108	0.080	0.055
Cr^{6+}	$K_2Cr_2O_7$			0.098	0.096	0.040	0.023
V^{5+}	NH_4VO_3	0.100	0.098	0.074	0.050	0.020	
ClO_3^-	$KClO_3$	0.102	0.098	0.084	0.062	0.054	
$S_2O_8^{2-}$	$(NH_4)_2S_2O_8$	0.100		0.103	0.104	0.119[b]	0.119[b]
Cl^-	NaCl	0.102	0.102		0.078	0.076	0.036
Br^-	KBr	0.095	0.082	0.074	0.016	0.016	
I^-	KI	0.100	0.106	0.093	0.040	0.014	
SCN^-	KSCN		0.102	0.093	0.060	0.034	
Al	Al powder					0.060	0.040
Mg	Mg powder					0.102	0.090
Si^{4+}	Na_2SiO_3				0.102	0.104	0.098[c]
H_2O_2	H_2O_2, 30% solution (diluted)	0.003 mg	0.015 mg	0.030 mg	0.060 mg	0.15 mg	0.24 mg
		0.105	0.108	0.114[b]	0.132[b]	0.119[b]	0.044[d]
		0.45 mg	0.75 mg	3.0 mg	5.0 mg		
		0.124[b]	0.113[b]	—[e]	—[e]		

[a] Recoveries obtained for 0.1, 0.2, 0.5, and 5.0 mg of NO_2^--N in the absence of nitrate were 0.022, 0.022, 0.018, and 0.162 mg, respectively [1]. [b] Solution had a slight amber tint. [c] Solution was filtered after distillation. [d] Color was yellowish-pink. [e] Most of the solution was lost by effervescence when the 2,4-xylenol solution was added.

unmodified method are as follows: NO_2^--N, 0.2; Fe^{2+} (and other reducing metal ions), 0.2; S^{2-}, 0.2; $S_2O_3^{2-}$, 0.1; SCN^-, 0.2; Mn^{7+}, 5; Cr^{6+}, 5; V^{5+}, 0.2; ClO_3^-, 0.2; $S_2O_8^{2-}$, 5; H_2O_2, 0.02; Cl^-, 0.2; Br^-, 0.1; I^-, 0.2; metals, none.

The non-interference of some ions (25 mg) was surprising, particularly for SO_3^{2-}, PO_2^{3-}, Fe^{3+}, and Ce^{4+}. Therefore, 50 mg of these ions were tested. It was found that recoveries of NO_3^--N in the presence of 50 mg of these ions were: SO_3^{2-}, 95%; PO_2^{3-}, 86%; Fe^{3+}, 98%; and Ce^{4+}, 60%.

Elimination of interference of metals

Solutions containing metals (as the elements) should be filtered as soon as possible. Prolonged standing before filtration will sometimes give slightly low results because of a slight reaction between the metal and water to produce some hydrogen.

Elimination of nitrite interference with sulfamic acid

Sulfamic acid was found to be more reliable than urea in eliminating nitrite interference. The acidity of sulfamic acid had no significant effect on the development of the color. A 10% solution of sulfamic acid was found to

be 1.05 M by titration with standard alkali. Digestion of the solution at about 60°C for 30 min after the addition of the sulfamic acid did not give better results than did the boiling treatment.

It is recommended that the method for the elimination of nitrite be confined to samples containing less than 50 mg of NO_2^--N (5.0 mg in the 10-ml aliquot). Slightly high results were obtained for samples containing 75 mg of NO_2^--N, and very high results were obtained with 100 mg of NO_2^--N present. In ordinary analytical work, nitrate usually predominates over nitrite so that the method will be applicable in almost all cases.

Not much effort was devoted to using procedures C and D sequentially, i.e. determining nitrate in solutions containing nitrite and reductants or oxidants. Preliminary work established that it would be difficult to check the use of procedures C and D sequentially because of chemical incompatibility of nitrite with reductants and oxidants. Nitrite acting as a reducing agent can react with Mn^{7+}, Cr^{6+}, and $S_2O_8^{2-}$ to give nitrate [9]; as an oxidant, it can react with Fe^{2+}, S^{2-}, and $S_2O_3^{2-}$ to give NO, which reacts with aerial oxygen to produce NO_2, which in turn reacts with water to give nitrate [9]. The extent of the reaction between nitrite and reductants and oxidants is difficult to predict, since it would depend on the nature and relative amounts of the reactants, as well as on the kind and amount of the other ions present, temperature, time of standing and pH. Sulfamic acid itself did not react with hydrogen peroxide to produce any interference with the nitrate color.

Good results were obtained when the sulfamic acid method (procedure C) and the precipitation with silver sulfate (procedure E) were used sequentially. However, it should be emphasized that the tests involving iodide and nitrite were conducted with freshly prepared neutral synthetic solutions of the potassium salts, with no other ions present. Nitrite can oxidize iodide but ordinarily the reaction takes place in acidic medium [9].

Elimination of interference of reductants and oxidants by use of hydrogen peroxide

Hydrogen peroxide in dilute sulfuric acid solution acts as an oxidizing and reducing agent and eliminates the interference of many reductants and oxidants. It oxidizes Fe^{2+}, S^{2-}, $S_2O_3^{2-}$, SCN^- and other strong reductants that could interfere with the method (Sn^{2+}, Cr^{2+}, Ti^{3+}, Cu^+, and Hg^+), while it reduces Mn^{7+} and Cr^{6+} [9]. Hydrogen peroxide behaves as an oxidant in the reaction $H_2O_2 + 2H^+ + 2e = 2H_2O$ ($E^\circ = +1.77$ V), and as a reductant in the reaction $2H^+ + O_2 + 2e = H_2O_2$ ($E^\circ = +0.68$ V) [10].

The iron(III) (25 mg), which catalyzes the decomposition of hydrogen peroxide [10], was found to be absolutely essential. Its action can be clearly demonstrated by the following experiment. Sulfuric acid (5 ml of 10%), 10 ml of hydrogen peroxide (30%) and about 110 ml of water were mixed and boiled vigorously for 30 min; no strong effervescence was noted. When a portion of the cooled solution was tested for peroxide with titanium solution [11], the intense orange solution showed that considerable peroxide remained

undecomposed. Then, 5 ml of the iron(III) reagent was added, and the solution was diluted to about 125 ml and boiled again for 30 min. Prior to the boiling there was considerable but even effervescence. On cooling, the testing with the titanium reagent was negative, indicating complete destruction of the hydrogen peroxide.

The Fe^{3+} seems to catalyze not only the destruction of the peroxide but also the oxidation of the reductants, especially in the case of S^{2-} and $S_2O_3^{2-}$. The S^{2-} is oxidized mostly to SO_4^{2-}, although some elemental sulfur (which does not interfere) is also produced. $S_2O_3^{2-}$ is oxidized to SO_4^{2-}.

Only 50 mg (5.0 mg in the 10-ml aliquot) of thiocyanate could be handled by the peroxide treatment. The presence of more SCN^- caused high results because of some oxidation to nitrate. It was thought initially that the high results might be due to nitrate in the KSCN used, but this was ruled out because the high results showed no pattern. The primary oxidation products of thiocyanate are probably CO_3^{2-}, NH_3, and SO_4^{2-}.

Only 15 mg of Cl^- or Br^-, and 10 mg of I^- (equivalent to 1.5 mg of Cl^- or Br^- and 1.0 mg of I^- in the 10-ml aliquot) can be present in samples subjected to the peroxide treatment. The presence of more halide caused high results (10—30% too high) for some unknown reason.

$S_2O_8^{2-}$ is eliminated during the peroxide treatment, probably because of decomposition (to SO_4^{2-} and O_2) [9], rather than any reaction involving hydrogen peroxide.

The hydrogen peroxide had no effect on V^{5+} and ClO_3^-, and the interference from these two ions could not be eliminated in this way. In experiments with ClO_3^-, any Cl^- produced by the reduction of ClO_3^- with hydrogen peroxide was removed with silver sulfate (very little Cl^- was detected).

No nitrate is lost during the boiling in the peroxide treatment since the vapor pressure of nitric acid from a very dilute nitric acid solution (ordinarily less than about 0.1% HNO_3) in a very dilute sulfuric acid solution is extremely low. This point was investigated by adding 5 ml of dilute sulfuric acid (10%) and 2.0 mg of NO_3^--N to 100-ml portions of water and boiling to volumes of 75, 50, 25, and 10 ml. Surprisingly, complete recoveries of NO_3^--N were obtained in all cases. Of course, if the solution were evaporated to the point at which the sulfuric acid started to fume (about 0.5 ml), all the nitrate would be lost.

The presence of halide during the boiling had no effect on the volatilization of nitrate. This was established by adding 100 mg of Cl^-, Br^-, or I^- to solutions containing 2.0 mg of NO_3^--N and 5 ml of dilute sulfuric acid (10%) and boiling for 30 min. On precipitating the halide with silver sulfate and analyzing for nitrate, complete recoveries were obtained. The experiments on the effect of halide during the boiling were somewhat academic because (as stated earlier) there is a recommended maximum limit of 15 mg for Cl^- and Br^- and 10 mg for I^-.

Dilute neutral solutions of nitrate were found to be quite stable towards reductants and oxidants at room temperature, so that the question of chemical incompatibility did not arise.

Correction method for nitrite with hydrogen peroxide

As indicated in procedure C, an alternative to the sulfamic acid method is to oxidize the nitrite to nitrate by hydrogen peroxide and then deduct NO_2^--N from the total NO_3^--N. The Fe^{3+} reagent seems to be essential for the oxidation. The correction method is especially advantageous when only a small amount of NO_2^--N is present.

The results obtained for the nitrite correction procedure (Table 3) are satisfactory although slightly low in some instances.

Elimination of halide interference by precipitation with silver sulfate

The amount of halide that can be handled is limited by the volume of silver sulfate solution (0.44%) that can be used while keeping the volume after filtration below 200 ml. Of course, the solution could be diluted further but this would decrease the sensitivity of the method.

An excess of silver sulfate does not seem to do any harm. Most of the I^- (but not Cl^- or Br^-) is released as free halogen and boiled off during the peroxide treatment. This has to be borne in mind in deciding how much silver sulfate solution to use.

Recommended limits and results for the procedures for the elimination of interferences

In view of the various considerations mentioned in the above paragraphs, the recommended maximum permissible limits (mg per 10-ml aliquot) for the elimination of interferences are as follows: NO_2^--N, 5; Fe^{2+}, 25; S^{2-}, 25; $S_2O_3^{2-}$, 25; SCN^-, 5; Mn^{7+}, 25; Cr^{7+}, 25; $S_2O_8^{2-}$, 25; H_2O_2, 100; Cl^-, 10; Br^-, 20; I^-, 25 (if the peroxide treatment is used the limits are Cl^-, 1.5; Br^-, 1.5; I^-, 1.0); metals, 25+.

The results obtained by the proposed methods for synthetic mixtures prepared from standard nitrate solution and solutions of the interferences (Table 4) were satisfactory. Analyses of solutions of the interferences without added nitrate showed that the chemicals used did not contain significant amounts of nitrate.

TABLE 3

Results for correction procedure for nitrite

NO_3^--N added (mg)	NO_2^--N added (mg)	Total NO_3^--N found (mg)[a]	NO_3^--N found after correction (mg)	NO_3^--N added (mg)	NO_2^--N added (mg)	Total NO_3^--N found (mg)[a]	NO_3^--N found after correction (mg)
1.00	0.00	0.102	0.102	0.50	0.50	0.092	0.042
0.00	0.50	0.053	0.003	1.00	1.00	0.194	0.094
0.00	1.00	0.100	0.000	1.00	0.50	0.144	0.094
0.00	1.50	0.155	0.005	0.50	1.00	0.148	0.048
0.00	2.00	0.194	−0.006				

[a]The amount found in the 10-ml aliquot. The dilution before aliquoting was 100 ml.

TABLE 4

Results for nitrate by the proposed methods for the elimination of interferences

Interference (mg)	NO_3^--N added (mg)	NO_3^--N in 10-ml aliquot (mg)[a]		Interference (mg)	NO_3^--N added (mg)	NO_3^--N in 10-ml aliquot (mg)[a]	
		Present	Found			Present	Found
25 NO_2^--N	0.00	0.000	0.005	250 $S_2O_8^{2-}$	0.00	0.000	0.000
50 NO_2^--N	0.00	0.000	0.005	250 $S_2O_8^{2-}$	0.75	0.075	0.076
75 NO_2^--N	0.00	0.000	0.030	250 $S_2O_8^{2-}$	1.50	0.150	0.152
25 NO_2^--N	0.50	0.050	0.060	100 Cl^-	0.00	0.000[b]	0.000
50 NO_2^--N	0.50	0.050	0.060	100 Cl^-	1.50	0.075[b]	0.072
75 NO_2^--N	0.50	0.050	0.065	100 Cl^-	3.00	0.150[b]	0.152
25 NO_2^--N	1.50	0.150	0.155	200 Br^-	0.00	0.000[b]	0.000
50 NO_2^--N	1.50	0.150	0.161	200 Br^-	1.50	0.075[b]	0.072
75 NO_2^--N	1.50	0.150	0.185	200 Br^-	3.00	0.150[b]	0.148
250 Fe^{2+}	0.00	0.000	0.005	250 I^-	0.00	0.000[b]	0.005
250 Fe^{2+}	0.75	0.075	0.072	250 I^-	1.50	0.075[b]	0.083
250 Fe^{2+}	1.50	0.150	0.148	250 I^-	3.00	0.150[b]	0.152
250 S^{2-}	0.00	0.000	0.005	100 Cl^- + 50 NO_2^--N	3.00	0.150[b]	0.155
250 S^{2-}	0.75	0.075	0.076	100 Br^- + 50 NO_2^--N	3.00	0.150[b]	0.158
250 S^{2-}	1.50	0.150	0.158	100 I^- + 50 NO_2^--N	3.00	0.150[b]	0.155
250 $S_2O_3^{2-}$	0.00	0.000	0.005	250 S^{2-} + 250 Cr^{6+}	1.50	0.150	0.152
250 $S_2O_3^{2-}$	0.75	0.075	0.076	100 Fe^{2+} + 100 $S_2O_3^{2-}$	1.50	0.150	0.155
250 $S_2O_3^{2-}$	1.50	0.150	0.152	100 Cr^{6+} + 100 Mn^{7+}	1.50	0.150	0.155
50 SCN^-	0.00	0.000	0.005	250 Fe^{2+} + 10 Cl^-	1.50	0.150	0.152
50 SCN^-	0.75	0.075	0.076	250 Cr^{7+} + 15 Cl^-	1.50	0.150	0.158
50 SCN^-	1.50	0.150	0.158	250 S^{2-} + 10 Br^-	1.50	0.150	0.148
250 Mn^{7+}	0.00	0.000	0.000	250 Fe^{2-} + 15 Br^-	1.50	0.150	0.158
250 Mn^{7+}	0.75	0.075	0.072	250 $S_2O_3^{2-}$ + 10 I^-	1.50	0.150	0.148
250 Mn^{7+}	1.50	0.150	0.148	250 S^{2-} + 10 I^-	1.50	0.150	0.161
250 Cr^{6+}	0.00	0.000	0.000	250 Mg	0.00	0.000	0.000
250 Cr^{6+}	0.75	0.075	0.072	250 Mg	0.75	0.075	0.072
250 Cr^{6+}	1.50	0.150	0.148	250 Mg	1.50	0.150	0.152
1000 H_2O_2	0.00	0.000	0.000	250 Al	0.00	0.000	0.000
1000 H_2O_2	0.75	0.075	0.072	250 Al	0.75	0.075	0.072
1000 H_2O_2	1.50	0.150	0.152	250 Al	1.50	0.150	0.148

[a]Unless otherwise specified, the dilution before aliquoting was 100 ml. [b]Dilution before aliquoting was 200 ml.

Applicability of the procedures

The method should be very useful for a variety of materials that are difficult to analyze. For example, it could be used to determine nitrate (present as an impurity or added as a brightener) in electroplating baths. It could certainly be used for the analysis of inorganic salts containing reducing or oxidizing ions, e.g. ammonium iodide, ammonium persulfate, iron(II) sulfate, iron(II) ammonium sulfate, potassium bromide, potassium chromate, potassium dichromate, potassium iodide, potassium permanganate, sodium sulfide, and sodium thiosulfate. Presently, the standard texts for the analysis of these salts give no method at all for nitrate, or give a method for total nitrogen which involves treatment with aluminum or Devarda's alloy in alkaline solution and distillation of the resultant ammonia [12, 13].

Various shades of turbid yellowish colors were obtained on adding the 2,4-xylenol solution to the concentrated sulfuric acid solutions containing the interferences described in this paper (before or after the preliminary treatments). This emphasizes the great value of the distillation technique, because the direct determination of the nitrate would be valueless.

REFERENCES

1 G. Norwitz and H. Gordon, Anal. Chim. Acta, 89 (1977) 177.
2 Am. Public Health Assoc., Standard Methods for the Examination of Water and Waste Water, 13th edn., Washington, DC, 1971, pp., 233, 234, 454.
3 F. Alten, B. Wandrowsky, and E. Hille, Bodenkd. Pflanzenernaehr., 1 (1936) 340.
4 H. Yagoda, Ind. Eng. Chem., Anal. Ed., 15 (1943) 27.
5 F. Werr, Fresenius Z. Anal. Chem., 109 (1937) 81.
6 H. Barnes, Analyst, 75 (1950) 388.
7 J. Buckett, W. D. Duffield, and R. F. Milton, Analyst, 80 (1955) 141.
8 A. C. Holler and R. V. Huch, Anal. Chem., 21 (1949) 1385.
9 A. B. Prescott and O. C. Johnson, Qualitative Chemical Analysis, 10th edn., Van Nostrand, New York, 1933, pp. 314, 322, 350, 472, 480, 522.
10 R. B. Heslop and K. Jones, Inorganic Chemistry, Elsevier, New York, 1976, p. 495.
11 F. D. Snell and C. T. Snell, Colorimetric Methods of Analysis, 3rd edn., Vol. II, Van Nostrand, New York, 1953, p. 882.
12 Am. Chem. Soc., Reagent Chemicals, 4th edn., Washington, DC, 1968.
13 J. Rosin, Reagent Chemicals and Standards, 5th edn., Van Nostrand, New York, 1967.

Analytica Chimica Acta, 98 (1978) 335—342

SPECTROPHOTOMETRIC DETERMINATION OF RUTHENIUM WITH 2,4,6-TRIS(2′-PYRIDYL)-S-TRIAZINE

YOSHIMI SASAKI

Department of Industrial Chemistry, Fukui Technical College, Geshi, Sabae, Fukui Prefecture (Japan)

(Received 5th December 1977)

SUMMARY

Ruthenium(III) reacts with 2,4,6-tris(2′-pyridyl)-s-triazine (TPTZ) in water—glycerol solution at pH 3—4, forming a red-purple complex (λ_{max} 505 nm) and the colour is developed fully by heating at 100° C for 35 min. On acidification with perchloric acid, the absorption peak shifts to 535 nm, and the absorbance increases by 30%. Moreover, the coloured TPTZ complexes of other metals such as iron(II), iron(III), cobalt(II), copper(II), and nickel(II) are destroyed. Beer's law is obeyed in the range 10—100 μg of ruthenium(III). The ruthenium—TPTZ complex can be extracted into nitrobenzene from aqueous solutions containing 0.5 mol dm^{-3} perchloric acid; Beer's law is then obeyed in the range of 4—40 μg of ruthenium(III). Common cations and anions do not interfere. Applications to synthetic mixtures and to plated brass are reported.

2,4,6-Tris(2′-pyridyl)-s-triazine (TPTZ) was first prepared by Case and Koft [1], and has been used for the colorimetric determinations of iron [2—4], ruthenium [5], and cobalt [6]. Embry and Ayres [5] reported the spectrophotometric determination of ruthenium with TPTZ in terms of the intensely coloured ruthenium complex formed in water—ethanol solution after heating at 87 ± 1° C for 1 h. This method can be improved in several respects by modifications designed to shorten the heating time, and improve the sensitivity and selectivity. Moreover, the ruthenium—TPTZ complex can be extracted into nitrobenzene from perchloric acid solutions, thus making the determination still more sensitive.

EXPERIMENTAL

Reagents

Ruthenium standard solution. Dissolve 1.132 g of ruthenium(III) trichloride monohydrate (extra-pure grade) in a small volume of 2 mol dm^{-3} hydrochloric acid, and dilute to 100 cm^3 with the same acid. This solution was standardized gravimetrically [7]; the mean result of 4 analyses was 5.05 mg Ru cm^{-3}. This solution was diluted 500 times with 0.1 mol dm^{-3} hydrochloric acid immediately before use.

TPTZ solution (0.01 mol dm^{-3}). Dissolve 1.562 g of TPTZ (extra-pure

grade) in a few drops of hydrochloric acid and dilute to 500 cm^3 with glycerol—water(2 + 1).

Acetate buffer. Mix 1 mol dm^{-3} sodium acetate and 1 mol dm^{-3} acetic acid in the ratio 1:3.

Other chemicals were all of extra-pure reagent grade.

Apparatus

A Hitachi Model 124 recording spectrophotometer, a Hitachi Model 101 spectrophotometer, with 1.0-cm cells, and a Hitachi-Horiba Model F 5 pH meter were used.

Recommended procedures

Procedure A for larger amount of ruthenium(10—100 μg). Place a suitable sample solution in a 25-cm^3 volumetric flask and add 7 cm^3 of the TPTZ solution and 3—5 cm^3 of acetate buffer pH 4.0. Dilute the solution to about 20 cm^3 with water, and heat in a boiling water bath for 35 min. After cooling, add 2.5 cm^3 of 60% perchloric acid and dilute to the mark with water. Mix well and measure the absorbance at 535 nm against a reagent blank.

Procedure B for smaller amount of ruthenium(4—40 μg). After the same treatment of the sample solution as described above, transfer the solution to a 100-cm^3 separating funnel. Add 25 cm^3 of water and 10.0 cm^3 of nitrobenzene, and shake for 5 min. Separate the nitrobenzene phase and measure the absorbance at 543 nm against a reagent blank.

RESULTS AND DISCUSSION

Development of the coloured ruthenium—TPTZ complex

Embry and Ayres [5] formed the ruthenium(III)—TPTZ complex in water—ethanol solution by heating at 87 ± 1°C for 1 h, but ethanol restricts the heating temperature to a few degrees below 90°C, so that the colour development remains incomplete. Replacement of ethanol by glycerol allowed the temperature to be increased to 100°C. Addition of 7 cm^3 of glycerol—water(2 + 1) mixture was found beneficial for 10 cm^3 of hydrochloric acid—ethanol(1 + 1) solution containing ruthenium(III); addition of 1 cm^3 of the mixture sufficed for test solutions containing no ethanol. The reagent solution was therefore prepared by dissolving TPTZ in glycerol—water (2 + 1). The glycerol did not interfere in the subsequent nitrobenzene extraction of the ruthenium—TPTZ complex.

The initial colour development was examined with a series of test solutions containing 50.5 μg of ruthenium(III) and varying amounts of TPTZ. About a 25-fold molar excess of the reagent over ruthenium was necessary to obtain a steady absorbance. When the pH was altered in Procedure A, the pH—absorbance plot showed a plateau between pH 2.5 and 6.0 with steep slopes on both sides.

During the first few minutes of heating, the absorbance of the initial

coloured solution increased rapidly; after 30 min, the absorbance reached a steady value and remained unchanged even on heating (Fig. 1). Good reproducibility was obtained after heating for 35 min. The developed colour was so stable that the absorbance was unchanged even after standing for 5 h; this was true for both the initial colour and the final colour in Procedure A.

To establish the optimum volume of 60% perchloric acid to be added to the initial coloured solution, Procedure A was used with varying volumes of 60% perchloric acid. Constant absorbances were obtained when 0.7—12.5 cm^3 of 60% perchloric acid was added, i.e. with 0.3—5 mol dm^{-3} perchloric acid in the final solution. Hydrochloric acid, sulfuric acid, and nitric acid of the same concentration behaved similarly, but the ruthenium—TPTZ complex could not be extracted with nitrobenzene from these solutions.

The absorption spectra shown in Fig. 2 indicate that the solution containing ruthenium(III) changes colour three times during the recommended procedure. The absorbances at each peak differ from each other: the absorbance at 535 nm (curve C) is 30% greater than that at 505 nm (curve B), and the absorbance at 543 nm (curve D) is 177% greater than that at 535 nm.

Composition of the ruthenium—TPTZ complex

For Job's method, the ruthenium—TPTZ complex was obtained by the initial step in Procedure A, with a series of solutions containing a total 2.0×10^{-4} mol dm^{-3} concentration of ruthenium(III) plus TPTZ. The continuous variations curves were obtained at different wavelengths (480 nm,

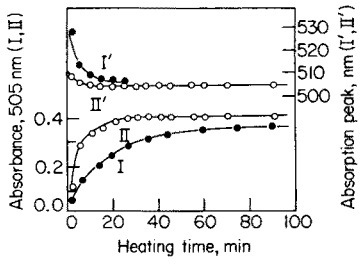

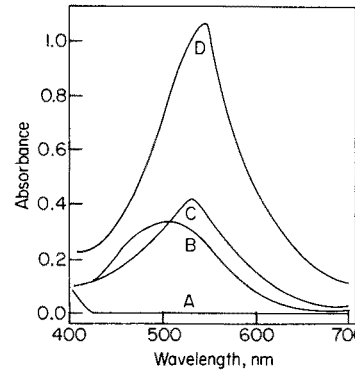

Fig. 1. Variations of the absorbance and of the absorption peak during colour developmen in Procedure A for 50.5 μg Ru(III) in 25 cm^3. (I) Heating at 87 ± 1° C. (II) Heating at 100° C. (I') Wavelength of the absorption peak of I. (II') Wavelength of the absorption pea of II.

Fig. 2. Absorption spectra of the ruthenium—TPTZ complex under various conditions for 40 μg Ru(III). (A) TPTZ reagent only (blank) against water. (B) Ruthenium—TPTZ complex in the initial coloured solution by Procedure A against reagent blank. (C) Ruthenium—TPTZ complex in the final coloured solution by Procedure A against reagent blanl (D) Ruthenium—TPTZ complex in nitrobenzene extracted from C by Procedure B against reagent blank.

505 nm, 520 nm, 540 nm, and 570 nm). All the peaks of the curves indicated a 1:2 molar composition for the ruthenium(III)—TPTZ complex, in contrast to the results of Embry and Ayres [5], which showed a 1:2 complex at 510 nm, and a 1:1 complex at 550 nm. This discrepancy can probably be attributed to differences between the composition in water—ethanol solution at 87 ± 1°C, and that in water—glycerol at 100°C. The heating to 100°C seems to lead to a definite composition of the complex. When Embry and Ayres' conditions were adopted, their results were confirmed in the present work.

The mole ratio method was also used. With a fixed (2.5×10^{-6} mol) amount of ruthenium(III), and varying amounts of TPTZ, Procedure A was followed as in the ordinary mole-ratio method. The absorbances obtained at 505 nm for the initial coloured solution and at 535 nm for the final solution were plotted against the amount of the reagent. The breaks in both curves confirmed the formation of a 1:2 ruthenium(III)—TPTZ complex.

Neither the initial red-purple complex nor the final purple complex in Procedure A was retained on a column of Dowex 1-X8 anion-exchange resin, but both were retained on a column of Dowex 50-W8 cation-exchange resin: therefore, the complexes were cationic.

The change in composition of the ruthenium—TPTZ complex during the initial colour development was studied in greater detail. When the ruthenium—TPTZ complex was formed, the initial blue turned to the final red colour on heating at 87 ± 1°C in ethanolic solution without glycerol; therefore two kinds of complex could be present in varying ratios. As shown by curve I′ in Fig. 1, the absorption peak shifted from 530 nm to 505 nm during the colour development. In contrast, when the solution was heated to 100°C in the presence of glycerol, the absorption peak remained at 505 nm and the final absorbance of curve II was 10% larger than that of curve I, (Fig. 1). The initial colour development in Procedure A was consistent with this fact. During the transformation of the colour on heating at 87 ± 1°C in the ethanolic solution without glycerol, the mixed coloured solution was submitted to paper electrophoresis; the red-purple 1:2 complex and the purple 1:1 complex could be separated from each other, with the 1:2 fraction predominating. However, when the water—glycerol solution was heated to 100°C, only the red-purple 1:2 complex was detected by electrophoresis.

Solvent extraction of the ruthenium—TPTZ complex

Among the various solvents tested, (nitrobenzene, isobutanol, phenylcarbinol, isobutyl methyl ketone, 1,2-dichloroethane, tributyl phosphate, ethyl acetate, chloroform, chlorobenzene, n-butyl acetate, diethyl ether, trichloroethylene, toluene, cyclohexane, and carbon tetrachloride), nitrobenzene gave the highest absorbance of the extracted ruthenium—TPTZ perchlorate ion pair.

The extraction with nitrobenzene in Procedure B was complete when the volume of ethanol was below 10%, with more than 10% ethanol, the extractior yield was somewhat lower. Therefore, in Procedure B, 25 cm^3 of water was

added to reduce the ethanol concentration below 10% where necessary. The extraction was complete in Procedure B with shaking times greater than 1 min.

Constant absorbances for the ruthenium—TPTZ perchlorate ion pair in nitrobenzene were obtained when the extraction was done from aqueous solutions containing 0.3—1.5 mol dm^{-3} perchloric acid; at acidities above 2 mol dm^{-3}, the absorbance of the organic phase began to decrease.

The colour change appearing in perchloric acid solution indicates the formation of a protonated complex, and this complex could be extracted with nitrobenzene, forming an ion pair with perchlorate. Continuous variations and slope methods showed that the ion-pair species is 1:1 between the ruthenium—TPTZ cation and the perchlorate anion.

Effect of diverse ions

Procedure A was applied to test solutions containing 50.5 μg of ruthenium(III) and varying amounts of other cations, and Procedure B was followed for test solutions containing 20.2 μg of ruthenium(III) and varying amounts of other cations. The results are shown in Table 1. No interferences were found from anions, which were examined with 0.4 mg of EDTA, 5 mg of the sodium salt of sulphate, citrate, phosphate or iodide, and 30 mg of the sodium salt of chloride, bromide, fluoride, nitrate or perchlorate. Iron(II), iron(III), cobalt(II), nickel(II), copper(II), and osmium(III) formed coloured complexes with TPTZ during the initial colour development of Procedure A. But these coloured TPTZ complexes, except that of osmium(III), were decolourized within 5 min by adding perchloric acid to the solution.

TABLE 1

Effect of diverse cations on the determination of ruthenium by Procedure A (50.5 μg Ru(III)) or B (20.2 μg Ru(III))

Metal	Added as	Amount (μg)	Procedure A		Procedure B	
			Ru found (μg)	Recovery (%)	Ru found (μg)	Recovery (%)
None	—	—	50.5	100	20.2	100
Ni(II)	$NiCl_2 6H_2O$	150	49.8	98	19.8	98
Zn(II)	$ZnSO_4 7H_2O$	600	50.5	100	20.1	100
Co(II)	$CoSO_4 7H_2O$	150	49.3	98	19.9	99
Cr(III)	$Cr(NO_3)_3 9H_2O$	100	50.0	99	20.0	100
Fe(III)	$FeCl_3 6H_2O$	100	50.2	99	20.1	100
Fe(II)	$FeSO_4 7H_2O$	100	49.8	99	19.9	99
Pb(II)	$Pb(NO_3)_2$	5000	50.0	99	19.9	99
Cu(II)	$CuSO_4 5H_2O$	800	50.0	99	19.7	98
Pt(IV)	H_2PtCl_6	300	51.7	102	20.5	101
Os(III)	$OsCl_3$	10	51.3	102	20.4	101
Rh(III)	$RhCl_3 3H_2O$	200	49.3	98	19.5	97
Ir(III)	$IrCl_3$	500	51.7	102	19.7	98
Au(III)	$HAuCl_4$	400	49.0	97	19.9	99
Pd(II)	$PdCl_2$	500	51.2	101	20.0	99

Calibration range and sensitivity

The optimum concentration ranges and sensitivities for Procedures A and B were as follows:

	Procedure A	Procedure B
Optimum range (1.00-cm path)	10—100 μg/25 cm^3	4—40 μg/10 cm^3
Specific absorptivity, ppm^{-1} cm^{-1}	0.24	0.27
Molar absorptivity, l mol^{-1} cm^{-1}	2.4×10^4	2.7×10^4

Determination of ruthenium in synthetic sample solutions

Ruthenium(III) was determined in the presence of platinum group metals or iron group metals by Procedures A and B. As shown in Table 2, the results were satisfactory without separation of ruthenium. Moreover, ruthenium(III) in sodium chloride was determined as a preliminary experiment for further application of this method.

Application to plated brass

A ruthenium-plated brass plate was obtained from an electroplating factory of a frame work manufacturer. This brass had been plated in three layers with nickel, nickel—palladium, and then ruthenium. In this case only the ruthenium of the uppermost layer should be released into solution. A 0.1—1-g sample of the plate was warmed in a flask with 2 cm^3 of sodium hydrochlorite—sodium hydroxide solution (10 g of sodium hydroxide in 50 cm^3 of sodium hydrochlorite solution containing 10% available chlorine). The resulting solution and washings were combined in a 25- or 50-cm^3 volumetric flask and 10 cm^3 of ethanol was added to reduce ruthenate to ruthenium dioxide. Then 7 cm^3 of 12 mol dm^{-3} hydrochloric acid was added to dissolve ruthenium dioxide to ruthenium(III) trichloride, and warmed to remove chlorine. After cooling, the solution was diluted to the mark with water. An aliquot (2 cm^3) of this solution was adjusted to pH 3—4 by adding

TABLE 2

Determination of ruthenium in synthetic sample solutions by Procedure A (50.5 μg Ru(III)) or B (20.2 μg Ru(III))

Addition	Procedure A		Procedure B	
	Ru found (μg)[a]	Recovery (%)	Ru found (μg)[a]	Recovery (%)
None	50.5 ± 0.4	100	20.2 ± 0.3	100
Composition A[b]	50.8 ± 0.5	101	20.1 ± 0.4	100
Composition B[c]	50.7 ± 0.5	100	19.8 ± 0.4	98
0.5 g NaCl	50.9 ± 0.6	101	19.7 ± 0.4	98
0.5 g NaCl, 50 μg Fe(II)	50.8 ± 0.5	101	20.4 ± 0.5	101

[a]The average value of 4 runs with standard deviation. [b]Composition A: 200 μg Ir(III), 200 μg Au(III), 200 μg Pt(IV), 200 μg Pd(II). [c]Composition B: 50 μg Fe(II), 50 μg Co(II), 50 μg Ni(II), 50 μg Cu(II).

TABLE 3

Determination of ruthenium of the uppermost layer of ruthenium-plated brass plate (For each brass, 4 samples were weighed out. Except where noted, sample solutions were diluted to 25 cm^3 and a 2-cm^3 aliquot was taken for Procedure A, a 20-cm^3 aliquot being used for the thiourea method. The results given are the averages of the 4 analyses with standard deviation.)

Sample[a]	Weight taken (g)	Ruthenium found (%)	
		Procedure A	Thiourea method
A (0.41% Ru)	0.137—0.408[b]	0.40 ± 0.006	0.39 ± 0.008
B (0.21% Ru)	0.254—0.311	0.22 ± 0.006	0.21 ± 0.01
C (0.12% Ru)	0.469—0.551	0.12 ± 0.01	0.12 ± 0.01
D (0.07,% Ru)	0.760—0.875	0.073 ± 0.004	0.070 ± 0.005
E	0.375—0.534	0.15 ± 0.01	0.16 ± 0.01

[a]The % Ru is given by the manufacturer: the value is estimated from the weight difference before and after the ruthenium plating. [b]For sample weights above 0.20 g, the sample solution was diluted to 50 cm^3 and a 2-cm^3 aliquot was taken for Procedure A. When a 20-cm^3 aliquot was used in the thiourea method, the absorbance was similar to the blank.

3—5 cm^3 of 1 mol dm^{-3} sodium acetate solution and sodium hydroxide solution. The colour was developed by Procedure A. The results for several samples are shown in Table 3.

To evaluate the recommended method, the thiourea method [8] was used to determine ruthenium in the same samples, because iron impurities in the reagents do not interfere with this method. The procedure was as follows: in a 25-cm^3 volumetric flask, an aliquot (20 cm^3) of the sample solution (which had been diluted to 25 cm^3) was mixed with 1 cm^3 of 10% thiourea solution and the mixture was diluted to just below the mark with hydrochloric acid and ethanol. The flask was placed for 10 min in a water bath at 85° C to develop the colour. After cooling, the mixture was diluted to the mark with hydrochloric acid—ethanol mixture, and the absorbance was measured at 620 nm. The results obtained by both methods for the same samples are noted in Table 3. The molar absorptivity of the ruthenium—TPTZ complex at its absorption peak (Procedure A) was about one order of magnitude larger than that of the ruthenium—thiourea complex. As shown in Table 3, the sample weight needed in the proposed method may be one tenth of that in the thiourea method. Analytical values obtained by the two methods are in good agreement, and the standard deviations are similar.

The author expresses his hearty thanks to Professor T. Kiba of Kanazawa University for advice and encouragement.

REFERENCES

1 F. H. Case and E. Koft, J. Am. Chem. Soc., 81 (1959) 905.
2 P. E. Colins, H. Diehl and G. F. Smith, Anal. Chem., 31 (1959) 1862.
3 C. C. Tsen, Anal. Chem., 38 (1959) 849.
4 A. A. Schilt and P. J. Taylor, Anal. Chem., 42 (1970) 220.
5 W. A. Embry and G. H. Ayres, Anal. Chem., 40 (1968) 1499.
6 M. J. Janmohamed and G. H. Ayres, Anal. Chem., 44 (1972) 2263.
7 Toshiyasu Kiba, K. Terada, Tomoe Kiba and K. Suzuki, Talanta, 19 (1972) 451.
8 G. H. Ayres and F. Young, Anal. Chem., 22 (1950) 1277.

Analytica Chimica Acta, 98 (1978) 343—348

CATALYTIC THERMOMETRIC TITRATION OF SILVER(I), MERCURY(II) AND PALLADIUM(II)

NOBUTOSHI KIBA* and MOTOHISA FUROSAWA

Department of Chemistry, Faculty of Engineering, Yamanashi University, Kofu-shi, 400 (Japan)

(Received 3rd January 1978)

SUMMARY

A thermometric method of end-point indication is described for catalytic titrations of micro amounts of silver, mercury or palladium. The indicator reaction is the iodide-catalysed Mn(III)—As(III) reaction, monitored with a thermistor probe, and the end-point is obtained from the recorded titration curves. Silver and mercury (0.5—500 μg) and palladium (0.2—500 μg) can be determined with relative errors and coefficients of variation of within 3%.

Since the possibility of using catalytic reactions for indication of end-points was pointed out by Yatsimirski and Fedorova [1], titration procedures with visual, potentiometric, biamperometric, spectrophotometric and thermometric catalytic end-points have been used for the determination of microgram quantities of material in solution [2].

Traces of iodine compounds and osmium(VIII) act as catalysts for the reduction of manganese(III) by arsenic(III) [3]. This has been applied to the standardization of permanganate solution with arsenic trioxide [4]. The catalytic action has been used also for the determination of organically bound iodine in rat thyroids by following the kinetics of the reaction photometrically [5], but the reactions has not been used for end-point indication in catalytic titrations.

The present paper describes a method for determining silver(I), mercury(II) and palladium(II) in the range 10^{-6}—10^{-3} M. Trivalent manganese was prepared by the reduction of permanganate with manganese(II) and was stabilized by the addition of metaphosphoric acid. The basic procedure is as follows. A stirred solution of the sample containing silver, mercury or palladium ions and fixed amounts of manganese(III), arsenic(III) and phosphoric acid is titrated with standard potassium iodide solution from a mechanically driven syringe burette. The rise in temperature based on the indicator reaction after the end-point is detected by a thermistor probe in a Wheatstone bridge circuit.

Several methods based on the inhibitory effects of metal ions on the iodide-catalysed Ce(IV)—As(III) reaction have been reported for catalytic

titrations of silver, gold, mercury, and palladium [6]. The range of the present method is similar to those of methods employing the Ce(IV)—As(III) reaction. However, the Ce(IV)—As(III) reaction method is inapplicable to samples containing phosphate because of the precipitation of cerium phosphate.

EXPERIMENTAL

Solutions

All solutions were prepared with deionized distilled water and ultra-reagent grade substances.

Mn(III) solution (ca. 0.02 M). Manganese(II) sulfate solution (50 ml, 1 M) was mixed with 500 ml of 7.5 M metaphosphoric acid. Then 60 ml of 0.2 M potassium permanganate solution was added slowly to the mixture over a 20-min interval with stirring. The solution was perfectly stable for 7 days; thereafter a red manganese orthophosphate precipitate appeared.

As(III) solution (ca. 0.1 M). Arsenic trioxide (10 g) was dissolved in 500 ml of 2 M sodium hydroxide solution, which was neutralized with 2 M sulfuric acid and diluted to 1 l with water.

Potassium iodide solution. Iodide stock solution (0.01 M) was prepared from potassium iodide dried in vacuo at 40°C for 24 h. The stock iodide solution was standardized against primary-standard silver nitrate solution. Other solutions (10^{-3} M and 10^{-4} M) were prepared by dilution daily.

Stock solutions (10^{-3} M) of silver(I), mercury(II) and palladium(II) were prepared by dissolving 0.1736 g of silver nitrate, 0.3178 g of mercury(II) acetate, and 0.2011 g of palladium sulfate, respectively, in 40 ml of (1 + 1) nitric acid and making up to 1 l with water. The dilute solutions were prepared just before the measurements.

Apparatus

A thermometric titrator with a recorder (TOA Electric, Tokyo) was used. The apparatus has been described in detail [7]. The titration cell was a 30-ml Dewar flask.

Procedure

The burette was filled with the appropriate standard iodide solution, depending on the metal concentration of the sample. An aliquot (5.00 ml) of the sample, 6 ml of Mn(III) solution, 2 ml of As(III) solution, and 7 ml of 5 M phosphoric acid were added to the titration cell. The cover with its attached thermistor, stirrer and burette tip was fitted; when the thermistor bridge recorder gave a steady trace, the synchronous burette motor was started to perform the titration. The recorder full scale sensitivity was 100 mV and the titration speed was 1 ml per 15 min.

All the titrations were carried out at room temperature (18—22°C).

Calibration curves were obtained by plotting chart travel against the amount of metal taken.

RESULTS AND DISCUSSION

The blank and the sharpness of the end-points were affected by the concentration of Mn(III) and As(III), acidity of titrand, concentration of titrant, and rate of addition of titrant. However, all these factors could be kept constant and the results were reproducible under a given set of experimental conditions. The sharpnesss of the temperature change at the end-point was greatly affected by the acidity of titrand. It is known that the catalytic reaction depends on the concentration of sulfuric acid [3, 5]. The effect of other mineral acids on the catalytic reaction has not been investigated. The magnitude of the catalytic action of iodide when a mineral acid, i.e. sulfuric acid, perchloric acid, nitric acid or phosphoric acid, was present in the titrand was studied. The angle θ, determined by extrapolation of the linear portions on either side of the equivalence point, was regarded as the magnitude of the catalytic action of iodide (Fig. 1). The results obtained with standard 10^{-3} M and 10^{-4} M iodide solutions are summarized in Fig. 2. The catalytic action of iodide was enhanced by small amounts of mineral acids, regardless of the kind of anionic species present, and a sharper end-point could be obtained. The catalytic action was depressed by high concentrations of acids except phosphoric acid. As shown in Fig. 2A, the catalytic action of iodide is greatest at 0.7 M for sulfuric acid, at 0.4 M for perchloric acid and at 0.6 M for nitric acid. An increase in the phosphoric acid concentration to 1.6 M increased the catalytic action; at higher concentrations of phosphoric acid the catalytic action remained unchanged, in contrast to the results with the other mineral acids tested. Results similar to those in Fig. 2A were obtained by the use of 10^{-4} M standard iodide solution. As shown in Fig. 2B maximal catalytic action of iodide was obtained at 0.7 M for sulfuric acid, 0.9 M for perchloric acid or 1 M for nitric acid. For phosphoric acid, the curve was identical in shape to that shown in Fig. 2A. Comparison of the results in Fig. 2 shows that the end-point becomes sharper with increasing titrant concentration. The effects of sulfuric acid and phosphoric acid on the reaction do not vary with the titrant concentration, whereas the effect of perchloric acid and nitric acid do vary.

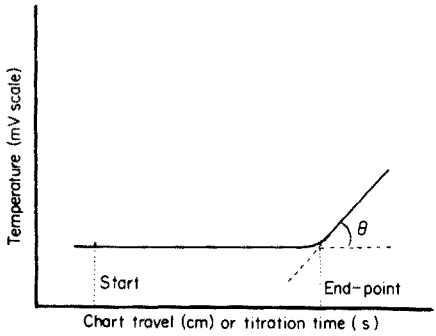

Fig. 1. Thermometric titration curve.

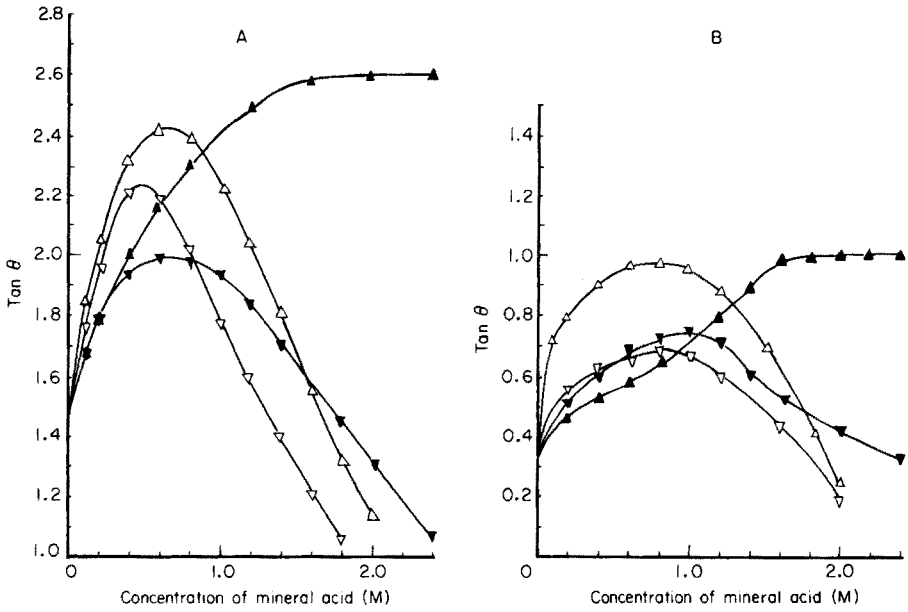

Fig. 2. Effects of mineral acids on the iodide-catalysed Mn(III)—As(III) reaction. (A) Titration of 2.005×10^{-5} M silver nitrate with 1.000×10^{-3} M iodide solution. (B) Titration of 2.005×10^{-6} M silver nitrate with 1.000×10^{-4} M iodide solution. △ H_2SO_4. ▲ H_3PO_4. ▼ HNO_3. ▽ $HClO_4$.

It is clear that smaller blanks and sharper end-points can be obtained when phosphoric acid or sulfuric acid is present; the concentration of sulfuric acid has to be adjusted to 0.7 M but strict adjustment of the phosphoric acid concentration is not necessary. Therefore, phosphoric acid was chosen for the analytical procedures.

The composition of the Mn(III) solutions also affected the blanks and sharpness of the end-points. Reactive Mn(III) solutions could be obtained with molar ratios of $MnSO_4$ to $KMnO_4$ ranging from 4.0 to 4.5. Above this ratio, titration curves displayed a gentle rise at the end-point, and sharp end-points could not be obtained; below this ratio, an excess of permanganate ion was present so that some As(III) was immediately oxidized. A stable temperature—time relationship could not be obtained because of the heat of reaction of permanganate with arsenite; the rise in temperature at the end-points became small. It is difficult to change manganese(II) to the trivalent state with permanganate unless sufficient metaphosphoric acid is present as complexing agent; the amount of metaphosphoric acid should be more than 20 times greater than the Mn(III) formed, otherwise a dark precipitate of hydrous manganese dioxide, which does not react with As(III), is formed. The final concentration of metaphosphoric acid employed in this study exceeded that of Mn(III) by at least 60 times.

Calibration curves to give molar concentrations or micrograms of metal ion in the aliquots titrated (5.00 ml) were prepared for each metal in three

TABLE 1

Titration of silver nitrate with potassium iodide

KI titrant (M)	Ag taken (μg)	Ag found (μg)	Error (%)	C.v. (n = 5) (%)
1×10^{-4}	0.551	0.535	−2.9	3.0
	1.081	1.054	−2.5	3.0
	2.162	2.140	−1.0	2.7
	5.405	5.433	+0.5	1.1
1×10^{-3}	7.56	7.58	+0.3	1.0
	10.81	10.84	+0.3	1.0
	54.05	53.83	−0.4	1.1
1×10^{-2}	75.69	75.76	+0.1	0.6
	108.1	108.3	+0.2	0.6
	216.2	216.6	+0.2	0.5
	540.5	540.0	−0.1	0.5

TABLE 2

Titration of mercury(II) acetate with potassium iodide

KI titrant (M)	Hg taken (μg)	Hg found (μg)	Error (%)	C.v. (n = 5) (%)
1×10^{-4}	0.598	0.580	−3.0	3.0
	1.396	1.356	−2.9	3.0
	3.988	3.879	−2.7	2.8
1×10^{-3}	9.970	9.850	−1.2	1.7
	19.94	19.77	−0.9	1.4
	39.88	39.77	−0.3	0.8
1×10^{-2}	99.70	99.90	+0.2	0.3
	199.4	199.8	+0.2	0.4
	398.8	399.7	+0.2	0.3
	598.2	597.6	−0.1	0.3

ranges (10^{-3}—10^{-4} M, 10^{-4}—10^{-5} M and 10^{-5}—10^{-6} M) with three iodide standard solutions (10^{-2} M, 10^{-3} and 10^{-4} M, respectively). The plot of chart travel (or time taken) against molar concentrations or micrograms of metal gave a linear relationship in each case. The results for metal solutions of known concentrations (Tables 1—3) show that silver, mercury or palladium in the range 0.20—500 μg could be determined with relative errors and coefficient of variation of within 3%.

Lead(II), bismuth(III), and thallium(I) could not be determined, and their presence did not affect the results for silver, mercury, and palladium. Under the experimental conditions, the Mn(III)—As(III) reaction was catalysed by about 10^{-6} mol of chloride or bromide ion. In the presence of these ions the temperature change at the end-point was not sharp and

TABLE 3

Titration of palladium(II) sulfate with potassium iodide

KI titrant (M)	Pd taken (μg)	Pd found (μg)	Error (%)	C.v. (n = 5) (%)
1×10^{-4}	0.211	0.205	−2.8	3.0
	0.528	0.515	−2.6	3.0
	1.056	1.030	−2.5	2.9
	2.112	2.059	−2.5	2.4
1×10^{-3}	5.28	5.36	+1.5	1.8
	10.56	10.69	+1.2	1.2
	21.12	21.32	+0.9	1.1
1×10^{-2}	52.80	53.04	+0.5	0.5
	105.6	105.4	−0.2	0.5
	211.2	211.8	+0.3	0.4
	528.0	529.5	+0.3	0.4

results were low, but less than 10^{-6} mol did not interfere. With silver, equivalent concentrations of sulfide, cyanide, and thiosulfate did not interfere but an equivalent concentration of thiocyanate led to obscure end-points. Sulfide and thiosulfate interfered with the titration of mercury(II) and could be determined by adding a known excess of standard mercury(II) solution to the sample solution and back-titrating with standard iodide solution. The presence of an equivalent concentration of cyanide or thiocyanate also led to obscure end-points for the titration of mercury(II). Further, cyanide and thiocyanate, which interfered quantitatively with the titration of palladium, could be determined by adding a known excess of standard palladium solution to the sample solution and back-titrating with standard iodide solution. Equivalent concentrations of sulfide and thiosulfate did not interfere with the titration of palladium.

REFERENCES

1 K. B. Yatsimirski and T. I. Fedorova, Proc. Acad. Sci. USSR, 143 (1962) 143.
2 H. Weisz, All. Prak. Chem., 22 (1971) 98; H. Weisz and S. Pantel, Fresenius Z. Anal. Chem., 264 (1973) 389; H. A. Mottola, CRC Crit. Rev. Anal. Chem., (1975) 229; H. Weisz, Angew. Chem. Int. Ed. Eng., 15 (1976) 150; H. Müler and G. Werner, Z. Chem., Leipzig, 16 (1976) 304; H. P. Hadjiioannou, Rev. Anal. Chem., 3 (1976) 82; N. Kiba, M. Furusawa and T. Takeuchi, Kagaku no Ryoiki, 31 (1977) 14.
3 R. Lang, Z. Anorg. Allg. Chem., 152 (1926) 197.
4 I. M. Kolthoff and R. Belcher, Volumetric Analysis III, Interscience, N.Y., 1957, p. 43.
5 W. Boguth and W. Schaeg, Mikrochim. Acta, (1967) 658.
6 H. Weisz, T. Kiss and D. Klockow, Fresenius Z. Anal. Chem., 247 (1969) 248; K. C. Burton and H. M. N. H. Irving, Anal. Chim. Acta, 52 (1970) 441; T. P. Hadjiioannou, E. A. Piperaki and D. S. Papastathopoulos, Anal. Chim. Acta, 68 (1974) 447; T. P. Hadjiioannou and M. M. Timotheou, Mikrochim. Acta, (1977) 61; F. Gaal and L. Bjelica, Chem. Anal., 21 (1976) 227.
7 N. Kiba and T. Takeuchi, Talanta, 20 (1973) 875.

Analytica Chimica Acta, 98 (1978) 349—356

THE METAL-COMPLEXING PROPERTIES OF *N*-BENZOYL-*N*-PHENYLHYDROXYLAMINE DERIVATIVES CONTAINING *N*-PHENYL RING SUBSTITUENTS

F. VERNON* and H. D. GUNAWARDHANA

Department of Chemistry and Applied Chemistry University of Salford, Salford, Lancs. M5 4WT (Gt. Britain)

(Received 17th October 1977)

SUMMARY

The syntheses and chelating properties of a number of *N*-benzoyl-*N*-phenylhydroxylamine derivatives substituted in the *N*-phenyl ring have been investigated. The acid dissociation constants, selective precipitation, solvent extraction and spectrophotometric properties of a range of metal chelates are compared with those of the corresponding 3,5-dinitrobenzoylphenylhydroxylamines. The *N*-phenyl ring substituents have only small effects on reagent acidity. If the substituents are in the *ortho* position, considerable selectivity is found because of steric hindrance. The use of an *o*-chloro derivative as a selective precipitant for iron(III) in the presence of cobalt, nickel, copper and aluminium, is described.

N-Benzoyl-*N*-phenylhydroxylamine (BPHA) has two oxygen atoms as the donor atoms in the chelate ring and is a "hard base", thus forming complexes non-selectivity with all hard and border-line acids. Selectivity for metal ions is achieved by pH control and by the use of masking agents. Since Shome [1, 2] first described the preparation and chelate-forming properties of BPHA, many derivatives have been prepared and studied; Majumdar [3] has described the preparation and properties of many BPHA analogues. *N*-Benzoyl-*o*-tolylhydroxylamine [4] and *N*-acetylsalicyloylphenylhydroxylamine [5] have been claimed as very selective reagents for uranium and titanium, respectively, whilst, under different conditions, the *o*-tolyl derivative has been reported as a very selective reagent for vanadium [6] although a similar claim has been made for the *p*-chlorophenyl derivative [7]. Much work has been done on vanadium extraction by BPHA derivatives; Tandon and Gupta [8] have claimed *N*-*p*-methoxybenzoyl-*m*-tolylhydroxylamine as the most sensitive and highly selective spectrophotometric reagent for this element.

Most of the work done on BPHA derivatives has involved substitution in the *C*-phenyl ring. Ryan and Lutwick [9], in an extensive survey, suggested that investigation into the effects of substitution in the *N*-phenyl ring would be rewarding, as a substituent in this ring should have greater effect on the acidity of the reagent. Whilst *N*-phenyl ring derivatives such as *o*-tolyl [6], *m*-tolyl [8], *p*-tolyl and *o*- and *p*-methoxyphenyl [10] and *p*-chlorophenyl

[7] compounds have been reported, few systematic surveys of the chelating behaviour of BPHA substituted in the *N*-phenyl ring have been reported. In this investigation, emphasis is placed on the properties of the *o*- and *p*-substituted derivatives of the *N*-phenyl ring of BPHA and, for a comparison, the corresponding *N*-(3,5-dinitrobenzoyl)phenylhydroxylamine.

EXPERIMENTAL

Preparation of BPHA derivatives

Reduction of the nitro compound. The nitro compound (0.4 mol; nitrobenzene, *o*- or *p*-nitrotoluene, *o*- or *p*-chloronitrobenzene, *o*-nitroanisole, *p*-nitroacetophenone, methyl *p*-nitrobenzoate or dimethyl-4-nitrophthalate) was suspended in a solution of 25 g of ammonium chloride in 400 ml of water by vigorous stirring. The suspension was heated to 45° C and 59 g of zinc powder was added at such a rate that the temperature was maintained at 60—65° C. After the addition of zinc, the stirring was continued for a further 15 min, after which time the mixture was filtered to remove zinc oxide and then saturated with sodium chloride and cooled in an ice bath, when the substituted phenylhydroxylamine crystallized. The product was filtered and immediately acylated.

Acylation. The substituted phenylhydroxylamine and excess of sodium hydrogencarbonate were stirred with ether at 0° C, and benzoyl chloride in ether was added dropwise until the reaction mixture gave a negative result with Tollens reagent. The stirring and cooling were continued for a further 90 min, after which time the mixture was filtered and the ether evaporated to yield the crude product. The purification step was as described by Shome [1], involving dissolution of the product in ammonia and precipitation with sulphuric acid. The purified BPHA derivative was crystallized from ethanol. For the production of a 3,5-dinitrobenzoyl derivative, the hydroxylamine compound in ether was treated with a solution of 3,5-dinitrobenzoyl chloride, with a slight excess of pyridine being added to maintain neutrality. Purification and crystallization procedures were as given for the benzoyl derivatives.

Acid dissociation constants

Spectrophotometric method. The purified BPHA (0.1 g) derivative was dissolved in 250 ml of 40:60 ethanol—water. A portion (5 ml) of this solution, together with 25 ml of buffer, was diluted to 50 ml with water, and the spectrum of the solution was plotted over the range 200—400 nm against a buffer blank, Two convenient wavelengths were chosen on either side of the isosbestic point and, from plots of absorbance values against pH, two values for pK_a were obtained. The mean value was taken as the pK_a of the reagent. Unicam SP800 and SP500 spectrophotometers were used. The phosphate buffers were produced by adding phosphoric acid or sodium hydroxide to 5% disodium hydrogenphosphate solutions to give a pH range of 5—10.

Potentiometric method. Perchloric acid (3 ml of 0.1 M) and sodium perchlorate (2 ml of 0.1 M) were pipetted into the titration cell, and 145 ml of water was added, followed by a suitable weight of BPHA derivative dissolved in 50 ml of ethanol. After degassing with nitrogen, the solution was titrated with 0.1 M sodium hydroxide, a blank on the perchlorates, alcohol and water also being determined. The pH at the half-neutralization point of the reagent was taken as the pK_a value in 25:75 ethanol—water. A Corning-EEL pH meter with glass indicator and silver—silver chloride reference electrodes was used.

Precipitation of metal complexes

A weighed amount of the reagent (a fourfold excess over the metal ion) was dissolved in methanol and a 0.1 M metal ion solution, together with 35 ml of 0.1 M hydrochloric acid, were added. The mixture was titrated with 2 M sodium acetate and the pH at which turbidity appeared was noted. Where no turbidity occurred after 10 ml of sodium acetate had been added, 1 ml of 0.880 ammonia was added to produce a pH of around 10. If no turbidity was observed the particular metal—BPHA derivative combination was recorded as "no precipitate".

Gravimetric determination of iron(III) with N-benzoyl-(o-chlorophenylhydroxylamine)

A suitable aliquot of the acidified sample solution (containing 10—50 mg of iron) was diluted to 150 ml and heated to boiling. *N*-Benzoyl-(*o*-chlorophenylhydroxylamine)solution in ethanol (50 ml of 0.5% w/v) was then added followed by sufficient 25% sodium acetate solution to bring the pH to 3.5. The solution was heated at 60—70° C for 1 h, allowed to cool, filtered through a tared No. 4 sintered glass crucible, washed with 25% ethanol in pH 3.5 buffer and then with water, and finally dried to constant weight at 100°C. (1 mg $Fe(C_{13}H_9NO_2Cl)_3 \equiv 0.0702$ mg Fe.)

Spectrophotometry of metal complexes

A 0.002 M solution of the reagent in chloroform was prepared. Into a separating funnel were placed 5 ml of this solution, 1 ml of 0.1 M metal ion solution and 5 ml of pH 5.0 acetate buffer. After shaking and separation, the absorbance of the chloroform layer against the reagent blank was recorded over the range 300—700 nm. Unchanged chloroform extracts were re-extracted in the presence of ammonia at pH 9.0.

RESULTS AND DISCUSSION

In the reduction of nitro compounds by zinc and ammonium chloride, a major factor is the steric effect of any *ortho* substituent, which makes the reduction difficult or impossible to bring about, depending upon the size of the *ortho* group. Thus *o*-methyl, *o*-chloro and *o*-methoxyphenylhydroxyl-

amines were obtained in low yield, whilst attempts to reduce *o*-nitroacetophenone, methyl *o*-nitrobenzoate and nitromesitylene to the corresponding hydroxylamines were unsuccessful. Wepster [11] has stated that the methyl group in *o*-nitrotoluene causes considerable steric inhibition to resonance between the nitro group and the ring, and that the presence of a second methyl group, as in 2,6-dimethylnitrobenzene, gives complete suppression of the resonance effect. This explains why the bulkier *ortho* groups and the di-*ortho* substitution in nitromesitylene did not lead to reduction to substituted hydroxylamines because of the out-of-plane distortion of ring and nitro group caused by substituents.

Effect of substituent on reagent acidity

The apparent acid dissociation constants of BPHA and some of its derivatives are given in Table 1. The values obtained by spectrophotometric and potentiometric methods differ because of the nature of the solvent. The spectrophotometric method is very sensitive and enables pK_a values to be determined in what is essentially an aqueous solution whereas solubility effects in the potentiometric method require the use of mixed solvents (25 : 75 ethanol—water). The two compounds 10 and 11 in Table 1 did not show a great difference in absorbance for the protonated and unprotonated forms hence only the potentiometric pK_a values are given. Table 1 shows the increase in acidity when the electron-attracting nitro groups are introduced into the *C*-phenyl ring. The suggestion by Ryan and Lutwick [9] that substitution into the *N*-phenyl ring should have large effects on the acidity of

TABLE 1

Acid dissociation constants of BPHA derivatives

	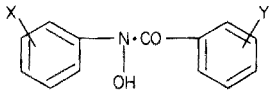 X	Y	pK_a Values: Spectrophotometric method	pK_a Values: Potentiometric method
1	H	H	8.35	9.60
2	*o*-CH_3	H	8.30	9.60
3	*p*-CH_3	H	8.40	9.80
4	*o*-Cl	H	8.10	9.40
5	*p*-Cl	H	8.09	9.55
6	*o*-OCH_3	H	8.50	
7	*p*-$COCH_3$	H	8.42	
8	*p*-$COOCH_3$	H	8.12	
9	H	3,5-$(NO_2)_2$	7.45	8.25
10	*p*-CH_3	3,5-$(NO_2)_2$		8.50
11	*p*-Cl	3,5-$(NO_2)_2$		8.15
12	*p*-$COCH_3$	3,5-$(NO_2)_2$	7.70	
13	*p*-$COOCH_3$	3,5-$(NO_2)_2$	7.68	

the reagents is seen to be not so. In fact, the most acidic compound prepared — *N*-3,5-dinitrobenzoyl-3,4-bis(carboxymethoxy)-phenylhydroxylamine — is not shown in Table 1 but was obtained by acylation of the product from reduction of dimethyl-4-nitrophthalate. With a spectrophotometric pK_a value of 7.10 compared with the value of 7.45 obtained for 3,5-dinitro-BPHA, it is obvious that two electron-attracting *N*-phenyl ring substituents have little effect. The potentiometrically determined pK_a values for several of the benzoyl derivatives given at the top of Table 1 are identical with values given by Majumdar and Das [12].

Precipitation of metal complexes

Table 2 gives the lowest pH values at which the various reagents precipitate with a selection of metal ions. It was found that, in general, a pH value 1.0 unit above that given in Table 2 was necessary for complete precipitation. Large effects caused by *ortho* substitution are apparent from Table 2: thus an *N*-*o*-tolyl derivative will precipitate copper, iron and nickel but not cobalt, whereas the *N*-*o*-chloro- and *N*-*o*-methoxy derivatives will precipitate copper and iron but neither cobalt nor nickel. Considering the performance of the various reagents with copper, which with BPHA forms a planar CuL_2 complex, it is apparent that steric hindrance to planarity — caused by an *ortho* substituent — plays a far more important rôle than does the acidity of the ligand. In the case of titanium complexes, which are precipitated from approximately 0.1 M acid solution regardless of ligand acidity, an *o*-methoxy substituent in the *N*-phenyl ring causes a large increase in precipitation pH to 5.6. It was also found that ligands 3—7 in Table 2 gave precipitates with molybdenum(VI) from 1 M acid. The *o*-methyl, *o*-chloro and *o*-methoxy derivatives also precipitated tungsten(VI) at pH 0.5, whereas the corresponding *para* derivatives did not form precipitates with tungsten(VI). This inhibiting effect of *p*-substituents with tungsten solutions has not so far been explained.

N-Benzoyl(*o*-chlorophenylhydroxylamine) was found to possess high

TABLE 2

The precipitation of metal complexes of BPHA derivatives, showing the lowest pH at which precipitation occurs. Positions X and Y are as in Table 1

	Substituents		Lowest pH for precipitation						
	X	Y	Co(II)	Cu(II)	Fe(II)	Fe(III)	Ni(II)	Ti(IV)	V(V)
1	H	H	5.0	3.0	4.1	2.8	5.0	1.2	No ppt
2	H	3,5-$(NO_2)_2$	5.7	3.9	1.9	1.9	6.2	0.7	0.7
3	*o*-CH_3	H	No ppt	5.3	4.3	2.6	8.4	1.0	1.9
4	*p*-CH_3	H	6.2	4.0	3.5	2.5	7.0	0.9	1.0
5	*o*-Cl	H	No ppt	5.6	3.5	2.5	No ppt	1.2	No ppt
6	*p*-Cl	H	6.0	3.2	2.4	1.9	5.9	0.5	0.3
7	*o*-OCH_3	H	No ppt	5.3	5.8	4.7	No ppt	5.6	No ppt
8	*p*-$COCH_3$	H	6.4	5.0	5.1	3.3	6.7	1.2	No ppt

selectivity for iron in the pH range 3.4—3.8. The precipitation procedure for iron, tested in the presence of 10-fold amounts of copper, cobalt and nickel and a 5-fold amount of aluminium, showed no interferences (Table 3). Two British Chemical Standards were analysed for iron by the method; a high-tensile brass (Fe 1.02%) gave values of 0.98, 1.00 and 1.01%, and an aluminium bronze (Fe 4.71%) gave values of 4.77, 4.75 and 4.74%.

Spectrophotometric properties of the metal complexes

Table 4 gives the spectrophotometric properties of the complexes of several ligands with the metals for which precipitation studies had been carried out. The molar absorptivities at the wavelengths of maximum absorption are given as a measure of the relative spectrophotometric sensitivities of the ligands. Some trends are apparent; thus the cobalt, copper, iron(III), vanadium and titanium complexes of the benzoyl reagents usually exhibit larger absorptivities than do the corresponding complexes of the 3,5-dinitrobenzoyl reagents. Iron(II) is unusual in this respect as the introduction of the nitro groups has very little effect, marginally enhancing the *p*-methyl derivative, having a large enhancing effect on the *p*-carboxy-methoxy derivative and the opposite effect on the *p*-chloro derivative. For all metals, the *o*-methyl complex provides a larger absorptivity than the *p*-methyl analogue.

Solvent extraction of iron and copper complexes

Percentage distribution curves as a function of pH were obtained for iron(III) and copper(II) with several of the ligands. The pH $_{\frac{1}{2}}$ values are given in Table 5. These values, the pH at which the complex is 50% extracted, are a measure of the relative complex stability constants and therefore of the separability of the two metals; obviously, a good iron—copper separation is not possible with any of the ligands. However, at low pH values the *o*-chloro derivative exhibited some selectivity for iron. At pH 3.5, copper is not extracted by this ligand in chloroform, whereas 20% of the iron(III) is extracted. The addition of ethanol enhanced the extractions: 25:75 alcohol —chloroform extracted no copper but 22% of the iron, whereas 40:60

TABLE 3

Percentage iron recoveries with *N*-benzoyl-(*o*-chlorophenylhydroxylamine) from solutions of various metal ions; 12.78 mg Fe was taken in each case

Ions present	pH of precipitation	Fe recovery (%)
1. 58 mg Co; 58 mg Ni; 5 mg Al	3.6	100.9
2. 12 mg Cu	3.5	98.9
3. 12 mg Cu	3.8	101.4
4. 127 mg Cu; 118 mg Co; 118 mg Ni; 54 mg Al	3.5	100.7 99.9 101.4

TABLE 4

Wavelengths of maximum absorption (λ_{nm}) and molar absorptivities (l mol^{-1} cm^{-1}) of metal complexes of BPHA derivatives. Positions X and Y are as in Table 1

Substituents			Co(II)		Cu(II)		Fe(II)		Fe(III)		Ti(IV)		V(V)	
	X	Y	λ	ϵ	λ	ϵ	λ	ϵ	λ	ϵ	λ	ϵ	λ	ϵ
1	H	H	—	—	335	714	440	900	450	1343	340	980	436	1430
2	*o*-CH_3	H	324	970	315	1856	442	1330	448	1486	328	1186	440	1730
3	*p*-CH_3	H	335	860	330	1050	448	1057	456	1371	346	700	440	1457
4	*p*-CH_3	3,5-$(NO_2)_2$	386	765	383	700	420	1114	430	1143	—	—	430	1000
5	*p*-Cl	H	342	900	338	870	444	1400	448	1570	352	486	434	1230
6	*p*-Cl	3,5-$(NO_2)_2$	393	720	378	690	436	1380	436	1440	382	85	380	810
7	*p*-$COOCH_3$	H	370	1143	346	650	436	535	446	580	352	330	436	565
8	*p*-$COOCH_3$	3,5-$(NO_2)_2$	384	690	379	410	430	800	430	870	380	175	383	680

TABLE 5

Solvent extraction data for iron(III) and copper(II) complexes of BPHA derivatives between aqueous solutions and chloroform. Positions X and Y are as in Table 1

	Substituents		$pH_{\frac{1}{2}}$ Values	
	X	Y	Iron(III) chelate	Copper(II) chelate
1	H	H	4.93	4.75
2	*o*-CH_3	H	5.25	4.85
3	*o*-Cl	H	5.50	5.20
4	*p*-Cl	H	4.90	4.65
5	*o*-OCH_3	H	5.60	4.92
6	*o*-CH_3	3,5-$(NO_2)_2$	4.85	5.00

alcohol—chloroform extracted 3% of the copper and 80% of the iron. Substitution of higher alcohols for the ethanol gave only a marginal further improvement in the selectivity for iron. There is, as yet, no explanation for this enhancement of extraction by alcohols, although the extracted species may be hydrogen-bonded to the alcohol molecules through the hydrophilic substituent on the chelate.

In conclusion, it is apparent that the effects on acidity and on spectrophotometric properties of the chelates are not large when BPHA is substituted in the *N*-phenyl ring. Spectrophotometric analysis will probably be limited to methods for iron and vanadium, as the other λ_{max} values lie in the ultraviolet. Selective precipitation techniques are certainly indicated with *o*-substituted reagents. As the results by solvent extraction show low selectivity, it is as precipitants that the *N*-phenyl-disubstituted BPHA derivatives show most promise.

REFERENCES

1 C. Shome, Analyst, 75 (1950) 27.
2 S. C. Shome, Anal. Chem., 23 (1951) 1187.
3 A. K. Majumdar, *N*-Benzoyl-*N*-phenylhydroxylamine and its Analogues, Pergamon Press, Oxford, 1972.
4 A. K. Majumdar, and M. K. Das, Anal. Chim. Acta, 50 (1970) 243.
5 C. P. Savariar and J. Joseph, Anal. Chim. Acta, 47 (1969) 347.
6 A. K. Majumdar and Gayatri Das, Anal. Chim. Acta, 31 (1964) 147.
7 A. K. Majumdar and Gayatri Das, J. Indian Chem. Soc., 42 (1965) 189.
8 S. G. Tandon and V. K. Gupta, Anal. Chim. Acta, 66 (1973) 39.
9 D. E. Ryan and G. D. Lutwick, Can. J. Chem., 32 (1954) 949.
10 T. Seshadri, J. Inorg. Nucl. Chem., 36 (1974) 519.
11 B. M. Wepster, in W. Klyne and P. B. De La Mare (Eds.), Progress of Stereochemistry, Vol. 2, Butterworths, London, 1958, p. 99.
12 A. K. Majumdar and Gayatri Das, Anal. Chim. Acta, 36 (1966) 454.

Analytica Chimica Acta, 98 (1978) 357—363

A STUDY OF 8-HYDROXYQUINOLINATES OF SOME TRIVALENT METAL IONS BY POTENTIOMETRY AND X-RAY PHOTOELECTRON SPECTROSCOPY

MICHAEL THOMPSON

Department of Chemistry, University of Toronto, 80 St. George Street, Toronto M5S 1A1, Ontario (Canada)

(Received 6th December 1977)

SUMMARY

The stability constants of aluminium(III), gallium(III), indium(III) and scandium(III) with 8-hydroxyquinoline and its 2-methyl derivative have been determined by potentiometric titration, with computation by the SCOGS program. In contrast to previous work, the results show that protonated species occur in several of the equilibria. The constants are discussed in terms of the nature of metal-to-ligand bonding in the complexes. X-ray photoelectron spectroscopy of the ligand coordinating atoms in the solid complexes confirms the significantly increased covalency of the gallium—oxygen bond compared to the same bond in the aluminium complex.

The chelating ligand 8-hydroxyquinoline (HQ) is an important analytical reagent for the Group IIIa and IIIb metals. It has been used extensively, and still features prominently, in separations of these metal ions by solvent extraction, as well as in spectrophotometric, spectrofluorimetric and other determinations. Therefore, it is not surprising that there have been many studies of the chemistry of these metal complexes. In particular, the debate concerning the nature of the aluminium(III)—2-methyl-8-hydroxyquinoline (HY) complex has become legendary [1]. Since the early measurements of the stability constants of the complexes of indium(III) and gallium(III) with HQ by solvent extraction methods [2—4], Corsini and co-workers [5, 6] have determined further values for the aluminium(III) and scandium(III) complexes of the parent ligand and its derivatives by potentiometric titration.

A study by far-infrared spectroscopy in chloroform solution indicated that the metal—oxygen bond in the aluminium(III) complex of HQ possesses a low degree of covalency [7]. This result was confirmed by proton magnetic resonance spectroscopy, which also indicated that the nitrogen atom of the ligand is co-ordinated to the metal atom [8].

The substantial increase in covalency of the gallium—oxygen bond over that of the corresponding aluminium and scandium bonds as evidenced by the He(I) photoelectron spectra of β-diketone complexes [9] prompted a study of this property in the 8-hydroxyquinolinates.

The present paper offers a re-evaluation of the solution equilibria for the Al(III), Ga(III), In(III) and Sc(III) 8-hydroxyquinolinates together with some x-ray photoelectron spectroscopic (x.p.s.) data on the solid complexes.

EXPERIMENTAL

Reagents

The perchlorates of Al(III), Ga(III), In(III) and Sc(III), obtained from commercial sources, were used without purification. Solutions of these salts (0.01 M) were standardized by both gravimetric and EDTA titrimetric procedures. 1,4-Dioxane was purified by refluxing over sodium for 24 h followed by fractional distillation. The hydrogen ion concentration of a 0.01 M solution of perchloric acid which contained sodium perchlorate (0.21 M) was determined titrimetrically with standard sodium hydroxide solution.

Apparatus

The potentiometric apparatus consisted of a Radiometer Model PHM 64 pH meter fitted with glass and calomel electrodes, titration cell, burettes, and constant-temperature water bath. The system was protected from CO_2.

Procedure

The potentiometric titrations of HQ and HY to obtain protonation constants, and in presence of Al(III), Ga(III), In(III) and Sc(III) to obtain formation constants, were carried out in the usual manner in 50% (v/v) aqueous 1,4-dioxane at ionic strength 0.1 and 25.0 ± 0.1°C, for metal-to-ligand ratios in the range 1:4 to 1:10. The Van Uitert and Haas parameter was 0.1 ± 0.01 and the pK_W value was 15.27. The constants were calculated by means of a modified version of the program SCOGS [10, 11]. The general procedure used in the computation of overall stability constants was to fix the values of the protonation constants and vary the models for solution equilibria involving the metal ions. To minimize the effects of hydrolysis data were deliberately taken from the acidic regions of the titration curves. Protonation constants are given as log K_{NH} or log K_{OH}. The overall stability constants of the metal chelates are given as log β_{pqn} for the species $M_pH_qL_n$ where M is Al(III), Ga(III), In(III) or Sc(III), and L is the 8-hydroxyquinoline-type anion (—q represents OH^-). Overall stability constants were not computed for the gallium(III)—HY system.

Metal chelates

The tris chelates of HQ with Al(III), Ga(III) and In(III) were prepared according to the procedures given by Hollingshead [12]. $Sc(Q)_3$, $Sc(Q)_3 \cdot H_2O$ and $Sc(Q)_3 \cdot QH$ were synthesized as reported earlier [13].

X-ray photoelectron spectroscopy

The C 1*s*, N 1*s* and O 1*s* binding energies of the solid metal 8-hydroxyquinolinates were measured by a McPherson ESCA36 x-ray photoelectron spectrometer with Mg K_α radiation. Generally the x.p. spectra were obtained from samples of the complexes pressed onto an aluminium backing plate. Background O 1*s* peaks from the Al support were carefully deconvoluted from the spectra. Several determinations of N 1*s* and O 1*s* binding energies were carried out with the C 1*s* signal as an internal standard.

RESULTS AND DISCUSSION

The $\beta_{1,01}$, $\beta_{1,02}$, and $\beta_{1,0,3}$ values for the Al(III)—HQ system were measured by Cassidy and Corsini [6] for comparison purposes with other HQ-based ligands. A similar computer model of the solution equilibria in the present work yielded the constants shown in Table 1. Initially, these data seem reasonable, but experience has shown that for a 'well-behaved' system the standard deviation in the titration value under the experimental conditions used in this work does not exceed approximately 1.0×10^{-2} ml. Furthermore, the second stepwise constant appears to be greater than the first. Inclusion of protonated species in the calculations gave the results for Al(III) shown in Table 2 where a somewhat better fit of titration data with the constants is achieved. These data emphasize the danger of using programs such as SCOGS without examination of the many possible equilibrium models for a particular set of data.

The overall constants for the HQ and HY complexes of Al(III), Ga(III), In(III) and Sc(III) obtained after an exhaustive study of possible equilibria are shown in Tables 2 and 3. Because of the high stability of the Ga(III) complex with HQ, the value for $\beta_{1,0,1}$ for this system is an estimate. The values for the Sc(III)—HY system can at best be regarded as approximate. Protonated species appear to be particularly prevalent in the equilibria involving Al(III), although they do occur in other instances. The value of the

TABLE 1

Overall stability constants for the Al(III)—HQ system including only metal and ligand anion in complex species (25° C, ionic strength 0.1, 50% (w/w) 1,4-dioxane[a]

Constant	Value found	SCOGS[b] σ
$\beta_{1,0,1}$	11.17	0.03
$\beta_{1,0,2}$	22.59	0.01
$\beta_{1,0,3}$	32.74	0.02

[a]HQ: $\log K_{NH} = 4.18$, $\log K_{OH} = 11.00$. [b]Standard deviation in titration value = 2.22×10^{-2} ml.

TABLE 2

Overall stability constants of 8-hydroxyquinoline complexes (25° C, ionic strength 0.1, 50% (v/v) 1,4-dioxane[a]

Metal ion	Constant	Value found	SCOGS σ	Standard deviation in titration value (ml)
Al(III)	$\beta_{1,1,1}$	14.56	0.02	5.07×10^{-3}
	$\beta_{1,1,2}$	25.73	0.03	
	$\beta_{1,0,2}$	22.53	0.02	
	$\beta_{1,0,3}$	33.08	0.01	
Ga(III)[b]	$\beta_{1,0,1}$	15.6	—	1.83×10^{-2}
	$\beta_{1,0,2}$	29.0	0.02	
	$\beta_{1,0,3}$	41.6	0.01	
In(III)	$\beta_{1,0,1}$	13.30	0.01	9.80×10^{-3}
	$\beta_{1,0,2}$	25.46	0.01	
	$\beta_{1,0,3}$	36.43	0.02	
Sc(III)	$\beta_{1,0,1}$	11.27	0.01	9.66×10^{-3}
	$\beta_{1,0,2}$	20.88	0.01	
	$\beta_{1,0,3}$	28.93	0.01	

[a]HQ: log K_{NH} = 4.18, log K_{OH} = 11.00. [b]$\beta_{1,0,1}$ for the Ga(III)—HQ complex is an estimate.

$\beta_{1,1,2}$ constant compared to that for $\beta_{1,0,2}$ for the Al(III)—HQ system implies that the site of protonation is the nitrogen atom. Undoubtedly, this result is associated with a balance of factors, viz., the affinity of a metal ion for the nitrogen atom compared to the proton, and the hydrogen ion concentration in the range where, for example, 1:1 and 1:2 M:L complexes occur

TABLE 3

Overall stability constants of 2-methyl-8-hydroxyquinoline complexes (25° C, ionic strength 0.1, 50% 1,4-dioxane)[a]

Metal ion	Constant	Value found	SCOGS σ	Standard deviation in titration value (ml)
Al(III)	$\beta_{1,1,1}$	15.08	0.02	8.56×10^{-3}
	$\beta_{1,1,2}$	25.24	0.02	
	$\beta_{1,0,2}$	20.52	0.04	
	$\beta_{1,0,3}$	30.53	0.01	
In(III)	$\beta_{1,2,2}$	32.00	0.08	1.29×10^{-2}
	$\beta_{1,0,2}$	25.97	0.05	
	$\beta_{1,-1,2}$	20.74	0.01	
Sc(III)	$\beta_{1,0,1}$	11.2	0.04	2.02×10^{-2}
	$\beta_{1,0,2}$	19.8	0.1	
	$\beta_{1,0,3}$	28.3	0.1	

[a]Log K_{NH} = 4.78, log K_{OH} = 11.44.

(and therefore the strength of the metal—oxygen interaction). The fractional degree of complexation, α, for two examples each of HQ and HY equilibria are shown in Figs. 1 and 2. Another factor contributing to the occurrence of protonated complex species could well be additional stability arising from intra-molecular hydrogen bonding. This effect is known to be important in the formation of solid 'adducts' such as UO_2 $(Q)_2 \cdot QH$ [14], Th $(Q)_4 \cdot QH$ [15] and Sc $(Q)_3 \cdot QH$ [13]. With regard to the uranium(VI) 'adduct', Hall et al. [16] have shown by x-ray crystallography that the additional ligand is coordinated through the oxygen atom and that the proton is probably situated on the nitrogen atom and hydrogen-bonded to a neighbouring ligand.

The $\beta_{1,0,2}$ values of Tables 1 and 2 show that the stabilities of the 8-hydroxyquinolinates lie in the order Ga>In>Al>Sc. To discuss this result in terms of metal-to-ligand bonding, it is instructive to use the equation developed by Steger and Corsini [5] for the relationship between stability constant and ligand basicity. Study of the complexes formed between some 8-hydroxyquinoline derivatives and various metal ions resulted in the expression:

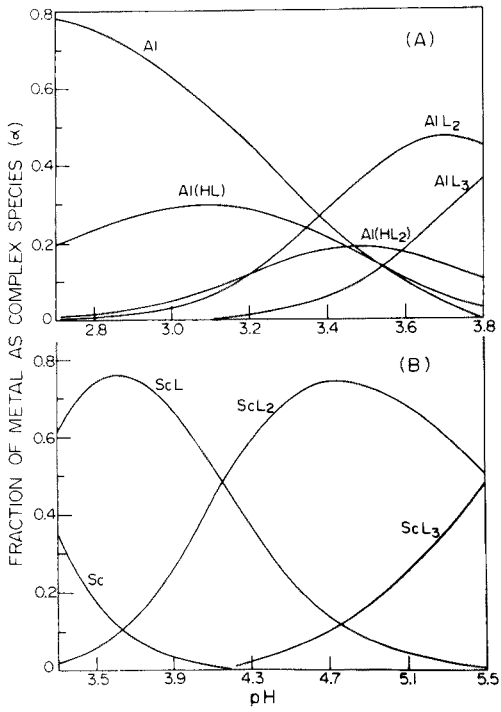

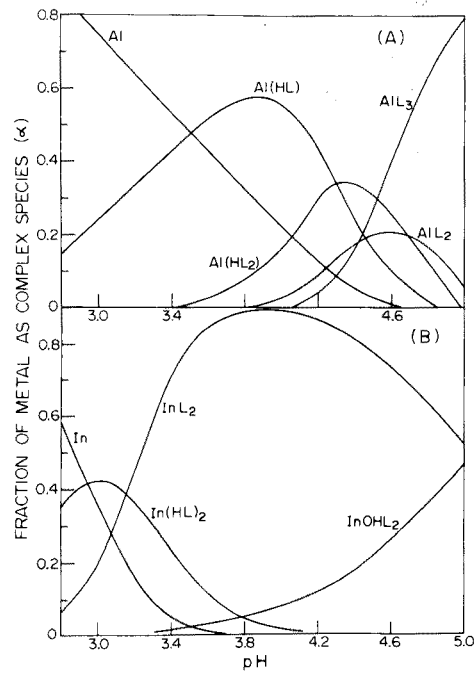

Fig. 1. (left) Fractional degree of complex formation (α) of 8-hydroxyquinoline complexes of (A) Al(III) and (B) Sc(III), as a function of pH.

Fig. 2. (right) Fractional degree of complex formation (α) of 2-methyl-8-hydroxyquinoline complexes of (A) Al(III) and (B) In(III) as a function of pH.

$$\log \beta_{ave} = m(0.177 \log K_{NH} + 0.123 \log K_{OH}) + b$$

where $\log \beta_{ave} = \frac{1}{3} \log \beta_{1,0,3}$ and m should equal the value of z/r (the ionic potential) for the metal ion in cases where bonding is predominantly electrostatic. Unfortunately, the parameter b was not interpreted; however, if this term is set at 0, at least some trends in the values of m calculated from the data of this work can be observed (Table 4). The substantially greater values of m for both the Ga(III) and In(III) systems compared to z/r indicate that the metal—oxygen bond in the HQ complexes of these metals is appreciably covalent, whereas in the case of Al(III) and Sc(III) the overall bonding must be predominantly electrostatic. It is not surprising, therefore, that the stability order shown in Tables 2 and 3 mirrors the electronegativity values for the elements although, obviously, such correlations should be treated with caution. Ultraviolet photoelectron spectroscopy of $M(HFA)_3$, where M is Al, Ga or Sc and HFA is hexafluoroacetylacetonate, has confirmed the significant increase in covalency in the gallium(III) metal—oxygen bonds of the complexes over those of aluminium(III) and scandium(III) [9].

An attempt was made to monitor the charge distribution at the coordinating atoms of the ligand by x.p.s. measurement of N 1*s* and O 1*s* binding energies of the solid chelates. The C 1*s* signal in the free ligand and the complexes should be very similar; therefore, this binding energy (284.6 eV) was used as an internal standard for the measurements (Table 5). As found for the U(VI) chelate of HQ [18], the slightly higher N 1*s* binding energies for the complexes compared to the corresponding value for the free ligand indicates transfer of some electron density from nitrogen to the metal atoms. The values for the series of compounds are too close to attach any significance to them in terms of metal-to-nitrogen bonding, but the similarity of the results for the three scandium compounds may reflect the reasonable accuracy of the calibration procedure. There was no evidence in the N 1*s* spectrum of $Sc(Q)_3 \cdot QH$ of the presence of a level corresponding to the $\overset{+}{N}$—H . . . . . O hydrogen bond, but it is possible that the expected peak [18] may be masked by the scandium $2p_{3/2}$ line which occurs at 401.9 eV. The O 1*s* binding energies of the ligands in the complexes are, with the single exception of the Ga(III) compound, lower than in the free ligand. This suggests that the

TABLE 4

Comparison of m values with z/r for complexes of HQ from $\log \beta_{ave} = m\,(0.177 \log K_{NH} + 0.123 \log K_{OH}) + b$ [5]

Metal ion	$\log \beta_{ave}$	m	z/r [17]
Al(III)	11.03	5.27	5.88
Ga(III)	13.9	6.64	4.84
In(III)	12.14	5.80	3.70
Sc(III)	9.64	4.60	4.21

TABLE 5

Binding energies of metal—8-hydroxyquinolates (eV) referenced to C 1*s* of HQ at 284.6 eV

Compound	N 1*s*	*O* 1*s*	Compound	N 1*s*	*O* 1*s*
HQ	398.5	532.2	$Sc(Q)_3$	399.0	531.3
$Al(Q)_3$	399.4	531.5	$Sc(Q)_3 \cdot H_2O$	399.2	531.2
$Ga(Q)_3$	399.1	532.4			533.0
$In(Q)_3$	399.5	531.8	$Sc(Q)_3 \cdot QH$	399.1	531.2

oxygen atoms of the former possess greater anionic character than the latter. Furthermore, the O 1*s* levels are in the order Ga>In>Al>Sc, which is the same as that shown by the stability measurements, thus confirming the significant covalent character of the gallium—oxygen bond. The O 1*s* level of the H_2O component of $Sc(Q)_3 \cdot H_2O$ is clearly distinguishable at the expected value of 533.0 eV.

Partial support for this work by the National Research Council of Canada is gratefully acknowledged.

REFERENCES

1 See A. Corsini, M. Thompson and D. Fowler, Anal. Chim. Acta, 86 (1976) 237.
2 A. P. Savostin, Zh. Neorg. Khim., 10 (1965) 2565.
3 Yu. A. Zolotov and V. G. Lambrev, Zh. Anal. Khim., 20 (1965) 1153.
4 G. K. Schweitzer and M. M. Anderson, J. Inorg. Nucl. Chem., 30 (1968) 1051.
5 H. F. Steger and A. Corsini, J. Inorg. Nucl. Chem., 35 (1973) 1621.
6 R. M. Cassidy and A. Corsini, Talanta, 21 (1974) 273.
7 R. Larson and O. Eskilsson, Acta Chem. Scand., 22 (1968) 1067.
8 B. C. Baker and D. T. Sawyer, Anal. Chem., 40 (1968) 1945.
9 S. Evans, A. Hamnett, A. F. Orchard and D. R. Lloyd, Faraday Disc. Chem. Soc., 54 (1972) 227.
10 I. G. Sayce, Talanta, 15 (1968) 1397; 18 (1971) 653.
11 I. G. Sayce and V. S. Sharma, Talanta, 19 (1972) 831.
12 R. G. W. Hollingshead, Oxine and Its Derivatives, Butterworths, London, 1954—56.
13 A. Corsini, M. Thompson and F. Toneguzzo, Can. J. Chem., 51 (1973) 1248.
14 A. Corsini, J. Abraham and M. Thompson, Talanta, 18 (1971) 481.
15 A. Corsini and J. Abraham, Anal. Chem., 42 (1970) 1528.
16 D. Hall, A. D. Rae and T. N. Waters, Acta Crystallogr., 22 (1967) 258.
17 D. D. Perrin, Organic Complexing Agents, Interscience, N.Y., 1964.
18 D. B. Adams, D. T. Clark, A. D. Baker and M. Thompson, Chem. Commun., (1971) 1600.

Analytica Chimica Acta, 98 (1978) 365—371

THE THERMAL DECOMPOSITION OF THE EXTRACTED COMPLEXES FORMED BY VANADYL CHLORIDE WITH TRI-n-OCTYLAMINE AND TRICAPRYLMETHYLAMMONIUM CHLORIDE

TAICHI SATO*, TAKATO NAKAMURA and HIROSHI WATANABE

Department of Applied Chemistry, Faculty of Engineering, Shizuoka University, Hamamatsu (Japan)

(Received 4th January 1978)

SUMMARY

The complexes, $(R_3NHVO(OH)Cl_2)_2$ and $(R_3R'NVO(OH)Cl_2)_2$, prepared by drying in vacuo the organic solutions from the extraction of aqueous vanadyl chloride solution with tri-n-octylamine (R_3N) and tricaprylmethylammonium chloride ($R_3R'NCl$) in benzene have been examined by thermogravimetric and differential thermal analyses, and the complexes and their thermally decomposed products by x-ray diffraction, visible-u.v. and i.r. spectrophotometry, and e.s.r. spectroscopy. The thermal decomposition of the complexes proceeds in the sequences: $(R_3NHVO(OH)Cl_2)_2 \rightarrow R_3NHVO(OH)Cl_2 \rightarrow VO(OH)Cl + V_2O_3 \rightarrow V_2O_5$ and $(R_3R'NVO(OH)Cl_2)_2 \rightarrow R_3R'NVO(OH)Cl_2 \rightarrow VO(OH)Cl + V_2O_3 \rightarrow V_2O_5 + V_2O_3 \rightarrow V_2O_5$. The structures of the complexes are discussed on the basis of the results obtained.

Previous papers [1] have reported that the complexes formed in the extraction of vanadium(IV) from hydrochloric acid solutions by tri-n-octylamine (R_3N, TOA) and tricaprylmethylammonium chloride ($R_3R'NCl$, Aliquat-336) have distorted octahedral structures with the stoichiometric composition $(R_3NHVO(OH)Cl_2)_2$ and $(R_3R'NVO(OH)Cl_2)_2$, respectively. To obtain further information on the composition of the metal complexes formed in the solvent extraction system, the thermal decomposition of the sulphato and nitrato complexes of uranium(V) [2] and of the chloro complexes of copper(II), zirconium(IV) and uranium(VI) with long-chain aliphatic amines have been investigated [3]. The present paper extends the work to the chloro complexes of vanadium(IV) with TOA and Aliquat-336.

EXPERIMENTAL

Chemicals

Tri-n-octylamine (Kao Soap Co. Ltd., used without purification) and tricaprylmethylammonium chloride (General Mills, purified by washing several times with aqueous sodium chloride solution and n-hexane [4]) were diluted with benzene. A 0.1 M solution of vanadium(IV) was prepared by dissolving vanadyl chloride in 0.06 M hydrochloric acid. Other chemicals were of analytical-reagent grade.

Preparation and analysis of complexes

On the basis of the distribution results, the organic solutions saturated with vanadium were prepared as follows: 0.05 M TOA or 0.082 M Aliquat-336 in benzene was shaken for 10 min with the aqueous solution of 0.1 M vanadyl chloride in 0.06 M hydrochloric acid containing 9.8 M lithium chloride at 20°C; the phases were separated by centrifugation and again equilibrated with a fresh aqueous solution; this procedure was repeated twelve times. The organic solutions so obtained were heated in vacuo at 50—60°C to remove benzene. For chemical analysis, the resulting materials were dissolved in benzene, and the chloride and water in portions of the solution were determined by Volhard and Karl Fischer titrations. The benzene solutions were then washed with 1 M nitric acid, and vanadium in the acidic layers was determined by EDTA with xylenol orange as indicator [5, 6].

The complexes obtained were examined by thermogravimetric and differential thermal analyses (t.g.a. and d.t.a.), and the complexes and their thermally decomposed products by i.r., x-ray diffraction, e.s.r. [1, 2, 7, 8]. For t.g.a. and d.t.a. the heating rate was 5°C min^{-1}. The thermal decomposition products were prepared by heating the sample at the temperature as stated for 1 h after heating at a rate of 5°C min^{-1}, on the basis of the results of thermal analysis.

RESULTS AND DISCUSSION

The d.t.a. curves for the vanadyl complexes (Fig. 1a) exhibit three endothermic peaks at 290, 340 and 400°C with TOA and at 255, 300 and 365°C with Aliquat-336. These endothermic peaks occur at points near the change of shape in the t.g.a. curves (Fig. 1b). In the i.r. spectrum of the vanadyl

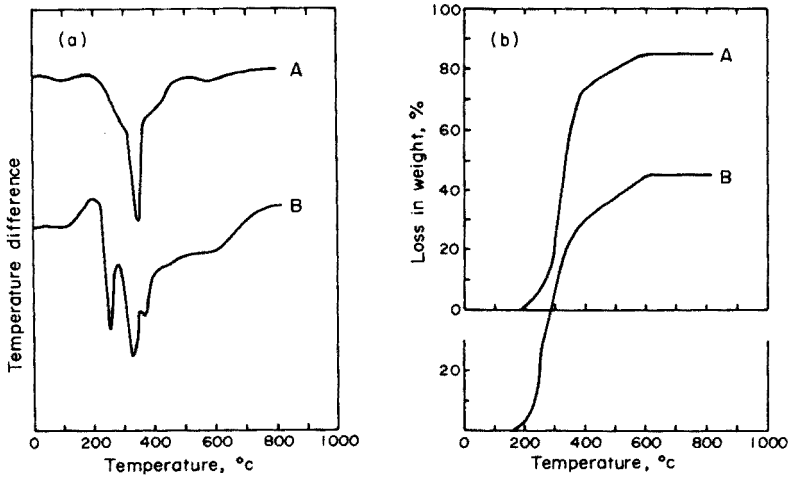

Fig. 1. D.t.a. curves (a) and t.g.a. curves (b) of the vanadyl complexes with A, TOA; B, Aliquat-336.

complex with TOA (Fig. 2a), the absorption assigned to the stretching frequency of the vanadyl group [5, 9] appears at 1005, 970, 954 and 935 cm^{-1} as a quartet band, indicating a lowering in the symmetry; the NH^+ stretching vibration at 2350 cm^{-1} in TOA hydrochloride shifts to 3000 cm^{-1} and the V—Cl stretching vibration appears at 430 cm^{-1}, confirming the formation of the chloro complex; the absorption of the OH stretching band appears at 3400 cm^{-1} and the OH bending bands at 1735 and 1620 cm^{-1}, implying the presence of the hydrolyzed species. When the complex is heated at 150°C, the V—O stretching vibration appears at 1000 cm^{-1}, and simultaneously the vanadyl group absorptions at 1005, 970, 954 and 935 cm^{-1} decrease in intensity; in addition, the NH^+ stretching band at 3000 cm^{-1} shifts to lower frequency at 2640 cm^{-1}. This is considered to result from dissociation of the dimeric complex, corresponding to the t.g.a. curve which exhibits the loss in weight. On heating at 200°C, the following changes are observed: the NH^+ band and the V=O absorptions at 970, 954 and 935 cm^{-1} disappear; the C—H stretching bands at 2920 and 2860 cm^{-1} and the CH_3 degenerate (and CH_2 scissoring) and symmetrical bending modes at 1465 and 1380 cm^{-1} decrease in intensity; a broad band centered around 1600 cm^{-1}, assigned to C=C and/or C=O bands, indicating the formation of an alkene and/or a carbonyl compound, appears; the V—Cl stretching band at 430 cm^{-1} decreases in intensity, and a band at 520 cm^{-1} appears. The increased intensity of the OH stretching vibration may be caused by the water molecule which enters a vacant site arising from the dissociation of the dimeric complex. These bands persist on heating at 300°C, but the bands due to TOA disappear at 350°C. Heating above 400°C produces absorptions at 1025, 850, 595, 395 and 280 cm^{-1} because of the formation of V_2O_5 [10].

In contrast, the vanadyl complex with Aliquat-336 (Fig. 2b) gives an i.r. spectrum similar to the complex with TOA. However, since the splitting in

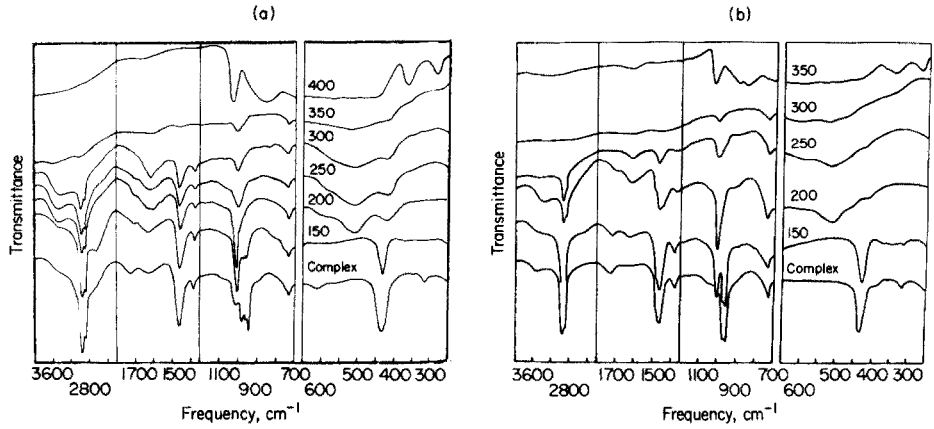

Fig. 2. Infrared spectra of the materials derived from the vanadyl complex with (a) TOA, (b) Aliquat-336 by heating to the stated temperatures (numbers on curves are heating temperatures, °C).

the V=O stretching bands at 968 and 955 cm^{-1} is less than that for the TOA complex, it is inferred that the symmetry of the latter is lower than that with Aliquat-336. The changes in the spectra of the thermally decomposed products from the Aliquat-336 complex are almost the same as those from the TOA complex, except that the absorptions caused by Aliquat-336 disappear at 300°C and the formation of V_2O_5 bands is observed at 350°C.

In the t.g.a. curves, weight losses of 23, 75, and 86% are observed on heating the vanadyl complex with TOA at 250, 400 and 600°C, respectively, and of 29, 71 and 85% with the Aliquat-336 complex at 300, 400 and 600°C, respectively, but a marked weight-loss at above 600°C is not shown by these complexes. The molar ratios, [Cl]/[V], in the thermally decomposed products obtained by heating the TOA complex at 300°C and that with Aliquat-336 at 250°C indicate values at 0.8 and 0.9, respectively (Table 1). The i.r. absorptions of TOA and Aliquat-336 decrease remarkably in intensity at the respective temperatures, while the OH bands become more intense. Accordingly, a compound such as VO(OH)Cl may be formed when some chlorine is removed by the thermal decomposition of the vanadyl complexes. In addition, the d.t.a. curve for the TOA hydrochloride reveals peaks at 285 and 335°C, arising from the formation of hydrocarbon by the cracking of the amine hydrochloride and carbonization [3].

The following interpretation may be given for the three endothermic reactions in the d.t.a. curves. The first is due to release of part of the co-ordinated chlorine; the second to thermal decomposition of the amines followed by carbonization; and the third to the removal of the remaining

TABLE 1

The composition of the products derived from the vanadyl complexes with TOA and Aliquat-336 by heating to the stated temperatures

Complex	Temp. (°C)	Loss in weight (%)	Molar ratio [Cl]/[V]
$R_3NHVO(OH)Cl_2$	100	0	2
	290	18	
	300	23	0.8
	360	69	
	400	75	0
	410	77	
	600	86	
$R_3R'NVO(OH)Cl_2$	100	0	2
	200	5	
	235	20	
	250	29	0.9
	300	48	
	330	63	
	350	67	0.1
	400	71	0
	600	85	

chlorine. It is evident that the vanadyl complex with TOA is more stable thermally than that with Aliquat-336. In the x-ray diffraction results (Table 2), the thermally decomposed products reveal the characteristic pattern of V_2O_3 at 300°C, although their diffraction lines are weak and broad, and the diffraction pattern of V_2O_5 at 400°C. At 350°C, however, the product derived from the complex with TOA shows the pattern characteristic of V_2O_3, while that with Aliquat-336 shows that of a mixture of V_2O_5 and V_2O_3.

The electronic spectra (Fig. 3a, b) indicate absorption bands at 12300 and 10600 cm^{-1} for the complex with TOA, and at 12200 and 10400 cm^{-1} for the complex with Aliquat-336, assigned to the transitions $^2B_2 \rightarrow {}^2B_1$ and $^2B_2 \rightarrow {}^2E(I)$, respectively. These bands are little influenced by heating at 150°C. This suggests that the crystal field effect around the vanadium(IV) ion still remains on heating, although the change in the V=O absorption bands is observed to a slight extent in the i.r. spectrum. In the e.s.r. results

TABLE 2

X-ray diffraction results of the products derived from the vanadyl complexes with TOA and Aliquat-336 by heating to the stated temperatures

Temperature (°C)	Phase detected	
	$R_3NHVO(OH)Cl_2$	$R_3R'NVO(OH)Cl_2$
200	Am[a]	Am
250	Am	Am
300	V_2O_3	V_2O_3
350	V_2O_3	$V_2O_5 + V_2O_3$
400	V_2O_5	V_2O_5
500	V_2O_5	V_2O_5
600	V_2O_5	V_2O_5

[a]Am indicates amorphous type.

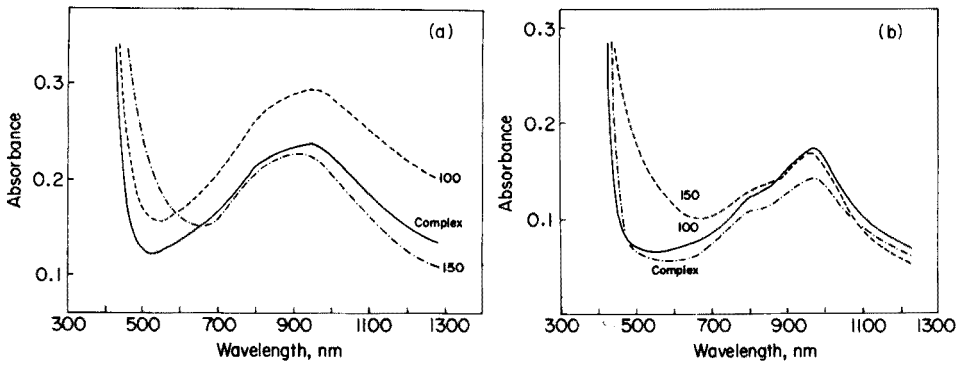

Fig. 3. Visible spectra of the materials derived from the vanadyl complex with (a) TOA, (b) Aliquat-336 by heating to the stated temperatures (numbers on curves are heating temperatures, °C).

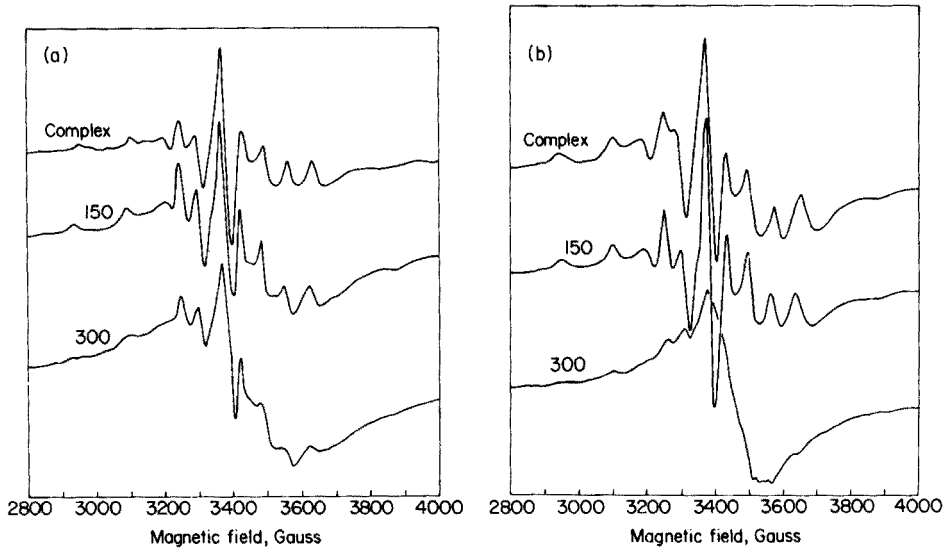

Fig. 4. E.s.r. spectra of the materials derived from the vanadyl complex with (a) TOA, (b) Aliquat-336 by heating to the stated temperatures (numbers on curves are heating temperatures, °C).

(Fig. 4a, b), the values of resonance parameters [10] are little influenced by heating at 150°C, in agreement with the electronic spectral results. At 200—300°C, the intensity of hyperfine lines decreases with increased heating temperature, because the internuclear V—V distance is reduced by cracking of the amines. In this case, however, as the position of the hyperfine lines does not change, it is deduced that the ligand field environment around the vanadium(IV) ion is constant, i.e. the conformation of the original species, VO(OH)Cl, is held during the thermal decomposition of the amines.

It is concluded that the thermal decomposition of the vanadyl complexes with TOA and Aliquat-336 proceeds in the sequences:

$$(R_3NHVO(OH)Cl_2)_2 \xrightarrow[\text{dissociation}]{150^\circ C} R_3NHVO(OH)Cl_2 \xrightarrow[\text{cracking}]{200-300^\circ C} VO(OH)Cl + V_2O_3 \xrightarrow{400^\circ C} V_2O_5$$

and

$$(R_3R'NVO(OH)Cl_2)_2 \xrightarrow[\text{dissociation}]{150^\circ C} R_3R'NVO(OH)Cl_2 \xrightarrow[\text{cracking}]{200-300^\circ C} VO(OH)Cl + V_2O_3 \xrightarrow{400^\circ C} V_2O_5$$

Accordingly if those complexes are assumed to have a point group C_{4v} symmetry, the proposed structures are supported on the basis of the results obtained.

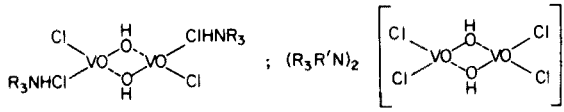

(I) (II)

We thank Mr. O. Terao for assistance with part of the experimental work, and the Kao Soap Co., Ltd. for a sample of TOA.

REFERENCES

1 T. Sato, S. Ikoma and T. Nakamura, J. Inorg. Nucl. Chem., 39 (1977) 395; T. Sato, T. Nakamura and O. Terao, J. Inorg. Nucl. Chem., 39 (1977) 401.
2 T. Sato, J. Inorg. Nucl. Chem., 26 (1964) 2229; 27 (1965) 240.
3 T. Sato and K. Adachi, J. Inorg. Nucl. Chem., 31 (1969) 1395; T. Sato and H. Watanabe, Anal. Chim. Acta, 54 (1971) 439; T. Sato, Anal. Chim. Acta, 77 (1975) 344.
4 T. Sato and H. Watanabe, Anal. Chim. Acta, 49 (1970) 463.
5 T. Sato and T. Takeda, J. Inorg. Nucl. Chem., 32 (1970) 3387.
6 J. Kinnumen and B. Wennerstrand, Chemist-Analyst, 46 (1957) 92.
7 T. Sato, T. Yamashita and F. Ozawa, Z. Anorg. Allg. Chem., 370 (1969) 202.
8 T. Sato, Z. Anorg. Allg. Chem., 376 (1970) 205.
9 E.g., P. A. Kiltz and D. Nicholls, J. Chem. Soc. A, (1966) 1175; J. Selbin, L. H. Holmes, Jr. and S. P. McGlynn, J. Inorg. Nucl. Chem., 25 (1963) 1359; D. N. Sathyanarayana and C. C. Patel, J. Inorg. Nucl. Chem., 30 (1968) 207.
10 J. R. Ferraro, Low-Frequency Vibrations of Inorganic and Coordination Compounds, Plenum Press, New York, 1971, p. 74.

Analytica Chimica Acta, 98 (1978) 373—383

A GRAVIMETRIC METHOD FOR THE DETERMINATION OF OXYGEN IN URANIUM OXIDES AND TERNARY URANIUM OXIDES BY ADDITION OF ALKALINE EARTH COMPOUNDS

TAKEO FUJINO*, HIROAKI TAGAWA, TAKEO ADACHI and HIROSHI HASHITANI

Chemistry Division, Japan Atomic Energy Research Institute, Tokai-mura, Ibaraki-ken (Japan)

(Received 5th December 1977)

SUMMARY

A simple gravimetric determination of oxygen in uranium oxides and ternary uranium oxides is described. In alkaline earth uranates which are formed by heating in air at 800—1100°C, uranium is in the hexavalent state over certain continuous ranges of alkaline earth-to-uranium ratios. Thus, if an alkaline earth uranate or a compound containing an alkaline earth element, e.g. MgO, is mixed with the oxide sample and heated in air under suitable conditions, oxygen can be determined from the weight change before and after the reaction. The standard deviation of the O:U ratio for a UO_{2+x} test sample is ±0.0008—0.001, if a correction is applied for atmospheric moisture absorbed during mixing.

Uranium oxides and oxides containing uranium and another metal (ternary oxides) are frequently non-stoichiometric with respect to oxygen; it is well known that the physicochemical properties of these compounds vary significantly with the degree of the non-stoichiometry. Precision and accuracy are therefore required in the determination of the oxygen-to-metal atom ratio of such oxides. Many methods have been proposed, but only a few are currently used [1]. They can be classified as wet chemical methods and dry methods. The wet chemical methods involve the determination of U(IV) and U(VI) by means of titration [2], coulometry [3] or polarography [4] after dissolution of the samples in a non-oxidizing medium such as phosphoric acid. Such methods can be applied to ternary oxides as well as uranium oxides. However, prevention of atmospheric oxidation of U(IV) and technical expertise are essential for satisfactory analyses. The precision of the redox titration methods with Cr(VI) or Ce(IV), which seem to be most widely used, is said to be good. Dharwadkar and Chandrasekharaiah [2] claimed a standard deviation of ±0.003 in O:U ratios for samples of $UO_{2.02}$ to U_3O_8, by adopting back-titration techniques; however, in routine use the deviations are usually of the order of ±0.01—0.02 [5].

The most frequently used dry methods for analyzing uranium oxides are the thermogravimetric techniques, in which the weight changes involved in the oxidation or reduction of the samples to a known O:U ratio (U_3O_8 or

UO_2) are measured. If uranium oxides are heated in air at 700—900°C, U_3O_8 is formed, but the compound has rather a wide range of non-stoichiometry, $U_3O_{8\pm x}$, where x may vary with history, amount and heating conditions of the samples [6, 7]. The problem of non-stoichiometry can be overcome practically by using UO_2 as reference material: $UO_{2.000}$ is obtained by heating in a mixture (10:1) of CO and CO_2 at 800—850°C or in hydrogen at 1150°C [8]. These dry methods are not applicable to the ternary uranium oxides because of the lack of standard compositions. The method of determining the O:U ratio through the lattice constant obtained by x-ray diffraction is useful, but is restricted to UO_{2+x} as a single phase. Other methods such as the solid galvanic cell, gas equilibration, mass spectrometry and electrical conductivity are not generally applied on account of experimental difficulties.

The present paper reports a simple thermogravimetric method which consists of heating a mixture of the oxide samples with alkaline earth compounds in air. The method can be used for the determination of oxygen not only in uranium oxides but also in ternary oxides, with a standard deviation of ±0.001.

PRINCIPLES OF THE METHOD

Alkaline earth uranates are known to be formed if carbonates, nitrates, chlorides, etc. of alkaline earth metals are mixed with calculated amounts of U_3O_8 or UO_2 and then the mixtures are heated in air at 800—1100°C [9]. Table 1 shows the main compounds formed; the ratio of alkaline earth metal to uranium atoms varies from 1:4 to 3:1 except for magnesium uranates. The characteristic of these uranates is that the formal valency of uranium* in the compounds is +6. The effect of adding alkali metal ions and/or alkaline earth metal ions to uranium oxides is to increase greatly the stability of U(VI) in the compounds; for comparison, the mean valency of uranium in U_3O_8 which is stable in air at 700—900°C is 5.333.

TABLE 1

Alkaline earth uranates formed by reaction at 800—1100°C in air ($Sr_2U_2O_7$ is not well established.)

M:U	1:4	1:3	1:2	2:3	1	2	3
		MgU_3O_{10}			$MgUO_4$		
	CaU_4O_{13}		CaU_2O_7	$Ca_2U_3O_{11}$	$CaUO_4$	Ca_2UO_5	Ca_3UO_6
	SrU_4O_{13}		(SrU_2O_7)	$Sr_2U_3O_{11}$	$SrUO_4$	Sr_2UO_5	Sr_3UO_6
			BaU_2O_7	$Ba_2U_3O_{11}$	$BaUO_4$	Ba_2UO_5	Ba_3UO_6

*This does not mean that the bonding is wholly ionic. The bonding in the UO_2^{2+} group in these uranates is covalent in character. However, the charge on the uranyl group is +2, there is no difference between UO_2^{2+} and $U^{6+} + 2O_2^{4-}$ with regard to the total charge. Therefore, the valency of uranium in the oxides was calculated simply from the charge neutrality condition taking the charge of alkaline earth ions as +2 and that of oxygen ion as −2.

Very little information is available about the valency of the uranium when the M:U ratio of alkaline earth to uranium atoms is between discrete values such as 1:4 and 1. However, there is experimental evidence that the magnesium uranate with Mg:U = 1:2 (between 1:3 and 1) is a mixture of MgU_3O_{10} and $MgUO_4$, i.e. U(VI) is present in this mixture [10, 11]. It therefore seems probable that the uranium remains hexavalent in the appropriate continuous range of M:U of the uranates in Table 1, where M indicates an alkaline earth metal.

Considering the case of possible magnesium uranates, let the free energy changes of the equations

$$MgO + U_3O_8 + \tfrac{1}{2}O_2 = MgU_3O_{10} \quad (1)$$

$$MgO + \tfrac{1}{3}U_3O_8 + \tfrac{1}{6}O_2 = MgUO_4 \quad (2)$$

be denoted as ΔG_1 and ΔG_2, respectively; these changes are negative. Provided that there are no other magnesium uranates in the range $1:3 < Mg:U < 1$, multiplication of eqn. (1) by $(p-1)/2$ and of eqn. (2) by $(3-p)/2$, followed by addition, gives

$$MgO + \frac{p}{3}U_3O_8 + \frac{p}{6}O_2 = \frac{p-1}{2}MgU_3O_{10} + \frac{3-p}{2}MgUO_4 \quad (3)$$

where $1 \leqslant p \leqslant 3$. The bulk composition on the right of eqn. (3) is MgU_pO_{1+3p}, in which Mg:U lies between 1:3 and 1. Because the free energy change of eqn. (3), $\Delta G_3 = (p-1)/2\,\Delta G_1 + (3-p)/2\,\Delta G_2$, is negative, the reaction yields a two-phase mixture of MgU_3O_{10} and $MgUO_4$, in which the mean uranium valency is +6. This statement that U(VI) is stable in mixtures of uranates was verified experimentally for the magnesium and the strontium uranates (see below).

These properties can be used to determine the oxygen in uranium oxides and ternary oxides. For example, if UO_{2+x} is mixed with Sr_2UO_5 and the mixture is heated in air, the reaction expressed as

$$UO_{2+x} + p \cdot Sr_2UO_5 + \frac{1-x}{2}O_2 = (Sr_{2p}U_{1+p}O_{3+5p}) \quad (4)$$

occurs under the condition $1/4 \leqslant 2p/(1+p) \leqslant 3$, where p is the mixing ratio. The parentheses on the right side of the equation indicate that the chemical formula is merely a bulky composition, the product actually formed being a two-phase mixture of the uranates. Equation (4) shows that the weight of the product is larger than the sum of the weights of the UO_{2+x} and the Sr_2UO_5 by the weight corresponding to $(1-x)/2$ mol of oxygen, from which the x value of UO_{2+x} can be calculated.

When the method is applied to a ternary uranium oxide, $Mg_yU_{1-y}O_{2+x}$, with a known magnesium content, y, then the reaction can be written as:

$$Mg_yU_{1-y}O_{2+x} + p \cdot MgUO_4 + \frac{1-x-2y}{2}O_2 = (Mg_{y+p}U_{1-y+p}O_{3-2y+4p}) \quad (5)$$

Here, $MgUO_4$ is used as the compound containing the alkaline earth elements instead of Sr_2UO_5 in eqn. (4). Equation (5) holds in the range $1/3 \leqslant (y + p)/(1 - y + p) \leqslant 1$; the weight increase in the product after heating corresponds to $(1 - x - 2y)/2\ O_2$, from which x can be obtained.

For the analysis of ternary uranium oxides with alkaline earth elements, the uranates to be added need not be restricted to those with a common alkaline earth element. For example, the oxygen in $Mg_yU_{1-y}O_{2+x}$ can be determined with Sr_2UO_5:

$$Mg_yU_{1-y}O_{2+x} + p \cdot Sr_2UO_5 + \frac{1-x-2y}{2}\ O_2 = (Mg_ySr_{2p}U_{1-y+p}O_{3-2y+5p}) \quad (6)$$

Uranium is known to be in the hexavalent state in quaternary uranium oxides containing two kinds of metals of alkali and/or alkaline earth elements in a certain range of the metal-to-uranium ratios [12, 13].

A characteristic of eqns. (4)—(6) is that the weight increase is independent of the mixing ratio, i.e. the value p does not enter into the O_2 terms. Accordingly, another modified method can be applied for the determination. If UO_{2+x}, for example, is mixed with large amounts of magnesium oxide and the mixture is heated in air at 800—900°C, the excess of MgO will be dispersed in the $MgUO_4$ formed, because magnesium uranates with an Mg:U ratio greater than 1 are unknown. The reaction is expressed as

$$UO_{2+x} + p \cdot MgO + \frac{1-x}{2}\ O_2 = MgUO_4 + (p-1) \cdot MgO \quad (7)$$

where the p value is larger than 1. The determination based on reaction (7) has the advantage that the effect of non-stoichiometry is practically negligible. Though narrow, the ranges of oxygen non-stoichiometry in the uranates are generally greater in the compounds with the smaller M:U ratios (M = alkaline earth element). When reaction (7) is used, the uranate with the greatest M:U ratio among the magnesium uranates, $MgUO_4$, is formed.

Although magnesium oxide is added here, it should be noted that other compounds can also be used, provided that they are stable in air at room temperature and not hygroscopic, and produce large weight increases on reaction.

EXPERIMENTAL

Apparatus

The reactions in air were performed in a SiC resistance furnace with a 20 × 20 × 40-cm sample chamber.

The x-ray powder photographs were taken with a Norelco 114.6-mm camera using nickel-filtered Cu Kα radiation.

Potentiometric titrations were made with a Hitachi—Horiba type F-7ss pH meter.

Chemicals

Triuranium octoxide, U_3O_8, was prepared by oxidizing uranium metal blocks in air in a quartz crucible. In order to avoid violent reaction, the temperature of the furnace was gradually raised to 800°C at a heating rate of about 50°C h^{-1} with the lid of the crucible almost closed. After cooling, the oxide was again heated at 800°C without the lid. The uranium metal used was the standard sample JAERI-U4, the minimum purity of which is 99.99% according to measurements of 18 impurity elements (total less than 40 ppm) [14]. Uranium dioxide, UO_{2+x}, was prepared by reducing the U_3O_8 in a stream of hydrogen at temperatures below 1000°C.

Reagent-grade magnesium oxide (heavy) was heated in air at 900°C before use. Strontium carbonate was obtained by adding ammonium carbonate to a solution of reagent-grade strontium nitrate; the precipitate was washed with water and then heated at 500°C to remove traces of ammonium carbonate.

The solid solution, $Mg_yU_{1-y}O_{2+x}$, was prepared as described earlier [15]. Magnesium monouranate, $MgUO_4$, was prepared by heating a mixture of the calculated amounts of MgO and U_3O_8 in air at 900°C. Strontium uranate, Sr_2UO_5, was obtained by heating a mixture of the calculated amounts of $SrCO_3$ and U_3O_8 in air at 1100°C [16].

General procedure

Weigh the sample of uranium oxide or ternary uranium oxide (0.5—2 g) on a microbalance with a precision of ±10 μg. Weigh an amount of the alkaline earth compound depending on the intended M:U ratio of the product (for relevant M:U ratios, see Results and Discussion). Mix the sample and the alkaline earth compound intimately in an agate mortar for about 20 min. Then, transfer the mixture to three or four quartz crucibles of cylindrical form (15-mm inner diameter and 15-mm height) which have been heated at 1000°C before use to ensure constant weight on heating. Gradually raise the temperature to the reaction temperature, 900°C, at a rate of about 100°C h^{-1}. Hold at the reaction temperature for 50 h, and then anneal at 800°C for 50 h. The annealing process is desirable to minimize the oxygen non-stoichiometry of the products. Cut the current of the furnace, to cool to 100—200°C, at which temperature the products are transferred to a silica-gel desiccator. Weigh after the crucibles have cooled to room temperature.

X-ray measurements

The x-ray diffraction measurements were made for the UO_{2+x} samples in glass capillaries. The lattice constants were obtained from the powder photographs by the Nelson—Riley treatment. The O:U atom ratios in the UO_{2+x} samples were calculated from the relation $a_0 = 5.4704 - 0.094x$ where a_0 is the lattice constant [17].

Determination of uranium(IV) by redox titration

Dissolve the uranate samples (about 0.5 g) in 1.5 M sulfuric acid in the presence of 20.00 ml of 0.05 N $K_2Cr_2O_7$ solution by heating to 60—70°C. Titrate the excess of Cr(VI) with 0.05 M iron(II) ammonium sulfate (Mohr's salt) by the potentiometric method. Standardize the titrant against pure uranium metal dissolved in sulfuric acid.

RESULTS AND DISCUSSION

To examine the validity of the proposed method, UO_{2+x} was considered the most suitable test sample, because the O:U ratio can be easily checked by x-ray diffraction; the lattice constant of the cubic UO_{2+x} changes quite significantly with the x value. An example of the weight changes before and after heating is shown in Table 2, where both determinations (1) and (2) were based on the reactions of eqn. (7). Column 3 of Table 2 shows the weights of the mixtures divided into the crucibles. It is not necessary to transfer all of the mixtures to the crucibles, but the fact that the sample powder absorbs atmospheric moisture during the mixing process must be taken into account because it causes systematic errors. The weights of the samples after standing in a silica-gel desiccator for 24 h (column 4, Table 2) show that the water once absorbed was not removed by silica gel.

The correction for absorbed water can be made by using reference samples which do not react in air on heating. Any discrepancy in the weight decrease caused by heating between ground and unground reference samples, must come from absorbed water because the other components of the atmosphere are common for these samples. Table 3 shows the results for MgO and $MgUO_4$. Heating in air was carried out together with the samples of determinations (1) and (2) in Table 2. The last column of Table 3 shows that both MgO and

TABLE 2

Weight changes when the oxygen of a UO_{2+x} test sample was determined by the proposed method
(Determination (1): 2.653485 g UO_{2+x}; 0.601660 g MgO; Mg:U atom ratio nearly 1.5. Determination (2): 2.211070 g UO_{2+x}; 0.332445 g MgO; Mg:U atom ratio nearly 1.0.)

Determination	Weight before heating (g)			Weight after heating (g)	
	After grinding	24 h in desiccator	Corrected for water	800°C, 50 h in air	900°C, 50 h 800°C, 50 h
(1)	0.991350	0.991370	0.989733	1.035605	1.036800
	0.794415	0.794390	0.793099	0.829500	0.830760
	0.707715	0.707685	0.706538	0.738675	0.740055
	0.716670	0.716705	0.715512	0.748770	0.749480
(2)	0.812485	0.812450	0.811230	0.850435	0.852205
	0.868485	0.868475	0.867157	0.908820	0.911040
	0.821885	0.821880	0.820628	0.859740	0.862150

TABLE 3

Absorption of atmospheric moisture by MgO and $MgUO_4$ during the grinding process (Grinding time: 20 min in an agate mortar.)

Sample	Initial weight (g)	Dried in desiccator (g)	900°C, 50 h; 800°C, 50 h (g)	Weight decrease (g)
MgO, ground	0.361595	0.361590	0.360355	0.001238
MgO, unground	0.482025	0.482040	0.481695	0.000338
$MgUO_4$, ground	0.780215	0.780190	0.779235	0.000968
$MgUO_4$, unground	1.002505	1.002490	1.002340	0.000158

$MgUO_4$ absorb water during grinding, and this constitutes the main part of the weight decrease. The weight decrease per gram of reference sample was 0.003424 and 0.001241 g for MgO and $MgUO_4$, respectively. The larger decrease for MgO is probably due to its voluminous nature, which gives a larger ratio of surface area to weight than for $MgUO_4$. In applying these correction factors for the mixtures of determinations (1) and (2), it was assumed that the correction factor is the same for UO_{2+x} and $MgUO_4$, which seems reasonable because the densities and particle sizes of the two compounds are not very different. The corrected weights are given in column 4 of Table 2.

The x values of the UO_{2+x} test sample were calculated by means of eqn. (7) from the data given in Table 2. The average results of the determinations where the mixtures were heated at 900°C in air for 50 h followed by annealing at 800°C for 50 h are shown in Table 4. Column 2 of Table 4 shows the x values without correction for absorbed water; these values are far larger than the value obtained by the x-ray method and the discrepancy between the averaged x values by determinations (1) and (2) is beyond the standard deviations.

These drawbacks can be overcome if a correction is applied for the absorbed water, as shown in column 3 of Table 4. The averaged x values for determinations (1) and (2) are consistent within the standard deviation and are in good accord with the x-ray value of 0.016 ± 0.002. Column 4 of

TABLE 4

Determination of the x value of the UO_{2+x} test sample (The x value from the x-ray method was 0.016 ± 0.002.)

Determination	Without H_2O correction	Corrected for H_2O	Corrected for H_2O and buoyancy
(1)	0.0496[a]	0.0159[a]	0.0165[a]
(2)	0.0466[b]	0.0172[b]	0.0176[b]

[a]Average of 4 determinations; in all cases the standard deviation was ±0.0008.
[b]Average of 3 determinations; in all cases the standard deviation was ±0.0008.

TABLE 5

Determination of the x values of $Mg_{0.2}U_{0.8}O_{2+x}$ and $Mg_{0.25}U_{0.75}O_{2+x}$, based on UO_{2+x} as standard sample
(For UO_{2+x}, x = 0.003 (±0.002) by the x-ray method. Compound added, Sr_2UO_5. Heating conditions were 900°C (50 h) then 800°C (50 h). For standardization, UO_{2+x} (1.329035 g) and Sr_2UO_5 (2.602985 g) were used. For $Mg_{0.2}U_{0.8}O_{2+x}$, the sample weight was 0.551980 g with 0.900190 g Sr_2UO_5. For $Mg_{0.25}U_{0.75}O_{2+x}$, the sample weight was 0.744050 g with 1.512300 g Sr_2UO_5.)

Sample	Mixture after grinding (g)	Corrected weight (g)	Weight after heating (g)	x value
UO_{2+x} (standard)	1.276060	1.272884	1.298295	
	1.499850	1.496662	1.526540	
	1.123120	1.120290	1.142655	
$Mg_{0.2}U_{0.8}O_{2+x}$	0.365740	0.364870	0.370315	0.0407
	0.339865	0.339057	0.344135	0.0387
	0.351245	0.350410	0.355645	0.0401
			Av.=	0.0398[a]
$Mg_{0.25}U_{0.75}O_{2+x}$	0.444895	0.443837	0.449155	0.0078
	0.540555	0.539270	0.545730	0.0079
	0.567075	0.565726	0.572480	0.0095
			Av. =	0.0084[a]

[a]Standard deviation is ±0.0008.

Table 4 shows the x values obtained when corrections were applied for both moisture and buoyancy; the effect of buoyancy is small and within the standard deviation, so that this correction is unnecessary until the standard deviation is diminished significantly. The error originates mainly from fluctuations in weighing. It is difficult, even with a microbalance, to measure the weight of a 0.5-g sample within ±10 μg, which causes an error of ±0.001 in the x value for a single determination. If the sample weight is several grams in each crucible, this error will be greatly decreased (by nearly an order of magnitude) and the buoyancy correction will become important.

The above method of correction can be used for absolute measurements of oxygen in the oxides. However, an alternative method can be based on the use of standard samples. The method cannot be applied for absolute measurements, but seems to be practical for routine work. If UO_{2+x} of known x value, for instance, is taken as the standard, and its x value is determined simultaneously with unknown samples, corrections for factors which may cause systematic errors are easily made. The standard x value of UO_{2+x} can be determined by the x-ray diffraction method.

The results for $Mg_{0.2}U_{0.8}O_{2+x}$ and $Mg_{0.25}U_{0.75}O_{2+x}$ by this method of correction are given in Table 5, where Sr_2UO_5 was used as the added compound. By means of the x value of the UO_{2+x}, 0.003 ± 0.002, determined by

the x-ray method, correction factors were calculated for the weights of the UO_{2+x} and Sr_2UO_5 mixtures before heating. The correction factor is simply the corrected weight of the mixture divided by the uncorrected weight and is applied to unknowns in the same batch of analyses. The x values for $Mg_{0.2}U_{0.8}O_{2+x}$ and $Mg_{0.25}U_{0.75}O_{2+x}$ were calculated according to eqn. (6) from the corrected weights and the weights after heating. The standard deviation is ±0.0008 (Table 5) but the error from the composition of the standard sample is ±0.002 (because the error in the lattice constant is ±0.0002 Å and the conversion factor from this constant to the composition is 1/0.094), hence the final standard deviation of this method must be about ±0.002. The x values by the redox titration method were 0.04 ± 0.01 and 0.01 ± 0.01 for $Mg_{0.2}U_{0.8}O_{2+x}$ and $Mg_{0.25}U_{0.75}O_{2+x}$, respectively, which indicates satisfactory agreement with the proposed method.

The above experiments were all done under standard heating conditions (900°C for 50 h; 800°C for 50 h). The effect of heating time was examined for the conditions 900°C for 10 h followed by 800°C for 10 h. The results are shown in Table 6. The averaged x value was 0.0272 ± 0.0007 for the same UO_{2+x} sample as in Table 4; this value is much higher than the x-ray value, which means that heating times of 10 h are insufficient for complete reaction. The reaction time, however, seems to be influenced by the supply of oxygen; if the reaction is conducted in a stream of oxygen, the time is materially shortened.

The reaction temperature has a greater effect on the reaction. Reaction at 800°C for 50 h is totally inadequate (Table 6). The products exhibited a heterogeneous tan color which was different from the pale yellow of $MgUO_4$; the color of uranates is known to darken if oxygen non-stoichiometry is introduced.

The relation of non-stoichiometry and M:U ratio is illustrated in Fig. 1 for magnesium uranates and strontium uranates. The M:U ratios examined were 0.9927, 0.7532, 0.4981, 0.3333, 0.2121 and 0.1617 for magnesium

TABLE 6

Effects of heating time and reaction temperature as illustrated for the x value of the UO_{2+x} test sample. (x value by the x-ray method, 0.016 ± 0.002.)

No.	Mg/U ≈ 1.5 800°C, 50 h[a]	Mg/U ≈ 2.0 900°C, 10 h; 800°C, 10 h[a]
1	0.0382	0.0280
2	0.0471	0.0264
3	0.0552	0.0266
4	0.0356	0.0277
Average	0.044 (±0.008)	0.0272 (±0.0007)

[a]Corrected for H_2O.

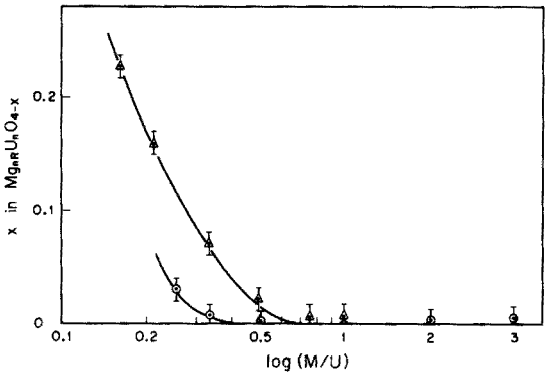

Fig. 1. Non-stoichiometry of the uranates as a function of M:U ratio (M = Mg, Sr). The original mixtures were MgO and U_3O_8 for magnesium uranates (▲) and $SrCO_3$ and U_3O_8 for strontium uranates (○). Reaction conditions: heating in air at 900°C for 50 h, cooling, grinding again, heating at 900°C for 50 h, and annealing at 800°C for 50 h.

uranates, and 2.9917, 2.0008, 1.0010, 0.5082, 0.3359 and 0.2553 for strontium uranates. The redox titration method was used. Non-stoichiometry is expressed as x in $M_{nR}U_nO_{4-x}$ where R is the M:U atom ratio and n is the factor which normalizes the amount of oxygen required for stoichiometry to 4. Figure 1 shows that magnesium uranates are nearly stoichiometric in the range $0.75 \leqslant Mg:U \leqslant 1$ whereas below 0.75 the non-stoichiometry becomes significant. Similar trends are also seen for strontium uranates, the range of de facto stoichiometry being $0.75 \leqslant Sr:U \leqslant 3$.

The method of determination described here can be applied within the above ranges of "stoichiometry", but the x values determined in Fig. 1 have standard deviations of ±0.01, so that it is safer to adopt larger M:U ratios in the proposed method. Jakeš and Křivý [19] have reported that the value of x in $MgUO_{4-x}$ is 0.0059, but the value is smaller in $MgUO_4$ prepared by annealing at 800°C in air for 50 h, since the x values for the UO_{2+x} test sample agreed well with the value by the x-ray method (Table 4) without taking into account the non-stoichiometry of the $MgUO_4$. In Fig. 1, the points could be connected by reasonably smooth curves which lay along the axis for M:U ratios above 0.75. These curves provide experimental support for the hexavalent state of uranium in uranates over certain continuous ranges of M:U ratios.

REFERENCES

1 T. M. Florence, in Analytical Methods in the Nuclear Fuel Cycle, Proceedings of a Symposium, Vienna, 29 November—3 December, 1971, IAEA, Vienna, 1972, p. 45.
2 D. R. Dharwadkar and M. S. Chandrasekharaiah, Anal. Chim. Acta, 45 (1969) 545.
3 R. W. Stromatt and R. E. Connally, Anal. Chem., 33 (1961) 345.
4 R. M. Burd and G. W. Goward, AEC-Reports WAPD-205 (1959).
5 See, e.g., U. Berndt, R. Tanamas and C. Keller, J. Solid State Chem., 17 (1976) 113.

6 G. S. Petit and C. A. Kienberger, Anal. Chim. Acta, 25 (1961) 579.
7 R. J. Ackerman and A. T. Chang, J. Inorg. Nucl. Chem., 39 (1977) 75.
8 G. C. Swanson, AEC-Reports LA-6083-T (1975).
9 C. Keller, Gmelin Handbuch der Anorganischen Chemie, No. 55, Uran C-3, Springer, Berlin, 1975, p. 77.
10 H. R. Hoekstra and J. J. Katz, J. Am. Chem. Soc., 74 (1952) 1683.
11 G. P. Polunina, L. M. Kovba and E. A. Ippolitova, in V. I. Spityn (Ed.), Investigations in the Fields of Uranium Chemistry, translated to AEC-Reports ANL-Trans-33, 1961, p. 224.
12 A. W. Sleight and R. Ward, Inorg. Chem., 1 (1962) 790.
13 S. Kemmler-Sack and I. Seemann, Z. Anorg. Allg. Chem., 411 (1975) 61.
14 H. Hashitani, A. Hoshino and T. Adachi, Japan Atomic Energy Research Institute Report, JAERI-M-5343 (1973).
15 T. Fujino and K. Naito, J. Inorg. Nucl. Chem., 32 (1970) 627.
16 H. Tagawa, T. Fujino and J. Tateno, Bull. Chem. Soc. Jpn., 50 (1977) 2940.
17 H. Nickel, Nukleonik, 8 (1966) 366.
18 K. Motojima, H. Hashitani and K. Katsuyama, J. Atomic Energy Soc. Jpn., 3 (1961) 855.
19 D. Jakeš and I. Křivý, J. Inorg. Nucl. Chem., 36 (1974) 3885.

Analytica Chimica Acta, 98 (1978) 385—387

Short Communication

THE CRITICAL BROMIDE CONCENTRATION IN AN OSCILLATING CHEMICAL SYSTEM

R. GYENGE

Research Institute for Pharmaceutical Chemistry, Budapest (Hungary)

E. KŐRÖS*

Institute of Inorganic and Analytical Chemistry, L. Eötvös University, Budapest (Hungary)

K. TÓTH and E. PUNGOR

Department of General and Analytical Chemistry, Technical University, Budapest (Hungary)

(Received 3rd January 1978)

In kinetic investigations of the Belousov—Zhabotinsky (BZ) oscillating reactions, knowledge of the critical bromide concentration ($[Br^-]_{crit}$) is of fundamental importance [1]. Recently, a preliminary study of the $Ru(bipy)_3^{2+}$-catalyzed reaction of malonic acid, bromate and sulphuric acid was reported [2]; it was of interest to establish whether this BZ system followed the same overall kinetics as when the catalyst was cerium(III), manganese(II) or $Fe(phen)_3^{2+}$. To obtain an accurate value for $[Br^-]_{crit}$, it was necessary to calibrate the bromide-selective electrode in the low bromide range between 10^{-4} and 10^{-7} M. The method applied has already been described [3]; here the determination of $[Br^-]_{crit}$ in the malonic acid—bromate—sulphuric acid—$Ru(bipy)_3^{2+}$ oscillating system is discussed.

Experimental

A Radelkis OH-404 Universal Coulometer was used in the constant-current mode for the coulometric generation of bromide by cathodic polarization of a silver—silver bromide electrode at a current density of 0.15 mA cm^{-2} [3].

The potentiometric cell, of design similar to that used earlier [3], was thermostated by a U-10 Thermostat at 20 ± 0.05° C and the solution was stirred magnetically. The change in bromide concentration was followed by a bromide-selective electrode (Orion Research 94-35) with a double-junction silver—silver chloride reference electrode (Radelkis OP-8201) connected via a salt bridge containing 10% potassium nitrate, because chloride ions inhibit the oscillating reaction. The electrode potential was measured on a Radelkis OP-205 Precision pH meter, connected to a Radelkis OH-814/1 potentiometric recorder for following the oscillating curves.

All reagents used were of analytical grade.

Results and discussion

During the BZ reaction, the concentration of bromide exhibits a temporal oscillation. The system goes from one kinetic state to the other, i.e. it switches on and off, when the bromide concentration passes through a critical value, called the critical bromide concentration. This value has been calculated from the kinetic data of the supposed elementary reaction steps [1].

To obtain an accurate experimental value for this critical value, the bromide selective electrode must be calibrated under the conditions of the BZ reaction. Calibrations were performed in solutions of various compositions and at a constant ionic strength; the curves obtained are shown in Fig. 1.

An attempt was made to measure the concentration of bromide under static conditions; in this case, the malonic acid was oxidized with bromate in the presence of cerium(III) or manganese(II) as catalyst. The system was thermostated at 15°C where the periodic oscillation required about 2 min, so that two samples could be withdrawn during one period. The sample was pipetted into a 40% acetate buffer solution in order to quench the chemical oscillation, and the potential was measured immediately. However, although the oscillation terminated at the pH of the buffer, the reaction proceeded at a non-negligible rate. Thus the bromide concentration changed, and the static method could not be applied.

Accordingly, the measurements were done under dynamic conditions [4] for the $Ru(bipy)_3^{2+}$-catalyzed BZ system. During the reaction the colour of the solution changed periodically from yellow to green, because of the transition from $[Ru(bipy)_3^{2+}]$ to $[Ru(bipy)_3^{3+}]$. The reaction mixture comprised 0.1 M potassium bromate, 0.4 M malonic acid, 0.5 M sulphuric acid and 4×10^{-3} M

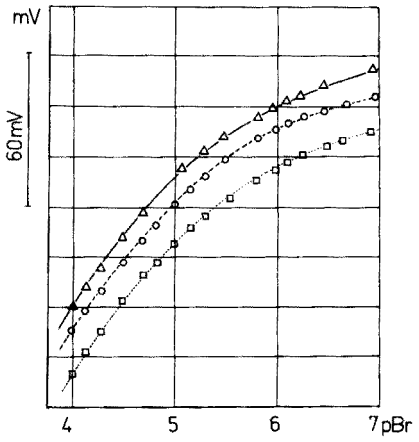

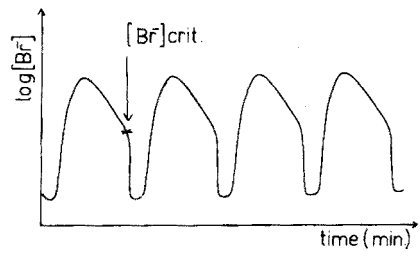

Fig. 1. Calibration curve of a bromide-selective electrode under the conditions of the oscillating reaction. (△) 10^{-1} M KNO_3; (○) 10^{-1} M KNO_3 + 0.25 M H_2SO_4; (□) 10^{-1} M KNO_3 + 0.25 M H_2SO_4 + 0.4 M malonic acid + 4×10^{-3} M $Ru(bipy)_3^{2+}$.

Fig. 2. Typical log[Br^-] vs. time curve of the system containing malonic acid—bromate—sulphuric acid—$Ru(bipy)_3^{2+}$.

$[Ru(bipy)_3^{2+}]$, the oscillatory reaction being initiated by addition of the catalyst. A typical $\log[Br^-]$ vs. time curve is illustrated in Fig. 2. The critical bromide ion concentration was evaluated from the second oscillation of the $\log[Br^-]$ vs. time curve by means of a calibration curve obtained by coulometric generation of bromide ions. This calibration plot was a smooth curve, showing a potential change of 47.5 mV over the pBr range 5—7, i.e. the range of the oscillating bromide concentration.

The average value of the critical bromide concentration was found to be 8×10^{-6} M, which is in very good agreement with the calculated value, 5×10^{-6} M. This indicates that the overall mechanism of the $Ru(bipy)_3^{2+}$-catalyzed BZ reaction is the same as that of the BZ systems investigated earlier.

REFERENCES

1 R. J. Field, E. Kőrös and R. M. Noyes, J. Am. Chem. Soc., 94 (1972) 8649.
2 E. Kőrös, L. Ladányi, V. Friedrich, Zs. Nagy and Á. Kiss, React. Kin. Cat. Lett., 1 (1974) 455.
3 R. Gyenge, K. Tóth, E. Pungor and E. Kőrös, Anal. Chim. Acta, 94 (1977) 111.
4 E. Kőrös and M. Burger, in E. Pungor (Ed.), Ion-Selective Electrodes, Akadémiai Kiadó, Budapest, 1973, p. 191.

Analytica Chimica Acta, 98 (1978) 389—392

Short Communication

STORAGE BEHAVIOUR OF INORGANIC MERCURY AND METHYLMERCURY CHLORIDE IN SEA WATER†

M. STOEPPLER* and W. MATTHES**

Institute of Chemistry, Institute 4, Applied Physical Chemistry, Nuclear Research Centre (KFA) Juelich, P.O. Box 1913, D-5170 Juelich (Federal Republic of Germany)

(Received 21st November 1977)

Mercury is well known as hazardous to man, and plays an important rôle in the aquatic food chain. Despite the low concentrations of dissolved (total) mercury in sea water — usually $<0.2\ \mu g\ l^{-1}$ from analyses carried out lately in different oceans [1—6] — the mercury content of marine organisms is quite high, because of accumulation processes, compared to the contents of other toxic metals, e.g. cadmium and lead. In some regions, high levels above the safe threshold have been found. This has been reported recently for some parts of the Mediterranean Sea [7—12] and may be attributed to man-made as well as to natural sources.

The predominant mercury species in marine organisms is methylmercury chloride [13—16], which is produced via biological transformation of ionic mercury at lower trophic levels [17, 18]. Thus, investigations on mercury in aquatic systems are highly desirable from the viewpoint of environmental safety as well as for improvement of basic scientific knowledge. As a prerequisite to tackling these problems, more information, particularly about the analytical discrimination of the most important mercury species, is urgently needed.

Losses of mercury from fresh water and distilled water are well known, although the mechanisms are a subject of controversy [20—25]. Experience gained during the analysis of sea waters for ultratrace levels of other toxic metals [26] indicated that the rather high content of competing ions in sea water should have a stabilizing effect, at least for relatively short storage times. Similar findings have been reported for inland waters by Mahan and Mahan [27]. Thus, a preliminary model study was done to establish defined conditions for sea-water storage so that the subsequent analysis for inorganic and total mercury would be as accurate as possible.

---

†Presented in part at the International Symposium on Microchemical Techniques, Davos, May, 1977.

**Present address, KFA, Central Unit of Chemical Analysis.

Experimental

Because of the proven influence of particulate matter on the storage behaviour of mercury in sea-water samples [28, 29], the experiments described below were done with carefully decanted sea-water samples spiked with ionic mercury and/or methylmercury chloride at the $\mu g\ l^{-1}$ level, and stored at ambient temperature.

The chemicals and acids used were of analytical grade (p.a., Merck). The 1-l polyethylene bottles (wall thickness, ca. 1 mm) had screw caps made from conventional high-pressure (linear) material. The glass containers were volumetric flasks made of Duran 50 (Schott, Mainz).

All the containers used were carefully treated with dilute acids in the following manner. The containers were filled with 5—6 M HNO_3 and shaken occasionally during about 48 h; they were then rinsed with three portions of quartz-distilled, mercury-free water.

During the storage periods of spiked sea-water samples, several aliquots were taken and analyzed for total as well as for inorganic mercury by an automated method (limit of determination, 0.01 μg Hg l^{-1}) based on pre-concentration of mercury on silver wool and subsequent a.a.s. [30].

Results and discussion

Initially, the spiked sea-water samples were stored as described above, at natural pH (about 8.4) in glass and polyethylene containers. In all cases, there was the expected rapid decrease of mercury concentration in solution, probably because of adsorption to the container wall and an additional conversion of methylmercury chloride to Hg^{2+}-ions. Figure 1 shows that this decrease was extremely rapid in polyethylene possibly because of an additional reduction mechanism.

When the samples were slightly acidified with 1 ml of concentrated HNO_3 or HCl per liter to about pH 2.5, the results for total mercury showed no change, within the analytical error of the a.a.s. method, during a storage time of about 2.5 months. In contrast, the degradation of methylmercury chloride proceeded quite quickly under identical conditions when HNO_3 was used for acidification (Fig. 2). For this reason, HCl was chosen for all further experiments on the long-term stability of sea-water samples spiked with ionic mercury and/or methylmercury chloride in glass and polyethylene containers.

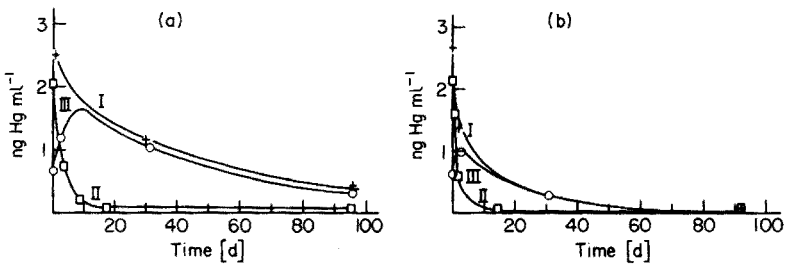

Fig. 1. Storage of sea water at natural pH spiked with 2.05 ng Hg ml^{-1} as CH_3 HgCl and 0.64 ng Hg ml^{-1} as $HgCl_2$. (a) Glass containers. (b) Polyethylene containers. I, Total Hg; II CH_3HgCl; III, $HgCl_2$. Storage time 94 days.

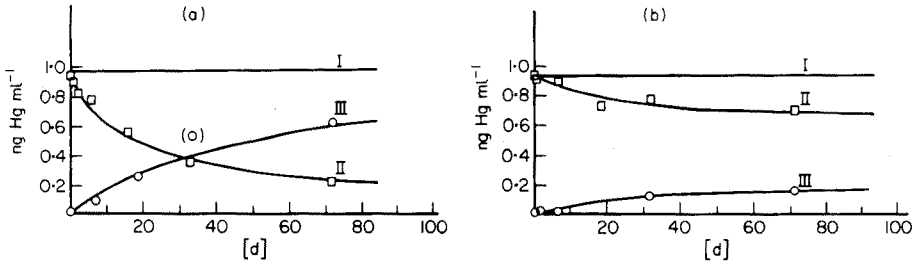

Fig. 2. Storage of spiked (2.05 ng Hg ml^{-1} as CH_3HgCl) sea water acidified to pH 2.5, in glass containers. (a) Nitric acid. (b) Hydrochloric acid. Curves I, II and III as in Fig. 1.

Sea-water samples acidified with 1 ml of 11 M HCl stored for about 90 days in volumetric flasks showed a significantly higher stability of the organic compound compared with samples stored in polyethylene (Fig. 3). Because of this and because polyethylene is markedly permeable for mercury vapour, so that the mercury concentration inside the container may increase if the external concentration exceeds 1 μg Hg m^{-3} [31] (which is possible in an analytical laboratory), it was decided to use only carefully cleaned glass bottles checked for mercury blanks. These findings about the superiority of glass confirm that the recent results of Carron and Agemian [32]. Further because light may affect the rate of conversion of methylmercury, real samples should be taken and stored only in brown glass bottles with tight screw-caps made from dense, rigid plastic material.

The preliminary results about the degradation of methylmercury chloride corroborate the observations of Kudo et al. [33] who used isotopically tagged CH_3HgCl and found a high exchange rate from the organic to the inorganic compound. Because of this degradation even in slightly acidified samples, the storage time should not exceed 10 days, and analysis for inorganic mercury should be done as quickly as possible after sampling.

Series of real samples with values well below 0.2 μg l^{-1} (total Hg) are now under study. For this purpose, a much more sensitive method — based on preconcentration on silver wool, with a limit of determination below 1 ng Hg l^{-1} — was developed for routine application [6]; cross-checks with a new voltammetric method of about the same sensitivity [34] are possible.

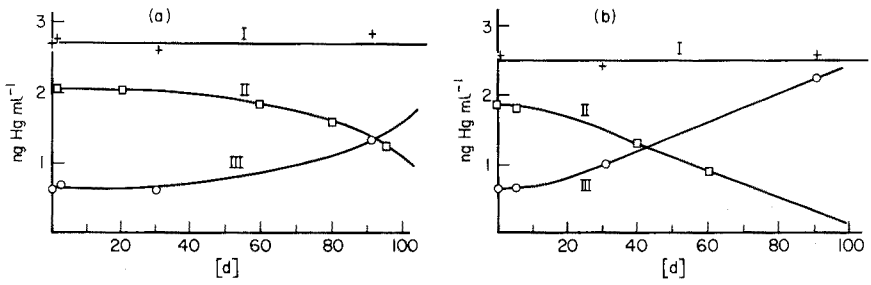

Fig. 3. Storage of spiked (as in Fig. 1) sea water at pH 2.5 (HCl). (a) Glass containers. (b) Polyethylene containers. Curves I, II and III as in Fig. 1.

The authors are grateful to Prof. Dr. H. W. Nürnberg, director of the Institute of Applied Physical Chemistry, for his continuous interest, and to Mr. R. Flucht for valuable technical assistance. Further thanks are due to the Bundesministerium für Forschung und Technologie, Bonn, for financial support of this work within the scope of the Environmental Specimen Bank Project under Contract UGB 0008.

REFERENCES

1 R. Chester, D. Gardner, J. P. Riley and J. Stoner, Mar. Poll. Bull., 2 (1973) 28.
2 A. Renzoni, E. Bacci and L. Falciai, Rev. Intern. Océanogr. Méd., 31, 32 (1973) 17.
3 J. Olafsson, Anal. Chim. Acta, 68 (1974) 207.
4 W. F. Fitzgerald, W. B. Lyons and C. D. Hunt, Anal. Chem., 46 (1974) 1882.
5 R. A. Fitzgerald, D. C. Gordon, Jr. and R. E. Cranston, Deep-Sea Res., 21 (1974) 139.
6 M. Stoeppler and R. Flucht, to be published.
7 Y. Thibaud, Science et Pêche, Bull. Inst. Pêche Marit., 209 (1971) 1.
8 G. Cumont, G. Viallex, H. Lelievre and P. Bobenrieth, Rev. Intern. Océanogr. Méd., 26 (1972) 95.
9 A. Renzoni and F. Baldi, Acqua and Aria, (1975) 597.
10 M. Stoeppler, F. Backhaus, W. Matthes, M. Bernhard and E. Schulte, Proc. Verb. XXVth. Congress and Plenary Assembly of ICSEM, Split, (1976) in press.
11 M. Stoeppler, M. Bernhard, F. Backhaus and E. Schulte, Mar. Poll. Bull, submitted.
12 A. Renzoni and M. Bernhard, private communication.
13 V. Zitko, B. J. Finlayson, D. J. Wildish, J. M. Anderson and A. C. Kohler, J. Fish Res. Bd. Can., 28 (1971) 1285.
14 A. V. Holden, J. Food Technol., 8 (1973) 1.
15 R. Doi and J. Ui, in P. A. Krenkel (Ed.), Heavy Metals in the Aquatic Environment, Pergamon, Oxford, 1975.
16 G. Westöö and B. Ohlin, Värföda 27 Suppl. No. 1, (1975) 12.
17 S. Jensen and A. Jernelöv, Nature, 223 (1969) 753.
18 B. H. Olson and R. H. Cooper, Nature, 252 (1974) 682.
19 F. E. Brinckman and W. P. Iverson, in T. M. Church (Ed.), ACS Symposium Series, Nr. 18, Marine Chemistry in the Coastal Environment, Am. Chem. Soc., 1975, p. 319.
20 R. M. Rosain and C. M. Wai, Anal. Chim. Acta, 65 (1973) 279.
21 H. L. Rook and J. Moody, Stabilization and Determination of Nanogram Quantities of Mercury in Water, 2nd Int. Conf. on Nuclear Methods in Environmental Research, Columbia, MO, July, 1974.
22 D. W. Newton and R. Ellis, Jr., Environ. Qual., 3 (1974) 20.
23 J. M. Lo and C. M. Wai, Anal. Chem., 47 (1975) 1869.
24 H. V. Weiss and W. H. Shipman, Anal. Chim. Acta, 81 (1976) 211.
25 D. R. Christmann and J. D. Ingle, Jr., Anal. Chim. Acta, 86 (1976) 53.
26 P. Valenta, L. Mart, H. W. Nürnberg and M. Stoeppler, Vom Wasser, 48 (1977) 89.
27 K. I. Mahan and S. E. Mahan, Anal. Chem., 49 (1977) 662.
28 R. A. Carr and P. E. Wilkniss, Environ. Sci. Technol., 7 (1973) 62.
29 I. Sanemasa, T. Deguchi, K. Urota, J. Tomooka and H. Nagai, Anal. Chim. Acta, 87 (1976) 479.
30 W. Matthes, R. Flucht and M. Stoeppler, Fresenius Z. Anal. Chem., in press.
31 M. H. Bothner and D. E. Robertson, Anal. Chem., 47 (1975) 592.
32 J. Carron and H. Agemian, Anal. Chim. Acta, 92 (1977) 61.
33 A. Kudo, H. Akagi, D. C. Mortimer and D. R. Miller, Environ. Sci. Technol., 11 (1977) 907.
34 L. Sipos, P. Valenta, H. W. Nürnberg and M. Branica, J. Electroanal. Chem., 77 (1977) 263.

Analytica Chimica Acta, 98 (1978) 393—396

Short Communication

DETERMINATION OF POSITIONAL ISOMER CONFIGURATION VIA PLASMA PROCESSING OF GAS CHROMATOGRAPHIC PEAKS

VELUPPILLAI PARAMASIGAMANI and WALTER A. AUE*

5637 Life Science Centre, Dalhousie University, Halifax, Nova Scotia (Canada)

(Received 15th November 1977)

It can be difficult to determine the configuration of a polysubstituted aromatic compound when several isomeric structures are possible and the compound is available either in very small amounts or in a complex mixture or both. N.m.r. and i.r. may not be sensitive enough, m.s. may not be able to distinguish between the possible structures, and the calculation of g.c. retention indices (in the absence of an authentic standard) requires data for many similar compounds which are usually not available.

Perhaps the oldest method of determining the configuration of positional isomers is to treat the substance chemically and count the number of isomers formed. This method is cumbersome and the possibility of error cannot be excluded. However, the use of g.c. coupled with in situ degradation of single peaks can render such a task considerably easier and faster in favourable cases.

Recently, the use of a low-energy plasma for obtaining product patterns from g.c. peaks was described [1]. After compounds have been separated on a first column, one peak is selected and routed through the plasma to the second column, which separates the products of the plasma reaction.

A variety of common substituents can be removed from aromatic rings by plasma processing. This communication illustrates the approach with a simple example, i.e. the "determination" of the isomeric configuration of all chlorinated benzenes. The isomers involved are the three dichloro-, three trichloro-, and three tetrachlorobenzenes; all of these are commercially available. The premise of this illustrative example is that these compounds are available but their isomeric configuration is not known.

Experimental

Figure 1 shows the schematic flow pattern used. Prepurified argon, after passage through an oxygen scavenger cartridge, was used as carrier gas. In the normal configuration the effluents from the first column were routed to the dummy column, while the reactor and second column were supplied with pure carrier gas. The four-port valve was turned when the first f.i.d.

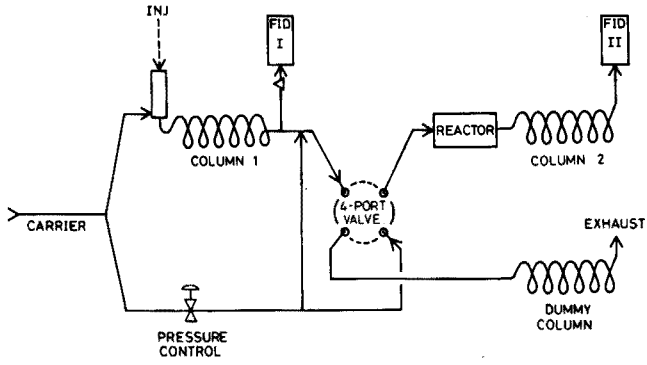

Fig. 1. Flow schematic diagram.

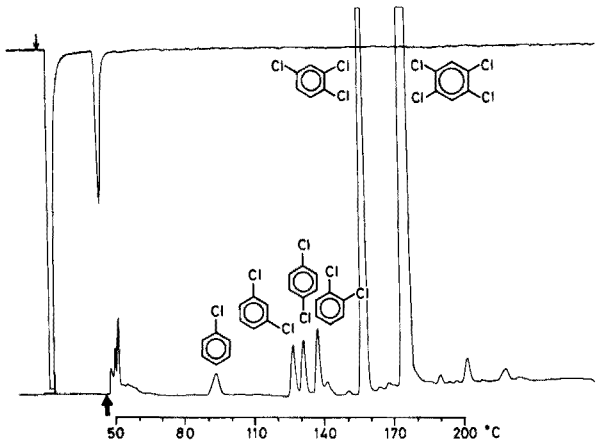

Fig. 2. Pattern from 1,2,4,5-tetrachlorobenzene. Top chromatogram: Column 1, isothermal at 185°C, f.i.d.-1. Bottom chromatogram: f.i.d.-2, temperature programmed.

signaled the emergence of the peak proper from the first column; the valve was returned to its normal position after the peak had passed on to the reactor and the second column. The lower black arrows in Figs. 2 and 3 mark the time when this peak passed through the reactor.

The first column was operated isothermally, the second column was temperature-programmed. The reactor contained a β-stimulated, mild discharge in argon.

Products were identified by comparisons of retention times, and occasional co-chromatography, with authentic standards. Confirmation of product structure by an independent method was not considered to be necessary in view of the simplicity of the product patterns.

Results and discussion

The primary products from a polyhalobenzene contain one less halogen. These are the predominant peaks in the chromatograms. Secondary products arise from these by further loss of halogen, etc.

Three tetrachlorobenzenes exist. Of these, 1,2,4,5-tetrachlorobenzene should give only *one* primary product, namely 1,2,4-trichlorobenzene. The latter should give all three dichlorobenzenes as secondary products. If removal of chlorine and acquisition of hydrogen occurs on a completely random basis (an unlikely situation), the three dichlorobenzenes should be present in equimolar amounts. Figure 2 shows the product pattern of 1,2,4,5-tetrachlorobenzene. It establishes the structure unequivocally.

The second tetrachlorobenzene, the 1,2,3,4-isomer, should give *two* isomers as primary products: 1,2,3- and 1,2,4-trichlorobenzene. These, in turn, should give the three dichlorobenzenes. If the rate constants for all processes involved are equal, the trichlorobenzenes should show a 1:1 ratio, and the ratios for the dichlorobenzenes would be 1,2-:1,3-:1,4- = 3:2:1. The peaks obtained had amplitude ratios of 1.0:1.7 for 1,2,3- and 1,2,4-trichlorobenzene, and 2.2:1.0:1.2 for 1,2-, 1,3- and 1,4-dichlorobenzene, respectively. These ratios can vary, depending on plasma conditions. The pattern obtained establishes the compound as the 1,2,3,4-tetrachloro isomer.

A similar reasoning predicts that the third isomer, 1,2,3,5-tetrachlorobenzene, yields *three* primary products, namely 1,2,4-, 1,2,3-, and 1,3,5-trichlorobenzene (2:1:1) and three secondary products, i.e. 1,2-, 1,3-, and 1,4-dichlorobenzene (2:3:1). The ratios obtained were 3.9:1.0:1.7, and 1.1:2.8:1.0, respectively. Again, the pattern establishes the isomer structure beyond any doubt.

For the plasma used in these experiments, reaction sequences can be quite complex and are often not well understood. At least four types of process must occur to an appreciable extent: ionization of the analyte molecule by argon metastables, followed by loss of chlorine and gain of hydrogen or gain of chlorine. (The latter was established in other experiments.) The initial reaction can, of course, also involve the radical elimination of chlorine by electron impact, etc. It would be unreasonable to expect isomers to behave exactly alike in these reactions; the observed ratios deviate from the ratios calculated. However, even the order of secondary products sometimes conforms to prediction, e.g. 1,3- > 1,2- > 1,4- from the 1,2,3,5-isomer.

The structure of trichlorobenzenes can be determined in a way similar to that of the tetrachlorobenzenes. 1,3,5-Trichlorobenzene yields 1,3-dichlorobenzene, 1,2,3-trichlorobenzene yields 1,2- and 1,3-dichlorobenzene (2:1; found 2.0:1.0); 1,2,4-trichlorobenzene yields all three isomers (1,2-:1,3-:1,4 = 1:1:1; found 1.0:1.1:1.7). Figure 3 shows an example of this series.

Dichlorobenzenes all yield chlorobenzene as the primary product and cannot be distinguished by the approach used so far. If, however, the trichlorobenzenes are available, the assignment is easy. A single primary

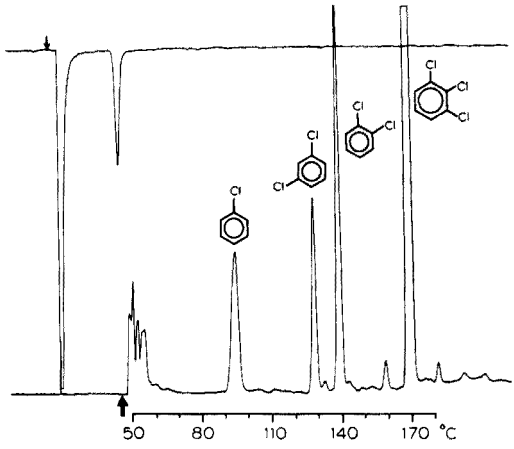

Fig. 3. Pattern from 1,2,3-trichlorobenzene. Conditions as for Fig. 2.

product from a trichlorobenzene must be the 1,3-isomer, two primary products from another one must be 1,2- and 1,3-, etc.

Thus it is possible to establish unequivocally the isomeric configuration of all polychlorobenzenes. Polybromo- and polyiodo-benzenes should follow the same pattern. Clearly, assignments become much more difficult, if not impossible, when more than one type of substituent or different aromatic structures are involved. It is also important to ensure, as far as possible, that all important products have been detected. While it may not be possible to identify all the positional isomers of a particular compound by this approach, particular isomers can often be distinguished. A further advantage of the g.c. approach is that a peak of interest from a complex mixture can be investigated. If other substances co-elute, it may be possible to detect the peak of interest and its products with a selective detector.

This study was supported by NRC grant A-9604 and AC grant 6099.

REFERENCE

1 W. A. Aue, V. Paramasigamani and S. Kapila, Mikrochim. Acta, in press.

Analytica Chimica Acta, 98 (1978) 397—399

Short Communication

SPECTROPHOTOFLUORIMETRIC DETERMINATION OF GADOLINIUM WITH TRIETHYLENETETRAMINE-*N*,*N*,*N*',*N*'',*N*''',*N*'''-HEXAACETIC ACID

TOMITSUGU TAKETATSU* and ATSUKO SATO

College of General Education, Kyushu University, Ropponmatsu, Fukuoka 810 (Japan)

(Received 7th December 1977)

The u.v. spectrophotometric determination of gadolinium is difficult because many lanthanides give absorption bands. It is particularly hard to find a simple, rapid method for the determination of micro amounts of gadolinium. Recently, fluorimetric methods for the metal have been described based on citric acid [1] and salicylic acid—rhodamine S [2]. The present communication reports a spectrophotofluorimetric determination of gadolinium with TTHA (triethylenetetramine-*N*,*N*,*N*',*N*'',*N*''',*N*'''-hexaacetic acid).

Experimental

Reagents and apparatus. Standard solutions of the metal ions were prepared by dissolving the 99.9% pure oxide (for all lanthanides except cerium) or the chloride (cerium) in dilute hydrochloric acid. The solutions were standardized by titration with EDTA (disodium salt) and xylenol orange indicator.

Standard solutions of NTA (nitrilotriacetic acid), EDTA, CyDTA (trans-1,2-cyclohexanediamine-*N*,*N*,*N*',*N*'-tetraacetic acid), DTPA (diethylene-triamine-*N*,*N*,*N*',*N*'',*N*''-pentaacetic acid) and TTHA were prepared by dissolving known amounts of the reagents (Dojin Co.) in dilute sodium hydroxide solutions. All other chemicals used were of analytical-reagent grade.

A Hitachi 204 spectrophotofluorimeter was used in combination with a high-pressure xenon tube.

Procedure. Transfer a dilute hydrochloric acid solution containing less than about 600 μg of gadolinium to a beaker. Add 2 ml of 0.02 M TTHA solution, adjust the pH to 3.2—3.4 with dilute hydrochloric acid and sodium hydroxide solution, transfer the solution to a 20-ml volumetric flask and dilute to volume with water. Transfer the solution to a 1-cm quartz cell and measure the fluorescence at 309 nm with excitation at 278 nm. Calculate the content of gadolinium from a calibration curve.

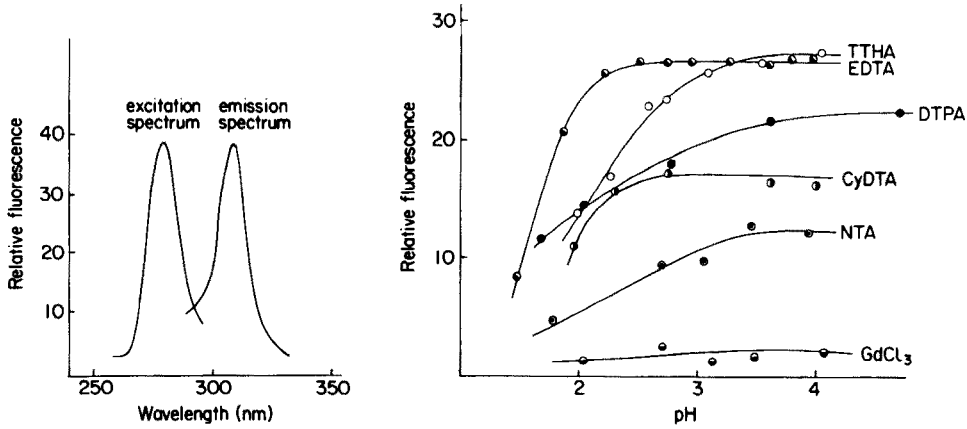

Fig. 1. Apparent excitation and emission spectra of the gadolinium—TTHA chelate. 10 μg Gd ml^{-1}; 5.48 × 10^{-3} M TTHA; pH 3.4.

Fig. 2. Variation of fluorescence intensity of various gadolinium chelates as a function of pH. 10 μg Gd ml^{-1}; 1 × 10^{-3} M aminopolycarboxylic acid. The maximum excitation and emission wavelengths are: 278 and 309 nm for TTHA, EDTA and DTPA; 280 and 310 nm for CyDTA; 281 and 309 nm for NTA; and 278 and 309 nm for $GdCl_3$.

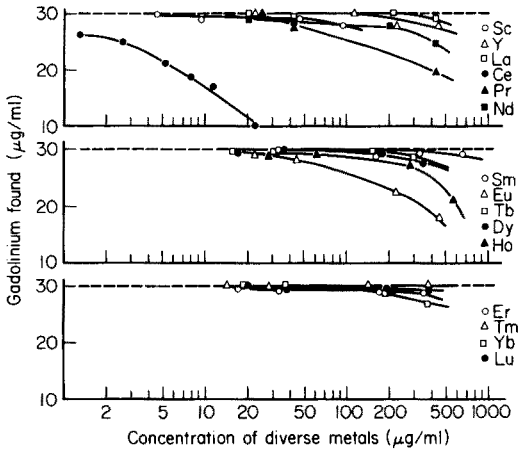

Fig. 3. Determination of gadolinium in synthetic samples containing diverse metal ions.

Results and discussion

Figure 1 shows the apparent excitation and fluorescence spectra of the solution (pH 3.3) containing the gadolinium—TTHA chelate.

Figure 2 shows the variation with pH of the relative fluorescence intensities of solutions containing the gadolinium chelates formed with different aminopolycarboxylic acids. Within the pH range 3.5—4.0, the order of the emission intensities is TTHA > EDTA > DTPA > CyDTA > NTA.

The emission intensity for the TTHA chelate is almost constant when the mole ratio of TTHA to gadolinium exceeds one, it remains constant for 24 h, and shows a linear relationship to the concentration of gadolinium in the range 1—30 $\mu g\ ml^{-1}$. Figure 3 shows how the values for gadolinium (30 $\mu g\ ml^{-1}$) are affected by the addition of diverse metal ions. Ten-fold amounts of yttrium, lanthanum, samarium, terbium, dysprosium, erbium, thulium and lutetium, or equal weights of scandium, praseodymium, neodymium, europium, holmium and ytterbium do not interfere. Cerium causes serious interference.

REFERENCES

1 E. A. Zhikareva, Yu. V. Zelyukova and N. S. Poluektov, Zh. Anal. Khim., 30 (1975) 2039.
2 A. T. Pilipenko, D. I. Bakardzhieva, A. I. Volkova and T. E. Get'man, Ukr. Khim. Zh., 37 (1971) 689.

Analytica Chimica Acta, 98 (1978) 401—404

Short Communication

THE DETERMINATION OF TRACES OF PHOSPHORUS IN SEMICONDUCTOR SILICON

PIER LUIGI BULDINI*
C.N.R., LAMEL Laboratory, Via de' Castagnoli 1, 40126 Bologna (Italy)
DIANA SANDRINI
Chemical Institute "G. Ciamician", University of Bologna, 40126 Bologna (Italy)
(Received 19th December 1977)

Traces of phosphorus have a strong effect on the electrical properties of silicon used in semiconductor devices, so that sensitive and reliable analytical methods are essential. Phosphorus in silicon is usually determined by activation analysis [1—5]; only Pohl and Bonsels [6] and Minns [7] seem to have used chemical methods which provide, within the limits of their sensitivity, adequate reliability and accuracy.

A general preliminary sample treatment based on matrix elimination has already been reported [8] for the determination of impurities in semiconductor silicon. The samples are dissolved in hydrofluoric acid and hydrogen peroxide in the presence of gold(III) as catalyst. After complete dissolution of the sample, the solution is evaporated to dryness in a filtered air flow, so that the silicon matrix volatilizes as hexafluorosilicic acid. After this treatment any phosphorus remains in the residue as phosphoric acid [6]. The present communication is concerned with applications of spectrophotometry and fluorimetry for the determination of the phosphorus present in this residue.

There is an abundant literature on the spectrophotometric determination of phosphorus as molybdophosphoric acid or molybdenum blue in aqueous or organic media. The direct determination of molybdophosphoric acid, after solvent extraction, in the u.v. range [9—11] is simple and offers advantageous possibilities for analysis of silicon. Highly sensitive fluorimetric methods for the determination of phosphate have been based on quinine molybdophosphate [12], rhodamine-B molybdophosphate [13], on fluorescence quenching by phosphate of the aluminium—morin [14, 15] or tin—flavonol complex [15, 16], and on the oxidizing action of molybdophosphoric acid on thiamine to produce fluorescent thiochrome [7, 17]. The thiamine method seemed most promising, because neither removal of excess of reagent nor fluorescent chelate preparation is required.

Experimental

Apparatus. A Perkin-Elmer Model 323 spectrophotometer and a Perkin-Elmer MPF 3 spectrofluorimeter fitted with a 150-W xenon arc lamp and an

R106 photomultiplier were used. Silica cells (10 mm) were used. The spectrofluorimeter was standardized with 10^{-7} M quinine sulphate in 0.05 M sulphuric acid, which was prepared daily from a suitable stock solution.

The silicon samples were dissolved in Teflon test tubes (25 mm i.d., 100 mm long).

Reagents. Solutions of the desired concentration were prepared daily by diluting the following stock solutions: 1000 μg P ml^{-1} solution from KH_2PO_4; 0.01 M thiaminium dichloride (Merck); 0.01 M (in molybdenum) from $(NH_4)_6Mo_7O_{24} \cdot 4H_2O$. Hydrofluoric acid was of electronic grade. All other chemicals were reagent grade. The solutions were stored in polyethylene bottles.

Sample processing and silicon volatilization. Clean the samples, generally as slices, carefully by ultrasonic washing and degreasing with trichloroethylene—acetone—methanol [18]. After etching with hydrofluoric—nitric acid (1 + 1), powder the samples finely in an agate container. Place 10—100 mg of sample in a Teflon test tube; add 3 drops of aqueous 1% $HAuCl_4$ solution and shake gently to wet the powder. Add 5 ml of 6 M HF and 2 ml of 36% H_2O_2. The reaction starts spontaneously. To complete the dissolution, place the covered tubes in a glycerol bath at 110°C for about 45 min. Then fit the tube with a Teflon plug adapted for passing filtered air, in order to eliminate silicon as hexafluorosilicic acid, which distils as an azeotrope with water and hydrofluoric acid.

After the solution has evaporated to dryness (ca. 2 h at 110°C), only a small gold residue and fluorosilicates of various metallic impurities remain.

Spectrophotometric determination of phosphoric acid. Silicate and fluorosilicate interfere in the spectrophotometric determination of phosphorus as molybdophosphoric acid, so that very selective extraction is required. The procedure based on extraction of molybdophosphoric acid with n-butyl acetate from 0.5 M HCl solution [19] is suitable.

To the residue in the Teflon test tube, containing 1—10 μg of phosphorus, add 5 ml of 1 M HCl, 5 ml of 2% ammonium molybdate and 5 ml of n-butyl acetate. Stopper the tube, shake for 2 min and allow the layers to separate. Transfer the organic solution to a 10-mm quartz cell and measure the absorbance at 315 nm against an n-butyl acetate reference.

Prepare a calibration graph by adding known quantities of the standard phosphorus solution to phosphorus-free silicon, or simply by using the standard phosphate solution, without processing silicon. The calibration graph is rectilinear up to 1.6 μg P ml^{-1} in the organic solution (ϵ 20,000 l mol^{-1} cm^{-1}).

Under these conditions, four analyses of a phosphorus-doped silicon (20—26-mg samples) gave a mean result of 100 ± 2 μg P g^{-1} from absorbance values in the range 0.25—0.295.

Fluorimetric determination of phosphoric acid. After sample processing and silicon volatilization as described above, complete elimination of residual fluorosilicate is mandatory. For this purpose, add to each Teflon test tube 1 ml of 0.36 M perchloric acid and again evaporate the solution to dryness

at 110°C with an efficient filtered air flow (for about 30 min); the residual fluorosilicates are thus converted to perchlorates. Cool the tubes to room temperature and add the following reagents: 4 ml of 0.36 M perchloric acid, 4 ml of 0.01 M ammonium molybdate and 4 ml of 0.001 thiaminium dichloride. Add 12 ml of 0.1 M borax (pH 9.4) to adjust the pH to the optimum value for maximum fluorescence. Then transfer the solution to a volumetric flask and dilute to 50 ml with twice-distilled water. Measure the fluorescence at 440 nm with a 370-nm excitation wavelength. Prepare a calibration graph by processing phosphorus-free silicon samples to which known quantities of the standard phosphorus solution have been added.

Under the recommended conditions, the calibration graph for phosphorus is linear up to about 0.6 μg in the measured solution (12 ppb). Four analyses of a phosphorus-doped silicon (35—40 mg samples) gave a mean result of 7.9 ± 0.2 μg P g^{-1} from fluorescence intensities in the range 70—77 (arbitrary units). Samples containing at least 5 μg P g^{-1} can be analyzed in this way; those containing up to 0.5 μg g^{-1} can be analyzed by decreasing the amounts of reagents in order to obtain a final volume of 10 ml.

The best working conditions chosen for the fluorimetric method are similar to those described by Holzbecher and Ryan [17]; it was verified that 0.2—1.0 M is the best starting acidity for molybdophosphoric acid formation, that the optimum molybdenum concentration for obtaining a high signal:blank ratio lies in the $2—7 \times 10^{-3}$ M range (at the time of molybdophosphoric acid formation), and that the amount of thiamine may vary in the $2—4 \times 10^{-4}$ M range without affecting the sample:blank fluorescence ratio, which is maximal for the final pH of 7.5—8.

TABLE 1

Determination of phosphorus in silicon samples

Sample[a]	Resistivity (ohm cm)	P[b] (μg g^{-1})	Fluorimetric				Spectrophotometric			
			No. of detns.	P (μg g^{-1})	s	s_r (%)	No. of detns.	P (μg g^{-1})	s	s_r (%)
W.Ch	4.2×10^{-2}	8.1	22	7.8	0.3	4	—	—	—	—
W.Ch	6.4×10^{-2}	4.0	16	4.4	0.4	9	—	—	—	—
M.	9.0×10^{-2}	2.2	14	2.4	0.2	9.5	—	—	—	—
M.	[d]	100[c]	11	90	2.7	3	8	91	1.8	2
M.	[d]	100[c]	14	101	3.4	3.4	12	99.5	2.3	2.3

[a]W. Ch.; Wacker Chemitronic GmbH, Burghausen (West Germany): M; Montedison S.p.A., Milan, (Italy).

[b]Phosphorus content derived from electrical measurements [20].

[c]Phosphorus obtained on similar samples by activation analysis.

[d]For heavily boron-phosphorus compensated samples, electrical measurements are not indicative.

Results and discussion

Table 1 shows the results obtained for some silicon samples, with a comparison of results obtained by electrical measurements [20]. The results indicate that both methods allow satisfactory determinations and are suitable for routine analysis. The precision and reliability of the spectrophotometric method are better than those of the fluorimetric method; the spectrophotometric method is less sensitive but its simplicity and rapidity offer many advantages. Because of the good reproducibility and linearity of the spectrophotometric calibration curve, standard runs in every series of analyses are unnecessary. The selectivity of the chemical reactions involved makes this method quite free from interferences. No complications were observed when Teflon vessels were replaced by polypropylene or polycarbonate vessels.

The fluorimetric method is much more sensitive than the spectrophotometric method and is limited only by the high fluorescence of the blanks. Teflon apparatus is essential in the sample processing to avoid interferences; polyethylene, polypropylene and polycarbonate vessels released fluorescent extractable materials, as found earlier by Kordan [21]. Despite careful standardization of the operations, the blank fluorescence was not easily reproducible; therefore, it is strongly recommended that each series of analyses should be checked with suitable standard control, instead of using a single calibration curve.

The authors thank Professors Pietro Lanza and Dario Nobili for their helpful discussions and suggestions and Dr. Paolo Ostoja for supplying standards and samples.

REFERENCES

1 F. Burkhardt, A. Mertens and C. Wagner, Phys. Stat. Sol. (a), 22 (1974) K45.
2 J. S. Makris and B. J. Masters, J. Electrochem. Soc., 120 (1973) 1252.
3 E. Ligeon, M. Bruel, A. Bontemps, G. Chambert and J. Monnier, J. Radioanal. Chem., 16 (1973) 537.
4 G. Restelli, F. Girardi, F. Mousty and A. Ostidich, Nucl. Instrum. Methods., 112 (1973) 581.
5 F. Mousty, P. Ostoja and L. Passari, J. Appl. Phys., 45 (1974) 4576.
6 F. A. Pohl and W. Bonsels, Mikrochim. Acta, (1962) 97.
7 R. E. Minns, Mikrochim. Acta, (1961) 354.
8 P. Lanza and M. T. Lippolis, Anal. Chim. Acta, 87 (1976) 27.
9 C. Wadelin and M. G. Mellon, Anal. Chem., 25 (1953) 1668.
10 M. A. De Sesa and L. B. Rogers, Anal. Chem., 26 (1954) 1381.
11 R. J. Jakubiec and D. F. Boltz, Mikrochim. Acta, (1970) 1199.
12 G. F. Kirkbright, R. Narayanaswamy and T. S. West, Analyst, 97 (1972) 174.
13 G. F. Kirkbright, R. Narayanaswamy and T. S. West, Anal. Chem., 43 (1971) 1434.
14 D. B. Land and S. M. Edmonds, Microchim. Acta, (1966) 1013.
15 J. C. Guyon and W. D. Shults, J. Am. Waterworks Assoc., 61 (1969) 403.
16 C. F. Coyle and C. E. White, Anal. Chem., 29 (1957) 1486.
17 J. Holzbecher and D. E. Ryan, Anal. Chim. Acta, 64 (1973) 147.
18 P. Lanza and P. L. Buldini, Anal. Chim. Acta, 85 (1976) 69.
19 S. J. Simon and D. F. Boltz, Anal. Chem., 47 (1975) 1758.
20 J. C. Irvin, The Bell System Tech. J., 41 (1962) 387.
21 H. A. Kordan, Science, 149 (1965) 1382.

Analytica Chimica Acta, 98 (1978) 405—406

Short Communication

LOSSES OF ELEMENTS DURING SAMPLE DECOMPOSITION IN AN ACID-DIGESTION BOMB

A. VAN EENBERGEN and E. BRUNINX*
Philips Research Laboratories, Eindhoven (The Netherlands)
(Received 27th January 1978)

Although acid-digestion bombs are extensively used, only scattered data are available on the possible losses of trace elements during the decomposition process [1—4]. A systematic examination of the losses in a Parr acid-digestion bomb [5] by means of radioactive nuclides of the elements, was therefore undertaken. Two acid mixtures were chosen: (a) $HNO_3/HClO_4$ (6 + 1) for the destruction of organic material; and (b) $HF/HClO_4$ (3 + 1), for the destruction of siliceous materials.

Experimental

The cleaned inner Teflon vessel (volume 25 ml) of the bomb was filled either with 125 mg of Orchard Leaves (NBS standard reference material 1571), 3 ml of concentrated nitric acid and 0.5 ml of concentrated perchloric acid, or with 150 mg of coarse powdered silica, 1.5 ml of concentrated hydrofluoric acid and 0.5 ml of concentrated perchloric acid. The radioactive nuclides were then added with carriers. For most elements, the amount of carrier added with the radionuclide was about 10 μg, but 5 mg was used for molybdenum because of its low specific activity. In addition, ruthenium, germanium and mercury were examined in the 0.5-μg range. In each run several elements were examined simultaneously; all experiments were carried out in duplicate.

The bomb was kept overnight in an oven at 140°C. After cooling and diluting, all radioactive nuclides were measured by computerized Ge(Li) γ-ray spectrometry. These data allowed the yield for each element to be computed. The standard deviation, 1s, for the yield of each nuclide was calculated from the duplicate determinations. Results are summarized in Table 1.

Results and discussion

The low molybdenum yield from the $HNO_3/HClO_4$ procedure is due to precipitation of molybdic acid; the lost molybdenum was found in the Teflon vessel. The same decomposition process also gives a small loss for the 0.5-μg range of germanium, probably as $GeCl_4$, although co-precipitation

TABLE 1

Recoveries after acid decomposition

Nuclide	Yield ± 1s (%) HNO_3—$HClO_4$	Yield ± 1s (%) HF—$HClO_4$	Nuclide	Yield ± 1s (%) HNO_3—$HClO_4$	Yield ± 1s HF—HClO
^{74}As	100 ± 5	99 ± 1	^{203}Hg	101 ± 1	100 ± 5
^{198}Au	101 ± 1	99 ± 2	^{203}Hg[a]	102 ± 2	97 ± 6
^{133}Ba	99 ± 2	100 ± 1	^{140}La	97 ± 2	—[b]
^{115m}Cd	102 ± 1	99 ± 5	^{54}Mn	98 ± 1	102 ± 1
^{60}Co	99 ± 1	100 ± 1	^{99}Mo[c]	32 ± 2	100 ± 3
^{51}Cr	97 ± 2	—	^{212}Pb	98 ± 1	105 ± 4
^{64}Cu	94 ± 4	99 ± 2	^{103}Ru	101 ± 1	84 ± 2
^{59}Fe	97 ± 1	103 ± 1	^{103}Ru[a]	100 ± 2	99 ± 1
^{72}Ga	101 ± 3	99 ± 1	^{46}Sc	99 ± 3	—[b]
^{68}Ge	94 ± 1	99 ± 7	^{75}Se	103 ± 3	100 ± 1
^{68}Ge[a]	88 ± 1	—	^{182}Ta	—[b]	100 ± 1
$^{175+181}Hf$	—[b]	100 ± 2	^{125}Te	101 ± 1	94 ± 3
			^{65}Zn	100 ± 1	104 ± 1

[a]Results for the 0.5-μg range. [b]Not examined because of precipitate formation. [c]Results for the 5-mg range.

with molybdenum cannot be excluded because both elements were used in the same experiment.

The ruthenium lost in the $HF/HClO_4$ procedure was also found in the Teflon vessel; the high yield at the lower ruthenium concentration cannot be explained.

From the yields mentioned in Table 1 and the known data for the elements Be, Se, I, Hg [2], and Si, Fe, Al, Ti, V, Ca, Mg, Na, K [3], it can safely be concluded that virtually no losses occur during the decomposition process, except for germanium and some elements which may precipitate under unfavourable conditions.

REFERENCES

1 R. Bock, Aufschlussmethoden der anorganischen und organischen Chemie, Verlag Chemie, 1971, p. 20, pp. 23—25 and pp. 46—48.
2 L. Kötz, G. Kaiser, P. Tschöpel and G. Tölg, Fresenius Z. Anal. Chem., 260 (1972) 207.
3 B. Bernas, Anal. Chem., 40 (1968) 1682.
4 G. Kaiser, E. Grallath, P. Tschöpel and G. Tölg, Fresenius Z. Anal. Chem., 259 (1972) 25
5 Parr bulletin 4745, Instructions for "Parr" 4745 acid digestion bomb. Parr Instrument Co., Moline, Ill.

Analytica Chimica Acta, 98 (1978) 407—409

Book Reviews

J. R. Green and D. Margerison, *Statistical Treatment of Experimental Data*, Elsevier, Amsterdam, 1977, xiv + 382 pp., US $34.95.

This book describes statistical methods applicable to experimental data which arise in the physical sciences. Dr. Green is a lecturer in the Department of Computational and Statistical Science and Dr. Margerison is a senior lecturer in Inorganic Physical and Industrial Chemistry at Liverpool University. Their aim was to give guidance to researchers who wish to understand statistical methodology in order to analyse their own experimental data.

The development of the material follows a traditional statistical textbook pattern. In chapters 2, 3 and 4 the reader meets probability theory, random variables, probability distributions and definitions of mean and variance. The next two chapters cover the estimation of unknown parameters of a probability distribution and the construction of confidence intervals. Hypothesis testing is the dominant feature of chapters 7, 8, 9 and 10 where tests on means and variances and goodness-of-fit tests are described. The remainder of the book describes various aspects of regression theory, including straight-line and polynomial regression, and weighted least-squares procedures.

My main criticism of this book is that, even though one of the authors is an experimentalist, the emphasis is on the mathematics of statistics. Chapters consist mainly of an account of general mathematical theory followed by brief numerical examples which illustrate the more elementary uses of what has gone before. Significantly the examples are in smaller type face than the mathematical text. No attempt is made to present a typical problem which involves experimental data as a guide to the determination of methods appropriate to an analysis of the data. To be fair to the authors, the theory is well presented but the book is better suited to a student of mathematics than an experimental scientist who might well be put off by the approach adopted.

The following sentence appears in the publisher's description of the book: "Neither a strong mathematical background nor a prior knowledge of probability or statistics is required in order to make use of this work". However, ideally the reader should have a good background knowledge of differential and integral calculus, vector and matrix algebra, and the principles of numerical analysis together with a strong bent toward the mathematical aspects of statistics.

M. V. Shotter

M. R. F. Ashworth, *The Determination of Sulphur-Containing Groups*, Vol. 3, Academic Press, London and New York, 1977, xi + 220 pp., price £11.00, $21.50.

This is the third volume in a series dealing with the analysis of organic sulphur compounds and it is concerned largely with analytical methods for compounds containing sulphide (—S—) or disulphide (—S—S—) groups attached to carbon atoms which are otherwise linked only to hydrogen or to other carbon atoms. Heterocyclic compounds that fall into these categories are, however, specifically excluded except for the more important thiophenes and biotin.

As in the previous volumes of this series the author has aimed to give a comprehensive review of the available methods without experimental details, but with a discussion of the advantages and disadvantages of each method and with references to the original literature. The methods described fall mainly into three categories — chemical, spectroscopic, and chromatographic; other methods such as polarography, catalysis (of the iodine—azide reaction) and microbiological methods are also mentioned. The large number of sub-headings in each chapter make for easy reference, as do the comprehensive subject and author indexes. The book is well produced and seems likely to become a standard source of information for those concerned with the analysis of sulphur compounds.

D. Leaver

A. J. Barnes and W. J. Orville-Thomas (Eds.), *Vibrational Spectroscopy — Modern Trends*, Elsevier, Amsterdam, 1977, xii + 442 pp., price Dfl. 122, $49.95.

This is a terrible tragedy. At the price of around £28, and for camera-ready typed copy, who can afford to purchase personal copies? Certainly not students, and yet this is the best text for students to appear for some time, as well as a text that will assist established spectroscopists to get up-to-date in the most efficient way possible.

After a brief introduction by (the late) Harry Hallam, the book is divided into 4 main sections, e.g. Lasers and their Applications, Experimental Methods, Theoretical Methods, and Applications to Problems in Molecular Structure; each of these is sub-divided to give a total of 26 chapters, each of around 15 pages. By selecting recognized authorities to write accounts of a wide range of current topics, and by setting a tight limit on the length of each contribution, the editors of the book have devised a successful way of producing a most readable and useful, balanced, concise, critical, and up-to-date text-book. The printing is bold and clear, mathematical

and other formulae are well set-out, the diagrams are excellent, and the author and subject indexes are comprehensive. Only two trivial misprints were noticed.

The standard of treatment is uniformly high, and it would be invidious to select any of the contributions for particular praise. The number of chapters is too large for details to be given of them all; the following selection is given solely to indicate the range of topics and the international status of the contributors. Principles of Lasers; Tuneable Infrared Lasers (both by J. J. Turner); Fourier Transform Spectroscopy (A. J. Barnes); Matrix Isolation (A. J. Barnes and H. E. Hallam); Highly Reactive and Unstable Species (G. C. Pimentel); High Temperature Species (I. R. Beattie); Resonance Raman Spectroscopy (R. J. H. Clark); Band Contour Analysis (W. H. Fletcher); Limitations of Force Constant Calculations (G. Zerbi); Barriers to Internal Rotation around Single Bonds (J. R. Durig); Transition Metal Co-ordination Compounds and their Analysis (A. Müller). Most of the chapters present a short, well-chosen list of literature references. A splendid book, therefore, for students, teachers, and spectroscopists.

D. M. W. Anderson

Alberto Frigerio and Emilio L. Ghisalberti (Eds.), *Mass Spectrometry in Drug Metabolism*, Plenum Press, New York and London, 1977, xii + 532 pp., price $51.

This expensive book presents the texts of most of the papers presented at the International Symposium on Mass Spectrometry in Drug Metabolism held in Milan in June 1976. Camera-ready typed copy has been used; the quality of the figures and formulae are satisfactory except where the direct reproduction of some computer print-out and other pre-set tabular data are concerned. The 32 papers are presented in the following sections: Identification of Drugs and Drug Metabolites; Quantitation of Drugs and Metabolites; Intermediates in the Metabolism of Drugs; Stable Isotope Labelling; Drug Abuse; and Developments in Methodology, the four papers in which constitute the main interest for analytical chemists, although several of the other papers contain interesting details of applications of g.c.-m.s., chemical ionisation m.s. etc.

Analytica Chimica Acta, 98 (1978) 410—411

FEDERATION OF EUROPEAN CHEMICAL SOCIETIES (FECS) WORKING PARTY ON ANALYTICAL CHEMISTRY (WPAC)

European Analytical Column 1

A resolution was passed at the seventh meeting of the WPAC/FECS in Davos, May 22, 1977, that the minutes of the WPAC meetings will be published in shortened form by the national analytical member societies in order to provide better information on the activities of this working party. The WPAC consists at the moment of 28 members representing 23 national societies of 17 European countries. The chairman is Prof. Dr. H. Malissa, Technical University, Vienna. WPAC activities are directed towards the practical needs of analytical chemistry in the European context, such as the organization of the Euroanalysis conferences, discussions of standardization in environmental analysis, and the treatment of educational problems in analytical chemistry.

At the seventh meeting of the WPAC, special consideration was given to the organization of the Euroanalysis III conference which will be held in Dublin during August 20—25, 1978, and to preparations for the Euroanalysis IV conference which will be held in Helsinki in 1981.

Like the earlier Euroanalysis meetings in Heidelberg (1972) and Budapest (1975), Euroanalysis III will emphasize both pure and applied aspects of analytical chemistry. The programme has been designed to appeal to the widest possible audience — from scientists engaged in the use of analytical techniques in problem solving to those involved in research and development of analytical techniques. The Conference will, therefore, present an excellent opportunity for participants to learn about the research work carried out in the laboratories of the member states of the Federation and its practical applications in many countries throughout the world. The scientific programme will consist of invited plenary and keynote lectures, contributed papers, poster sessions, round-table discussions and panel discussions.

The round-table discussions will be devoted to two further main activities of the WPAC: standardization in environmental analysis (Standard Reference Materials, SRM, and Standard Reference Criteria, SRC) and education in analytical chemistry. Invited plenary and keynote lecturers will describe their ideas and act as discussion starters.

The creation of a special discussion group on SRM was proposed by Prof. Malissa at the Davos meeting. Practical work has already been done in establishing dust SRMs by laboratories in Austria, Hungary, Yugoslavia and Germany.

The aim of the round-table discussion on education in analytical chemistry is to create a European model of teaching analytical chemistry in such a way

that the growing demands of technology, medicine and environmental research can be met by analytical chemists graduating from European universities. This does not necessarily mean that "classical analytical chemistry" should be abandoned, but certainly that modern methods of analysis should be included in the teaching plans of more universities. In order to consider the best model, every member country will present two posters on the actual and the "optimal" methods of teaching analytical chemistry in that country. In two special lectures, the needs of industry and of government will be discussed.

At the Davos meeting it was also resolved to support the creation of a European Museum of Analytical Chemistry to collect, conserve and demonstrate valuable prototypes of pioneering analytical instrumentation and original publications.

Colleagues who are interested in cooperating in any of the fields described above are requested to contact the Secretary of the WPAC: Prof. Dr. R. Kellner, Institut für Analytische Chemie und Mikrochemie, Technical University, Getreidemarkt 9, A 1060 Wien, Austria.

ANALYTICA CHIMICA ACTA, Vol. 98 (1978)

AUTHOR INDEX

(continued from outside of cover)

Printed in The Netherlands

VOL. 98 No. 2 ANALYTICA CHIMICA ACTA JUNE 1, 1978

CONTENTS

(continued on inside of cover)